Scientific Publications of the American Museum of Natural History

American Museum Novitates
Bulletin of the American Museum of Natural History
Anthropological Papers of the American Museum of Natural History

Publications Committee
Robert S. Voss, Chair

Board of Editors
Jin Meng, Paleontology
Lorenzo Prendini, Invertebrate Zoology
Robert S. Voss, Vertebrate Zoology
Peter M. Whiteley, Anthropology

Managing Editor
Mary Knight

Submission procedures can be found at http://research.amnh.org/scipubs

All issues of *Novitates* and *Bulletin* are available on the web (http://digitallibrary.amnh.org/dspace). Order printed copies on the web from:
http://shop.amnh.org/a701/shop-by-category/books/scientific-publications.html

or via standard mail from:
American Museum of Natural History—Scientific Publications
Central Park West at 79th Street
New York, NY 10024

♾ This paper meets the requirements of ANSI/NISO Z39.48-1992 (permanence of paper).

On the cover: Reconstruction of *Azendohsaurus madagaskarensis* from the ?Middle to Upper Triassic, Isalo group, Madagascar. Drawing by Matth Celeskey.

AMNH BULLETIN 398

2015

Postcranial Osteology of *Azendohsaurus madagaskarensis* (?Middle to Upper Triassic, Isalo Group, Madagascar) and Its Systematic Position among Stem Archosaur Reptiles

Sterling J. Nesbitt, John J. Flynn,
Adam C. Pritchard, J. Michael Parrish,
Lovasoa Ranivoharimanana, and André R. Wyss

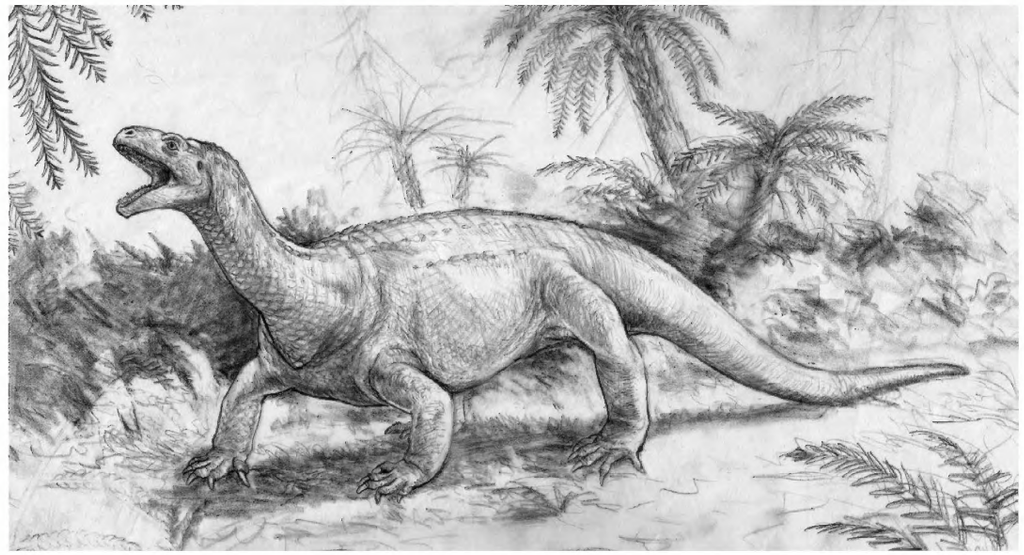

BULLETIN OF THE AMERICAN MUSEUM OF NATURAL HISTORY

POSTCRANIAL OSTEOLOGY OF *AZENDOHSAURUS MADAGASKARENSIS* (?MIDDLE TO UPPER TRIASSIC, ISALO GROUP, MADAGASCAR) AND ITS SYSTEMATIC POSITION AMONG STEM ARCHOSAUR REPTILES

STERLING J. NESBITT
Center for Integrative Research, Field Museum of Natural History;
Division of Paleontology, American Museum of Natural History;
Department of Geosciences, Virginia Polytechnic Institute and State University, Blacksburg

JOHN J. FLYNN
Richard Gilder Graduate School and Division of Paleontology
American Museum of Natural History

ADAM C. PRITCHARD
Department of Anatomical Sciences, Stony Brook University,
Stony Brook, New York

J. MICHAEL PARRISH
College of Science, San Jose State University, San Jose, California

LOVASOA RANIVOHARIMANANA
Département de Paléontologie et d'Anthropologie Biologique,
Université d'Antananarivo, Madagascar

ANDRÉ R. WYSS
Department of Geological Sciences, University of California at Santa Barbara;
Division of Paleontology, American Museum of Natural History

BULLETIN OF THE AMERICAN MUSEUM OF NATURAL HISTORY
Number 398, 126 pp., 81 figures, 12 tables
Issued December 7, 2015

Copyright © American Museum of Natural History 2015 ISSN 0003-0090

CONTENTS

Abstract 4
Introduction 4
Institutional acronyms 5
Methods 6
Geological context 7
Systematic paleontology 9
  Archosauromorpha 9
  Allokotosauria 9
  Azendohsaurus 10
  Azendohsaurus madagaskarensis 10
    Holotype 10
    Paratypes 10
    Referred Material 10
    Locality 10
    Revised Diagnosis 11
Description 11
  Axial Skeleton 11
    Vertebral column (general) 11
    Cervical vertebrae 13
    Trunk vertebrae 21
    Sacral vertebrae 25
    Caudal vertebrae 27
    Ribs 31
    Gastralia 33
    Chevrons 33
  Pectoral girdle 35
    Clavicle 35
    Interclavicle 36
    Scapula 37
    Coracoid 39
  Forelimb 40
    Humerus 40
    Radius 42
    Ulna 43
    Manus 44
      Radiale 47
      Intermedium 48
      Ulnare 50
      Lateral centrale 51
      Medial centrale 51
      First–fourth distal carpals 51
      Metacarpals 53
      Manual digits 54
      Terminal phalanges 55
  Pelvic girdle 57
    Ilium 57
    Pubis 60
    Ischium 61
  Hind limb 62
    Femur 62

Tibia 64
Fibula 65
Pes 66
Astragalus 68
Calcaneum 73
Distal tarsals 75
Metatarsals 76
Pedal digits 78
Phylogenetic analysis 79
Taxon and character sampling 79
Tree search strategy 81
Results and Discussion 81
Allokotosauria: tree topology and clade support 84
Allokotosauria + Archosauriformes 84
Allokotosauria 85
Azendohsauridae + Trilophosauridae 86
Azendohsauridae 86
Trilophosauridae 87
Trilophosaurus 88
Implications for the divergence of Archosauromorpha 92
Convergence and the prevalence of herbivory in Triassic Archosauromorpha 93
Conclusions and perspective 96
Acknowledgments 97
References 97
Appendix 1. Referred material of *Azendohsaurus madagaskarensis* 106
Appendix 2. The manus of *Trilophosaurus buettneri* 108
Appendix 3. Extended description of newly added terminal taxa in the phylogenetic analysis 111
Appendix 4. Phylogenetic characters 113
Appendix 5. Character scores 124

ABSTRACT

During the Triassic, archosauromorphs became one of the first groups of diapsid reptiles to diversify in terms of body size and morphological disparity in both terrestrial and marine ecosystems across Pangaea. This seemingly rapid divergence, and the numerous unique body plans stemming from it, concomitantly has confounded reconstructions of archosauromorph relationships. Teasing apart homology from homoplasy of anatomical characters in this broad suite of body types remains an enormous challenge with the current sample of taxa. Here, we present the postcranial anatomy of *Azendohsaurus madagaskarensis*, an early archosauromorph from ?Middle to Upper Triassic strata of Madagascar. *Azendohsaurus madagaskarensis* is known from nearly the entire skeleton in an ontogenetically variable sample. The holotype locality consists of a monotypic bone bed; preservation ranges from complete but disarticulated bones to articulated sections of the skeleton. *Azendohsaurus madagaskarensis* embodies an aberrant constellation of archosauromorph features, including an elongated neck, a short, stocky tail, robust limbs, and unexpectedly short digits terminating in large recurved unguals on the manus and pes. Together with the cranium, the postcrania reveal *A. madagaskarensis* to be another representative of a growing coterie of highly apomorphic and bizarre Triassic archosauromorphs. At the same time, recovery and description of the full anatomy of *A. madagaskarensis* helps to identify a monophyletic grouping of specialized taxa that includes the North American Late Triassic–aged archosauromorphs *Trilophosaurus, Spinosuchus,* and *Teraterpeton*, Indian *Pamelaria*, and Moroccan *Azendohsaurus laaroussii*. Moreover, information derived from the skeleton of *A. madagaskarensis* solidifies the systematic position of these taxa among other archosauromorphs. Using the most comprehensively sampled phylogenetic analysis of early archosauromorphs, we found the clade encompassing the aforementioned taxa as the nearest outgroup of *Prolacerta broomi* + Archosauriformes. The newly recognized clade containing *Azendohsaurus, Trilophosaurus, Spinosuchus, Pamelaria,* and *Teraterpeton* demonstrates high morphological disparity even within a closely related group of archosauromorphs, underscores the polyphyly of protorosaurs (= prolacertiforms), and suggests that most major divergences within this group occurred in the Triassic. Furthermore, our results indicate that craniodental character states ascribed to a herbivorous diet were much more pervasive across Triassic Archosauromorpha than previously conjectured.

INTRODUCTION

The initial diversification of Archosauria during the Triassic has been the focus of voluminous research (e.g., Romer, 1956; Charig, 1980; Benton, 1983; Gauthier, 1986; Benton and Clark, 1988; Sereno, 1991; Parrish, 1993; Juul, 1994; Nesbitt, 2003, 2011; Nesbitt et al., 2011; Brusatte et al., 2008; 2011; Butler et al., 2011) because this clade: (1) includes two important extant groups, crocodylians and birds; (2) is a classic example of an adaptive radiation; and (3) has recently been the focus of many groundbreaking macroevolutionary studies. Archosauria is just one component of a larger radiation of Archosauromorpha (stem archosaurs and the crown clade Archosauria) that arose either just prior to the end of the Permian or soon after the end-Permian extinction (Ezcurra et al., 2014). Stem archosaur interrelationships have received some attention (Benton, 1985; Gauthier et al., 1988a, 1988b; Dilkes, 1998; Muller, 2004; Ezcurra et al., 2014; Pritchard et al., 2015), but a consensus is elusive. Disagreement about relationships partially reflects the tremendous divergence among taxa (e.g., *Trilophosaurus*, *Tanystropheus*, long-necked "protorosaurs") with extremely long ghost lineages. Moreover, the membership of Archosauromorpha remains fluid. Currently, it is unclear whether turtles (Cao et al., 2000; Bhullar and Bever, 2009), drepanosaurids (Dilkes, 1998), sauropterygians (Caldwell, 1996), or other extinct clades (e.g., Ichthyosauria; Caldwell, 1996) are archosauromorphs. Placement of these clades at the base of Archosauromorpha would have a profound influence on our understanding of character evolution and macroevolutionary patterns within the group.

Even relationships among the clades that are clearly part of Archosauromorpha, such as archosauriforms, rhynchosaurs, and tanystropheids, are challenging because these

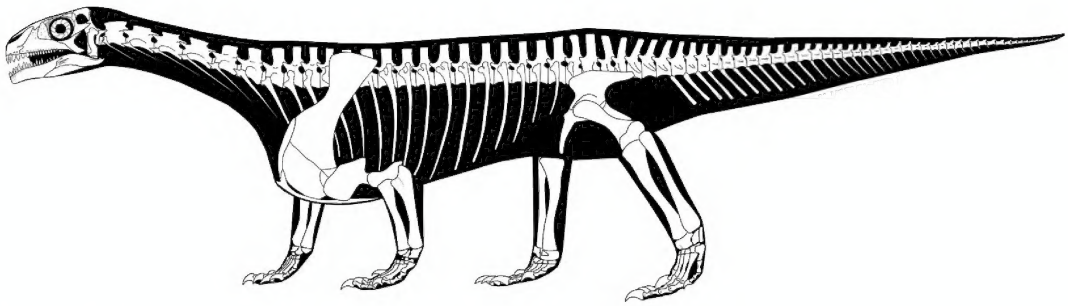

Fig. 1. Skeletal reconstruction of *Azendohsaurus madagaskarensis*.

clades appear "fully derived" at their first appearance in the fossil record, providing few clues to assist in teasing out plesiomorphy from homoplasy and derived character states. Additionally, bizarre taxa such as *Trilophosaurus* and *Teraterpeton* do not clearly fit into any of the monophyletic components of the clade. The problem of the phylogenetic placement of early archosauromorph taxa often owes less to incomplete skeletal records of these taxa (although that is sometime a major factor) than to a lack of understanding about which character states are plesiomorphic for Archosauromorpha.

To help resolve uncertainties involving character transformations among early archosauromorphs, we continue our morphological description of the early archosauromorph *Azendohsaurus madagaskarensis* (fig. 1) from the ?Middle to Upper Triassic Isalo Group of Madagascar. Our most recent work (Flynn et al., 2010) on *A. madagaskarensis* focused on naming the taxon, a description of its cranial anatomy, and a rejection of the taxon's previously accepted dinosaurian affinities (Dutuit, 1972; Gauffre, 1993; Flynn et al., 1999). The cranial morphology of *A. madagaskarensis* revealed an enigmatic taxon combining a patchwork of seemingly dinosaurian dental characters and various plesiomorphic characters indicative of an earlier-diverging position within Archosauromorpha (Flynn, et al., 2010). Herein we describe and thoroughly illustrate the known, almost entire, postcranial skeleton of *A. madagaskarensis*. We provide a complete diagnosis for the taxon, compare it to other early archosauromorphs, and determine its affinities based on the most comprehensive phylogenetic analysis focused on Triassic noncrown archosauromorphs undertaken to date. Finally, we discuss the implications of the phylogenetic placement of *A. madagaskarensis* on our understanding of the relationships of other aberrant archosauromorphs. We also use the well-preserved material of *A. madagaskarensis* to reinterpret portions of the skeletal anatomy of several other archosauromorphs.

In the description below, we compare *Azendohsaurus madagaskarensis* to many archosauromorphs, but preferentially focus our comparisons on the Triassic archosauromorphs with the most complete skeletal records, such as *Trilophosaurus buettneri*, *Mesosuchus browni, Proterosuchus fergusi*, *Protorosaurus speneri*, and *Tanystropheus longobardicus*.

INSTITUTIONAL ACRONYMS

AMNH	American Museum of Natural History, New York
BP	Evolutionary Studies Institute (formerly Bernard Price Institute for Palaeontological Research), University of the Witswatersrand, Johannesburg, South Africa
FMNH	Field Museum of Natural History, Chicago, Illinois
GPIT	Paläontologische Sammlung der Universität Tübingen, Tübingen, Germany
GR	Ruth Hall Museum of Paleontology, Ghost Ranch, New Mexico
ISIR	Geological Studies Unit of the Indian Statistical Institute, Kolkata, India

IVPP Institute of Vertebrate Paleontology and Paleoanthropology, Beijing, China
MCSN Museo Civico di Storia Naturale di Milano, Milan, Italy
MCSNB Museo Civico di Storia Naturale Enrico Caffi, Bergamo, Italy
MCZ Museum of Comparative Zoology, Cambridge, Massachusetts
MFSN Museo Friulano di Storia Naturale, Udine, Italy
MNHN (and MTD) Muséum National d'Histoire Natu relle, Paris, France
NHMUK Natural History Museum, London, United Kingdom
NMK Naturkundmuseum im Ottoneum, Kassel, Germany
NMMNHS New Mexico Museum of Natural History and Science, Albuquerque, New Mexico
NMQR National Museum, Blomfontein, South Africa
NMT National Museum of Tanzania, Dar es Salaam, Tanzania
NSM Nova Scotia Museum of Natural History in Halifax, Nova Scotia, Canada
PIMUZ Paläontologisches Institut un Museum, Zürich, Switzerland
PIN Paleontological Institute of the Russian Academy of Sciences, Moscow, Russia
PVSJ División de Paleontología de Vertebrados del Museo de Ciencias Naturales y Universidad Nacional de San Juan, San Juan, Argentina
SAM Iziko South African Museum, Cape Town, South Africa
SMNS Staatliches Museum für Naturkunde, Stuttgart, Germany
TTU-P Museum of Texas Tech University, Lubbock, Texas
UA Université d'Antannanarivo, Antannanarivo, Madagascar
UCMP University of California Museum of Paleontology, Berkeley, California
UFRGS Instituto de Geociências, Universidade Federal do Rio Grande do Sul, Porto Alegre, Brazil
UMMP University of Michigan Museum of Paleontology, Ann Arbor, Michigan
USNM National Museum of Natural History, Washington, DC
VMNH Virginia Museum of Natural History, Martinsville, Virginia
WMsN Westfäliches Museum für Naturkunde, Münster, Germany

METHODS

Permits

Fieldwork was conducted under permit from Ministère des Mines de Madagascar and in collaboration with the Ministère de l'Enseignement Supérieur et de la Recherche Scientifique de Madagascar.

Fieldwork and Preparation

Field crews from the Field Museum of Natural History, University of California Santa Barbara, and University of Antananarivo (see Acknowledgments) excavated the type locality of *A. madagaskarensis* in southwestern Madagascar from 1997 until 1999 (fig. 2). Specimens were excavated with hand tools (e.g., small shovels, rock hammers) using standard paleontological techniques and consolidated with cyanoacrylate glues; they were wrapped in locally obtained tissue paper and then secured by tape, or encapsulated in metal cans or plaster jackets when necessary for transport. Specimens were shipped to the Field Museum of Natural History for preparation by staff and volunteer preparators (see Acknowledgments). The red clay matrix and thin calcium carbonate veneer adhering to the surfaces of fossils were removed with microjacks (www.paleotools.com) and pin-vices holding carbide needles; fine-scale preparation was undertaken under magnifiers or stereomicroscopes. Surface coats of thin B-72 were applied to protect the surfaces of many of the bones. Cyanoacrylate glues and epoxies (e.g., 2-ton) were used to secure fragile areas or bond breaks.

The material of *Azendohsaurus madagaskarensis* is permanently housed at the University of Antananarivo (including the holotype and other material) and the Field Museum of Natural History. Most specimens

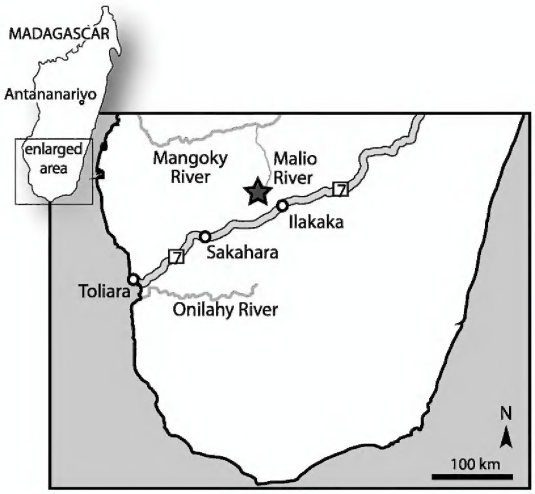

Fig. 2. Map of the location of the holotype locality of *Azendohsaurus madagaskarensis*.

are referred to throughout the text by their original field collection number (see appendix 1) and these specimen identification numbers will always be kept with the specimens at both institutions. Most specimens permanently housed at the University of Antananarivo were molded, and casts are deposited at the Field Museum of Natural History. Preparation volunteers and staff molded and cast specimens at the FMNH. Elements were embedded in plastaline modeling clay and encased in room temperature vulcanizing tin-cured silicone rubber, typically in two or three part molds. Surfaces were cleaned with acetone applied by brush.

GEOLOGICAL CONTEXT

The geological and geographic provenance of the *Azendohsaurus madagaskarensis* sample is detailed in Flynn et al. (2010), and consequently just a few of the more pertinent details are highlighted here. The monospecific sample derives from a single, geographically tightly circumscribed locality (M-28) within tens of meters of the east (right) bank of the Malio River immediately west of the western boundary of Isalo National Park, which itself lies between the cities of Ranohira and Sakaraha (prior to the fairly recent discovery of sapphires in Quaternary gravels near Ilakaka and the ensuing mining boom, Ranohira and Sakaraha were the largest centers of habitation in the region). Fossils of *A. madagaskarensis* were recovered along ~100 m of strike of a less than 1 m thick stratigraphic interval. The fossiliferous unit, which dips nearly horizontally, is exposed at midelevation along a ~15 m high portion of an uplifted river terrace. As a result, the fossiliferous horizon projects into a steep slope of outcroup exposures. We thus were able to excavate specimens over a swath of only a few meters wide into this slope.

Fossils of *A. madagaskarensis* have been recovered exclusively from a lens of red, fine-grained sequence of overbank deposits in the limited area just described (M-28) (fig. 3). Reduced (green) ovoid granules and flakes, ≤1 cm in diameter, occur sporadically through the fossiliferous mudstone. Several aspects of this occurrence are curious. First, numerous other terrestrial vertebrate taxa (see Flynn et al., 2000, for summary) have been recovered from the same formation from many locations within a 20–30 km radius of the *A. madagaskarensis* site. Although many of these other sites are lithologically indistinguishable from M-28, none have yielded *A. madagaskarensis*. Similarly, none of the dozen or so reptile and synapsid taxa (see below) occurring at these other locations are recorded at M-28. Many of the best-preserved specimens from other locations, particularly rhynchosaurs and traversodontids, are derived from medium-grained, well-sorted channel sands. Whether the current restriction of *A. madagaskarensis* to a single monotypic bone bed, reflects profound habitat partitioning between it and other components of the assemblage, a taphonomic/depositional bias (*A. madagaskarensis* being the largest-bodied taxon in the entire assemblage), behavioral factors, or some other cause, remains to be established.

Azendohsaurus madagaskarensis and other elements of the Triassic assemblage from the Malio River drainage are derived from basal levels of a lithostratigraphical unit that is classically termed the Isalo II (Besairie, 1936; 1972)—of the Isalo Group, or the Makay Formation (Razafimbelo, 1987). The age of the fossiliferous unit is best constrained by vertebrate biostratigraphy of a single cynodont

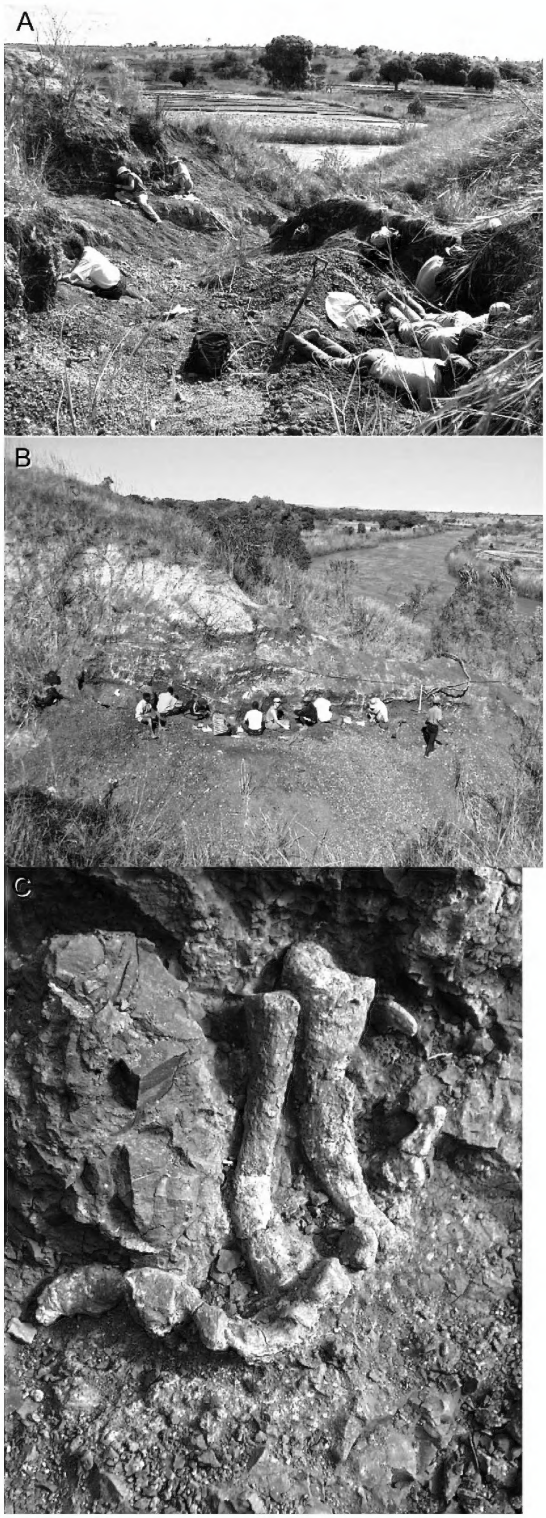

and the absence of certain Late Triassic archosauriforms otherwise found throughout Pangaea. The shared presence of *Menadon besairiei* in the Makay Formation and the Ladinian *Santacruzodon* Assemblage Zone (AZ) of the Brazilian Santa Maria Formation suggests that the Makay Formation is also Ladinian or late Middle Triassic in age (Melo et al., 2010; Schultz and Langer, 2010). Moreover, the *Santacruzodon* AZ is biostratigraphically correlated with the Chañares Formation of northwestern Argentina. The latter unit has been recently considered to be late Middle Triassic–early Late Triassic in age by Desojo et al. (2011), a hypothesis further bolstered by radioisotopic dating (Irmis et al., 2013). The possible extension of these South American units into the early Late Triassic and the shared presence of the *Massetognathus-Santacruzodon* clade with the Makay Formation provide further evidence for a late Middle Triassic–early Late Triassic age for the Makay Formation. Additionally, we note that dinosaurs and other archosauriform taxa (e.g., phytosaurs, aetosaurs) typically found in Upper Triassic deposits of neighboring areas (e.g., Maleri Formation of India; Chatterjee, 1978) are absent thus far in the Makay Formation. The Makay Formation thus is almost certainly older (by an unknown span) than units producing the earliest dinosaurs, including the Ischigualasto Formation of Argentina and Santa Maria Series of Brazil (see Flynn et al., 1999; 2000).

As mentioned, the remains of *A. madagaskarensis* have been recovered solely from a monotypic bone bed. Of the hundreds of elements removed from the small quarry, none obviously pertain to any other taxon. Specimens range from incomplete isolated elements to articulated partial skeletons, sometimes preserved in life position (e.g., the upright manus in fig. 3C). As discussed more fully below in conjunction with the

←

Fig. 3. The holotype locality of *Azendohsaurus madagaskarensis* near the Malio River in southern Madagascar (**A**) during the second year of excavation in 1998, (**B**) during the third year of excavation in 1999, and (**C**) a photograph of the articulated right manus (FMNH PR 3820) in situ. All photographs by William Simpson.

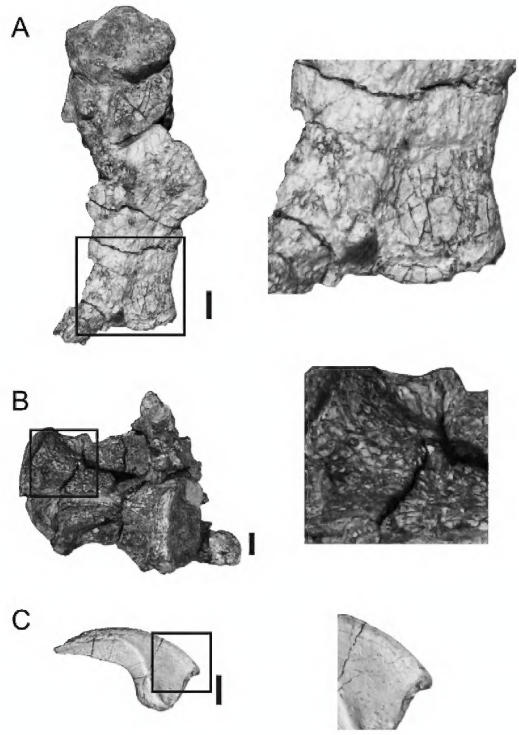

Fig. 4. The various states of preservation of bones from the *Azendohsaurus madagaskarensis*. A poorly preserved humerus (UA 8-28-97-143) (**A**) in ventral view and close-up (right); a heavily cracked cervical vertebra (UA 7-12-99-564) (**B**) in ventral view and close-up (right); and an exquisitely preserved pedal ungual (FMNH PR 3815) (**C**) in lateral view and close-up (right). Scales = 1 cm.

description of particular elements, the sample exhibits a size range of roughly 25% from the smallest to the largest specimens, reflecting ontogenetic variation, intraspecific variation, and/or sexual dimorphism; these factors cannot be differentiated from one another in the context of the given sample.

The quality of preservation of the *A. madagaskarensis* sample varies considerably but is generally excellent. Some postmortem disturbance (by other organisms) and deformation (by geological processes) is evident in the sample, possibly the result of soft-sediment deformation or trampling. Given the multiple duplicates of most elements in the assemblage, little ambiguity about original morphology exists. The surfaces of the bones vary from heavily cracked (weathering stage 3 or 4 of Behrensmeyer, 1978; fig. 4A) to pristine (fig. 4C) suggesting that some were exposed at the surface for many years before burial, whereas others were rapidly and completely buried. In general, the bones with heavily cracked surfaces tend to be isolated, whereas the articulated sections, for the most part, tend to be better preserved. Diagenetic factors may have been responsible for cracking in some specimens (e.g., fig. 4B). The cracking in this specimen (UA 7-12-99-564) is similar to the bones from the Triassic Santa Maria Formation that were cracked and displaced as a consequence of calcite cementation during or after initial fossilization (see Holz and Schultz, 1998).

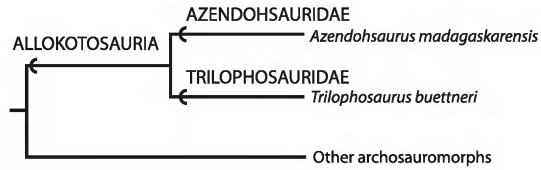

Fig. 5. Illustration of the phylogenetic use of Allokotosauria, Azendohsauridae, and Trilophosauridae for this paper. Curved lines mark stem groups.

SYSTEMATIC PALEONTOLOGY

Archosauromorpha Huene, 1946 (sensu Benton, 1985)
Allokotosauria (new)

DEFINITION: The least-inclusive clade containing *Azendohsaurus madagaskarensis*, Flynn et al., 2010, and *Trilophosaurus buettneri*, Case, 1928a, but not *Tanystropheus longobardicus*, Bassani, 1886, *Proterosuchus fergusi*, Broom, 1903, *Protorosaurus speneri* von Meyer, 1830, or *Rhynchosaurus articeps* Owen, 1842 (fig. 5).

DIAGNOSIS: Lateral surface of orbital margin of frontal rugose (char. 237, state 1, abbreviated to 237-1; this simplification is followed throughout the text); posterior side of quadrate head expanded and hooked (207-1); and prominent tubercle developed superior to glenoid fossa of scapula (146-0). These unambiguous character states most conspicuously diagnose Allokotosauria, but are only a subset of the full unambiguous character state set that characterizes the clade (see Results and Discussion).

REMARKS: Here we recognize a clade containing *Azendohsaurus*-like taxa (in Azendohsauridae) paired with *Trilophosaurus*-like taxa (in Trilophosauridae). Allokotosauria, meaning "strange reptiles" in Greek, contains a bizarre suite of Triassic-aged archosauromorph taxa with a high disparity of craniodental features typically associated with herbivory. Given the previous difficulty with finding a well-supported position of *Trilophosaurus* and kin within Archosauromorpha (Dilkes, 1998), and the currently fluid state of understanding both the interrelationships of early Archosauromorpha and their placement within Diapsida, we err on the side of caution in naming this clade. As defined, the stem-based clade name Allokotosauria is used to refer to Azendohsauridae and Trilophosauridae and their closest relatives exclusive of other archosauromorphs. If Azendohsauridae and Trilophosauridae are found to be more distantly related in future analyses, Allokotosauria would thus serve no purpose and should summarily be abandoned. Azendohsauridae and Trilophosauridae currently appear to share a number of apomorphies exclusive of other archosauromorph groups, supporting the monophyly and value of naming this new clade (see below).

Azendohsauridae (new)

DEFINITION: The most inclusive clade containing *Azendohsaurus madagaskarensis*, Flynn et al., 2010, but not *Trilophosaurus buettneri*, Case, 1928a, *Tanystropheus longobardicus* (Bassani, 1886), *Proterosuchus fergusi*, Broom, 1903, *Protorosaurus speneri* von Meyer, 1830, *Rhynchosaurus articeps* Owen, 1842, or *Passer domesticus* Linnaeus, 1758 (fig. 5).

DIAGNOSIS: A prominent anteroposteriorly oriented ridge is present on the medial surface of the maxilla (201-1); the dorsal apex of the maxilla is a separate, distinct process with a posteriorly concave margin (202-1); the crowns of the upper dentition are lower (i.e., apicobasally shorter) than those of the lower dentition (211-1).

REMARKS: Here we use Azendohsauridae to refer to *Azendohsaurus madagaskarensis*-like taxa from the Triassic. This stem-based definition specifies the most completely known taxon, *Azendohsaurus madagaskarensis*, to distinguish members of Archosauromorpha that are more closely related to *A. madagaskarensis* than to any other clade within Archosauromorpha (e.g., Trilophosauridae, Rhynchosauria) and thus the name would be applied regardless of whether the phylogenetic position of *Azendohsaurus madagaskarensis* would change in the future relative to various basal archosauromorphs.

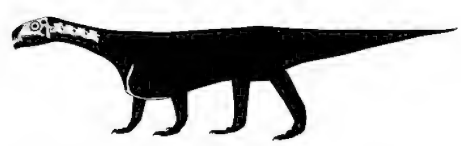

Fig. 6. Elements present in the holotype of *Azendohsaurus madagaskarensis* (UA 7-20-99-653).

Azendohsaurus Dutuit, 1972
Azendohsaurus madagaskarensis Flynn et al., 2010

HOLOTYPE: UA 7-20-99-653 (field number 7-20-99-653) (figs. 3–12), a nearly complete skull with associated vertebrae (fig. 6).

PARATYPES: FMNH PR 2751 (field number 8-30-98-376), nearly complete disarticulated skull (associated with postcranial specimens, FMNH PR 2788, FMNH PR 2789, FMNH PR 2792 and possibly FMNH PR 2796).

REFERRED MATERIAL: See appendix 1.

LOCALITY: Basal Isalo IIof Besairie (1972), termed the Makay Formation by Razafimbelo (1987); drainage of the Malio River, Morondava Basin, southwestern Madagascar (fig. 2). Locality details are on file at the AMNH and FMNH. Cynodonts (*Dadadon isaloi*, Flynn et al., 2000; *Menadon besairiei*, Flynn et al., 2000; *Chiniquodon kalanoro*, Kammerer et al., 2010), rhynchosaurs (*Isalorhynchus genovefae* Buffetaut, 1983, Whatley, 2005), a kannemeyeriifrom dicynodont (Flynn et al., 1999), an enigmatic archosaur (Nesbitt et al., unpublished data) and dinosauromorphs (Kammerer et al., unpublished data) occur in the Makay Formation within a 10 km radius of the *Azendohsaurus* producing locality. The stratigraphic relationships among these localities are not well

understood because most outcrops are isolated and difficult to trace.

Revised Diagnosis (see also Flynn et al., 2010): *Azendohsaurus madagaskarensis* is a medium-sized (2–3 m in length), early-diverging archosauromorph with large palatal teeth, a pineal foramen, and lanceolate, or leaf-shaped, teeth. Based solely on the holotype, *Azendohsaurus madagaskarensis* differs from all other archosauromorphs in possessing a unique combination of character states, including: ventral curvature of the anterior portion of the dentary; a robust dorsal process of the maxilla, the base of which occurs on the anterior third of the bone; a concave anterior margin of the dorsal process of the maxilla; lanceolate teeth with denticles; a series of small nutrient foramina on the medial surface of the maxilla; elongated cervical vertebrae with small epipophyses dorsal to the postzygapophyses (unknown in *A. laaroussii*); and a posteriorly expanded, T-shaped interclavicle (unknown in *A. laaroussii*).

Azendohsaurus madagaskarensis is distinguished from *Azendohsaurus laaroussii* by a lower maxillary tooth count (11–13, vs. 15–16 for the Moroccan form); apicobasally longer teeth in both maxillae and dentaries; more densely packed serrations in both maxillary and dentary teeth (fig. 7), the absence of a mediolateral swelling at the base of the dentary teeth (fig. 7); and a prominent longitudinal keel on the medial surface of the maxilla present only on the posterior half of the maxilla, as opposed to occurrence along its entire length in *A. laaroussii*.

Furthermore, we have identified seven additional possible autapomorphies present in the postcranial elements now referred to *Azendohsaurus madagaskarensis* (see figures in the description). These include: (1) a small tuber located on the ventrolateral surface of the prezygapophyseal stalk in the middle to posterior cervical vertebrae; (2) a well-defined fossa at the base of the neural spine, just posterior to the prezygapophyses in the second sacral vertebra; (3) the lateral side of the calcaneal tuber expanded laterally and ventrally, with the ventral expansion being clearly visible in proximal view; (4) deep fossae between well-developed laminae in the posterior cervical vertebrae (autapomorphy among non-archosaurian archosauromorphs, but these structures are found in some crown-group archosaurs and *Aenigmastropheus parrintoni* [Ezcurra et al., 2014]); (5) hyposphene-hypantra intervertebral articulations in the posterior cervical, anterior trunk, and sacral vertebrae (autapomorphy among non-archosaurian archosauromorphs, but these structures are found in some crown-group archosaurs); (6) proximal projection on the proximal surface of metatarsal IV; and (7) an oval and proximodistally oriented tuber on the lateral surface of the scapula that nearly contacts the edge of the glenoid fossa.

DESCRIPTION

Axial Skeleton

Vertebral Column: A complete vertebral column is not available from any single individual of *Azendohsaurus madagaskarensis*. Instead, we present a composite axial column (fig. 8) assembled from short, articulated sections of vertebrae, associated (but not articulated) vertebrae from several individual specimens, and isolated vertebrae found throughout the monospecific bone bed. For example, FMNH PR 2751 and UA 7-20-99-653 both preserve the anterior cervical series, including the atlas and axis—in addition to nearly complete skulls (Flynn et al., 2010).

Full descriptions of the intracolumnar variation of the vertebrae are presented below, but a few general introductory comments about the vertebral column of *Azendohsaurus madagaskarensis* are warranted. The neck of *A. madagaskarensis* is long, as in "protorosaurs" (e.g., *Macrocnemus bassanii*, *Prolacerta broomi*, *Protorosaurus speneri*) and in sauropodomorph dinosaurs (e.g., *Plateosaurus engelhardti*), poposauroids (e.g., *Xilousuchus sapingensis*), and early neotheropods (*Coelophysis bauri*). The cervical vertebrae immediately posterior to the axis are the longest, maintaining a similar length from the third through fifth cervical elements. Vertebrae become progressively shorter posteriorly, with this trend continuing to the pelvis. The anterior articular facets of the anterior cervical vertebrae are elevated

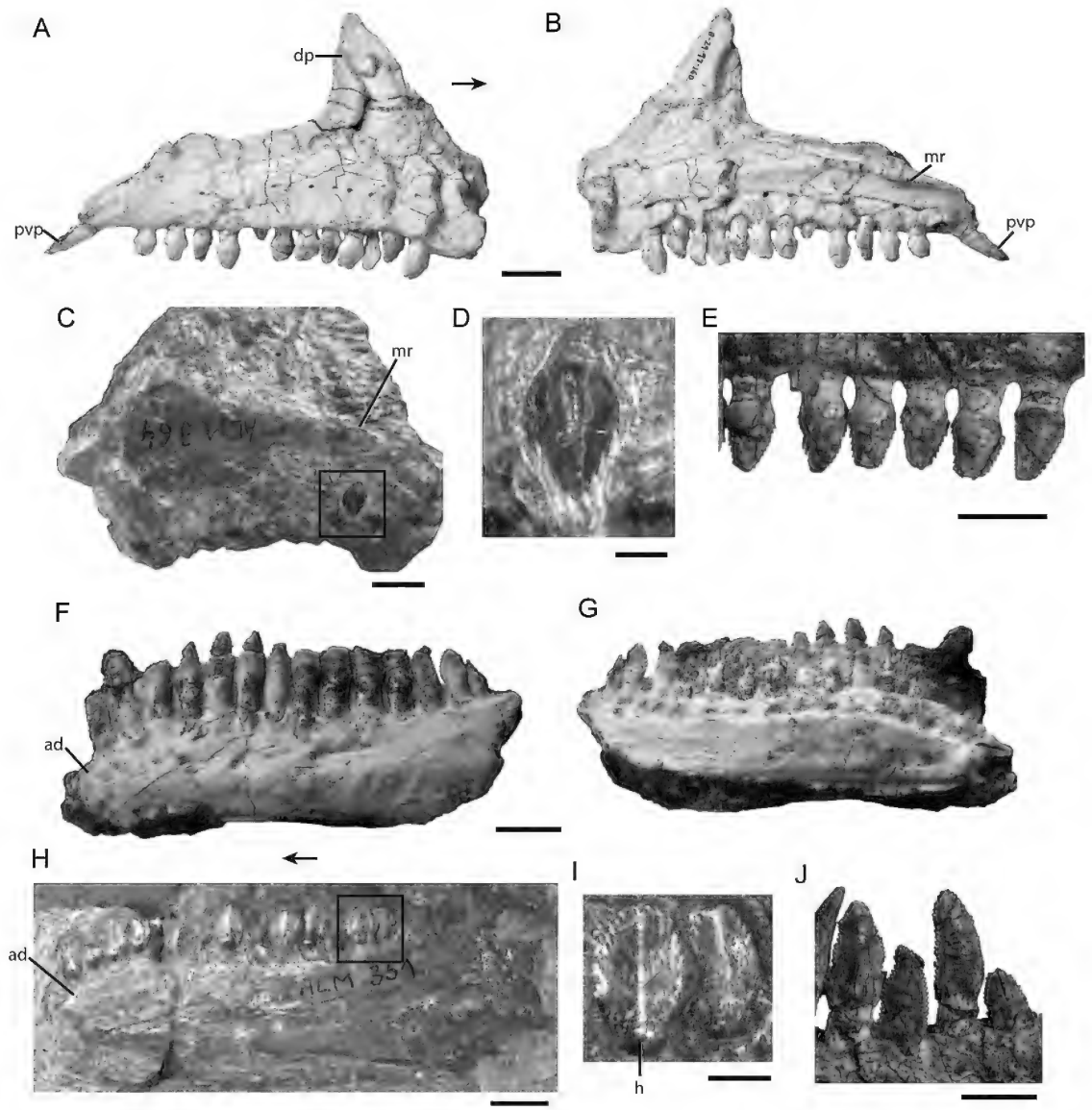

Fig. 7. Comparison between the tooth-bearing elements and teeth of *Azendohsaurus madagaskarensis* (**A–B**, **E–G**, **J**) and *Azendohsaurus laaroussii* (**C–D**, **H–I**). Right maxilla of *A. madagaskarensis* (FMNH PR 2756) in (**A**) lateral and (**B**) medial views. Left maxilla of *A. laaroussii* (MNHN-ALM 364) in (**C**) medial view with a close up of a posterior maxillary tooth in (**D**) medial view. Middle to posterior maxillary teeth of *A. madagaskarensis* (FMNH PR 2751) in (**E**) lateral view. Left dentary of *A. madagaskarensis* (unnumbered) in (**F**) lateral and (**G**) medial views. Left dentary of *A. laaroussii* (MNHN-ALM 351) in (**H**) lateral view with a close-up of a posterior dentary teeth in **I**, lateral view. Middle dentary teeth of *A. madagaskarensis* (FMNH PR 2751) in **J**, lateral view. Scales = 1 cm in **A–C**, **E–H**, **I**; scales = 5 mm in **D**, **I**. Arrows indicate anterior direction. Abbreviations: **ad,** anteroventral deflection; **dp,** dorsal process; **h,** heel; **mr,** medial ridge; **pvp,** posteroventral process.

dorsally relative to their corresponding posterior articular facets, indicating that the head and neck were raised above the level of the trunk vertebrae.

The shape and height of the neural spines of *Azendohsaurus madagaskarensis* are highly variable throughout the axial vertebral column. The neural spines of the anterior

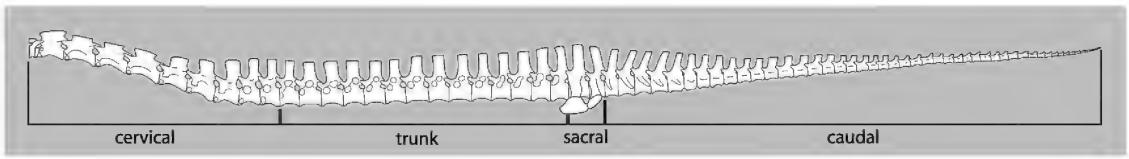

Fig. 8. The reconstructed vertebral column of *Azendohsaurus madagaskarensis*.

cervical vertebrae are anteroposteriorly long and low, whereas they are anteroposteriorly short and tall on the posterior cervical vertebrae (presacral vertebrae 7–9). Neural spines of the posterior trunk vertebrae (= dorsals) are inclined anterodorsally, whereas they slant posterodorsally on the anterior caudal vertebrae (fig. 8). All other neural spines are nearly vertically oriented. All centra are amphicoelous. Amphicoely is common among early archosauromorphs (e.g., Gottmann-Quesada and Sander, 2009; Gow, 1975), with procoely occurring in *Trilophosaurus buettneri* (TMM 31025-140) and a subclade of Tanystropheidae (Olsen, 1979; Pritchard et al., 2015).

The number of vertebrae in each region of the axial column is difficult to estimate because of gaps in the articulated series of vertebrae throughout the column. We estimate 24 presacral vertebrae based on gradual transitions of centrum length, positions of diapophyses and parapophyses, and the sizes and shapes of the corresponding prezygapophyses and postzygapophyses. Two sacral vertebrae are present, based on the morphology of the sacral ribs and the two sacral rib scars on the medial side of the ilium (see below). The number of caudal vertebrae is the most uncertain. Nevertheless, the tail of *Azendohsaurus madagaskarensis* appears short compared to those of other early archosauromorphs with preserved caudal series, such as *Langobardisaurus pandolfii*, *Protorosaurus speneri*, and *Trilophosaurus buettneri*. We estimate the caudal vertebral count to be between 45 and 55, with centra decreasing in length distally.

Postaxial vertebral intercentra do not occur in *Azendohsaurus madagaskarensis*, based on three lines of evidence. First, no intercentra have been found between any of the articulated segments of presacral vertebrae. Second, the ventral edges of the anterior and posterior articular faces of the presacral centra are not beveled to any degree, leaving no room for intercentra. Third, no isolated postaxial intercentra have been recovered from the extensive, multi-individual, monospecific bone bed. Postaxial intercentra also are absent in Tanystropheidae (see Pritchard et al., 2015) and Archosauria (Nesbitt, 2011).

Vertebrae of *A. madagaskarensis* vary in size by roughly 25% across individuals in the sample. In all instances, however, the neural arch is completely fused to the centrum and no suture between the two vertebral components is apparent. It should be noted that neurocentral fusion occurs early in ontogeny in some other early archosauromorphs (see Nosotti, 2007). In some cases, a slightly raised rim demarks the contact between the neural arch and the centrum, but, even in those vertebrae, the suture is completely obliterated. Thus, given the size variation, in spite of fusion without evidence of a suture, *A. madagaskarensis* continued to grow after the neural arch and centrum had fused (see below).

Cervical Vertebrae: The complete atlas and axis are best preserved as disarticulated elements in the holotype UA 7-20-99-653 (fig. 9A–D) and as partial specimens in FMNH PR 3823 (fig. 9E–F) and FMNH PR 3818. Originally in articulation, the atlas and axis of UA 7-20-99-653 were partially disarticulated for study, whereas in FMNH PR 3823 these elements remain articulated, but are missing the atlantal neural arch and proatlas. The atlas of *A. madagaskarensis* consists of six elements: paired proatlantes, paired neural arches, the atlantal centrum (fused to the axial intercentrum), and the atlantal intercentrum. The left proatlas lies on the dorsal surface of the neural arch of the atlas whereas the right element lies within the foramen magnum of the skull of specimen UA 7-20-99-653 (labeled "pa" in Flynn et al., 2010: fig. 2). The dorsoventrally compressed,

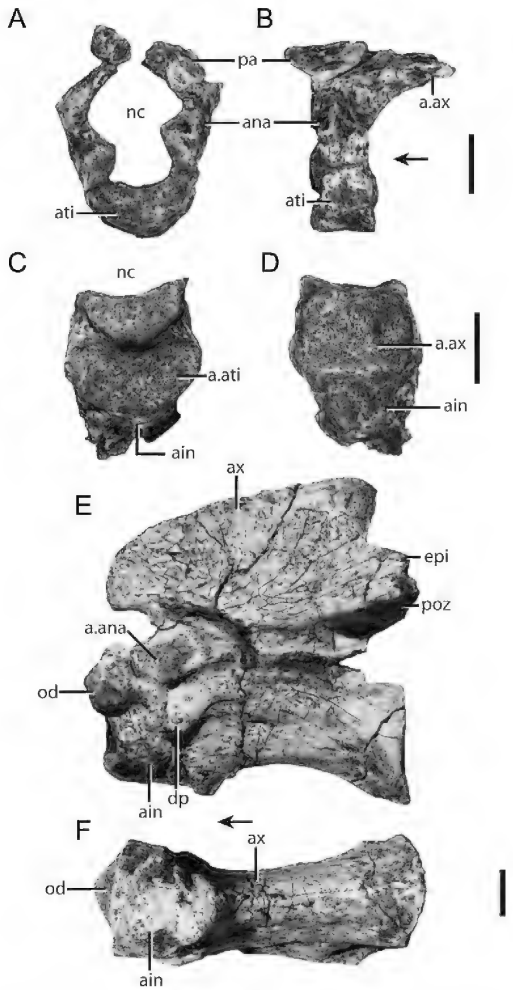

Fig. 9. Atlas and axis of *Azendohsaurus madagaskarensis*. Atlas (UA 7-20-99-653) in (**A**) anterior and (**B**) left lateral view. Odontoid process and axis intercentrum (UA 7-20-99-653) in (**C**) anterior and (**D**) posterior views. Articulated odontoid, axis intercentrum, and axis (FMNH PR 3823) in (**E**) left lateral and (**F**) ventral views. Scales = 1 cm. Arrows indicate anterior direction. Abbreviations: **a.,** articulates with; **ain,** axis intercentrum; **ana,** atlas neural arch; **ati,** atlas intercentrum; **ax,** axis; **dp,** diapophysis; **epi,** epipophysis; **nc,** neural canal; **od,** odontoid; **pa,** proatlas; **poz,** postzygapophysis.

oval proatlas is similar to that in other archosauromorphs, such as *Trilophosaurus buettneri* (TMM 31025-140) and the crocodylomorph *Hesperosuchus agilis* (Colbert, 1952). Proatlas elements are present in a variety of diapsids as either paired elements that lack bone-to-bone articulations (e.g., *Sphenodon*) or as fused bones (e.g., crocodylians) (Romer, 1956), but these are rarely preserved. The left atlantal neural arch of UA 7-20-99-653 appears complete, and includes a prominent, winglike posterior expansion at its dorsal end. In articulation, this posterior process lies on the anterolateral surface of the neural arch of the atlas, a condition widespread in reptiles (e.g., Reisz, 1981; Broili and Schroeder, 1934). A thin ridge lies on the dorsal surface of the posterior process and terminates in a point posteriorly. Medially the atlantal neural arches are dorsoventrally thin, failing to meet at the midline in UA 7-20-99-653. The atlantal intercentrum, a prominent crescent-shaped structure in anterior view, articulates with the ventral surfaces of the two neural arches, and posteriorly with the atlantal centrum. The anterior surfaces of the atlantal intercentrum and the two neural spine elements form a hemispherical concavity for articulation with the occipital condyle. The convex posterior surface of the atlantal intercentrum mirrors a concave surface of the axial centrum just ventral to the odontoid process. No rib attachments occur on the lateral or ventral surfaces of the intercentrum of the atlas, but the presence of ribs attaching elsewhere cannot be ruled out (see below).

The anteroposteriorly foreshortened atlantal centrum is tall and almost completely fused to the intercentrum of the axis (fig. 10), as in *Trilophosaurus buettneri* (TMM 31025-140). Unfused odontoid complexes occur in *Mesosuchus browni* (Dilkes, 1998), *Proterosuchus fergusi* (Broili and Schröder, 1934), and *Tanystropheus longobardicus* (Wild, 1973). The anterior surface of the bone in *A. madagaskarensis* is complex, with a mediolaterally expanded crescent-shaped odontoid process at its dorsal half overlying a crescent-shaped concavity that articulates with the atlantal intercentrum. The odontoid process of *A. madagaskarensis* is relatively wider than that of *Trilophosaurus buettneri* (TMM 31025-140). The posterior face of the atlantal centrum of *A. madagaskarensis* forms an ovoid concavity that is taller than wide, articulating with the convex anterior surface of the centrum of the axis. The presence of a rib fragment ventrolateral to the atlantal centrum on the right side suggests that an

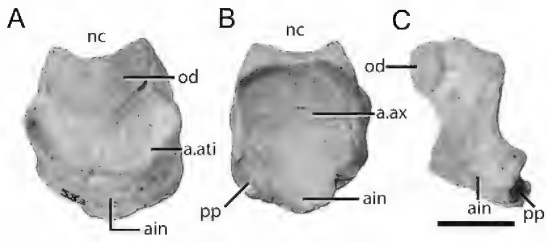

Fig. 10. The fused odontoid and axis intercentrum of *Azendohsaurus madagaskarensis* (FMNH PR 3818) in (**A**) anterior, (**B**) posterior, and (**C**) left lateral views. Scale = 1 cm. Abbreviations: **a.,** articulates with; **ain,** axis intercentrum; **ati,** atlas intercentrum; **ax,** axis; **nc,** neural canal; **od,** odontoid; **pp,** parapophysis.

atlantal rib was present, despite the lack of a clear rib facet on the centrum.

The axis is preserved in the holotype, UA 7-20-99-653, as part of an articulated series (fig. 11), and in FMNH PR 3823 (fig. 9E–F) and FMNH PR 3818. All three axes preserve the axis intercentrum, which contacts the anteroventral surface of the axial centrum. This wedge-shaped element is partially fused to the atlas centrum in UA 7-20-99-653 and FMNH PR 3823, but completely fused in FMNH PR 3818 without any remnants of a suture (fig. 10). In all three specimens, the axis intercentrum remains independent of the centrum. The dorsal extent of the axis intercentrum reaches the ventral extent of the axial diapophysis. The axis parapophysis lies entirely on the axis intercentrum, an arrangement best seen in FMNH PR 3818 (fig. 12). The facets of the parapophysis are directed posteriorly at the ventral edge of the lateral sides of the axis intercentrum.

The broad subrectangular neural spine of the main body of the axis is just over twice as long anteroposteriorly as it is tall. The neural spine inclines slightly posterodorsally and the posterior termination is expanded slightly transversely. The dorsal margin of the axial neural spine is inclined posterodorsally in *Proterosuchus alexanderi* (NMQR 1484; Broili and Schröder, 1934), *Protorosaurus speneri* (Gottmann-Quesada and Sander, 2009), and *Trilophosaurus buettneri* (TMM 31025-140). It is inclined anterodorsally in tanystropheids (e.g., *Macrocnemus bassanii* [MCSN V 457], *Tanystropheus longobardicus* [PIMUZ T/2819)]).

The anterior aspect of the axial neural spine differs in the three *Azendohsaurus* specimens, but the anterior end overhangs the rest of the axis in all of them; in UA 7-20-99-653, the anterior end tapers to a point dorsally, whereas in FMNH PR 3823 and FMNH PR 3818 the anterior edge is rounded (fig. 12). The posterior edge of the neural spine also differs among the three specimens; the posterior surface exhibits a midline groove in UA 7-20-99-653 and FMNH PR 3818, whereas in FMNH PR 3823 a thin vertical ridge occurs on the midline.

The anteriorly short, semicircular prezygapophyses face dorsolaterally, articulating with the neural arches of the atlas. A slight ridge connecting the lateral edge of the prezygapophysis with the anterior extent of the postzygapophysis (= interzygapophyseal lamina sensu Wilson, 1999) occurs in all three specimens, but is most prominent in the largest (FMNH PR 3823). The flat articular surfaces of the postzygapophyses are deflected dorsally about 20° from horizontal in posterior view. Laminae extending from near the dorsal surface of the neural spine to the dorsal margin of the postzygapophyses, and a thinner one between the postzygapophyses, frame a deep, triangular, and posteriorly facing fossa at the midline of the neural arch. Epipophyses lie on the dorsal surface of the postzygapophyses but do not extend posteriorly to the articular surface of the postzygapophyses. Similar small projections occur in a variety of early archosauromorphs, including *Mesosuchus browni* (SAM-PK-5882), tanystropheids (e.g., Wild, 1973; Pritchard et al., 2015), *Teraterpeton hrynewichorum* (Sues, 2003), *Trilophosaurus buettneri* (TMM 31025-140), and *Spinosuchus caseanus* (Spielmann et al., 2009). The postzygapophyses extend about 30° laterally from the midline whereas the postzygapophyses of *T. buettneri* (TMM 31025-140) project 45° laterally from the midline. The neural canal is circular in both anterior and posterior views.

The gently convex anterior surface of the axis centrum is subtriangular and pointed ventrally in anterior view. The slightly ventrally directed anterior articular surface of the centrum is convex in UA 7-20-99-653, whereas the ventral half of the anterior face is

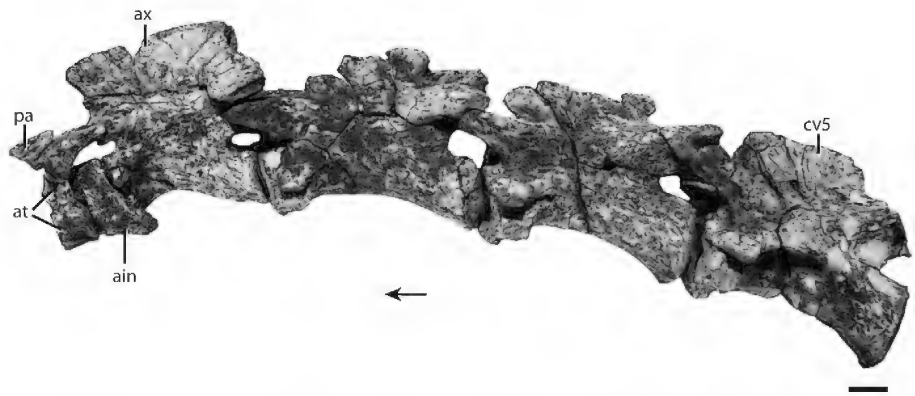

Fig. 11. Articulated cervical vertebrae of *Azendohsaurus madagaskarensis* (UA 7-20-99-653) in lateral view. Scale = 1 cm. Arrow indicates anterior direction. Abbreviations: **ain,** axis intercentrum; **at,** atlas; **ax,** axis; **cv5,** cervical vertebra 5, **pa,** proatlas.

concave in FMNH PR 3818. In lateral view, the axis centrum is parallelogram shaped, with the anterior articular surface elevated dorsally relative to the posterior articulation, suggesting a curved neck in life. A similar parallelogram-shaped axis is present in *Trilophosaurus buettneri* (Gregory, 1945) and, to a lesser degree, in other archosauromorphs with elongated necks (e.g., *Macrocnemus bassanii*, MCSN V 457; *Prolacerta broomi*, BP/1 2675, UCMP 37151; Gow, 1975). In *Azendohsaurus madagaskarensis,* the diapophysis is poorly developed and anteriorly bordered by the atlas centrum. A fossa is located ventral to the diapophysis, but this fossa shallows posteriorly anterior to the anteroposterior midpoint of the centrum. The posterior articular surface of the centrum is deeply concave, to a degree unmatched throughout the rest of the vertebral column. In contrast, this surface is convex in *Trilophosaurus buettneri* (Gregory, 1945) and slightly concave in a South American rhynchosaur (MCZ 1529). The ventral surface of the centrum bears a distinct ventral keel at the midline in all three preserved *Azendohsaurus* axes. In UA 7-20-99-653 and FMNH PR 3818 the keel extends along the entire length of the centrum, whereas in FMNH PR 3823 it is highly incomplete. The ventral keel of FMNH PR 3818 is much more ventrally expanded than in the other specimens (fig. 12).

The **anterior cervical vertebrae** of *A. madagaskarensis* occur in articulation in the holotype (UA 7-20-99-653; fig. 11) and in one larger individual (FMNH PR 2788); they are also known from disarticulated examples throughout the quarry (e.g., FMNH PR 2791; fig. 13). The anterior cervical vertebrae are elongated relative to the mid- to posterior dorsal vertebrae (fig. 8). The axis of UA 7-20-99-653 is considerably shorter than the third through fifth cervical vertebrae, which are all similar in length. A similar pattern occurs in *Macrocnemus bassanii* (MCSN V 457), *Prolacerta broomi* (UCMP 37151), and *Trilophosaurus buettneri* (TMM 31025-140). In *Tanystropheus longobardicus*, vertebrae lengthen from the axis to the eighth or ninth cervical vertebra (MCSN BES 1018; Wild, 1973), before shortening to the ultimate (13th) cervical vertebra (Rieppel et al., 2010).

The anterior cervical neural spines of *A. madagaskarensis* are about twice as long (anteroposteriorly) as tall (dorsoventrally). Similarly low anterior cervical neural spines occur in *Langobardisaurus pandolfii* (MCSNB 2883), *Macrocnemus fuyuanensis* (MCSN V 457; Jiang et al., 2011), and *Prolacerta broomi* (UCMP 37151; Gow, 1975). In *A. madagaskarensis*, the anterior cervical neural spines are transversely compressed into thin blades, resembling those in *Prolacerta broomi* (UCMP 37151) and *Trilophosaurus buettneri* (TMM 31025-140). The anterodorsal portion of the neural spine overhangs the base of the neural spine in some anterior cervical vertebrae (e.g., the fourth cervical of UA 7-20-99-653; fig. 11) whereas the anterior edge of the

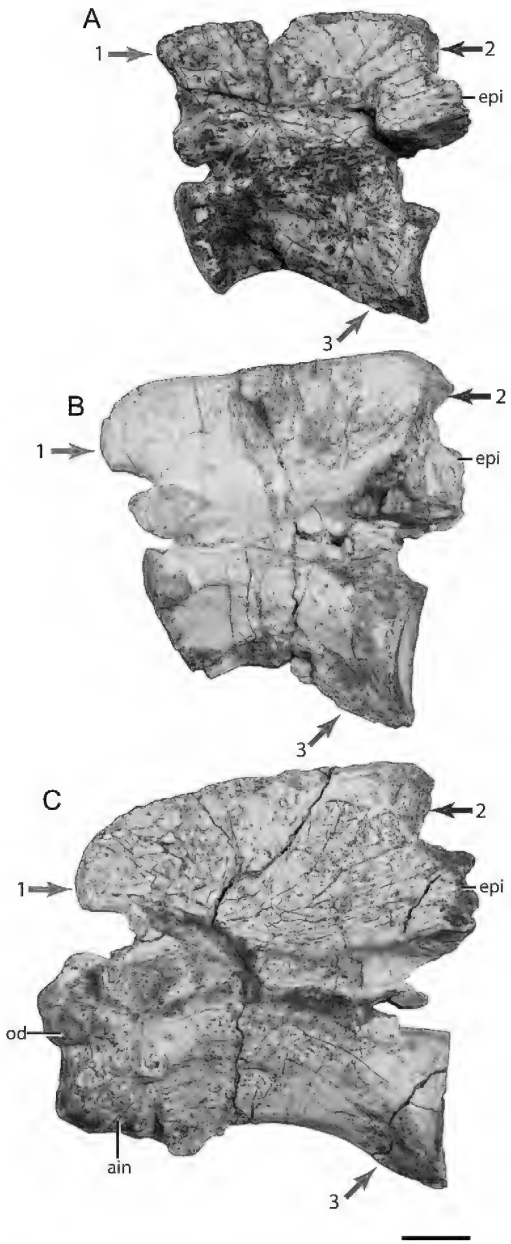

Fig. 12. Variation in the axis of *Azendohsaurus madagaskarensis*. Axis of the (**A**) holotype (UA 7-20-99-653) in left lateral view, (**B**) FMNH PR 3818 in left lateral view, and (**C**) FMNH PR 3823 in left lateral view. The **1** arrows highlight variation of the anterior portion of neural spine. The **2** arrows highlight variation of the posterior edge of the neural spine. The **3** arrows highlight variation of the ventral keel. Scale = 1 cm. Abbreviations: **ain,** axis intercentrum; **epi,** epipophysis; **od,** odontoid.

neural spine is vertical in a much larger anterior cervical vertebra (FMNH PR 2791; fig. 13). The orientation of the posterior edge of the neural spine also varies; the posterodorsal corner of the neural spine in the fourth cervical vertebra of UA 7-20-99-653 overhangs the base of the neural spine, whereas the posterior edge of the neural spine is vertical in the fifth cervical vertebra in this specimen and in the larger FMNH PR 2791. The neural spines of the anterior cervicals consistently overhang the anterior margins of their bases in tanystropheids (Peyer, 1937; Wild, 1973; Dilkes, 1998; Pritchard et al., 2015) and in *Prolacerta broomi* (BP/1/2675).

The neural arches of the anterior cervical vertebrae bear well developed pre- and postzygapophyses that extend horizontally in lateral view; the articular facets are angled 30° (medially and laterally in the transverse plane, respectively). Shallow fossae occur at the base of the neural spine, between the prezygapophyses anteriorly and the postzygapophyses posteriorly. Similarly positioned but substantially deeper pits are known in some tanystropheids (Wild, 1973; Pritchard et al., 2015), and likely represent attachment sites for the interspinous ligaments. In dorsal view, the pre- and postzygapophyses project about 30° (medially and laterally in the transverse plane, respectively), but do not diverge anterolaterally to the degree seen in *Spinosuchus caseanus* (Spielmann et al., 2009) and *Trilophosaurus buettneri* (TMM 31885-140).

In the fourth cervical vertebra of UA 7-20-99-653, a small knob is located on the ventrolateral surface of the prezygapophyseal stalk; this feature is more prominently expressed in FMNH PR 2791 (fig. 13). Knobs are inconsistently present on the anterior cervical vertebrae. For example, the third and fifth cervical elements of the same specimen (UA 7-20-99-653) lack this structure. The knob is also present in other cervical vertebrae (see below) and may represent an autapomorphy of *A. madagaskarensis*. A ventrally deflected shelf (with respect to the midline) occurs between the postzygapophyses of the third cervical vertebra of UA 7-20-99-653. This structure is distinct from the well-developed, mediolaterally horizontal shelf linking the medial

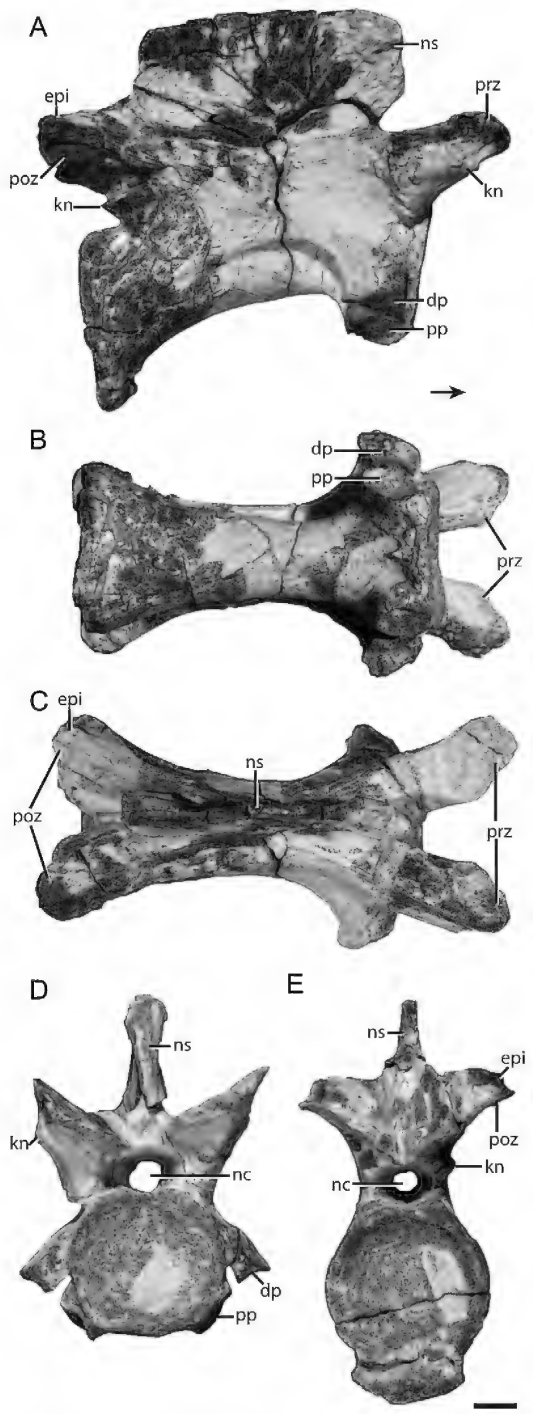

Fig. 13. Anterior cervical vertebra of *Azendohsaurus madagaskarensis* (FMNH PR 2791) in (**A**) right lateral, (**B**) ventral, (**C**) dorsal, (**D**) anterior, and (**E**) posterior views. Scale = 1 cm. Arrow indicates anterior direction. Abbreviations: **dp,** diapophysis; **epi,** epipophysis;**kn,** knob; **nc,** neural canal; **ns,** neural spine; **poz,** postzygapophysis; **pp,** parapophysis; **prz,** prezygapophyses.

margins of the postzygapophyses in the anterior cervical vertebrae of *T. buettneri* (TMM 31885-140) and *Spinosuchus caseanus* (Spielmann et al., 2009)—a possible synapomorphy of those two taxa (Spielmann et al., 2009; see below). Epipophyses occur dorsal to the postzygapophyses but fail to extend posteriorly beyond the articular surface of the postzygapophyses, resembling the conditions in *Langobardisaurus pandolfii* (MCSNB 2883), *Macrocnemus bassanii* (MCSN V 457), and in tanystropheid cervical vertebrae from the Hayden Quarry (GR 269). A slight extension of epipophyses beyond the level of the articular facet occurs in *Trilophosaurus buettneri* (TMM 31025-140), and an even greater extension occurs in species of *Tanystropheus* (MCSN BES SC 1018; Wild, 1973). A small ridge occurs medial to the postzygapophysis in FMNH PR 2791. Just anterior and ventral to the articular surface of the postzygapophysis in the anterior cervical of UA 7-20-99-653 lies a small notch, prominently seen in FMNH PR 2791 (fig. 13). A small ridge that projects posteriorly beyond the lateral wall of the neural canal frames the notch ventrally. Hyposphene-hypantrum intervertebral articulations are absent in the anterior cervical vertebrae. The neural canal is circular in both anterior and posterior views.

The centra of the third through fifth cervical vertebrae of *A. madagaskarensis* are three times longer than high (fig. 11), as in *Protorosaurus speneri* (Gottmann-Quesada and Sander, 2009) and *Trilophosaurus buettneri* (TMM 31025-140). Cervical centra are proportionally more elongate in Tanystropheidae (e.g., Wild, 1973; Pritchard et al., 2015), and proportionally shorter in both late-diverging rhynchosaurs (e.g., Montefeltro et al., 2013) and *Erythrosuchus africanus* (NHMUK R 3592; Gower, 2003). As with the axis, the cervical centra in *A. madagaskarensis* are parallelogram shaped, where the anterior articular surface is positioned dorsal to the posterior articular surface in lateral view. The anterior and posterior articular

surfaces of the cervical vertebrae are circular and concave. The diapophyses and parapophyses are situated on pedicles distinct from but located near the anterior rim of the centrum, as in most early archosauromorphs (e.g., Gow, 1975; Gregory, 1945). These articular surfaces are anteroposteriorly elongate and concave in *A. madagaskarensis*. The diapophyses and parapophyses very nearly contact each other in the anteriormost cervicals, but quickly diverge posteriorly in UA 7-20-99-653, as in archosauromorphs basal to *Erythrosuchus* (Gower, 2003). The diapophysis projects ventrolaterally and the parapophysis laterally. A dorsally convex crescentic fossa indents the centra laterally, originating between the diapophyses and parapophyses and arching posteriorly. The length and relative depth of these fossae increase posteriorly within the vertebral column, as seen in the articulated series of the holotype (UA 7-20-99-653). A weak midline keel occurs ventrally on the anterior cervicals, as in most early archosauromorphs (Pritchard et al., 2015).

A **midcervical vertebra**, possibly the fifth or sixth presacral vertebra, of *A. madagaskarensis* is represented in specimen UA 8-28-9-141 (fig. 14). This element is shorter than more anterior vertebrae, but longer than the more posterior cervicals, a pattern similar to *Trilophosaurus buettneri* (Gregory, 1945) and *Spinosuchus caseanus* (Spielmann et al., 2009). This contrasts with *Protorosaurus speneri* (Gottmann-Quesada and Sander, 2009) and Tanystropheidae (Peyer, 1937; Wild, 1973), wherein the midcervical centra are proportionally the longest.

In *A. madagaskarensis*, the neural spines of the midcervicals are shorter anteroposteriorly than those of the anterior cervicals. The neural spines are oval in cross section—the major axis of which is oriented anteroposteriorly—and their tips are slightly expanded transversely. They are canted slightly anteriorly, as in some of the more posterior cervical vertebrae (e.g., FMNH PR 3818). The anterior edge of the neural spine is flat, whereas a thin vertical ridge occurs along the midline posteriorly.

Deep, dorsally opening fossae are present at the base of the neural spine between the prezygapophyses and postzygapophyses. Similar fossae are seen in some archosauromorphs (e.g., *Erythrosuchus africanus*, Gower, 2001; *Prolacerta broomi*, BP/1/2675). A shallow fossa occurs between the base of the neural spine and the prezygapophyses, and a much deeper one between the base of the neural spine and the postzygapophyses. The articular facets are more inclined in the midcervical than in the anterior cervical vertebrae; the prezygapophyses and postzygapophyses are banked 45° to the horizontal plane. A knob similar to that seen in the anterior cervical vertebrae occurs on the lateral side of the prezygapophyses (fig. 14). Deep, anteriorly opening fossae are present lateral to the neural canal, just ventral to the articular facets of the prezygapophyses (fig. 14). Fossae of this kind have not been reported in any non-archosaurian archosauromorph to date, but do occur in theropod dinosaurs such as coelophysoids (e.g., AMNH FR 2701, cervical vertebra).

A distinct gap occurs between the prezygapophyses of the midcervicals of *A. madagaskarensis* (fig. 14), resembling the hypantra of saurischian dinosaurs and those of a variety of pseudosuchians (see Nesbitt, 2011). In support of the view that this feature represents a true hypantrum in *A. madagaskarensis*, a ventrally elongated lamina of bone resembling the hyposphene of saurischian dinosaurs is present between the postzygapophyses in the same midcervical vertebra. The *A. madagaskarensis* hypantrum clearly extends ventral to the articular facets of the postzygapophyses and its ventral surface is flush with the dorsal border of the neural canal. A hyposphene-hypantrum intervertebral articulation in *A. madagaskarensis*, restricted to the midcervical vertebrae, represents the first occurrence of this feature among non-archosauriform archosauromorphs. Epipophyses adorn the dorsal surface of the postzygapophyses but do not extend posterior to the articular surfaces. A rounded ridge separates the postzygapophyseal articular surface from a shallow, anteroventral fossa.

The centra of the midcervical vertebra in *A. madagaskarensis* are less parallelogram shaped than those of the anterior cervical vertebrae. The surface area of the anterior articular surface is larger than the posterior;

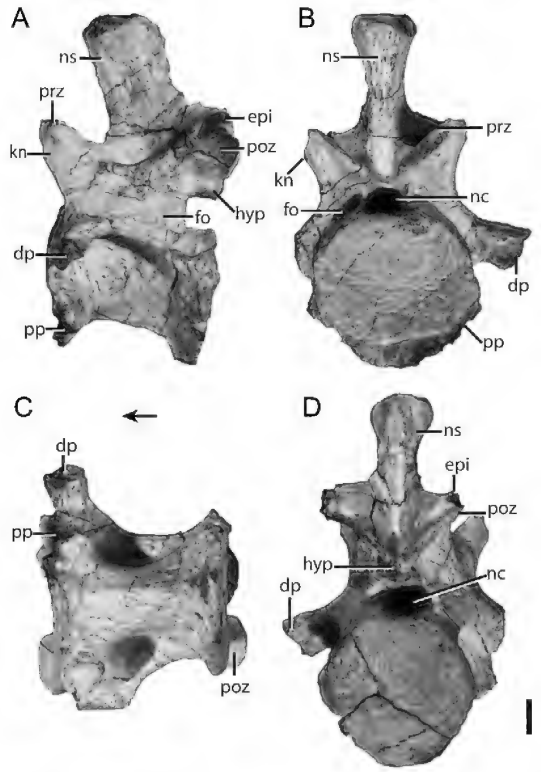

Fig. 14. Midcervical vertebra of *Azendohsaurus madagaskarensis* (UA 8-28-97-141) in (**A**) left lateral, (**B**) anterior, (**C**) ventral, and (**D**) posterior views. Scale = 1 cm. Arrow indicates anterior direction. Abbreviations: **dp,** diapophysis; **epi,** epipophysis; **hyp**, hyposphene; **kn,** knob; **nc,** neural canal; **ns,** neural spine; **poz,** postzygapophysis; **pp,** parapophysis; **prz,** prezygapophyses.

both are round. Shallow fossae ventral to the posterior diapophyseal laminae span the length of the centrum laterally. A fine, anterolaterally oriented lamina subdivides this fossa on one side (left) of UA 8-28-97-141. Similar laminae occur in a number of archosauriforms (Butler et al., 2012). The diapophysis projects ventrolaterally. Its concave articular surface is smaller than that of the parapophysis. The articular surface of the parapophysis lies on the lateral edge of the anterior articular surface of the centrum. The ventral surface of the centrum bears a midline keel that fails to meet the anterior margin of the centrum.

Two isolated **posterior cervical vertebrae** (UA 8-30-98-349; fig. 15; FMNH PR 3818; fig. 16) that likely correspond to the eight or ninth presacral vertebrae of *A. madagaskarensis* are well preserved. The neural spines, positioned on the posterior half of the centrum, are much more transversely expanded than those of the anterior cervical vertebrae, resulting in a subcircular cross section. The vertically oriented neural spine flares laterally at its dorsal end but does not form a distinct "spine table" as occurs in phytosaurs (e.g., Butler et al., 2012: fig. 7) and aetosaurs (e.g., *Desmatosuchus spurensis*, MNA V9300; Parker, 2008). The edges of the dorsal surface of the neural spine are distinctly convex. A midline ridge is present posteriorly, whereas the neural spine is concave anteriorly.

As on the midcervicals, the pre- and postzygapophyses of UA 8-30-98-349 are angled about 45° from horizontal (medially and laterally in the transverse plane, respectively) and, thus, are comparatively more steeply oriented than in the anterior cervical vertebrae. The pre- and postzygapophyses meet their counterparts at the midline at an acute angle. The dorsal tips of the articular surface of the pre- and postzygapophyses taper to a point; distinct epipophyses occur on the dorsal margin of the postzygapophyses. Rounded knobs lateral to the prezygapophyses are larger than those in more anterior elements of the vertebral column.

A complicated set of laminae (figs. 15, 16) connects the prezygapophyses, postzygapophyses, diapophyses, and parapophyses of the posterior cervical vertebrae, structures more typical of archosaurs than of basal saurians. Although laminae have been described in non-archosaurian archosauromorphs (Ezcurra et al., 2014), they are not present among all archosauromorphs. Three deep fossae (anterior, ventral, and posterior) occur at the base of the diapophysis. Employing the terminology of Wilson (1999), a paradiapophyseal lamina that joins the ventral surface of the diapophyses with the parapophysis together with a vertical centroprezygapophyseal lamina that connects the ventral portion of the prezygapophysis with the centrum frame a deep anterior fossa just lateral to the neural canal (fig. 16). The ventral fossa, the deepest of the three, is bordered anteriorly by the paradiapophyseal lamina and posteriorly by the centrodiapophyseal lamina that con-

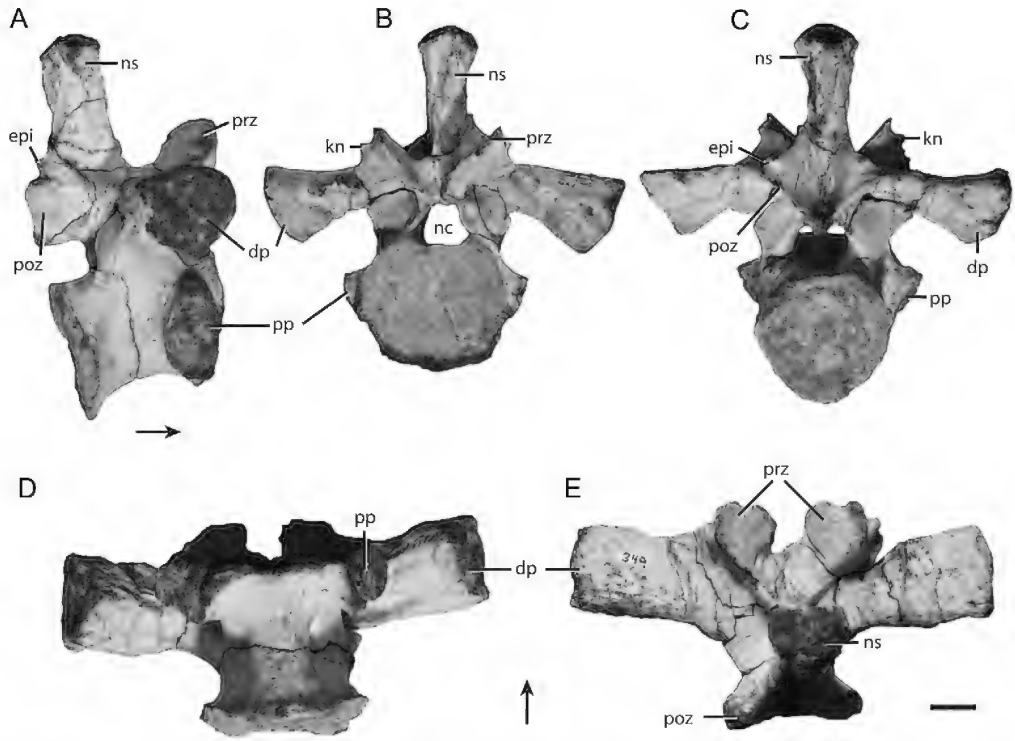

Fig. 15. Posterior cervical vertebra of *Azendohsaurus madagaskarensis* (UA 8-30-98-349) in (**A**) right lateral, (**B**) anterior, (**C**) posterior, (**D**) ventral, and (**E**) dorsal views. Scale = 1 cm. Arrows indicate anterior direction. Abbreviations: **dp,** diapophysis; **epi,** epipophysis; **kn,** knob; **nc,** neural canal; **ns,** neural spine; **poz,** postzygapophysis; **pp,** parapophysis; **prz,** prezygapophyses.

nects the ventral surface of the diapophyses with the posterior portion of the centrum. The fossa posterior to the diapophysis is roofed by the postzygodiapophyseal lamina, which extends from the posterior side of the diapophysis to the postzygapophysis. Similar, but less pronoumced laminae occur in *Trilophosaurus buettneri* and *Spinosuchus caseanus* (Spielmann et al., 2009). In *A. madagaskarensis*, the diapophyses, which are deflected ventrolaterally at their distal tips, expand laterally, making them club shaped. The articular surfaces are distinctly concave. The parapophysis arises from the anterior margin of the centrum and the major axis of its oval articular surface is vertically oriented.

The centrum is rectangular, lacking any vertical offset between the anterior and posterior surfaces. The anterior and posterior articular surfaces are round, the former much larger than the latter. No ventral beveling is present, in contrast to the condition in archosauromorphs with vertebral intercentra (e.g., *Proterosuchus alexanderi* [NMQR 1484], *Trilophosaurus buettneri* [TMM 31025-140]). A shallow fossa occurs laterally near the contact between the neural arch and the centrum. A ventral keel is absent.

TRUNK VERTEBRAE: Trunk vertebrae (= dorsals; presacral vertebrae ~11–24) of *A. madagaskarensis* are well represented in the Malio River bone bed, either in articulated series (e.g., FMNH PR 2789, fig. 17) or as isolated elements (e.g., FMNH PR 2779, fig. 18; UA 8-26-98-250, fig. 19).

The anterior trunk vertebrae are best represented by the spectacularly preserved FMNH PR 2779 (fig.18). The neural spine is mediolaterally compressed; its ventral base is about as long (anteroposteriorly) as the centrum, whereas its dorsal margin is one-third shorter, resulting in the anterior margin of the neural spine angled posterodorsally. The dorsal surface of the neural spine is unexpanded and dorsally convex in lateral

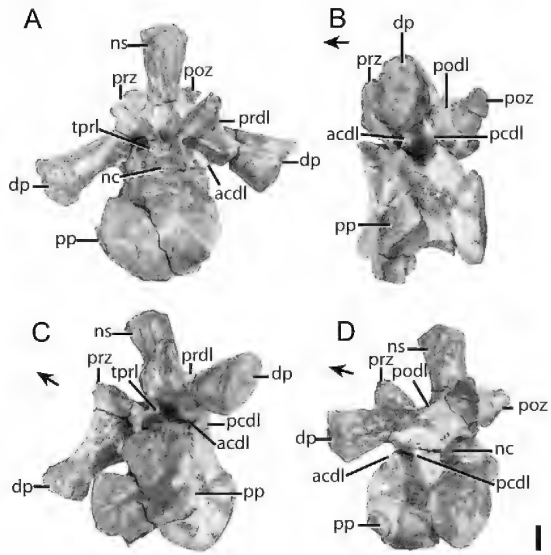

Fig. 16. Posterior cervical vertebra of *Azendohsaurus madagaskarensis* (FMNH PR 3818) in (**A**) anterior, (**B**) ventrolateral, (**C**) anteroventral, and (**D**) posterolateral views. Scale = 1 cm. Arrow indicates anterior directions. Abbreviations: **acdl,** anterior centrodiapophyseal lamina; **dp,** diapophysis; **hyp,** hyposphene; **nc,** neural canal; **ns,** neural spine; **pcdl,** posterior centrodiapophyseal lamina; **podl,** postzygadiapophyseal lamina; **poz,** postzygapophysis; **pp,** parapophysis; **prdl,** prezygadiapophyseal lamina; **prz,** prezygapophyses; **tprl,** intraprezygapopohyseal lamina.

view. Posteriorly, the neural spine bifurcates ventrally into thin laminae that terminate at the dorsal margin of the postzygapophyses; these laminae and the postzygapophyses together frame a posteriorly oriented interspinous fossa at the midline. A similarly positioned, but substantially deeper fossa is known in some tanystropheids (Pritchard et al., 2015). No corresponding fossae occur at the bases of the neural arches between the prezygapophyses in the anterior trunk vertebrae—in contrast to the cervical vertebrae, where one is present. A ventrally deep fossa with mediolaterally oriented striations is present lateral to the base of the neural spine, immediately medial to the articular surface of the diapophysis. This structure is divided by a rounded ridge of bone from a second, more anterior fossa that sits lateral to the base of the neural spine (fig. 18E).

The articular surfaces of the pre- and postzygapophyses are deflected about 45° to the horizontal (medially and laterally in the transverse plane, respectively), as in the mid- and posterior cervical regions. Weakly developed hyposphene-hypantrum intervertebral articulations are present in FMNH PR 2779 (fig. 18). The hypantrum (fig. 18) exists as a small gap between the prezygapophyses; it is located roughly half the distance between the anterior ends of the prezygapophyses and the base of the neural spine. The hyposphene arises from a vertically oriented lamina at the midline between the postzygapophyses. This lamina reaches the posterior end of the postzygapophyses and roofs the neural canal.

The well-developed laminae between the diapophyses, parapophyses, neural arches, and centra of the anterior trunk vertebrae of *Azendohsaurus madagaskarensis* resemble those of its posterior cervical vertebrae, as well as the anterior trunk vertebrae of *Erythrosuchus africanus* (Gower, 2003), *Aenigmastropheus parrintoni* (Ezcurra et al., 2014), and certain archosaurs (e.g., paracrocodylomorphs, saurischians). The diapophysis and prezygapophysis are connected by the prezygadiapophyseal lamina, the parapophysis by the paradiapophyseal lamina, the posterior portion of the centrum by the posterior centrodiapophyseal lamina, and the postzygapophysis by the postzygapodiapophyseal lamina (fig. 18). As in the posterior cervical vertebrae, three well-defined

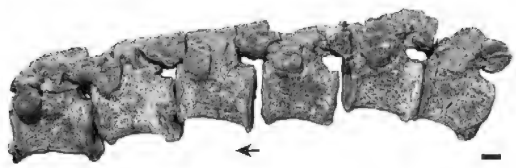

Fig. 17. Articulated trunk vertebrae of *Azendohsaurus madagaskarensis* (FMNH PR 2789) in lateral view. Scale = 1 cm. Arrow indicates anterior direction.

fossae are present among laminae radiating from the diapophysis, with the one ventral to the diapophysis the deepest. This fossa is clearly separated from the more ventrally located lateral centrum fossa. Smaller, shallow fossae lie within a fossa formed by the postzygapodiapophyseal and posterior centrodiapophyseal laminae. Compared to the trunk vertebrae of *Spinosuchus caseanus* (UMMP 7507), material referred to *Tanystropheus conspicuus* (Wild, 1973), and *Trilophosaurus buettneri* (TMM 31025-173 but now cataloged as FMNH PR 259), the vertebral laminae of *A. madagaskarensis* are better developed and, consequently, the fossae framed by them are much deeper. In *S. caseanus* and *T. buettneri,* the prezygadiapophyseal and postzygapodiapophyseal laminae are present, but given that the parapophysis is either absent or fused with the diapophysis, the paradiapophyseal and posterior centrodiapophyseal laminae are absent.

In *A. madagaskarensis*, the concave articular facets of the diapophysis and parapophysis are about the same size in the anterior trunk vertebrae. The diapophysis projects laterally and is inclined slightly dorsally, whereas the parapophysis projects directly laterally. The diapophysis sits ventral to the dorsal margin of the prezygapophysis.

In lateral view, the centra of the anterior trunk vertebrae are rectangular, their anterior and posterior articular facets are vertical, and the ventral margins are slightly concave. The circular anterior and posterior articular facets are both concave. A distinct lateral fossa is centered on the centrum below the neural arch. This feature is absent in the trunk vertebrae of *Trilophosaurus buettneri* (TMM 31025-173, now cataloged as FMNH PR 259).

Specimen UA 8-26-98-250 (fig. 19) represents a midtrunk vertebra from a much

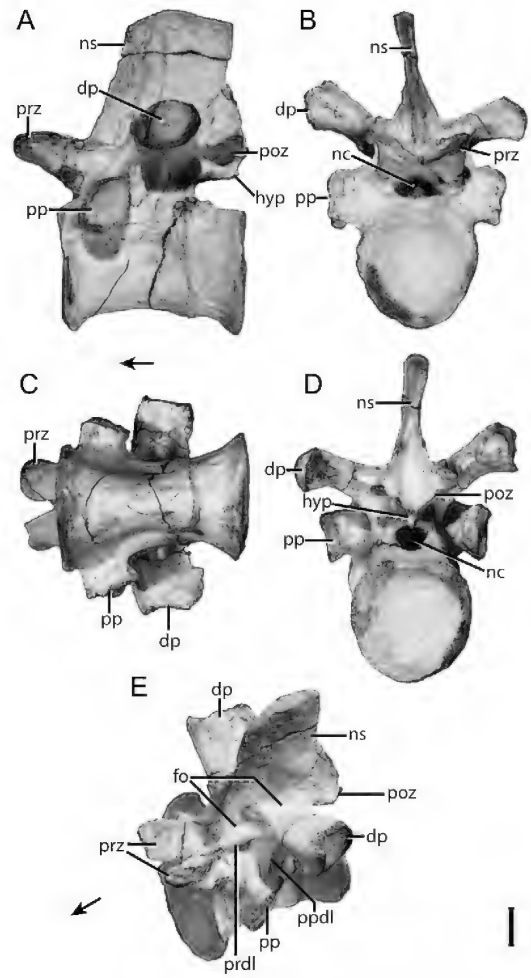

Fig. 18. Trunk vertebra of *Azendohsaurus madagaskarensis* (FMNH PR 2779) in (**A**) left lateral, (**B**) anterior, (**C**) ventral, (**D**) posterior, and (E) anterolateral views. Scale = 1 cm. Arrows indicate anterior direction. Abbreviations: **dp,** diapophysis; **fo,** fossa; **hyp,** hyposphene; **nc,** neural canal; **ns,** neural spine; **prdl,** prezygadiapophyseal lamina; **poz,** postzygapophysis; **pp,** parapophysis; **ppdl,** paradiapophyseal lamina; **prz,** prezygapophyses.

smaller individual than that represented by FMNH PR 2779. In general, the former element resembles the anterior trunk vertebrae, sharing the same set of laminae, fossae, and hyposphene-hypantrum intervertebral articulations. The midtrunk vertebrae (UA 8-26-98-250) differ from the anterior trunk vertebrae in having mediolaterally thicker neural spines and in lacking lateral fossae on the centra. The lack of lateral fossae in UA

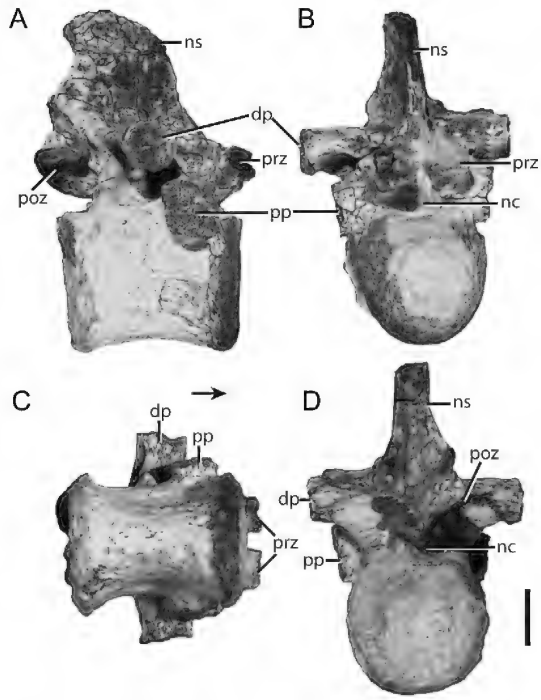

Fig. 19. Trunk vertebra of *Azendohsaurus madagaskarensis* (UA 8-26-98-250) in (**A**) right lateral, (**B**) anterior, (**C**) ventral, and (**D**) posterior views. Scale = 1 cm. Arrow indicates anterior direction. Abbreviations: **dp,** diapophysis; **nc,** neural canal; **ns,** neural spine; **poz,** postzygapophysis; **pp,** parapophysis; **prz,** prezygapophyses.

8-26-98-250 may simply reflect the small size of the specimen, given the presence of this feature in the midtrunk vertebrae of larger specimens of *A. madagaskarensis* (e.g., FMNH PR 2789).

The vertebral series of FMNH PR 2789 spans the midtrunk to posterior-trunk vertebral transition (fig. 19). Preservation of FMNH PR 2789 is poorer than that of FMNH PR 2779 (fig. 18), but most general features are nonetheless discernable throughout the series in the former specimen. A few incremental changes occur posteriorly. The diapophysis and parapophysis converge posteriorly in the trunk region; consequently the paradiapophyseal lamina shortens and eventually disappears as the diapophysis and the parapophysis merge into a single articular facet (fig. 20). A similar convergence of costal facets occurs in the trunk series of tanystropheids (Wild, 1973; Pritchard et al., 2015) and in early archosauriforms (Hughes, 1963; Gower, 2003), although the position within the column where this convergence occurs varies among those taxa. In *A. madagaskarensis*, the deep fossa framed by the paradiapophyseal and posterior centrodiapophyseal diminishes (and then disappears) posteriorly. Centra become less transversely "waisted" and shorter posteriorly (table 1). Because of preservation, it is unclear whether hyposphene-hypantrum intervertebral articulations occur in the middle to posterior trunk vertebrae.

The last trunk vertebra (FMNH PR 2780, fig. 21; FMNH PR 3822; fig. 22) was recovered in association with the first sacral vertebra. The former differs strikingly from other trunk vertebrae. The neural spine, which sits over the posterior half of the centrum, is oval in cross section, with an anteroposteriorly oriented major axis; its dorsal portion is expanded laterally. The pre- and postzygapophyses are slanted ~45° to the horizontal (medially and laterally in the transverse plane, respectively); no hyposphene-hypantrum intervertebral articulations are present. All vertebral laminae and nearly all the fossae surrounding the diapophysis are absent, apart from a shallow fossa ventral to the confluent diapophysis-parapophysis. The articular surfaces of the diapophysis-parapophysis are nearly vertical, with a slight posterodorsal cant; these surfaces are greatly reduced in area relative to their counterparts in the midtrunk vertebrae. In FMNH PR 2780 (fig. 21), a rib is partially fused to the diapophysis-parapophysis on both sides of the element. Fusion of ribs to their respective posterior trunk vertebrae creates a distinct lumbar region in *Langobardisaurus tonelloi* (MFSN 1921), *Proterosuchus fergusi* (Cruickshank, 1972), and *Tanytrachelos ahynis* (VMNH 120015).

The centrum of FMNH PR 2780 is the shortest within the presacral vertebral series. Its concave anterior and posterior articular facets are larger in surface area than in any other presacral vertebrae. The posterior articular facet of the centrum matches the anterior articular facet of the first sacral vertebra in size. The lateral edges of the anterior articular facet of the first sacral vertebra articulate against the laterally deflected edges of the

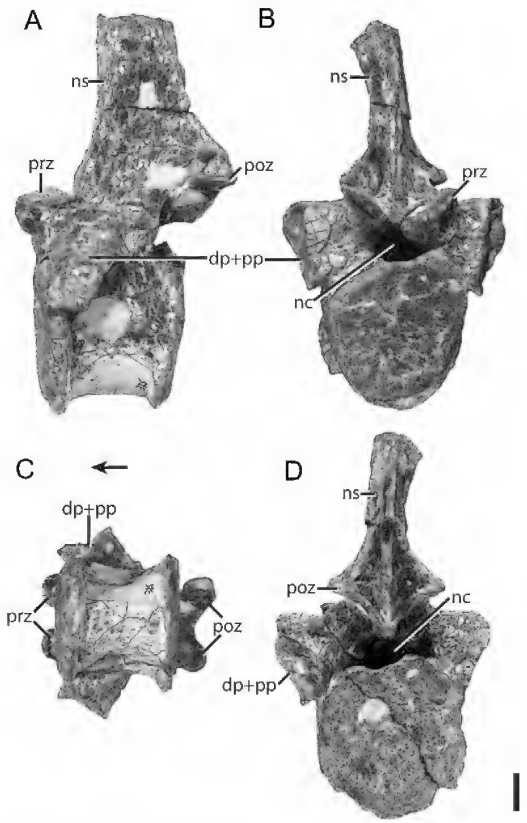

Fig. 20. Posterior trunk vertebra of *Azendohsaurus madagaskarensis* (UA 8-29-98-325) in (**A**) left lateral, (**B**) anterior, (**C**) ventral, and (**D**) posterior views. Scale = 1 cm. Arrow indicates anterior direction. Abbreviations: **dp+pp,** diapophysis and parapophysis; **nc,** neural canal; **ns,** neural spine; **poz,** postzygapophysis; **prz,** prezygapophyses.

posterior articular facet of the centrum of the last trunk vertebra. The centrum of FMNH PR 2780 bears a fossa located on the lateral side in the center of the body.

A second, much smaller, last trunk vertebra (FMNH PR 3822, fig. 22) was recovered in association with a first sacral vertebra. Apart from size, this vertebra exhibits only minor differences from FMNH PR 2780 (fig. 21). For example, the dorsal margin of the neural arch of FMNH PR 3822 is more expanded laterally and anteriorly. The prezygapophyses lie at a much lower angle (~10°–20°) to the horizontal (medially and laterally, respectively) than in FMNH PR 2780, a difference apparently unrelated to postmortem deformation. The ribs of

TABLE 1
Measurements of the articulated presacral vertebrae (in mm) of *Azendohsaurus madagaskarensis*
Abbreviation: est, estimated.

Specimen	Order in series	Anterior-posterior length
UA 7-20-99-653 (fig. 11)	axis	38
	presacral #3	52
	presacral #4	52
	presacral #5	52
FMNH PR 2788	presacral #3	60
	presacral #4	70
	presacral #5	75
FMNH PR 2784	presacral #6	50
	presacral #7	42
FMNH PR 2783	presacral #8	37
	presacral #9	34
	presacral #10	34 est
FMNH PR 2789 (fig. 17)	presacral A	40
	presacral B	39
	presacral C	36
	presacral D	33
	presacral E	33
	presacral F	31
	presacral G	32

FMNH PR 3822 are completely fused with the diapophysis + parapophysis, implying that this union occurred early in ontogeny. These ribs, although complete, are short (~10 mm) and project directly laterally.

SACRAL VERTEBRAE: All sacral vertebrae known from the *Azendohsaurus madagaskarensis* bone bed are disarticulated. Nevertheless, vertebrae from the sample that bear sacral ribs fall into two distinct morphological classes; this, coupled with the presence of a pair of sacral scars on the medial surface of the ilium (see below), suggests that *A. madagaskarensis* retained the plesiomorphic amniote and archosauromorph condition of having two sacral vertebrae. Although not found in articulation, first (FMNH PR 2780) and second (FMNH PR 2777) sacral vertebrae likely belong to the same individual, given their compatibility in size, proximity in the quarry, and precise correspondence of articulation surfaces when rearticulated (fig. 23). Other sacral vertebrae were recov-

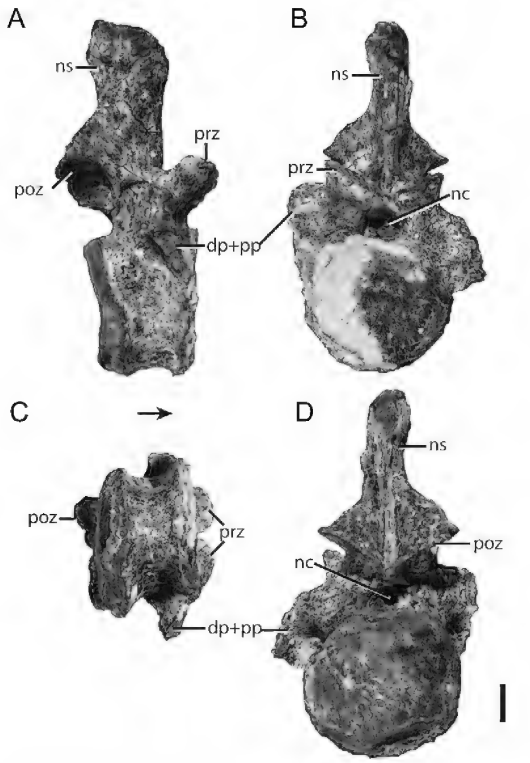

Fig. 21. Posteriormost trunk vertebra of *Azendohsaurus madagaskarensis* (FMNH PR 2780) in (**A**) right lateral, (**B**) anterior, (**C**) ventral, and (**D**) posterior views. Scale = 1 cm. Arrow indicates anterior direction. Abbreviations: **dp+pp,** diapophysis and parapophysis; **nc,** neural canal; **ns,** neural spine; **poz,** postzygapophysis; **prz,** prezygapophyses.

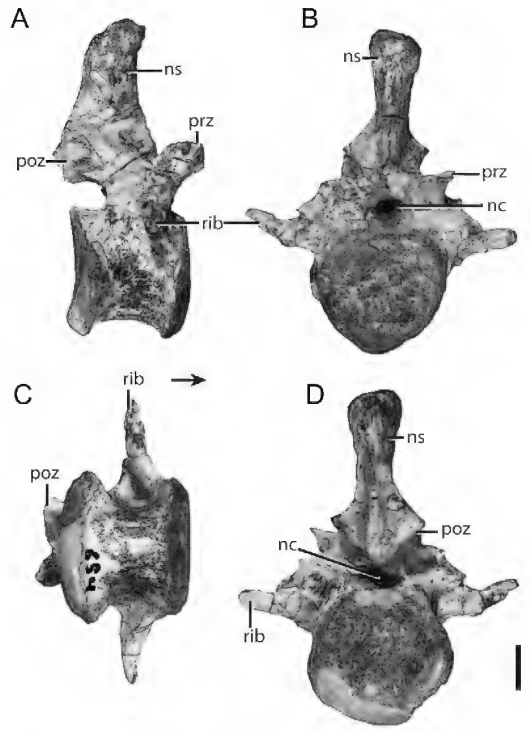

Fig. 22. Posteriormost trunk vertebra of *Azendohsaurus madagaskarensis* (FMNH PR 3822) in (**A**) right lateral, (**B**) anterior, (**C**) ventral, and (**D**) posterior views. Scale = 1 cm. Arrow indicates anterior direction. Abbreviations: **nc,** neural canal; **ns,** neural spine; **poz,** postzygapophysis; **prz,** prezygapophyses.

ered from the quarry (see appendix 1), but the following description centers principally on FMNH PR 2780 and FMNH PR 2777.

The first sacral vertebra (FMNH PR 2780, fig. 23A–C) is larger and more robust than the second. The anteroposteriorly short neural spine, transversely expanded at its dorsal margin, sits over the posterior half of the centrum. The prezygapophyseal facets in the first sacral are comparable in size to those in the posterior dorsal region, whereas the postzygapophyseal facets are roughly half the size of those of the posterior trunk vertebrae. The pre- and postzygapophyses are angled about 45° and 60° medially and laterally to the transverse plane, respectively. Ventrally, the postzygapophyses are ~5 mm apart; their articular surfaces are roughly level with the dorsal margin of the neural canal. By themselves, the ventral portions of the postzygapophyses do not appear to form a distinct hyposphene, but they fit into a well-defined gap in the second sacral vertebra when in articulation, which resembles a hypantrum.

The anterior articular surface of the centrum is much larger and more concave than in its posterior counterpart. The concavity of the anterior surface extends about one-third the length of the centrum. Ventrally, the centrum is flat and lacks the anteroposteriorly oriented groove present in *Trilophosaurus buettneri* (TMM 31025-140) and the ridge present in *Tanystropheus conspicuus* (Wild, 1973). The entire lateral surface of the centrum is fused with the first sacral rib.

The first sacral vertebra and rib lack a clear suture, but a raised area on the ventral

surface of the centrum marks the contact between the two elements. The main body of the first sacral rib is directed 30° ventrally from horizontal in the mediolateral direction (fig. 23). The posterior surface of the sacral rib bears a fossa whereas the anterior surface is slightly convex. The articulation surface of the first sacral rib is similar to that in certain early archosauriforms (e.g., *Erythrosuchus africanus*; Hughes, 1963) in that it is dorsoventrally much deeper than those of *Proterosaurus speneri* (Gottmann-Quesada and Sander, 2009), *Tanystropheus conspicuus* (Wild, 1973), or *Trilophosaurus buettneri* (TMM 31025-140). The articular surface of the first sacral rib indicates that the ilium was held nearly vertically. In lateral view, the articular surface is comma shaped, with the "tail" of the comma projecting anteriorly. A fossa occurs immediately dorsal to the "tail" of the articular surface; whether this fossa contacted the ilium is uncertain. The anterior portion of the articular surface extends well anterior of the centrum; its posterior edge bears a small platform for articulation with the anterior edge of the second sacral rib.

On the second sacral vertebra (FMNH PR 2777; fig. 23) a well-defined fossa marks the base of the neural spine immediately posterior of the prezygapophyses, a possible autapomorphy of *A. madagaskarensis*. The dorsal portion of the neural spine is incomplete in FMNH PR 2777 and in all other specimens. A pair of thin, paramedian, vertically oriented laminae lie on the anterior edge of the neural spine, terminating at the base of the articular surface of the prezygapophyses. The small prezygapophyses, angled ~55°, are separated medially by a large, median gap that accepts the hyposphene of the first sacral vertebra. The postzygapophyses are larger than the prezygapophyses and are deflected about 45° laterally in the mediolateral plane. The articular surfaces of the postzygapophyses are separated by ~5 mm medially. A deep, posterolaterally opening pit lies anterior to the articular surfaces of the postzygapophyses.

The concave anterior and posterior articular surfaces of the centrum of the second sacral vertebra are subequal in size. The centrum is transversely convex ventrally. The second sacral rib occupies the entire lateral portion of the centrum (fig. 23I). As in the first sacral rib, the second sacral rib is completely fused to the centrum with no sign of a suture. The second sacral rib extends laterally from the centrum and is inclined slightly ventrally. The dorsal surface of the sacral rib is nearly flat and tapers posteriorly at its lateral margin where it meets the posterior edge of the ilium. Fossae occur dorsolateral and lateral to the centrum on the anterior surface of the main body of the second sacral rib. Posteriorly, this rib is convex. Laterally, the second sacral rib expands anteroventrally; it ends anteriorly in a flat surface that articulates with the posterior edge of the second sacral vertebra. The iliac articular surface is irregularly rounded. The second sacral rib is not bifurcated laterally in *A. madagaskarensis* as the bifurcated form in *Langobardisaurus pandolfii* (MCSNB 2883), *Mesosuchus browni* (SAM 6046), *Proterosuchus alexanderi* (NMQR 1484), and *Tanystropheus longobardicus* (MCSN BES SC 265).

CAUDAL VERTEBRAE: The caudal vertebral skeleton is well represented by isolated vertebrae (e.g., FMNH PR 2775, fig. 24) and segments of articulated elements (e.g., UA 8-29-97-169, fig. 25). A proximalmost caudal vertebra is represented by FMNH PR 2775 (fig. 24). The neural spine, broken in FMNH PR 2775, is complete in the proximalmost caudal from a partially articulated series (fig. 25) spanning the region where chevrons are present. The neural spines of the anterior caudal vertebrae are canted posteriorly. The neural spines are mediolaterally compressed at their bases and gradually become rounder in cross section distally. The dorsal surface of each neural spine is flat. Posteriorly, a deep, vertically oriented gap divides the postzygapophyses at the base of each neural spine. In FMNH PR 2775, the anterior portion of the base of the neural spine bifurcates into thin laminae; each leads to the articular surface of the prezygapophyses and the gap between the laminae is deep. This gap narrows posteriorly within the anterior caudal vertebral series, disappearing altogether at the first caudal vertebra (the fourth caudal) that possesses articular surfaces for a chevron. The pre- and postzygapophyses are angled ~45° (medially and laterally in the transverse plane, respectively). Hyposphene-hypantrum intervertebral articulations are absent. Similarly

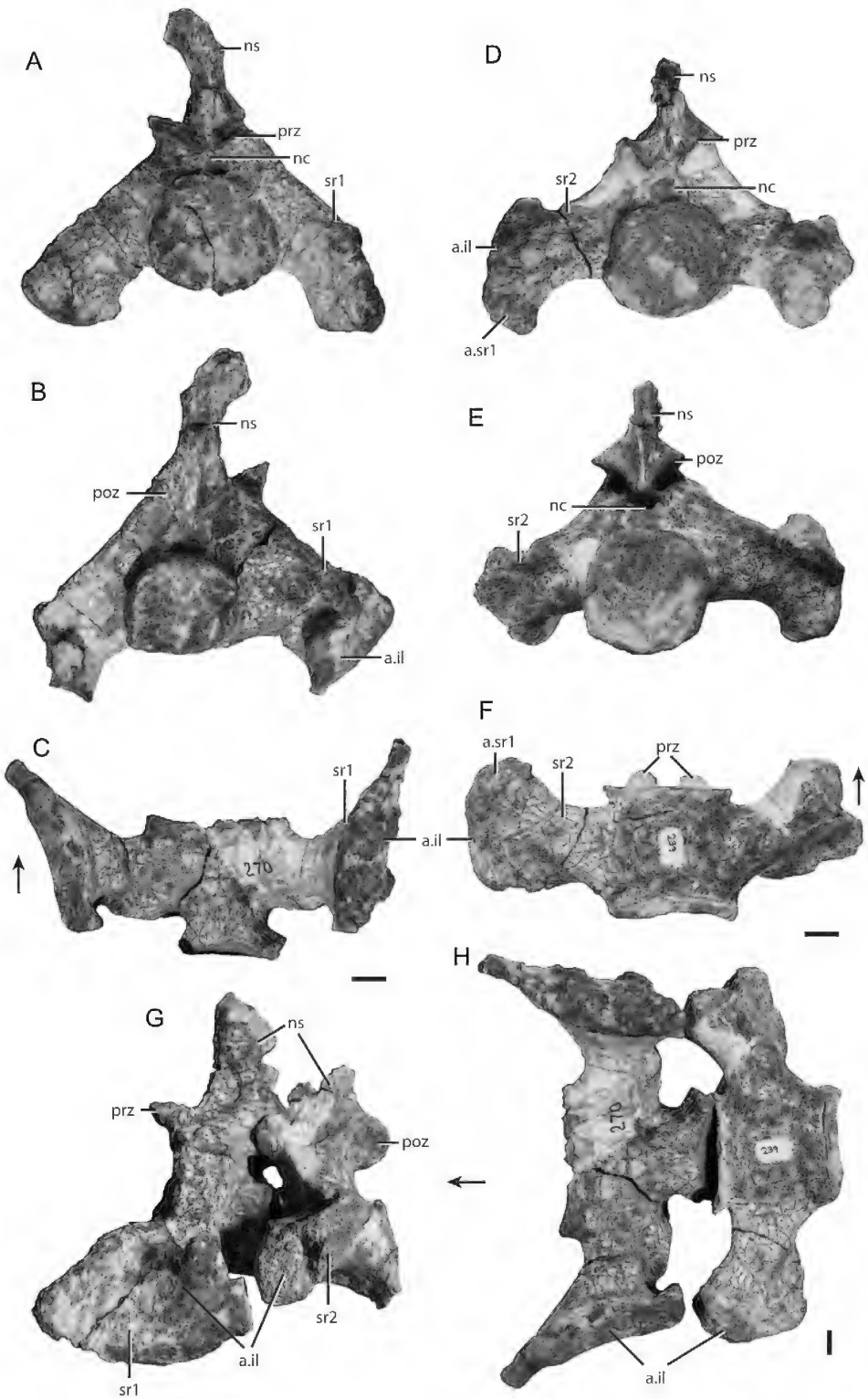
A
ns
prz
nc
sr1
B
ns
poz
sr1
a.il
C
sr1
a.il
270
D
ns
prz
sr2
nc
a.il
a.sr1
E
ns
poz
nc
sr2
F
a.sr1
sr2
prz
G
ns
prz
poz
sr2
a.il
sr1
H
270
a.il
I

oriented zygapophyses occur in tanystropheid vertebrae (e.g., GR 284, 291) and *Trilophosaurus buettneri* (TMM 31025-140). More steeply inclined zygapophyseal articulations occur in late-diverging rhynchosaurs (e.g., Benton, 1983).

The transverse processes of the anterior caudal vertebrae are completely fused to their centra without any trace of sutures. Unfused caudal ribs are known in early diapsids such as *Araeoscelis gracilis* (Reisz et al., 1984) and *Petrolacosaurus kansensis* (Reisz, 1981), but also in some archosauriforms (e.g., *Doswellia kaltenbachi*, Dilkes and Sues, 2009). In *A. madagaskarensis* the transverse processes slant posteroventrally (in the horizontal plane) and ventrally about 30° to the horizontal plane. In dorsal view, the dorsoventrally flattened processes arc posterolaterally and their tapered tips are posteriorly directed, similar to the condition in species of *Macrocnemus* (Peyer, 1937; Li et al., 2007). Straight, posterolaterally angled caudal transverse processes occur in many early archosauromorphs (e.g., *Mesosuchus browni,* SAM-PK 6046; species of *Langobardisaurus,* MCSNB 4860, MFSN 1921; "*Chasmatosaurus" yuani,* Young, 1936).

In *A. madagaskarensis* a small fossa occurs anterior to the juncture of the transverse process and centrum in the anterior caudals. This fossa disappears posteriorly in the caudal series, beginning with the first caudal vertebra that bears a chevron. The anterior and posterior articular facets of the centra are rounded and concave. The body of each centrum is waisted in shape only minimally; no chevron facet is evident on the posteroventral edge of FMNH PR 2775. No complete articulated series of the anteriormost caudal vertebrae is known, but chevron facets are evidently present either on the third or fourth caudal vertebra (fig. 25).

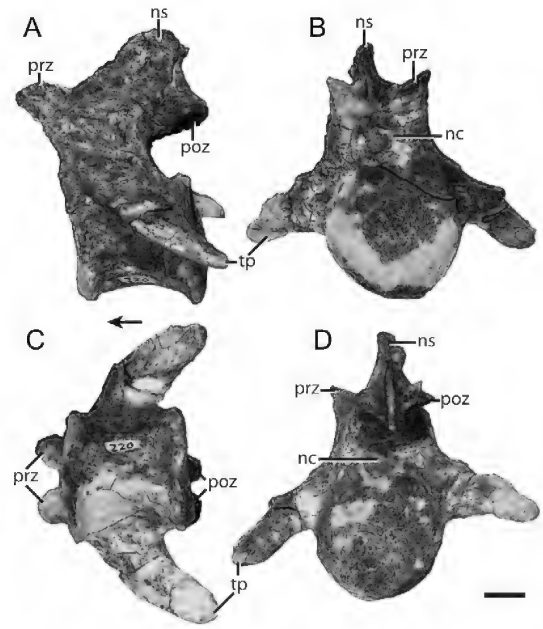

Fig. 24. Anterior caudal vertebra of *Azendohsaurus madagaskarensis* (FMNH PR 2775) in (**A**) left lateral, (**B**) anterior, (**C**) ventral, and (**D**) posterior views. Scale = 1 cm. Arrow indicates anterior direction. Abbreviations: **nc,** neural canal; **ns,** neural spine; **poz,** postzygapophysis; **prz,** prezygapophyses; **tp,** transverse process.

The middle caudal vertebrae of *A. madagaskarensis* are represented by a long articulated series (UA 7-15-99-600, fig. 26A), a shorter articulated series (FMNH PR 2778, fig. 26B–C), and an isolated element (FMNH PR 3822, fig. 27). The neural spines of all midcaudal vertebrae are canted posteriorly, with anterior edges slanted posterodorsally, whereas the posterior edges are vertical. Most of the dorsal ends of the neural spines are broken in the midcaudal vertebrae, except for the isolated specimen (FMNH PR 3822, fig. 27). In that specimen, the neural spine is oval in cross section with an

←

Fig. 23. Sacral vertebrae of *Azendohsaurus madagaskarensis*. First sacral vertebra (FMNH PR 2780) in (**A**) anterior, (**B**) posterior, and (**C**) ventral view. Second sacral vertebra (FMNH PR 2777) in (**D**) anterior, (**E**) posterior, and (**F**) and ventral view. Rearticulated sacral vertebrae (FMNH PR 2780 and FMNH PR 2777) in (**G**) lateral view and (**H**) in ventral view. Scales = 1 cm. Arrows indicate anterior direction. Abbreviations: **a.,** articulates with; **il,** ilium; **nc,** neural canal; **ns,** neural spine; **poz,** postzygapophysis; **prz,** prezygapophyses; **sr1,** sacral rib one; **sr2,** sacral rib 2.

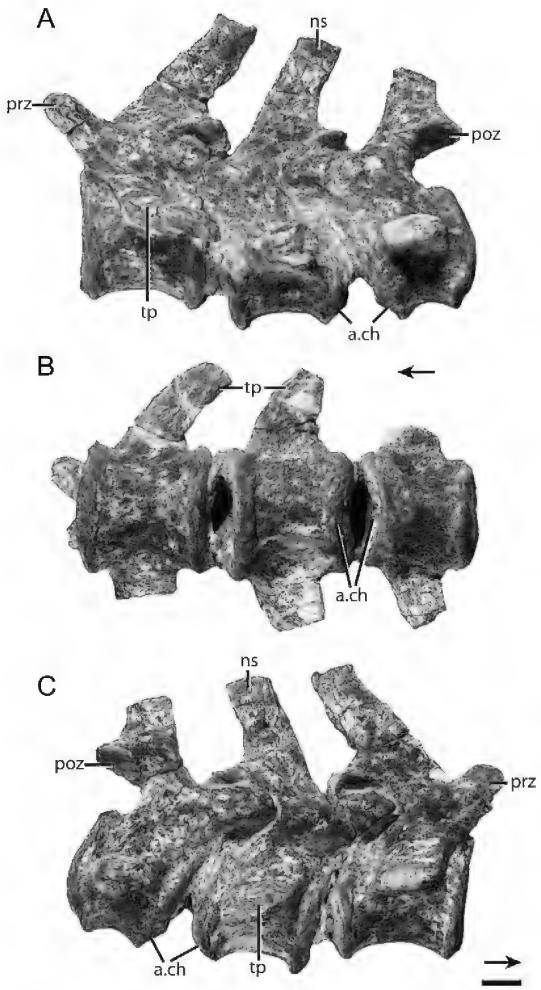

Fig. 25. Three articulated anterior caudal vertebrae of *Azendohsaurus madagaskarensis* (UA 8-29-97-169) in (**A**) left lateral, (**B**) ventral, and (**C**) right lateral views. Scale = 1 cm. Arrows indicate anterior direction. Abbreviations: **a.,** articulates with; **ch,** chevron; **ns,** neural spine; **poz,** postzygapophysis; **prz,** prezygapophyses; **tp,** transverse process.

anteroposteriorly oriented long axis; the dorsal edge is slightly rounded and the base of the neural spine overlies the posterior third of the centrum. Neural spine height decreases posteriorly in the articulated series (UA 7-15-99-600, fig. 26A). The postzygapophyses extend well posterior of the posterior edge of the centrum, and the prezygapophyses are widely spaced from each other. Both the pre- and postzygapophyses are angled about 45° (medially and laterally in the transverse plane, respectively); this angle varies slightly throughout the articulated midcaudal vertebral series, perhaps due to crushing.

The transverse processes of the midcaudal vertebrae originate in the anteroposterior midpoint area of the centrum. They project posterolaterally and are deflected slightly ventrally at their tips. They are dorsoventrally compressed and squared off laterally. The neural spines decrease in length posteriorly (UA 7-15-99-600, fig. 26A). The anterior and posterior articular facets of the centrum are rounded and angle slightly toward the center of the centrum at their ventral edges. A shallow groove marks the ventral surface at the midline. A similar groove occurs in *Trilophosaurus buettneri* (TMM 31025-140), whereas strong ridges frame a deeper groove in tanystropheid caudal vertebrae (Pritchard et al., 2015) (although crushing of the specimens may exacerbate these ridges). All midcaudal vertebrae in *A. madagaskarensis* bear a well-defined chevron facet on the posteroventral portion of the centrum.

The distal caudal vertebrae of *A. madagaskarensis* are represented by an articulated series (FMNH PR 2774) and isolated elements (FMNH PR 2772, fig. 26D; UA 7-15-99-599, fig. 28). The distal caudal vertebrae do not increase in length distally, in contrast to the condition in *Trilophosaurus buettneri* (TMM 31025-140; Gregory, 1945) in which centra of the distal caudal vertebrae are longer than those of the anterior caudal vertebrae. The distal caudal vertebrae of *A. madagaskarensis* decrease in length posteriorly (table 2), and this decrease in length in *A. madagaskarensis* occurs more anteriorly than in the caudal series of *Mesosuchus browni* (SAM 7416), *Protorosaurus speneri* (Gottmann-Quesada and Sander, 2009), "*Chasmatosaurus*" *yuani* (Young, 1936), and tanystropheids (e.g., MCSN BES SC 111, MFSN 1921). In *A. madagaskarensis*, the neural spines of the distal caudal vertebrate are mediolaterally compressed and have low, bladelike dorsal margins. The articular facets of the prezygapophyses of the distal caudal vertebrae differ from those of other caudals in being distinctly concave and in having a horizontal ventral portion and a vertical dorsal portion. Similar cupping of the prezygapophyses occurs in *Spinosuchus caseanus*

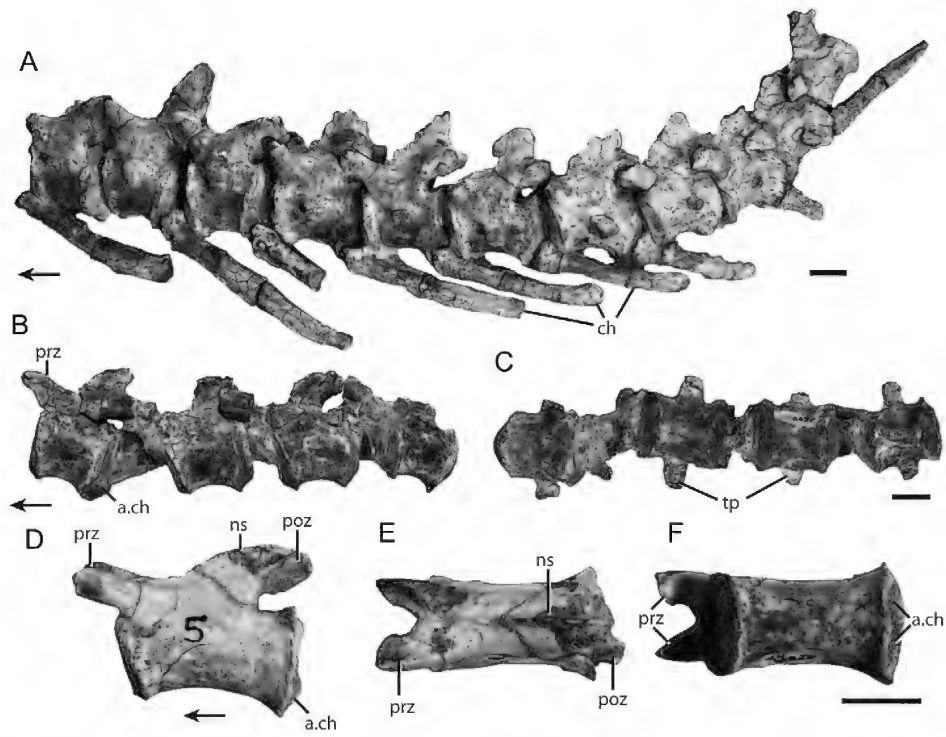

Fig. 26. Caudal vertebrae of *Azendohsaurus madagaskarensis*. Articulated middle caudal vertebrae (UA 7-15-99-600) in (**A**) left lateral view. Articulated middle caudal vertebrae (FMNH PR 2778) in (**B**) lateral (reversed) and (**C**) ventral views. An isolated distal caudal vertebra (FMNH PR 2772) in (**D**) left lateral, (**E**) dorsal, and (**F**) ventral views. Scales = 1 cm. Arrows indicate anterior direction. Abbreviations: **a.,** articulates with; **ch,** chevron; **ns,** neural spine; **poz,** postzygapophysis; **prz,** prezygapophyses; **tp,** transverse process.

(Spielmann et al., 2009) and in *Trilophosaurus buettneri* (TMM 31025-140). The postzygapophyses are simple flat surfaces deflected 45° laterally to the transverse plane. The short, laterally directed transverse processes of the middle and more anterior distal caudal vertebrae give rise to an anteroposteriorly trending ridge in the more distal caudal vertebrae. The anterior and posterior articular facets of the centra are concave centrally, with a large rounded marginal ridge circumscribing the central depression. A shallow midline groove marks the ventral surfaces of the centra; articular surfaces for the chevrons occur posteroventrally. Chevron facets reach the end, or nearly the end, of the caudal series. The distal tip of the tail is not preserved in available specimens.

Ribs: Ribs of *Azendohsaurus madagaskarensis* occur abundantly throughout the bone bed. Most were recovered disarticulated, and, unfortunately, displacement during fossilization precludes the secure assignation of ribs to particular vertebrae. Few ribs are complete.

All cervical ribs have distinct anterior processes (e.g., FMNH PR 2751, fig. 29; FMNH PR 3819, fig. 30A–B), a widespread feature within Archosauromorpha (Hoffstetter and Gasc, 1969; Dilkes, 1998; Gottmann-Quesada and Sander, 2009). The first cervical rib occurs on the axis. The anterior cervical ribs (FMNH PR 2751; fig. 29) are thin and circular in cross section. Their shafts parallel the long axis of the cervical vertebrae, and are at least as long as the centrum to which they attach. None are complete, making it difficult to assess their original length. Similarly shaped cervical ribs are widespread among early archosauromorphs, occurring in *Proterosuchus* (Cruickshank, 1972), *Protorosaurus speneri* (Gottmann-Quesada and Sander, 2009), tanystropheids (e.g., Peyer,

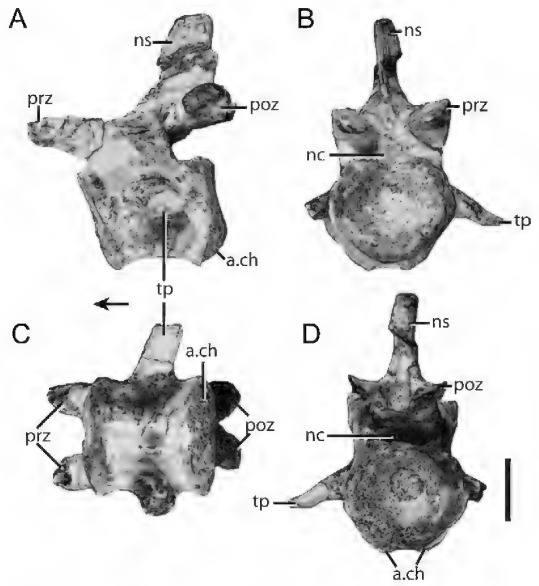

Fig. 27. Middle caudal vertebra of *Azendohsaurus madagaskarensis* (FMNH PR 3822) in (**A**) left lateral, (**B**) anterior, (**C**) ventral, and (**D**) posterior views. Scale = 1 cm. Arrow indicates anterior direction. Abbreviations: **a.,** articulates with; **ch,** chevron; **nc,** neural canal; **ns,** neural spine; **poz,** postzygapophysis; **prz,** prezygapophyses; **tp,** transverse process.

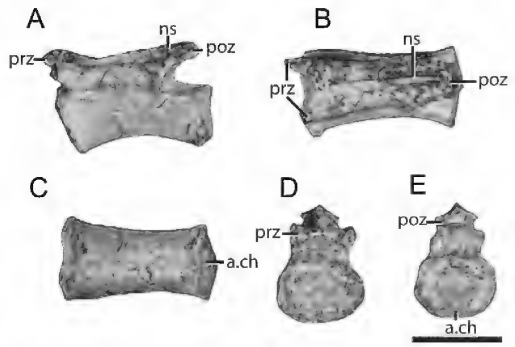

Fig. 28. Distal caudal vertebra of *Azendohsaurus madagaskarensis* (UA 7-15-99-599) in (**A**) left lateral, (**B**) dorsal, (**C**) ventral, (**D**) anterior, and (**E**) posterior views. Scale = 1 cm. Abbreviations: **a.,** articulates with; **ch,** chevron; **ns,** neural spine; **poz,** postzygapophysis; **prz,** prezygapophyses.

1937; Wild, 1973), and *Trilophosaurus buettneri* (TMM 31025-140; Gregory, 1945). The middle and posterior cervical ribs are more robust than their anterior counterparts. The capitulae and tuberculae are about equal in size. The tapered distal ends of the middle to posterior cervical ribs bear a shallow facet medially, perhaps indicating contact with the preceding cervical rib, and therefore a rigid cervical rib series, as has been suggested to occur in *Tanystropheus longobardicus* (Tschanz, 1988).

The anterior trunk costal series is best represented by an unusually well-preserved right rib, associated with a similarly exquisitely preserved anterior trunk vertebra (FMNH PR 2779; fig. 30C). The subequal capitulum and tuberculum are separated by a span of thin bone as in *Tanystropheus longobardicus* (Wild, 1973). Proximally, the dorsolateral edge of the proximal portion, which connects the tuberculum to the rib shaft, is bladelike. A rounded fossa occurs on the posterior side, ventrolateral to the gap between the capitulum and tuberculum. The shaft is oval in cross section, and its major axis is oriented anteroposteriorly for much of the length of the rib. The posterior surface of the shaft is grooved, whereas the proximal third of the dorsolateral surface is flat. The rib ends bluntly, tapering little in diameter relative to the shaft. The length (= 270 mm) and laterally oriented curvature of the anterior trunk rib indicates that the anterior trunk of *A. madagaskarensis* was deep and barrel shaped (fig. 1). The long scapular blade is consistent with this interpretation (see below).

The middle and posterior trunk ribs are represented by isolated specimens (UA 7-16-99-621, fig. 30E–F; UA 8-28-98-297, fig. 30G–H) and a partial series of partially articulated trunk vertebrae and incompletely preserved ribs (FMNH PR 2789, fig. 17). The middle to posterior trunk ribs are generally similar to those associated with the anterior trunk vertebrae, differing mainly in the following respects in their morphology: The shafts of the middle to posterior trunk ribs are nearly circular in cross section throughout their length. The fossae on the posterior sides of the proximal ends of the anterior trunk vertebrae are absent in the more posterior trunk vertebrae. The capitulum and tuberculum converge posteriorly as the diapophyses and parapophyses of the posterior trunk vertebrae converge; the capitulum and tuberculum are conjoined on the more posterior

TABLE 2
Measurements of the articulated caudal vertebrae (in mm) of *Azendohsaurus madagaskarensis*

Specimen	Order in series	Anterior-posterior length	Chevron length
Midcaudals	Caudal A	24	51
UA 7-15-99-600	Caudal B	24	X
(fig. 26A)	Caudal C	24	60
	Caudal D	23	X
	Caudal E	22	47
	Caudal F	20	42
	Caudal G	20	40
	Caudal H	20	39
	Caudal I	20	X
	Caudal J	20	X
	Caudal K	20	44
Distal caudals			
FMNH			
PR 2774	Caudal A	22	34
	Caudal B	22	33
	Caudal C	22	X
	Caudal D	22	28
	Caudal E	22	28
	Caudal F	21	X
	Caudal G	20	X
Distalmost caudals			
FMNH			
PR 2772	Caudal A	19	
	Caudal B	19	
	Caudal C	18	
	Caudal D	18	
	Caudal E	16	
	Caudal F	16	
	Caudal G	15	
	Caudal H	13	

trunk ribs. The 10 mm–long posteriormost trunk rib is fused to its corresponding vertebra (fig. 22). A similar convergence of the capitulae and tuberculae occurs in *Tanystropheus* (Wild, 1973). The degree of lateral curvature and the length of the trunk ribs both appear to decrease posteriorly.

GASTRALIA: A series of small, very delicate gastralia are preserved in association, but not in direct articulation, with a trunk rib in specimen FMNH PR 2760 (fig. 31). These elongate, cylindrical elements can be identified as gastralia based on their size and similarity to these elements in other diapsids, but they are too few in number and too disarticulated to provide information about

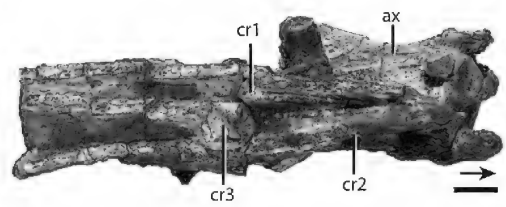

Fig. 29. The first three cervical ribs of *Azendohsaurus madagaskarensis* in articulation (FMNH PR 2751) in ventral view. Scale = 1 cm. Arrow indicates anterior direction. Abbreviations: **ax,** axis; **cr1,** first cervical rib; **cr2**, second cervical rib; **cr3**, third cervical rib.

the detailed organization of the gastralial basket. One element exhibits a bend of ~90° typical of gastralia (fig. 31).

Ossified gastralia occur in diapsids plesiomorphically (e.g., *Petrolacosaurus kansensis*). The nonsquamate lepidosaur *Sphenodon punctatus* (FMNH 197942) is characterized by a large number of ossified gastralia that nearly articulate with one another (= gastralial basket) whereas squamates lack ossified gastralia. In archosauromorphs, large numbers of gastralia are found in *Protorosaurus speneri* (Gottmann-Quesada and Sander, 2009: fig. 11), tanystropheids (e.g., *Tanystropheus longobardicus*, MCSN BES SC 1018), archosauriforms (e.g., *Proterosuchus alexanderi*, NMQR 1484, *Euparkeria capensis*, SAM 5867), and rhynchosaurs (e.g., *Mesosuchus browni*, SAM-PK-5882; *Rhynchosaurus articeps*, Benton, 1990). Given the rarity of gastralia in the *Azendohsaurus* quarry, it is unlikely that this taxon had an extensive gastralial basket like that of *Proterosuchus alexanderi* (NMQR 1484). The nearly articulated skeleton of *Trilophosaurus buettneri* (TMM 31025-140) includes many gastralia, but their arrangement is indiscernible (Gregory, 1945).

CHEVRONS: Chevrons of *A. madagaskarensis* were recovered both as isolated elements (e.g., FMNH PR 2773, fig. 32) and in articulation (e.g., UA 7-15-99-600, fig. 26A; FMNH PR 2774). Articulated examples show that the chevrons decrease in length gradually posteriorly. Facets on the posteroventral portion of the caudal vertebrae suggest that chevrons are present from the third or fourth caudal vertebra to the tip of the tail. The position of the anteriormost

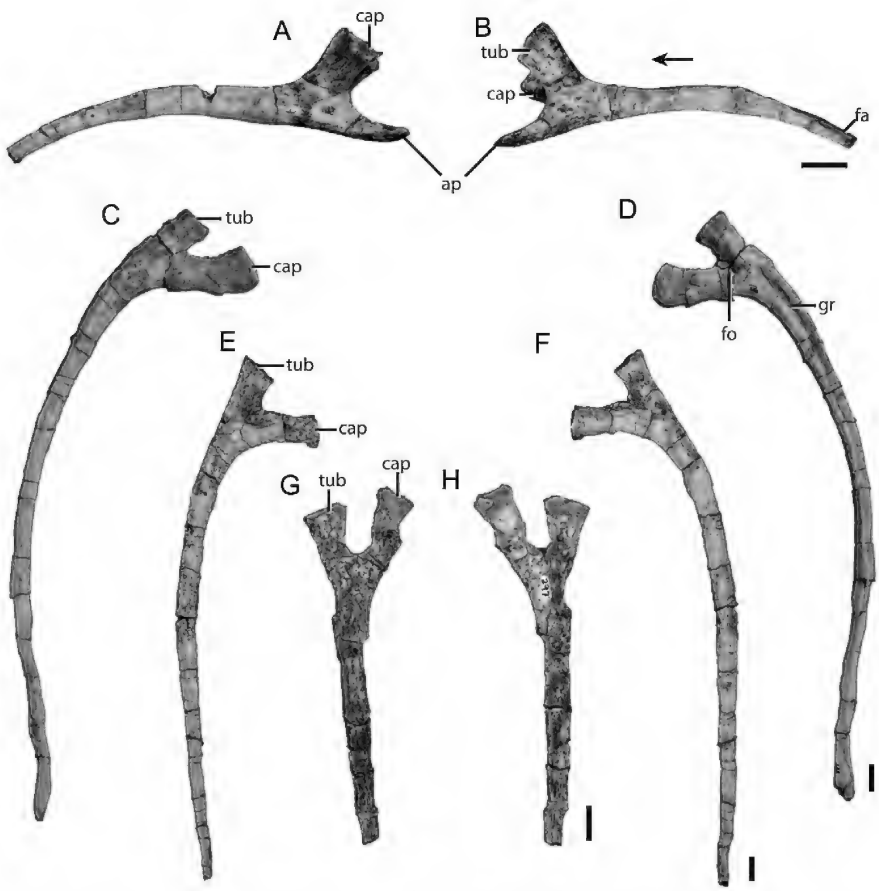

Fig. 30. Presacral ribs of *Azendohsaurus madagaskarensis*. Left middle cervical rib (FMNH PR 3819) in (**A**) ventral and (**B**) lateral views. Right anterior trunk rib (FMNH PR 2779) in (**C**) anterior and (**D**) posterior views. Left midtrunk rib (UA 7-16-99-621) in (**E**) posterior and (**F**) anterior views. Right posterior trunk rib (UA 8-28-98-297) in (**G**) anterior and (**H**) posterior views. Scales = 1 cm. Abbreviations: **ap,** anterior process; **cap,** capitulum; **fa,** facet; **fo,** fossa; **gr,** groove; **tub,** tuberculum.

chevron is variable in early archosauromorphs, occurring between the second and third caudals in *Trilophosaurus buettneri* (per Gregory, 1945), the third and fourth caudals in *Protorosaurus speneri* (Gottmann-Quesada and Sander, 2009), and the seventh and eighth caudals in *Tanystropheus longobardicus* (Wild, 1973). In *A. madagaskarensis* the chevrons project posteroventrally about 45° from the horizontal. The proximal portions of the chevrons are expanded mediolaterally relative to the more distal shaft. An articular facet at the proximal surface spans the entire width of the chevron, even though the anterior edge is notched at the midline. *Trilophosaurus buettneri* (TMM 31025-140) and *Youngina capensis* (Gow, 1975) exhibit similar proximal articulations, although both lack the midline notch. By contrast, the proximal chevron articulations in *Langobardisaurus pandolfii* (MCSNB 2883) and *Tanystropheus longobardicus* (Wild, 1973) are bipartite and separated by a broad gap.

The proximal articular surface and the remainder of the chevron are penetrated by an anteroposteriorly oriented opening. In the anterior chevrons (FMNH PR 2773, fig. 32A–B), the anterior and posterior edges of the shafts bear a weakly developed ridge on the midline. In lateral view, the shafts of the more anterior chevrons expand slightly, but not to the same extent as in *Trilophosaurus buettneri* (TMM 31025-140). A slight expansion of the distal ends of the anterior

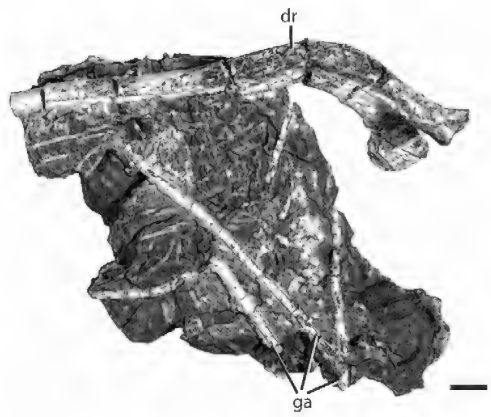

Fig. 31. Gastralia and a trunk rib of *Azendohsaurus madagaskarensis* (FMNH PR 2756). Scale = 1 cm. Abbreviations: **dr,** trunk rib; **ga,** gastralia.

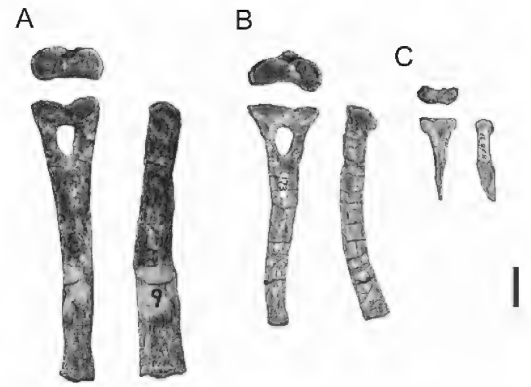

Fig. 32. Chevron of *Azendohsaurus madagaskarensis*. Anterior chevron (FMNH PR 2773) (**A**) in proximal (top), anterior (left), and left lateral (right). Midtail chevron (FMNH PR 2773) (**B**) in proximal (top), anterior (left), and left lateral (right). Posterior portion of the tail chevron (FMNH PR 2772) (**C**) in proximal (top), anterior (left), and left lateral (right). Scale = 1 cm.

chevrons also occurs in *Langobardisaurus pandolfii* (MFSN 1921). Besides the anterior and posterior ridges, the cross sections of the more anterior chevrons in *A. madagaskarensis* are nearly circular, becoming more oval distally with the long axes oriented anteroposteriorly. The distal surfaces have a slightly flared, circumscribing rim, and the middle of the distal ends bear a slight hump.

The proximal articular surfaces of the most posterior chevrons (FMNH PR 2772, fig. 32C) resemble those of the more anterior elements. In posterior chevrons, the midline ridges on the anterior and posterior sides of the shaft are well developed, and the shafts are mediolaterally compressed. The posterior chevrons are posteroventrally recurved and taper distally (fig. 32C).

Pectoral Girdle

Clavicle: No single complete clavicle is known from the quarry, but fragments of the dorsal half of left (FMNH PR 2795) and right (UA 8-30-98-355) clavicles (fig. 33) and the proximal portion of a right one from the holotype (UA 7-20-99-653) provide a comprehensive view of the element's structure (fig. 33). The clavicle fragments were not found in articulation, meaning that the patterns of articulation between the scapula and interclavicle and the clavicles must be inferred from articular surfaces. The proximal portion of the clavicle consists of an anteroposteriorly expanded head that is dorsoventrally compressed into a thin blade. A ridge on the dorsal surface tapers medially to a fine point; the ridge appears to form part of the articular surface for the interclavicle. The ventral surface of the clavicle is convex.

The shaft of the clavicle twists from a horizontal orientation medially to a vertical orientation dorsally; the middle portion of the shaft is oval in cross section, with its long axis aligned anteroposteriorly. The distal tip of the element tapers anteriorly and is thickened relative to the posterior edge (fig. 33). The thickened anterior edge and thin posterior edge of the dorsal portion of the clavicle create a medially concave and laterally convex cross section. We infer that the concave ventral surface contacted the acromion process of the scapula, as in other diapsids. The thin posterior edge bears a rugose area medially, possibly marking attachment sites of the ligaments connecting the scapula and clavicle.

Comparisons between the clavicles of *A. madagaskarensis* and those of other early archosauromorphs are limited by the paucity of three-dimensionally preserved elements in other taxa. *Azendohsaurus madagaskarensis* is similar to *Tanystropheus longobardicus* (MCSN BES SC 1018) in that the clavicles in both appear to have thickened, anterodorsally tapering anterior margins and the

proximal ends are narrower than the shaft. In contrast, the proximal portions of the clavicles of *Mesosuchus browni* (SAM 6536) and *Proterosuchus alexanderi* (NMQR 1484) are greatly expanded relative to the midshaft, with their dorsal portions long and gradually tapering. Proximally expanded clavicles also occur in early diapsids such as *Claudiosaurus germaini* (MNHN 1978-6-1) and *Araeoscelis gracilis* (Reisz et al., 1984). The clavicle is slightly expanded proximally in a drepanosaurid from northern New Mexico (Harris and Downs, 2002). The clavicle of *Prolacerta broomi* (BP/1/2675) bears a thickened anterior margin but is otherwise far more robust than that of *A. madagaskarensis*. We were unable to make direct comparisons with the lone clavicle of *Trilophosaurus buettneri,* as this unnumbered specimen described, but not figured, by Gregory (1945) cannot currently be located.

INTERCLAVICLE: Three nearly complete interclavicles (fig. 34; FMNH PR 2781, FMNH PR 2760, UA 7-16-99-620) are known for *A. madagaskarensis*. Specimen FMNH PR 2781 (fig. 34A–B) appears to be undistorted, retaining its three-dimensional architecture, whereas UA 7-16-99-620 (fig. 34 C–D) is pathologically malformed such that the posterior process is torqued strongly to the right. The interclavicle of *A. madagaskarensis* is a large, robust element with a prominent paddle-shaped posterior process. The anterior portion consists of an anteriorly pointed prominence at the midline and laterally directed processes that articulated with the clavicles. A similar anterior process occurs in *Protorosaurus speneri* (Gottmann-Quesada and Sander, 2009: fig. 19), and anterior processes also occur in *Araeoscelis gracilis* (Reisz et al., 1984) and *Petrolacosaurus kansensis* (Reisz, 1981). Other early archosauromorphs lack an anterior process, as the anterior surface of the interclavicle in most forms, including *Mesosuchus browni* (Dilkes, 1998), *Prolacerta broomi* (BP/1/2675), *Proterosuchus alexanderi* (NMQR 1484; Dilkes, 1998), and *Tanystropheus longobardicus* (Wild, 1973), is notched along the midline rather than possessing an anteriorly projecting process. The dorsoventrally compressed lateral processes taper laterally and terminate in a slightly thickened margin

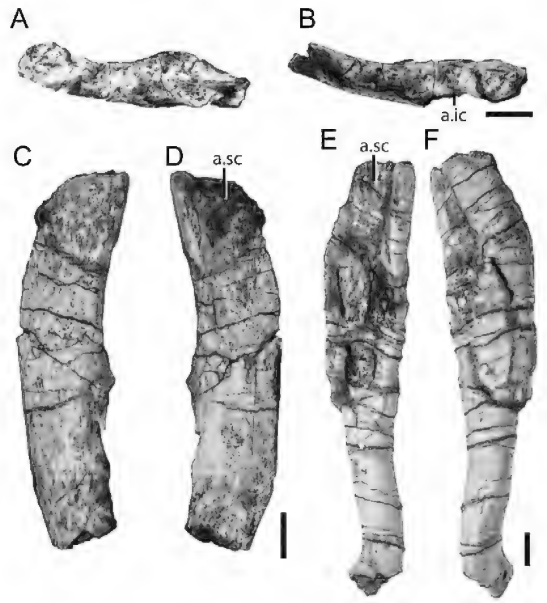

Fig. 33. Clavicles of *Azendohsaurus madagaskarensis*. Proximal portion of the right clavicle (UA 7-20-99-653) in (**A**) dorsal and (**B**) ventral views. Dorsal half of the right clavicle (UA 8-30-98-355) in (**C**) lateral and (**D**) medial views. Dorsal half of the left clavicle (FMNH PR 2795) in (**E**) lateral and (**F**) medial views. Scales = 1 cm. Abbreviations: **a.,** articulates with; **ic,** interclavicle; **sc,** scapula.

(fig. 34B). Both the anterior and posterior rims of the lateral processes taper to bladelike edges. The dorsal surfaces of the lateral processes are smooth whereas the ventral surfaces bear a slightly concave articular surface for the clavicles. These surfaces appear to extend the length of the lateral processes but do not meet at the midline. They are poorly defined in *A. madagaskarensis* and "*Scaphonyx*" *fischeri* (MCZ 1636), in contrast to the deep, distinct facets seen in *Trilophosaurus buettneri* (TMM 31025-144). The lateral processes of *A. madagaskarensis* project directly laterally, as in *Prolacerta broomi* (BP/1/2675), *Proterosuchus alexanderi* (NMQR 1484), and *Tanystropheus longobardicus* (Haas, 1970), in contrast to the condition in *Trilophosaurus buettneri* (TMM 31025-144) where they project posterolaterally.

The posterior process of the interclavicle of *A. madagaskarensis* becomes oval in cross section immediately posterior to the lateral processes, with the greater expansion oriented

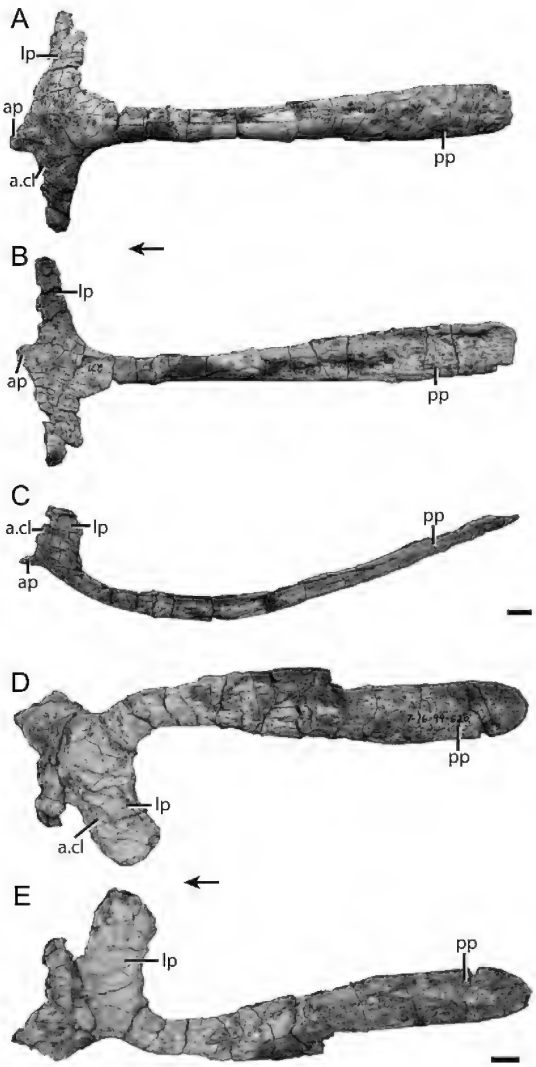

Fig. 34. Interclavicles of *Azendohsaurus madagaskarensis*. Interclavicle (FMNH PR 2781) in (**A**) ventral, (**B**) dorsal, and (**C**) left lateral views. Pathological interclavicle (UA 7-16-99-620) in (**D**) ventral and (**E**) dorsal views. Scales = 1 cm. Arrows indicate anterior direction. Abbreviations: **a.,** articulates with; **ap,** anterior process; **cl,** clavicle; **lp,** lateral process; **pp,** posterior process.

mediolaterally. More posteriorly, the process becomes dorsoventrally flattened, concave dorsally, and convex ventrally; it terminates as a laterally expanded "paddle." The interclavicle also is expanded posteriorly in *Trilophosaurus buettneri* (TMM 31025-144), "*Scaphonyx*" *fischeri* (MCZ 1636), and *Mesosuchus browni* (SAM 6536), whereas it has a similar width posteriorly (subrectangular in ventral view) in *Protorosaurus speneri* (Gottmann-Quesada and Sander, 2009), *Petrolacosaurus kansensis* (Reisz, 1981), *Prolacerta broomi* (BP/1/2675), *Proterosuchus alexanderi* (NMQR 1484), *Tanystropheus longobardicus* (Wild, 1973), and *Youngina capensis* (Gow, 1975). The dorsal and ventral surfaces of the posterior end of the posterior process bear anteroposteriorly oriented grooves in *A. madagaskarensis* (especially prominent in FMNH PR 2760).

SCAPULA: The scapula of *A. madagaskarensis* is known best from three nearly complete elements, two left (UA 8-27-98-292 and FMNH PR 2798; fig. 35) and one right (FMNH PR 2771). All exhibit some degree of natural lateral body curvature, but small cracks permeating the specimens suggest some degradation of original three-dimensional architecture. A thickened proximal region bears a posteroventrally directed glenoid. The glenoid projects laterally, as in other early archosauromorphs, but the scapular portion of the glenoid is clearly more posteriorly oriented in *A. madagaskarensis* than in *Trilophosaurus buettneri* (TMM 30125-140), *Mesosuchus browni* (Dilkes, 1998), *Prolacerta broomi* (BP/1/2675), *Proterosuchus fergusi* (NMQR 1484), *Protorosaurus speneri* (Gottmann-Quesada and Sanders, 2009), *Tanystropheus longobardicus* (MCSN BES SC 1018), or *Youngina capensis* (AMNH FR 5561). The posterior deflection of the glenoid in *A. madagaskarensis* may indicate a fairly upright orientation of the humerus (see below). Roughly half of the glenoid fossa is composed of the scapula, as in FMNH PR 2771 (fig. 36). A low, short, and poorly defined ridge separates the ventral portion of the glenoid from the rugose articulation surface for the coracoid. A prominent tuber lies just dorsal to the glenoid on the posterolateral portion of the scapula. This tuber, the probable insertion site of the scapular head of the *m. triceps brachii* based on comparisons with extant lepidosaurs [Romer, 1922, 1944] and archosaurs [Romer, 1922; Meers, 2003]), is oval, with a proximodistally oriented long axis; it nearly contacts the edge of the glenoid fossa. In contrast, the corresponding tuber in *Trilophosaurus buettneri* (TMM 31025-68R) is circular and

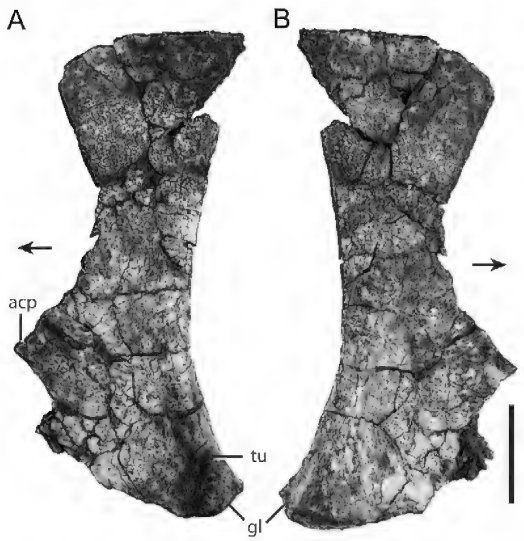

Fig. 35. Left scapula of *Azendohsaurus madagaskarensis* (FMNH PR 2798) in (**A**) lateral and (**B**) medial views. Scale = 5 cm. Arrows indicate anterior direction. Abbreviations: **acp,** acromian process; **gl,** glenoid; **tu,** tuber.

positioned well dorsal of the glenoid rim. Other early archosauromorphs, such as rhynchosaurs, have little or no scar in this region (e.g., *Teyumbaita sulcognathus*, UFRGS-PV-0232T) or only a slight depression (e.g., *Proterosuchus alexanderi*, NMQR 1484).

The region anterior to the glenoid fossa is flat and lacks the raised acromion process typical of archosaurs (Nesbitt, 2011) and some non-archosaurian archosauriforms (e.g., *Pseudochampsa ischigualastensis,*Trotteyn et al., 2012), late diverging rhynchosaurs (Montefeltro et al., 2013), and turtles (Gaffney, 1990). The well-preserved anteroproximal region of FMNH PR 2771 (fig. 38) shows that the anterior edge of the glenoid is distinctly notched at the articulation between the scapula and coracoid. No such notch occurs in *Protorosaurus speneri* (Gottmann-Quesada and Sanders, 2009), *Mesosuchus browni* (Dilkes, 1998), *Prolacerta broomi* (BP/1/2675), *Tanystropheus longobardicus* (MCSN BES SC 1018), or *Proterosuchus alexanderi* (NMQR 1484). *Trilophosaurus buettneri* also appears to lack an anterior notch, but this portion of the scapula is typically broken (e.g., TMM 31025-68R) or reconstructed (e.g., TMM 31025-68B),

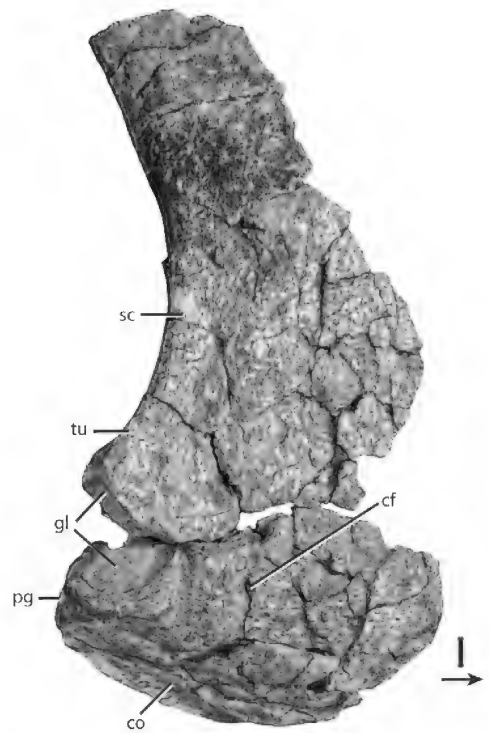

Fig. 36. Articulated right coracoid and scapula of *Azendohsaurus madagaskarensis* (FMNH PR 2771) in lateral view. Scale = 1 cm. Arrow indicates anterior direction. Abbreviations: **cf,** coracoid foramen; **co,** coracoid; **gl,** glenoid; **pg,** postglenoid process; **sc,** scapula; **tu,** tuber.

hindering accurate interpretation. In *A. madagaskarensis*, the ventral surface of the proximal portion of the scapula is flat and slightly concave posteriorly medial to the glenoid. The scapula and the coracoid meet at a sigmoidal contact at the proximal margin of the scapula (fig. 38). The scapula and coracoid, preserved nearly in articulation in FMNH PR 2771, show no sign of the fusion that is observed in several archosaurs (e.g., coelophysoid dinosaurs).

The scapular blade of *A. madagaskarensis* is preserved completely in FMNH PR 2798. The scapular blade is particularly tall in *A. madagaskarensis* and *Trilophosaurus buettneri* (TMM 31025-68R) relative to those in other archosauromorphs except *Jesairosaurus lehmani* (MNHN ZAR 6). In *Jesairosaurus* the scapula is about twice as tall as wide at the proximal margin, whereas in other early archosauromorphs, the scapula is about 1.5

times as tall as wide proximally (e.g., *Proterosuchus alexanderi*, NMQR 1484; *Prolacerta broomi*, BP/1/2675; *Mesosuchus browni,* SAM 6536; *Protorosaurus spenceri*, PSM 4). Late-diverging tanystropheids (e.g., *Tanystropheus longobardicus*, MCSN BES SC 1018; *Tanytrachelos ahynis*, VMNH 120046) exhibit proportionally shorter scapulae, reflecting their posterodorsally arched blades. The scapular blade of *A. madagaskarensis* is thin mediolaterally; its posterior edge is slightly thicker than its anterior edge. The anterior and posterior margins of the scapular blade are concave in lateral view. Although a concave posterior edge is plesiomorphic for diapsids (e.g. Reisz, 1981; Reisz et al., 1984), a concave anterior margin is unusual for early archosauromorphs. A concave anterior scapular margin also occurs in *Trilophosaurus buettneri* (TMM 31025-140), *Teraterpeton hrynewichorum* (Sues, 2003), and rhynchosaurs (e.g., *M. browni*, SAM 6536; *Teyumbaita sulcognathus*, Montefeltro et al., 2013). In nearly all other early archosauromorphs the anterior scapular margin is slightly concave, straight, or convex (e.g., *Proterosuchus alexanderi*, NMQR 1484; *Prolacerta broomi*, BP/1/2675; *Tanystropheus longobardicus*, MCSN BES SC 1018). The distal end of the scapular blade of *A. madagaskarensis* is asymmetrical in lateral view; the posterior portion is pointed and more distally expanded than the rounded anterior portion. The distal edge is nearly flat in dorsal view.

Coracoid: The coracoid of *Azendohsaurus madagaskarensis* is best represented by a complete, well-preserved specimen from the left side (FMNH PR 3822; fig. 37) and a nearly complete specimen from the right side (FMNH PR 2771; fig. 36). In lateral view, the coracoid of *A. madagaskarensis* is oval in outline, with an anteroposteriorly oriented long axis. The prominent glenoid fossa is located on the proximoposterior edge of the coracoid, with the coracoid component of the glenoid fossa lying proximoposterolaterally. The coracoid portion of the glenoid is much great than that of the scapula, as is common in early diapsids (e.g., *Petrolacosaurus kansensis*, Reisz, 1984; *Youngina capensis*, AMNH FR 5561). The glenoid is slightly concave anteriorly and convex posteriorly. A small notch occurs just medial to the medial margin of the glenoid. The postglenoid process of *A. madagaskarensis* is distinct, consisting of ventral and lateral components separated by a well-rounded ridge. It produces a shallow, mediolaterally directed shelf clearly seen in proximal (fig. 37B) but not lateral or ventral views (fig. 37A). After the glenoid region, the postglenoid process forms the mediolaterally thickest part of the coracoid. A small groove separates the posterior half of the ventral rim of the glenoid's articular surface from the postglenoid process. The postglenoid process of *A. madagaskarensis* is atypical for early archosauromorphs, being more similar to those of early crocodylomorphs (Clark, in Benton and Clark, 1988) than to other plausible close relatives of *Azendohsaurus*. The coracoids of most early archosauromorphs end immediately posterior to the glenoid fossa and are simply rounded in this area (e.g., *Proterosuchus alexanderi*, NMQR 1484; *Prolacerta broomi*, BP/1/2675; *Protorosaurus speneri*, PSM 4). The postglenoid process appears to be slightly expanded in *Sarmatosuchus otschevi* (Gower and Sennikov, 1997) and *Tanystropheus longobardicus* (Wild, 1973; MCSN BES SC 1018). The postglenoid processes of *Trilophosaurus buettneri* (TMM 31025-140) and *Trilophosaurus jacobsi* (NMMNHS P-44279) are very large and proportionally longer than those of *A. madagaskarensis*. The postglenoid processes of *T. buettneri* and *A. madagaskarensis* are similar in bearing a mediolaterally expanded surface; in *T. buettneri* (TMM 31025-140) this shelf diminishes in prominence posteriorly. The condition in *Mesosuchus browni* (SAM 6536) is unclear owing to poor preservation, but other rhynchosaurs lack a postglenoid process (e.g., *Teyumbaita sulcognathus*, UFRGS-PV-0232T).

The body of the coracoid anterior to the glenoid fossa is distinctly convex in lateral and ventral views, and concave in medial view. A small coracoid foramen pierces the element just anterior to the glenoid. On the lateral surface, a rounded ridge extends from just ventral to the coracoid foramen to the thin anterior edge of the element. This ridge is not evident in *Trilophosaurus buettneri* (TMM 31025-68B), *Prolacerta broomi* (BP/

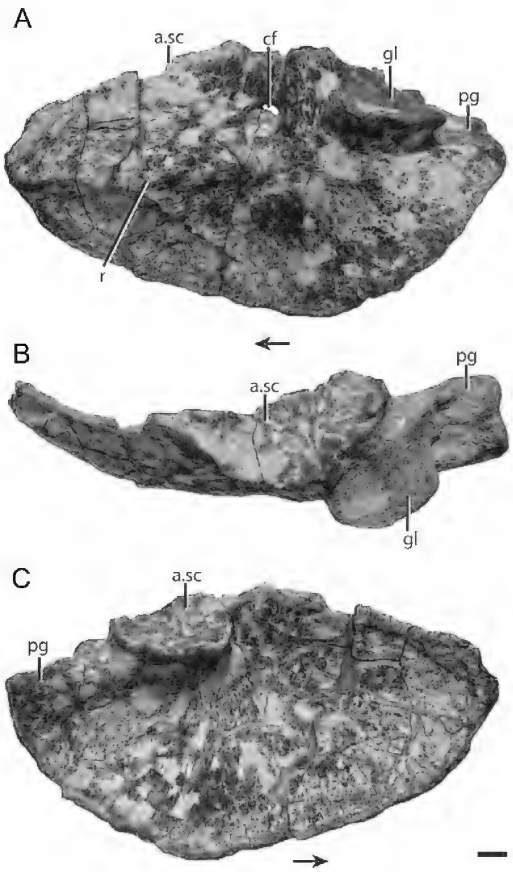

Fig. 37. Left coracoid of *Azendohsaurus madagaskarensis* (FMNH PR 3822) in (**A**) lateral, (**B**) proximal, and (**C**) medial views. Scale = 1 cm. Arrows indicate anterior direction. Abbreviations: **a.,** articulates with; **cf,** coracoid foramen; **gl,** glenoid; **pg,** postglenoid process; **sc,** scapula.

1/2675), or *Proterosuchus alexanderi* (NMQR 1484).

Forelimb

Humerus: Humeri, well represented in the *A. madagaskarensis* sample, vary considerably in size, ranging from 157–200+ mm in length (table 3). The two best-preserved specimens, FMNH PR 2755 (fig. 38) and the smaller FMNH PR 3817 (fig. 39) are illustrated, but information from others (e.g., FMNH PR 3816, FMNH PR 2760) is incorporated in the description below. The proximal and distal surfaces are poorly ossified in most specimens (although not to the extent observed in *Erythrosuchus africanus*, AMNH FARB 5595, NHMUK R3592). Many specimens are slightly distorted from crushing; for example, the right and left humeri from a single individual (FMNH PR 3816) differ somewhat in maximum length, proximal width, and distal width (see measurements). Nevertheless, the original three-dimensional shape is generally retained in most specimens.

The humerus is transversely expanded proximally and distally, producing a highly waisted midshaft. In proximal view, the long axes of the proximal and distal ends are offset roughly 30° (in proximal view) relative to one another in most specimens. The proximal end bears a prominent anteroventral fossa, framed anterolaterally by the deltopectoral crest and posteromedially by a rounded ridge. The robust deltopectoral crest, lengthened ventrally and projecting anteroventrally, is continuous with the proximal surface of the humerus, as is common in early archosauromorphs (e.g., *Protorosaurus speneri*, Gottmann-Quesada and Sander, 2009; *Tanystropheus longobardicus*, MCSN BES SC 1018; *Trilophosaurus buettneri*, TMM 31025-140). The crest terminates distally where a prominent fossa ends near the midshaft. The proximal articular surface forms a long, crescentic shape (concave anteroventrally) in proximal view. The central part of the proximal surface is expanded dorsally into a highly concave head that articulates with the glenoid fossa of the scapula and coracoid. A prominent ridge on the anterodorsal surface of the proximal portion of the humerus extends from dorsal of the deltopectoral crest to proximal of the midshaft. No such ridge occurs in *Prolacerta broomi* (BP/1/2675) or *Trilophosaurus buettneri* (TMM 31025-140). Shallow fossae occur anterior and posterior to this ridge. Another fossa is present on the dorsal surface, just distal to the proximal surface and anterior to the posterior surface of the humerus. A swollen, striation-covered hump occurs distal to this depression. Dorsally, a distinct muscle scar lies just proximal to the midshaft. The depth, length, and shape of this scar vary considerably within the sample. For example, the scar is shallow and short (~10 mm) in FMNH PR 2755 (fig. 38), deep and short (~10 mm) in FMNH PR 3816, and deep and

TABLE 3
Measurements of humeri (in mm) of *Azendohsaurus madagaskarensis*
Abbreviations: est, estimated; inc, incomplete.

Specimen	Side	Length	Proximal width	Distal width
FMNH PR 2755 (fig. 38)	right	191	100	91
UA 8-25-98-213	left	157	90	75
FMNH PR 2760	right	190	106	90
UA 8-29-98-340	left	189 inc	109	91
UA 9-5-980-457	left	203	106	97
FMNH PR 3816	left	183	92	79
FMNH PR 3816	right	191	95	90
FMNH PR 3817 (fig. 39)	left	195	96	85
UA 7-16-99-620	left	200 est	97	88

elongated (~30 mm) in FMNH PR 2760. The middle portion of the shaft is circular in cross section.

The humerus is less transversely expanded distally than proximally. The dorsal surface of the distal end is slightly concave whereas the ventral surface is flat. The medially expanded entepicondyle is rounded and bears unfinished bone on its medial surface. In dorsal view, a sharp change in angle occurs at the intersection of the compact and the spongier, unfinished bone. A similar "squared-off" entepicondyle is present in *Trilophosaurus buettneri* (TMM 31025-140; Gregory, 1945), *Trilophosaurus jacobsi* (NM MNHS P-39936), and "*Chasmatosaurus*" *yuani* (Young, 1963). Articular surfaces for

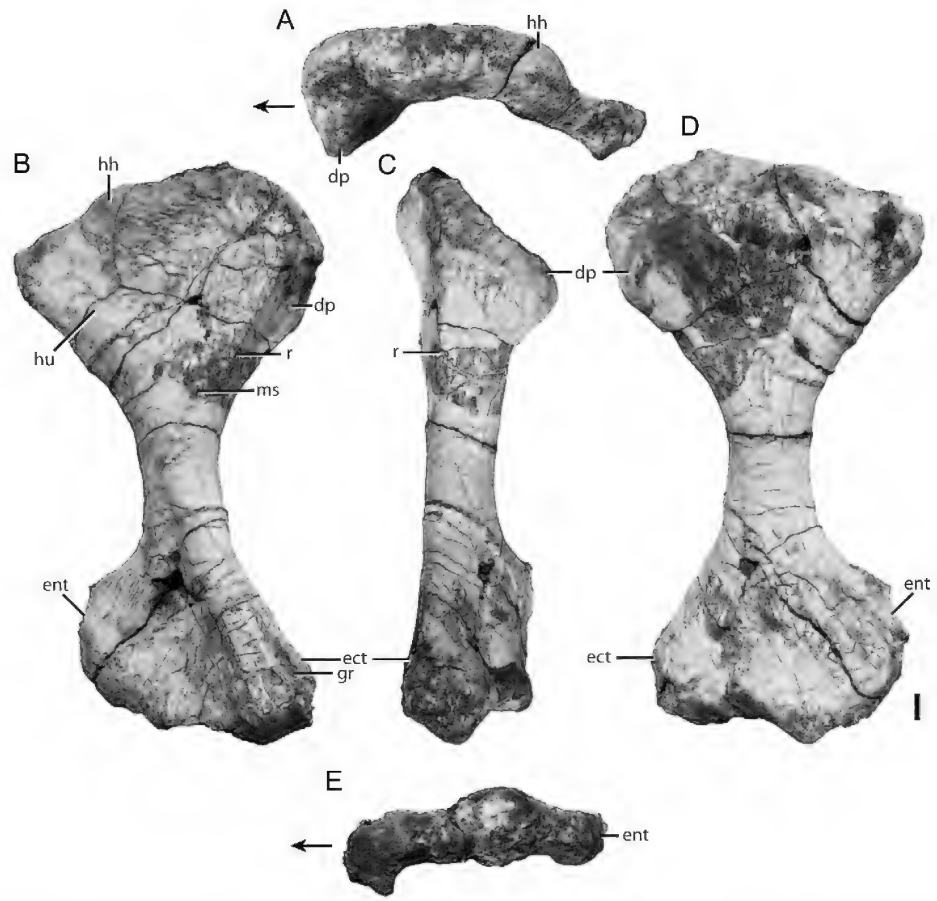

Fig. 38. Right humerus of *Azendohsaurus madagaskarensis* (FMNH PR 2755) in (**A**) proximal, (**B**) dorsal, (**C**) anterolateral, (**D**) ventral, and (**E**) distal views. Scale = 1 cm. Arrows indicate anterior direction. Abbreviations: **dp,** deltopectoral crest; **ect,** ectepicondyle; **ent,** entepocondyle; **gr,** groove; **hh,** humeral head; **hu,** hump; **ms,** muscle scar; **r,** ridge.

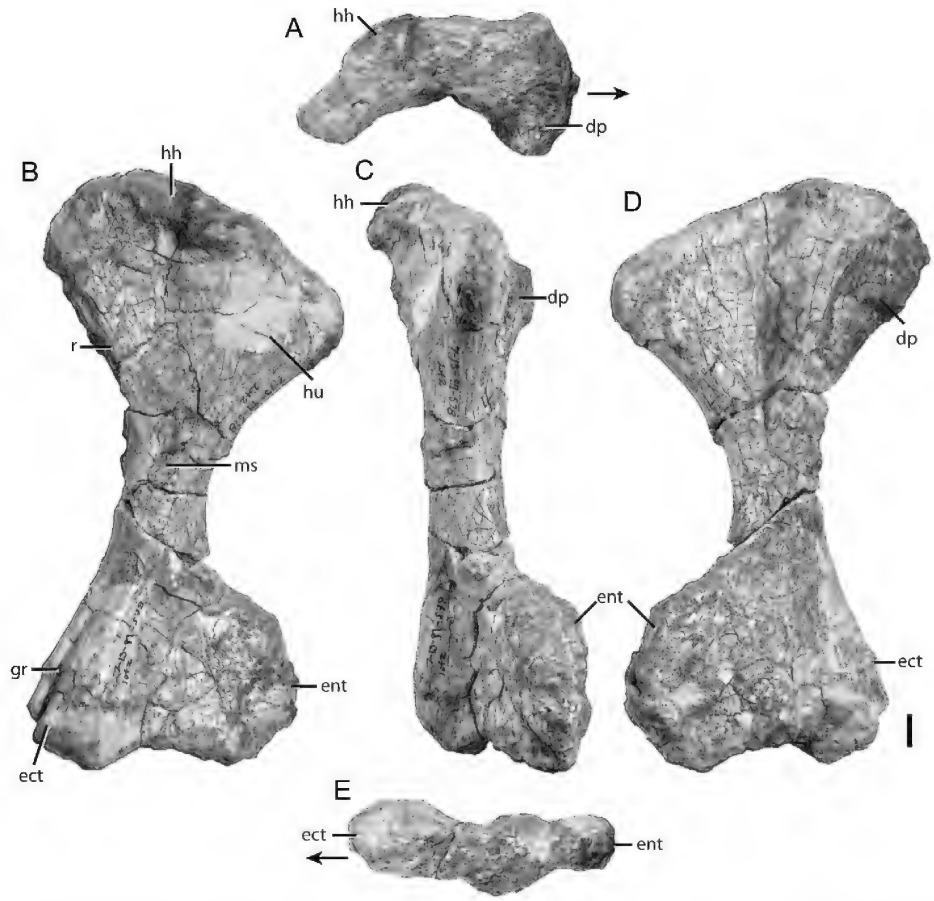

Fig. 39. Left humerus of *Azendohsaurus madagaskarensis* (FMNH PR 3817) in (**A**) proximal, (**B**) dorsal, (**C**) anterolateral, (**D**) ventral, and (**E**) distal views. Scale = 1 cm. Arrows indicate anterior direction. Abbreviations: **dp,** deltopectoral crest; **ect,** ectepicondyle; **ent,** entepocondyle; **gr,** groove; **hh,** humeral head; **hu,** hump; **ms,** muscle scar; **r,** ridge.

the radius and ulna occupy roughly the lateral two-thirds of the distal surface. The ulnar articulation is flat distally, whereas the radial articulation is flat ventrodistally and laps onto the ventral surface. The articular surfaces are poorly ossified, in contrast to the better-defined and rounded condyles in *Trilophosaurus buettneri* (TMM 31025-140) and in many early diapsids (e.g., *Araeoscelis gracilis*, MCZ 2043). The entepicondyle and ectepicondyle are separated by a broad fossa on the distal surface. An ectepicondylar groove is present in all specimens, but its breadth and depth vary depending on the degree of postmortem or postdepositional crushing. This groove is particularly prominent in FMNH PR 2760, encircling the distal end and creating a small, dorsally hooked pendant on the lateral side of the element. A similar structure is illustrated for *Tanystropheus conspicuus* by Wild (1973).

RADIUS: Radii, well represented within the *A. madagaskarensis* bone bed, typically are found associated (UA 8-29-27-153; fig. 40, FMNH PR 3816; fig. 41; UA 9-5-98-449) or articulated (FMNH PR 2793 and FMNH PR 3820) with the ulna and/or elements of the manus.

This stocky element is slightly expanded proximally and distally; it ranges from 112 to 157 mm in length (table 4) within the sample. The proximal surface of the radius is mostly concave and D-shaped in proximal view; its flat medial side articulates with the anteromedial surface of the proximal portion of the ulna. The anteromedial portion of the

Fig. 40. Left radius of *Azendohsaurus madagaskarensis* (UA 8-29-97-153) in (**A**) proximal, (**B**) anterior, (**C**) medial, (**D**) medial, (**E**) lateral and (**F**) distal views. Scale = 1 cm. Arrows indicate anterior direction.

proximal surface is raised relative to the remainder of the proximal surface, as in *Trilophosaurus buettneri* (Gregory, 1945). No such raised margin occurs in *Mesosuchus browni* (SAM 8552), tanystropheids (e.g., MCSN BES SC 1018; MFSN 1921), or *Proterosuchus fergusi* (Cruickshank, 1972). In *A. madagaskarensis* a rounded ridge originates on the anterior portion of the radius and forms the anterior extent of the radius for much of the length of the element, with a much sharper ridge marking the lateral side of the proximal third of the shaft. This sharp lateral ridge is most pronounced in larger specimens (e.g., FMNH PR 3820). The shaft of the radius, bowed anteromedially, is circular in cross section at the midshaft. The distal end of the radius is compressed mediolaterally, giving the distal surface an oval outline. The distal surface is convex laterally and concave medially.

ULNA: The ulnae of *A. madagaskarensis* are well represented in the sample (figs. 42, 43). In general, the ulna is moderately expanded distally relative to its midshaft width, whereas the proximal end is greatly expanded and more than twice the width of the midshaft. Ulnae range in length from 134 to 177 mm (table 5). The ulna is compressed mediolaterally, and is curved such that it is convex laterally, with the distal third of the bone bowed anterolaterally. The robust, knoblike olecranon process is raised dorsally at the anterior portion of the proximal surface. The olecranon of *A. madagaskarensis* is proportionally similar to that of *Proterosuchus alexanderi* (NMQR 1484). The proximal portion of the ulna in *Trilophosaurus*

Fig. 41. Left radius of *Azendohsaurus madagaskarensis* (FMNH PR 3816) in (**A**) proximal, (**B**) anterior, (**C**) posterior, and (**D**) distal views. Scale = 1 cm. Arrows indicate anterior direction.

buettneri (TMM 31025-140) differs in exhibiting a proximodistally shorter olecranon and lesser development of the anterolateral tuber. *Mesosuchus browni* (SAM 6046) and *Rhynchosaurus* (Benton, 1990) exhibit similarly weak development of the proximal portion of the ulna. *Langobardisaurus tonelloi* (MFSN 1921), *Macrocnemus bassanii* (MCSN BES SC 111; Peyer, 1937), and *Tanystropheus longobardicus* (MCSN BES SC 265) exhibit little to no development of the olecranon process.

The humeral articular surface of the ulna is gently concave. In proximal view, a distinct, anterolaterally projecting ridge marks the lateral articulation with the radius. A similar ridge occurs in *Trilophosaurus buettneri* (Gregory, 1945). The medial side is concave along most of its proximal half. A marked, rounded muscle scar occurs on the anteromedial edge, about 1 cm distal to the proximal surface of the ulna (fig. 43C). This scar is likely to represent the insertion locations of the *m. biceps brachii* and *m. brachialis* as described by Abdala and Diogo (2010) (= *m. brachialis inferior* sensu Romer, 1944, and Dilkes, 2000), which are reported to have a common insertion in lepidosaurs and crocodylians (Romer, 1944; Dilkes, 2000), although Meers (2003) reports no *m. brachialis* attachment sites on the ulnae of crocodylians.

In undistorted specimens, the long axis of the distal end of the ulna is aligned at approximately a 30° angle (in proximal view) to that of the proximal end. The midshaft is mediolaterally compressed, resulting in an oval cross section. A muscle scar on that anterior surface, near its distal end, may be the attachment site for the *m. abductor pollicis longus* (Haines, 1939; Abdala and Diogo, 2010). The distal surface is convex and compressed mediolaterally.

MANUS: The manus of *A. madagaskarensis* is almost completely known (fig. 44) from a minimum of five individuals, ranging from associated, disarticulated examples (UA 98-98-498; fig. 45) to a nearly complete and articulated specimen (FMNH PR 3820,

TABLE 4
Measurements of radii (in mm) of *Azendohsaurus madagaskarensis*

Specimen	Side	Length	Proximal width	Distal width
UA 8-29-97-153 (fig. 40)	left	110	31	25
UA 8-28-98-307	left	146	31	34
FMNH PR 2793	left	X	35	38
FMNH PR 2760	left	151	35	33
FMNH PR 2760	right	147	35	33
UA 9-5-98-449	left	161	38	34
FMNH PR 2797	left	147	35	34
FMNH PR 3816 (fig. 41)	left	128	32	26
UA 7-15-99-592	left	140	38	31
FMNH PR 3820	right	138	27	32

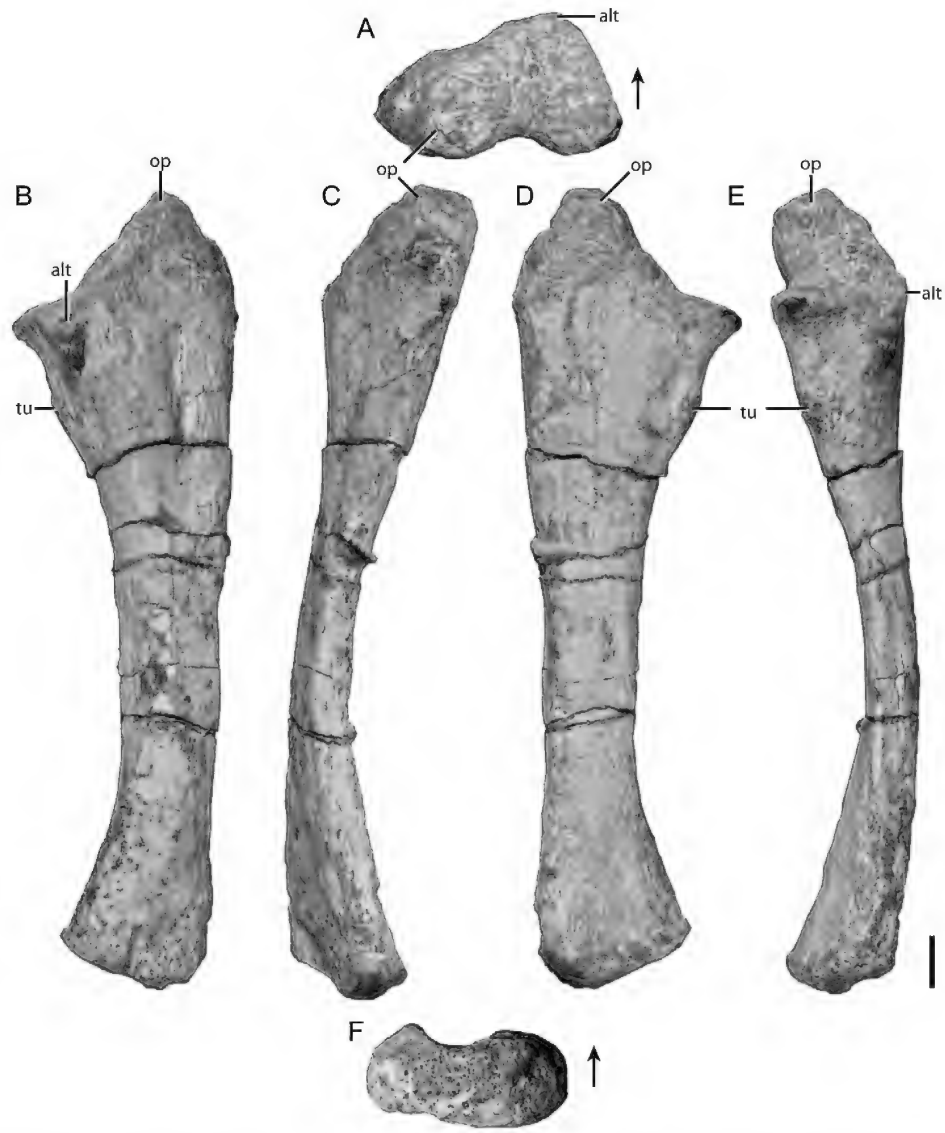

Fig. 42. Left ulna of *Azendohsaurus madagaskarensis* (UA 8-29-97-153) in (**A**) proximal, (**B**) anterior, (**C**) lateral, (**D**) posterior, (**E**) medial, and (**F**) distal views. Scale = 1 cm. Arrows indicate anterior direction. Abbreviations: **alt,** anterolateral tuber; **op,** olecranon process; **tu,** tuber.

fig. 46, table 6). In all specimens, the carpals, metacarpals, and phalanges are well ossified. The phalangeal formula is 2-3-4-5-3 (fig. 44), as in early diapsids (Reisz, 1981), *Protorosaurus speneri* (Gottmann-Quesada and Sander, 2009), *Rhynchosaurus articeps* (Benton, 1990), *Macrocnemus bassanii* (MCSN BES SC 111), and *Langobardisaurus tonelloi* (MFSN 1921). *Tanystropheus longobardicus* and *Tanytrachelos ahynis* differ in having four phalanges in the fourth digit (Nosotti, 2007; Pritchard et al., 2015).

In *A. madagaskarensis* the metacarpals diverge from the carpals in a smooth arc; digits I and V are not significantly divergent from the rest of the manus, in contrast to the divergent condition in *T. buettneri* (TMM-31025-140; Gregory, 1945). The manual

TABLE 5
Measurements of ulnae (in mm) of *Azendohsaurus madagaskarensis*

Specimen	Side	Length	Proximal width	Distal width
UA 8-29-97-153 (fig. 42)	left	137	39	28
FMNH PR 2790	left	170	54	39
FMNH PR 2793	left	153	51	40
UA 8-30-98-348	left	154	44	31
FMNH PR 2760	right	154	48	35
FMNH PR 2760	left	165	49	38
UA 9-5-98-449	left	181	53	35
FMNH PR 2797	left	168	53	39
FMNH PR 3816 (fig. 43)	left	155	44	30
FMNH PR 3820	right	150	44	34

digits are relatively short but are nearly symmetrical in dorsal view; the longest is digit III, which measures ~86% of the length of the ulna from the same limb. Digit V, the shortest, is barely exceeded in length by digit I; digits II and IV are also nearly equal in length to each other, but all are considerably shorter than digit III.

Nine carpals are preserved in FMNH PR 3820 including the radiale, intermedium, ulnare, lateral centrale, medial centrale, and the first, second, third, and fourth distal carpals (fig. 46). Carpals are fully ossified and bear distinct articular surfaces for the ulna, radius, metacarpals, or other carpals. A fifth distal carpal is not ossified in available specimens, nor does a clear articular facet for such an element exist on the ulnare or fourth distal carpal. A fifth distal carpal is absent in *Proterosuchus fergusi* (Cruickshank, 1972) and *Protorosaurus speneri* (Gottmann-Quesada and Sander, 2009). Tanystropheids lose additional distal carpals; *Tanystropheus longobardicus* (MCSN BES SC 1018; Wild, 1973) possesses only two. A pisiform, present in *Araeoscelis gracilis* (Vaughn, 1955), *Sphenodon punctatus* (FMNH 197942), and *Trilophosaurus buettneri* (TMM 31025-140; see appendix 2), is not recognized in the sample for *A. madagaskarensis*.

The manus of *A. madagaskarensis* is an important addition to our understanding of the evolution of the archosauromorph skeleton, as completely articulated, well-ossified

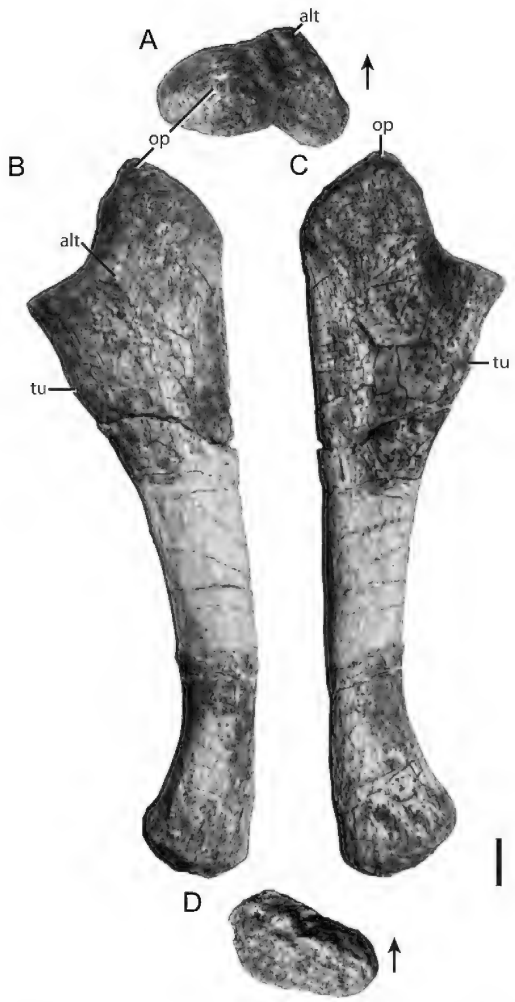

Fig. 43. Left ulna of *Azendohsaurus madagaskarensis* (FMNH PR 3816) in (**A**) proximal, (**B**) anterior, (**C**) posterior, and (**D**) distal views. Scale = 1 cm. Arrows indicate anterior direction. Abbreviations: **alt,** anterolateral tuber; **op,** olecranon process; **tu,** tuber.

hands are exceedingly rare for early members of the group. For example, the hands of most non-dinosaurian archosauromorphs are rarely preserved and those that are known are usually poorly ossified (e.g., *Macrocnemus bassanii*, MCSN BES SC 111; *Tanystropheus longobardicus*, MCSN BES SC 1018), or are slightly disarticulated, preventing a secure identification of carpal elements (e.g., "*Chasmatosaurus*" *yuani*, Young, 1936). Among early archosauromorphs, three-dimensional, well-preserved mani are described only for

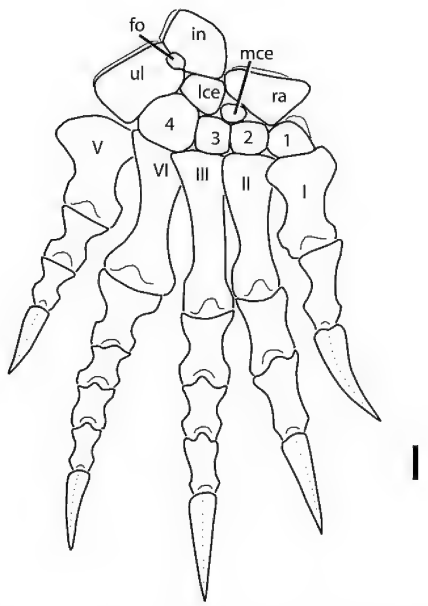

Fig. 44. Reconstruction of the right manus of *Azendohsaurus madagaskarensis* in dorsal view. Scale = 1 cm. Abbreviations: **fo,** foramen; **in,** intermedium; **lce,** lateral centrale; **mce,** median centrale; **ra,** radiale; **ul,** ulnare; **1,** distal carpal 1; **2,** distal carpal 2; **3,** distal carpal 3; **4,** distal carpal 4; **I,** digit I; **II,** digit II; **III,** digit III; **IV,** digit IV; **V,** digit V.

Noteosuchus colletti (Carroll, 1976), *Isalorhynchus genovefae* (Whatley, 2005), and *Trilophosaurus buettneri* (Gregory, 1945). In the case of *Trilophosaurus buettneri*, the identification of the proximal carpal elements is incorrect in the original description (Gregory, 1945). Fortunately, one of us (S.J.N.) recovered a partially articulated hand among the remains from the original *Trilophosaurus* Quarry at Otis Chalk, Texas. Using this new specimen and the nearly complete manus presented by Gregory (1945; fig. 10), we were able to reconstruct nearly the entire manus of *T. buettneri* (see appendix 2 for description), and use this as a comparison with the manus of *A. madagaskarensis*. The following description of *A. madagaskarensis* centers on a largely articulated right manus (FMNH PR 3820; fig. 46) supplemented by observations of FMNH PR 2797 (partial metacarpal and carpal series of the left manus, largest individual); FMNH PR 2793 (articulated proximal carpals of right manus); FMNH PR 2760 (left and right disarticulated and incomplete mani; fig. 45); FMNH PR 3817 (disarticulated, incomplete left manus, smallest individual); and UA 9-8-98-498 (fragmentary left manus).

The **radiale** can be identified confidently only in FMNH PR 3820 (fig. 46) and FMNH PR 3817. In the smallest manus recovered (FMNH PR 3817) the radiale was disarticulated from the rest of the carpals, whereas in FMNH PR 3820 the radiale is in near articulation with the rest of the carpals, but is slightly rotated anteriorly, with the lateral surface exposed in ventral view. Ventrally, the radiale is triangular, with the long side oriented mediolaterally on the proximal surface (fig. 46). The ventrolaterally directed lateral surface bears a shallow fossa for articulation with the first distal carpal, whereas the medioventrally deflected medial surface articulates with the medial centrale. Distally, the radiale tapers and meets the second distal carpal at its apex. The dorsal surface of the element is poorly ossified; the well-ossified ventral surface is penetrated by three or four centrally located foramina. The longitudinal ridge of the dorsal surface of the radiale of *Petrolacosaurus kansensis* (Reisz, 1981) is evidently absent in *Azendohsaurus*. The proximal surface of the radiale consists of a rounded, dorsally oriented region and a mediolaterally elongated region with a corresponding shallow fossa. The proximal surface of the radiale is much smaller than the distal surface of the radius of the same individual, suggesting that a significant amount of cartilage lay between the two elements in life rather than a significant bony articulation occurring between these bones. The smaller radiale, FMNH PR 3817, bears a relatively smaller proximal surface for articulation with the radius, suggesting that this part of the element ossified more fully through ontogeny.

There is no confirmed radiale in any known *Trilophosaurus buettneri* specimen (see appendix 2), nor in *Protorosaurus speneri* (Gottmann-Quesada and Sander, 2009). An ovoid radiale is reported in the early rhynchosaur *Noteosuchus colletti* (Carroll, 1976). An ossified radiale is not known in any tanystropheids; the elements identified by Kuhn-Schnyder (1959), Wild (1973), and Nosotti

Fig. 45. Left metacarpals (**A–E**) of *Azendohsaurus madagaskarensis* in (from top down) proximal, dorsal, lateral, ventral, and distal views. (**A**) Metacarpal I (UA 9-8-98-498); (**B**) metacarpal II (FMNH PR 2756); (**C**) metacarpal III FMNH PR 2756); (**D**) metacarpal IV (FMNH PR 2756); (**E**) metacarpal V (FMNH PR 3820) (reversed). Scale = 1 cm. Arrows indicate dorsal direction. Abbreviations: **dc1,** distal carpal one.

(2007) are actually intermedia (see Pritchard et al., 2015). Among early diapsids, disk-like radialia are known in *Petrolacosaurus kansensis* (Reisz, 1981), *Araeoscelis gracilis* (Vaughn, 1955), *Hovasaurus boulei*, and *Thadeosaurus colcanapi* (Caldwell, 1994).

The **intermedium** is preserved in articulation in FMNH PR 3820 (figs. 46, 47),

TABLE 6
Measurements of the complete right manus (in mm; figs. 46, 52) of *Azendohsaurus madagaskarensis* (FMNH PR 3820)
Abbreviation: inc, incomplete.

Digit	Element	Length from dorsal surface	Length from ventral surface	Digit length
I				79
	metacarpal I	29	29	
	phalanx I-1	25	35	
	phalanx I-2	25 inc	25 inc	
II				122
	metacarpal II	40	40	
	phalanx II-1	23	29	
	phalanx II-2	23	33	
	phalanx II-3	36	36	
III				138
	metacarpal III	49	49	
	phalanx III-1	19	24	
	phalanx III-2	18	26	
	phalanx III-3	19	29	
	phalanx III-4	33	33	
IV				119
	metacarpal IV	29	29	
	phalanx IV-1	19	22	
	phalanx IV-2	16	22	
	phalanx IV-3	15	21	
	phalanx IV-4	15	21	
	phalanx IV-5	25	25	
V				82
	metacarpal V	31	31	
	phalanx V-1	15	18	
	phalanx V-2	15	18	
	phalanx V-3	21	21	

FMNH PR 2793, and FMNH PR 2797, and disarticulated in the left manus of FMNH PR 2760. Compact bone forms the dorsal and ventral surfaces of the intermedium, whereas spongy, unfinished bone circumscribes the edges of the element. The dorsal surface is nearly smooth, whereas the ventral surface is covered in small pits and disorganized ridges. The ventral surface slopes toward a rounded notch located laterally. The overall shape and locations of the articular facet appear to be conserved throughout ontogeny, judging from comparison of the smallest (FMNH PR 3820, proximodistal length = 25 mm) and largest (FMNH PR 2797, proximodistal length = 30 mm) specimens.

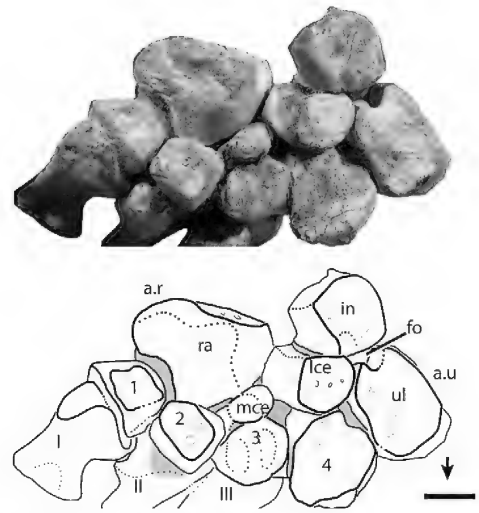

Fig. 46. Partially articulated right manus of *Azendohsaurus madagaskarensis* (FMNH PR 3820) in ventral view. Scale = 1 cm. Arrow indicates anterior direction. Gray in drawings represents matrix. Abbreviations: **a.,** articulates with; **fo,** foramen; **in,** intermedium; **lce,** lateral centrale; **mce,** median centrale; **r,** radius; **ra,** radiale; **u,** ulna; **ul,** ulnare; **1,** distal carpal I; **2,** distal carpal II; **3,** distal carpal III; **4,** distal carpal IV; **I,** digit one; **II,** digit two; **III,** digit three.

The robust, dorsoventrally compressed intermedium articulates with the ulna proximolaterally, the ulnare laterally, the lateral centrale distally, and the radiale medially. A similarly compressed intermedium occurs in *Protorosaurus speneri* (Gottmann-Quesada and Sander, 2009), *Noteosuchus colletti* (Carroll, 1976), and *Trilophosaurus buettneri* (TMM 31025-140). Taller, narrower intermedia occur in araeoscelids (Vaughn, 1955; Reisz, 1981) and tanystropheids (MCSN BES SC 1018). In *A. madagaskarensis*, the lateral contact between the intermedium and the ulnare is restricted to a dorsoventrally elongated, convex surface near the ulnar articulation. Ventral to this articulation, both the intermedium and the ulnare contribute to the border of a foramen that penetrates the manus (figs. 46, 47). This foramen is present in most amniotes plesiomorphically (see Romer, 1956), early diapsids (e.g., Vaughn, 1955; Reisz, 1981), *Protorosaurus speneri* (Gottmann-Quesada and Sander, 2009), tanystropheids (e.g., MCSN BES SC 1018), rhynchosaurs (e.g., Carroll, 1976), *Trilopho-*

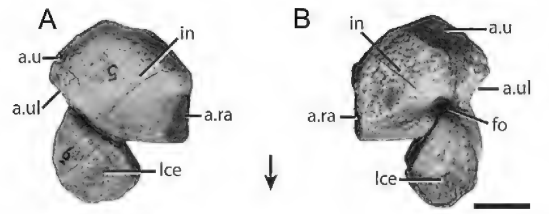

Fig. 47. Slight disarticulated right carpal elements, the intermedium and lateral centrale, of *Azendohsaurus madagaskarensis* (FMNH PR 3820) in (**A**) dorsal and (**B**) ventral views. Scale = 1 cm. Arrow indicates anterior direction. Abbreviations: **a.,** articulates with; **in,** intermedium; **fo,** foramen; **lce,** lateral centrale; **ra,** radiale; **u,** ulna; **ul,** ulnare.

saurus buettneri (TMM 31025-140), and *Sphenodon punctatus* (FMNH 197942), but is absent in those squamates possessing an intermedium (e.g., *Varanus salvator*, FMNH 31358) and in Archosauria (e.g., *Herrerasaurus ischigualstensis*; Sereno, 1994). The lateral centrale likely forms the ventral border of the perforating foramen, but this is not clearly observable in any specimen of *A. madasgaskarensis*. The convex distal surface of the intermedium articulates with the correspondingly concave proximal surface of the lateral centrale. This surface is clearly visible in FMNH PR 3820, as both elements are slightly displaced from their original positions, revealing the articular surface. In *Trilophosaurus buettneri* (TMM 31025-140), this surface of the intermedium is flat. In *A. madagaskarensis*, the articulation surface for the radiale is slightly convex and triangular in medial view. This articulation is separated from the rest of the medial surface by a deep concavity on the medial half of the dorsal surface. This concavity deepens medially where it reaches the medial edge of the intermedium. The proximomedial edge of the intermedium does not articulate with other elements. The proximolateral surface of the intermedium articulates with the mediodistal edge of the ulna. The articulation surface is expanded distally where it meets the articulation surface for the ulna and ulnare. The articulation between the carpus and ulna thus spans the intermedium and ulnare.

The general shape of the intermedium in *A. madagaskarensis* and the locations and shapes of its articular surfaces closely match those of *Trilophosaurus buettneri* (see appendix 2) and *Sphenodon punctatus* (FMNH 197942). The intermedium of *T. buettneri* (TMM 31025-140) is more proximodistally elongated than that of *A. madagaskarensis,* and its proximomedial edge is composed of finished bone. In contrast, this edge is consistently composed of unfinished bone in *A. madagaskarensis.*

The **ulnare** is preserved in articulation in FMNH PR 3820 (fig. 46), FMNH PR 2793, FMNH PR 2797, and FMNH PR 3817, and disarticulated in the right manus of FMNH PR 2760 (fig. 48). The ulnare is the largest carpal in the manus, forming much of the lateral side of the carpal row. Compact bone covers the dorsal, ventral, and medial surfaces of the element whereas unfinished bone envelops the remainder of the element. As with the intermedium, the overall shape and articular surfaces of the ulnare vary little from the smallest (FMNH PR 3817, proximodistal length = 15 mm) to the largest (FMNH PR 2797, proximodistal length = 25 mm) specimen.

The ulnare articulates with the ulna proximally, the intermedium proximomedially, the lateral centrale distomedially, and the fourth distal carpal ventrally. A similar pattern occurs in most early diapsids (Vaughn, 1955; Reisz, 1981). The articular surface with the ulna is distinctly concave and oval in proximal view. The medial side of the ulnare bears a proximal articulation surface with the intermedium and a distal articulation surface with the lateral centrale; these two surfaces are completely separated by the lateral wall of the perforating foramen. The proximal articular surface with the intermedium is concave, mirroring its slightly convex counterpart. This articulation surface spans the medial face of the ulnare, whereas in *Trilophosaurus buettneri* (TMM 31025-140) it is restricted to the anterior two-thirds of the ulnare. The bisecting channel that forms the lateral border of the perforating foramen trends dorsodistally; its concave surface is dotted with small foramina. Ventrally, the medial side of the ulnare articulates with the lateral centrale. This convex articular surface expands ventromedially from the main body of the ulnare, forming a small process that fits into a concave surface on the lateral side

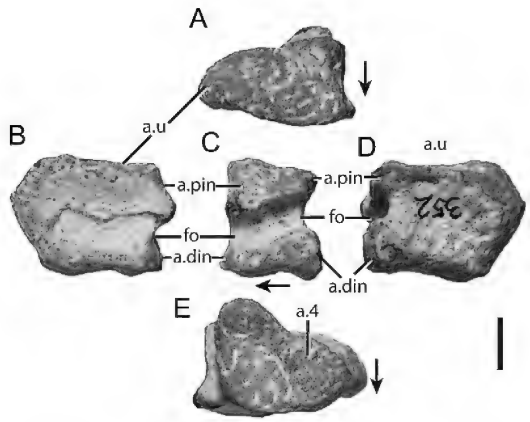

Fig. 48. Right ulnare of *Azendohsaurus madagaskarensis* (FMNH PR 2760) in (**A**) proximal, (**B**) anterior, (**C**) medial, (**D**) posterior, and (**E**) distal views. Scale = 1 cm. Arrows indicate anterior direction. Abbreviations: **a.,** articulates with; **din,** distal facet for the intermedium; **fo,** foramen; **pin,** proximal articulation for the intermedium; **u,** ulna; **4,** fourth carpal.

of the first distal carpal, as observed in FMNH PR 2793. The ventral surface of the ulnare articulates with the fourth distal carpal. The articular face is triangular, with a small ventromedial projection (expressed in medial view) for articulation with the medial centrale. The lateral side of the ulnare does not articulate with other elements; there is no clear facet for a pisiform, in contrast to one seen on the ventrolateral edge of the ulnare of *T. buettneri* (originally identified as the radiale by Gregory, 1945; see appendix 2) (TMM 31025-140).

The **lateral centrale** occurs in near articulation in FMNH PR 3820 (fig. 46), FMNH PR 2793, and FMNH PR 2797, and disarticulated in the right manus of FMNH PR 2760. None of the specimens are in precise articulation. The dorsal and ventral faces of this rectangular element are covered in finished bone, each bearing small central foramina. The lateral centrale articulates with the intermedium proximally, the ulnare proximolaterally, the third and fourth distal carpals distally, and likely the medial centrale medially. Most of the articular facets are flat (e.g., third and fourth distal carpal articular surface) or slightly concave (e.g., ulnare articular surface). The lateral centrale is about five times larger than the medial centrale. The lateral centrale of *Trilophosaurus buettneri* (TMM 31025-140; now lost) is similar in overall proportions to that of *A. madagaskarensis*. In contrast, the lateral centrale in *Sphenodon punctatus* (FMNH 197942) is tiny (fig. 49). Lateral centralia occur in early diapsids, such as *Hovasaurus boulei* and *Thadeosaurus colcanapi* (Caldwell, 1994) and one has been reported in the early rhynchosaur *Noteosuchus colletti* (Carroll, 1976).

The **medial centrale** is preserved only in the largely articulated manus of FMNH PR 3820 (fig. 46). This rounded element is the smallest carpal. The lack of distinguishing features of this element prevents a positive identification from disarticulated remains of *A. madagaskarensis*. In articulated specimens it is nestled between the second and third distal carpals, radiale, and lateral centrale. The medial centrale is flanked by the radiale dorsolaterally, second distal carpal ventrolaterally, third distal carpal ventromedially, and lateral centrale dorsomedially. The surfaces of this element are poorly ossified, and clear facets for surrounding carpals are lacking. Among saurians, *Sphenodon punctatus* (FMNH 197 942) has a medial centrale, but this element is much larger proportionally and more elongated mediolaterally than that of *A. madagaskarensis*. Proportionally larger medial centralia also occur in early diapsids (e.g., *Petrolacosaurus kansensis*, Reisz, 1981; *Hovasaurus boulei*; *Thadeosaurus colcanapi* Caldwell, 1994). Small and rounded medial centralia, reminiscent of those in *A. madagaskarensis,* have been reported in *Protorosaurus speneri* (Gottmann-Quesada and Sander, 2009) and *Noteosuchus colletti* (Carroll, 1976). It is unclear whether *Trilophosaurus buettneri* has a medial manual centrale.

The **first–fourth distal carpals** are preserved in articulation in FMNH PR 3820 (fig. 46), partial articulation in FMNH PR 2797, and disarticulated in FMNH PR 3817 and the right manus of FMNH PR 2760. The first distal carpal is confidently identified only in FMNH PR 3820 and UA 9-8-98-498 in which it is in near articulation with metacarpal I. The first distal carpal is wedge shaped and thins medially. Finished bone surfaces are present on the dorsal and ventral surfaces only. The element is crescent shaped

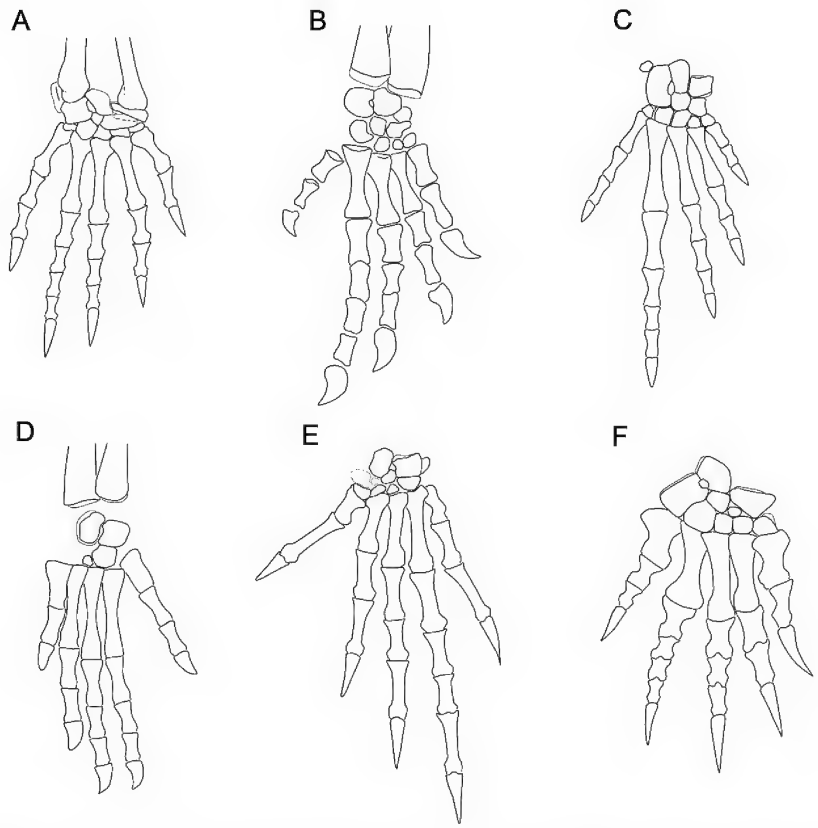

Fig. 49. The manus of diapsid reptiles in dorsal view. (**A**) Right manus of *Sphenodon punctatus* (FMNH 197942). (**B**) Right manus of *Protorosaurus spenceri* (WMsN P 47361) (redrawn from Gottmann-Quesada and Sander, 2009). (**C**) Right manus of *Petrolacosaurus kansensis* (modified from Reisz, 1981). (**D**) Left manus of *Tanystropheus longobardicus* (MSNM BES SC 1018). (**E**) Left manus of *Trilophosaurus buettneri* (redrawn from Gregory, 1945; see appendix 2). (**F**) Right manus of *Azendohsaurus madagaskarensis*.

dorsally, and slightly concave. The first distal carpal is the second largest element of the distal carpal series, as in *Trilophosaurus buettneri* (TMM 31025-141), *Macrocnemus bassanii* (Rieppel, 1989), and *Noteosuchus colletti* (Carroll, 1976). These proportions suggest an ossification sequence of the distal carpals similar to that in early diapsids (Caldwell, 1994), wherein the first distal carpal is the second to appear. In *A. madagaskarensis,* the first distal carpal articulates with metacarpal I distally, the second distal carpal medially, and the radiale proximally. The articular surfaces with the radiale and second distal carpal are flat, whereas the articular surface with metacarpal I is distinctly convex. This convex surface matches a distinctly concave surface on the proximal surface of metacarpal I, as in *T. buettneri* (TMM 31025-141).

The **second and third distal carpals** are cuboid, with the latter slightly larger than the former, as expected from the ossification sequences of carpals in early diapsids (Caldwell, 1994). Finished bone caps the dorsal and ventral surfaces, each bearing a small central foramen. Both distal carpals overlie their respective metacarpals, the long axes of the distal carpals paralleling the long axes of the metacarpals. The distal surfaces of the second and third distal carpals are flat, matching the proximal surfaces of their respective metacarpals.

The **fourth distal carpal** is preserved in articulation in FMNH PR 3820 (fig. 46), FMNH PR 2797, and FMNH PR 3817, and

as a disarticulated element in both mani of FMNH PR 2760 (fig. 50). The fourth distal carpal, the largest element of the distal carpal series, is about twice the size of the first distal carpal, as in most early diapsids (Caldwell, 1994), *Protorosaurus speneri* (Gottmann-Quesada and Sander, 2009), *Sphenodon punctatus*, and many squamates (Renous-Lécuru, 1973). Finished bone caps the dorsal and ventral surfaces, both of which bear small central foramina. The dorsal surface is distinctly concave and is much smaller than the flat ventral surface. The fourth distal carpal bears distinct facets for the ulnare proximolaterally, metacarpal IV distally, the third distal carpal medially, and the lateral centrale proximomedially. The articular surfaces with the ulnare and the third distal carpal are concave; concavities and convexities on the distal articular surface precisely match the proximal surface of metacarpal IV. The fourth distal carpal appears not to contact metacarpal V.

All **metacarpals** from *A. madagaskarensis* are known. Metacarpals I–IV occur in articulation in FMNH PR 3820 (fig. 46); most elements were recovered in both mani of FMNH PR 2760, but were disarticulated (fig. 51). The shafts of metacarpals I–V are subparallel, but the distal articular surfaces are generally directed away from the central axis of metacarpal III. The distal articular surfaces of metacarpals I and II are canted medially whereas the distal articular surfaces of metacarpals IV and V are canted laterally. Metacarpals II–V bear clear medial articular surfaces proximally, for articulation with neighboring elements, yielding lateral imbrication whereby more medial metacarpals overlap their lateral counterparts. A similar pattern occurs in *Protorosaurus speneri* (Gottmann-Quesada and Sander, 2009), *Macrocnemus bassanii* (MCSN BES SC 111), *Langobardisaurus tonelloi* (MFSN 1921), and *Tanystropheus longobardicus* (MCSN BES SC 1018). In proximal view, the metacarpals fit together precisely. The proximal surfaces of metacarpals II–IV are nearly flat and lack the distinct proximolateral processes seen in *Trilophosaurus buettneri* (TMM 31025-140). Such processes are also lacking in *Protorosaurus speneri* (Gottmann-Quesada and Sander, 2009), tanystropheids (e.g., MCSN BES SC 1018), and rhynchosaurs (Carroll, 1976).

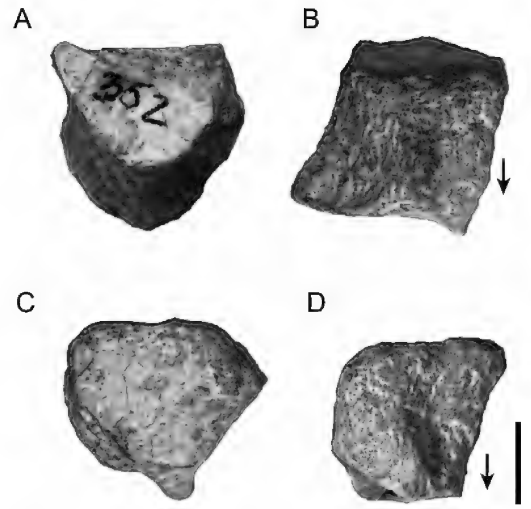

Fig. 50. Fourth distal carpal of *Azendohsaurus madagaskarensis* (FMNH PR 2756) in (**A**) dorsal, (**B**) proximal, (**C**) ventral, and (**D**) distal views. Scale = 1 cm. Arrows indicate anterior direction.

Metacarpal I is rarely preserved in the *A. madagaskarensis* sample; it is known from FMNH PR 3820 (fig. 46), FMNH PR 3817, and UA 9-8-98-498 (fig. 45). The length of metacarpal I equals that of metacarpal V, as in early diapsids (e.g., Caldwell, 1994) and most early archosauromorphs (e.g., *Tanystropheus longobardicus* MCSN BES SC 1018; Benton, 1990; Gottmann-Quesada and Sander, 2009). Metacarpal I is concave proximally. As a result, a small process on the medial side of the proximal portion almost reaches the proximal surface of the distal carpal series. A small, proximal facet on the lateral edge articulates with metacarpal II. The shaft of metacarpal I is nearly as broad (particularly proximally) as it is long. The main body of metacarpal I is asymmetrical, the lateral side being more distally expanded than the medial side (fig. 45). Consequently, the distal surface of metacarpal I is triangular rather than rectangular as it is in metacarpals II–V. Additionally, the medial ligament pit is shifted onto the dorsal surface, and an overhanging ridge transects much of the dorsal surface of the distal end. The lateral ligament pit is located in its usual position on the lateral side of the element. The medial ligament pit of metacarpal I of *Trilopho-*

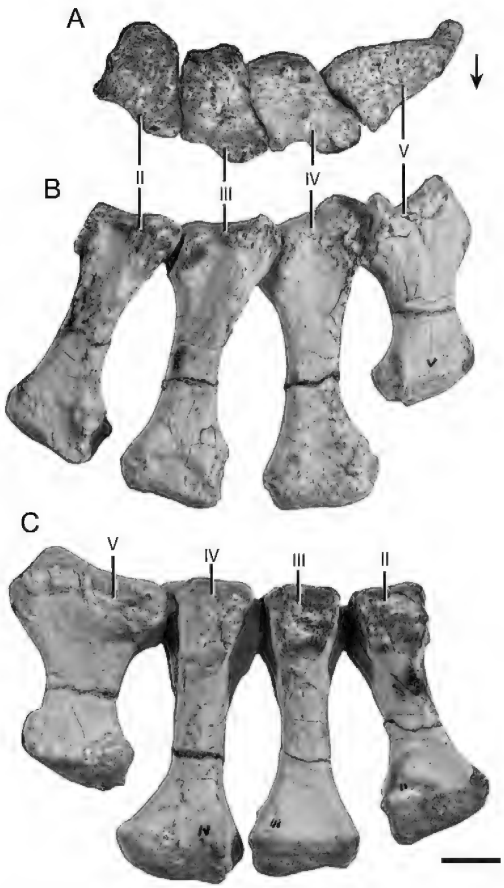

Fig. 51. Articulated left metacarpals of *Azendohsaurus madagaskarensis* (FMNH PR 2756) in (**A**) proximal, (**B**) dorsal, and (**C**) ventral views. Scale = 1 cm. Arrow indicates dorsal direction. Abbreviations: **II,** digit two; **III,** digit three; **IV,** digit four; **V,** digit five.

saurus buettneri (TMM 31025-140) is also positioned dorsally, but not to the degree seen in *A. madagaskarensis*. The orientation of the distal surface of metacarpal I directs the rest of the digit away from digit II.

Metacarpals II–IV (figs. 45, 51) are similar in the following regards: all bear distinct facets proximomedially for articulation with the immediately medial metacarpal, as well as a small concave region just ventral to these articular surfaces; all have short proximodorsal processes that dorsally overlap the laterally adjacent metacarpal. All have shallow medial and deep lateral ligament pits (as in *Trilophosaurus buettneri,* TMM 31025-140). The distal surfaces are nearly rectangular in outline in distal view, and their distal halves are nearly symmetrical. Metacarpals increase in length laterally beginning with metacarpal II. Sharp ridges occur dorsolaterally, just proximal to the midshaft of metacarpals II and III, but more prominently on the former. No such ridge is present in metacarpal IV.

Metacarpal V is represented by a number of specimens (FMNH PR 3820; fig. 45; 8-FMNH PR 2793; FMNH PR 2797), but has not been recovered articulated with other metacarpals. Nevertheless, the articular facet on the ventrolateral side of metacarpal IV and the articular facet on the medial side of the proximal portion of metacarpal V demonstrate that metacarpal V is clearly part of the metacarpal arc and is not divergent from the other metacarpals. The proximal portion of metacarpal V is divided into a convex area that articulates with metacarpal IV, a concave region that likely articulated with a cartilaginous fifth distal carpal, and a laterally deflected proximal process. The lateral, tablike proximal process projects ventrolaterally and extends ventrally to near midshaft. A similar but less strongly developed process occurs in *Trilophosaurus buettneri* (TMM 31025-140). Mimicking metacarpal I, the shaft of metacarpal V is subequal in length and width, and its body is strongly asymmetric along the proximodistal axis. The medial side of the distal end is deep dorsoventrally. A shallow ligament pit occurs medially, but the lateral side tapers without such a pit. This results in a laterally deflected, triangular outline of the distal surface.

All **manual digits** are preserved in FMNH PR 3820 (figs. 46, 52), with only minor disarticulation at some of the joints. In other specimens, the manual phalanges associated with the metacarpals are disarticulated. Nonterminal phalanges are generally similar in form, but differ slightly in mediolateral symmetry and length. The manual phalanges of *A. madagaskarensis* are short, similar to those in late diverging rhynchosaurs (Benton, 1990; Whatley, 2005) and "*Chasmatosaurus*" *yuani* (Young, 1936); the few manual phalanges reported for *Teraterpeton hrynewichorum* are very short (Sues, 2003). Slightly longer phalanges occur in *Langobardisaurus pandolfii* (MFSN 1921), *Protorosaurus speneri* (Gottmann-Quesada and Sander, 2009),

and *Tanystropheus longobardicus* (MCSN BES SC 1018), but the greatest proportional elongation occurs in *Trilophosaurus buettneri* (Gregory, 1945). In *A. madagaskarensis* pha - langes are longer ventrally than dorsally, the result of a strongly developed proximoventral process (table 6). The proximal articular surfaces are concave dorsoventrally, with strongly developed marginal ridges encircling their proximal surfaces. The shafts of the nonterminal phalanges are waisted relative to the articular ends, and are oval in cross section at midshaft (with a longer mediolateral axis). The distal articular ends, which are more expanded mediolaterally than dorsoventrally, are distinctly convex. Phalanges lack ligament pits medially, but bear marked ones laterally except in the penultimate phalanges of each digit (see below).

Proximally, the first phalanges in digits I–IV are nearly symmetrical mediolaterally and are wider than the more distal phalanges. The distal articular surfaces are canted medially, extending more distally on the lateral than the medial side. The first phalanx of digit I resembles the penultimate phalanges of the other digits in being highly asymmetrical proximally; a long medial process lies ventral to the distal articular facet of metacarpal I.

The second phalanges in digits III and IV are similar in form but shorter than phalanx 1 of their respective digits. The medial cant of the distal surface is more exaggerated in these phalanges; proximally, an elongated medial process underlies phalanx 1. The second and third phalanges of digit IV are nearly indistinguishable. The penultimate phalanx of each digit is unique relative to its more proximal phalangeal counterparts. These highly asymmetrical elements bear medial processes on the ventral surfaces of their proximal ends (figs. 52, 53). These tonguelike processes completely underlie the distal articular surfaces of the preceding phalages, similar to the condition in the early turtle *Proganochelys quenstedti* and some more recent turtles (Gaffney, 1990). In all digits, the penultimate phalanx is about the same length as the preceding phalanx, as in most early archosauromorphs (fig. 49). The penultimate phalanx is decidedly not the longest one, in contrast to the condition in *Trilophosaurus buettneri* (Gregory, 1945). The distal articular surface is grooved slightly at the midline. The medial and lateral sides of the distal ends converge dorsally, as in *T. buettneri* (TMM 31025-140), and both sides bear deep ligament pits.

The **terminal phalanges**, or unguals, are well preserved in a number of specimens (e.g., FMNH PR 3820, UA 9-8-98-498, FMNH PR 2760). All unguals are mediolaterally compressed, dorsoventrally tall, thin distally, and taper to sharp distal points (fig. 54), as in most early archosauromorphs (e.g., "*Chasmatosaurus*" *yuani*, Young, 1936; *Prolacerta broomi*, BP/1/2675). The unguals increase in overall size (e.g., depth) and length medially, with the ungual on digit V about half the length of that on digit I. The articular facet with the penultimate phalanx is concave. A small groove separates the proximal articular surface from a well-developed, rounded tubercle on the ventral surface of the ungual. This tubercle is also similarly well developed in *Trilophosaurus buettneri* and *Trilophosaurus jacobsi* (Gregory, 1945; Spielmann et al., 2005; 2008), but not in other early archosauromorphs (e.g. *Tanystropheus longobardicus*, MCSN BES SC 1018; *Teraterpeton hrynewichorum*, Sues, 2003). In *A. madagaskarensis* the tubercle is shifted ventrodistally relative to the proximal articular surface. The small groove separating the proximal articular surface from the ventral tubercle continues distally as a deep groove on both the medial and lateral sides. This dorsally open groove reaches the dorsal surface of the ungual near its tip. The dorsal edge of each ungual is rounded along most of its length, but becomes flatter distally. In ventral view, the proximal half of the ungual is rounded in the smaller elements (e.g., manual ungual V in FMNH PR 3820) but flat ventrally in larger ones (e.g., manual ungual I or II in FMNH PR 2760).

The curvature of the unguals is similar across specimens. Curvature, using Feduccia's (1993) measure, varies from ~95° to 125°, with larger unguals having a higher degree of curvature. The unguals of digits III–V of FMNH PR 3820 are gently arched proximodistally, whereas the larger unguals of FMNH PR 2760 are straight near their distal ends (fig. 54).

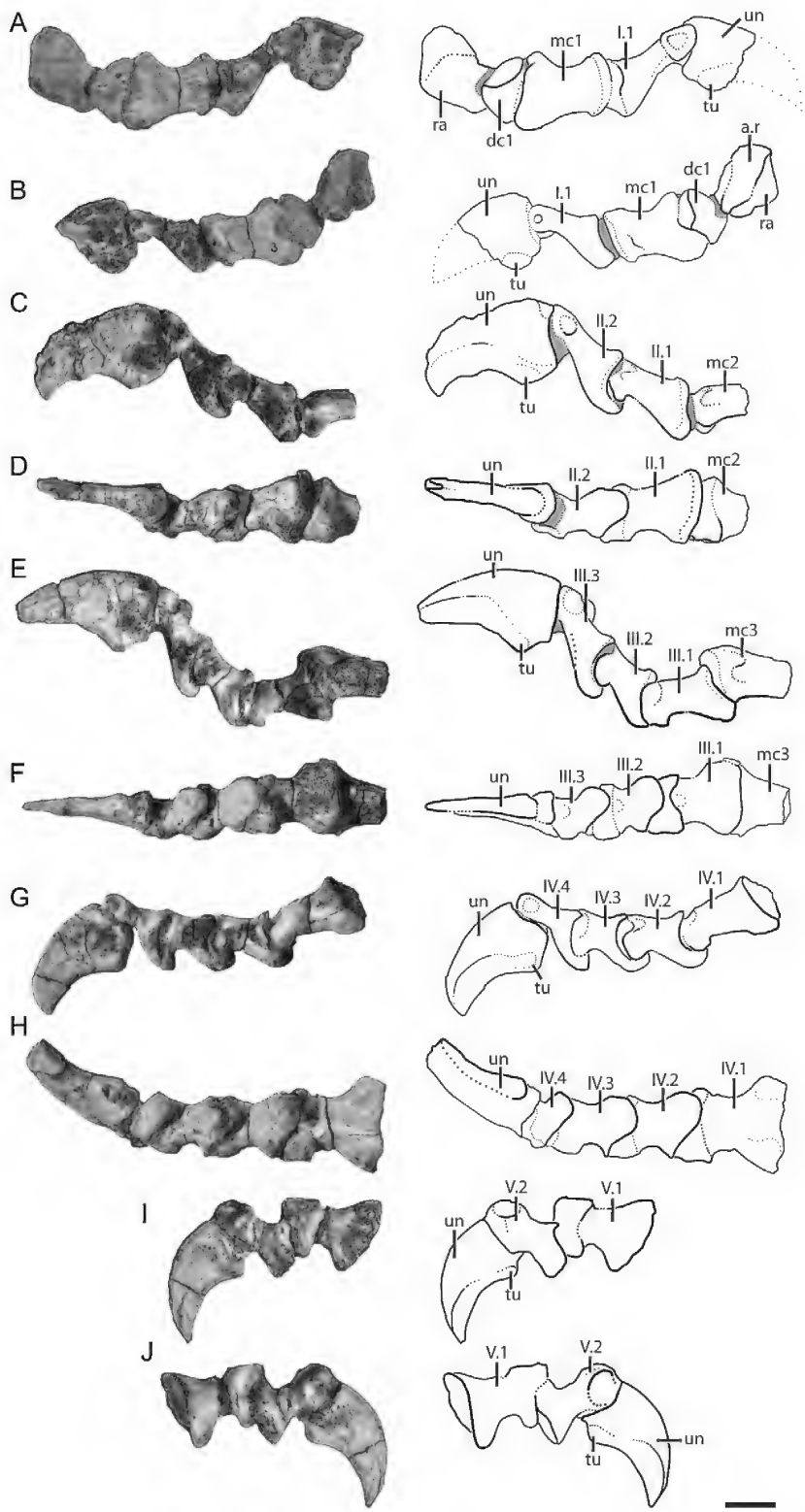
A
B
C
D
E
F
G
H
I
J
un
mc1
I.1
ra
dc1
tu
a.r
II.2
II.1
mc2
III.3
III.2
III.1
mc3
IV.4
IV.3
IV.2
IV.1
V.2
V.1

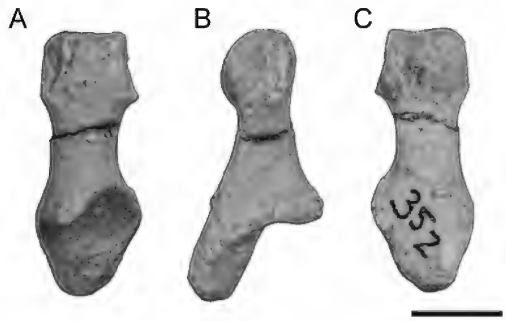

Fig. 53. Penultimate phalanx of the left manus of *Azendohsaurus madagaskarensis* (FMNH PR 2760) in (**A**) dorsal, (**B**) lateral, and (**C**) ventral views. Scale = 1 cm.

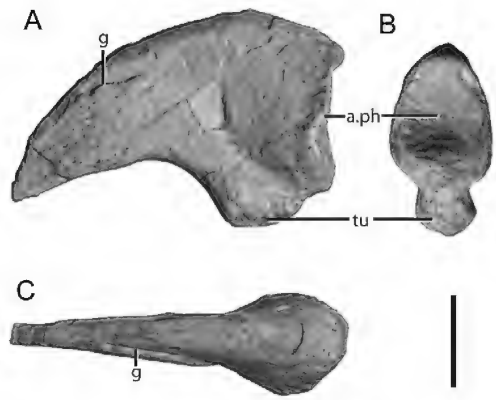

Fig. 54. A manual ungual of *Azendohsaurus madagaskarensis* (UA 9-8-98-497) in (**A**) left lateral, (**B**) proximal, and (**C**) dorsal views. Scale = 1 cm. Abbreviations: **a.,** articulates with; **g,** groove; **ph,** phalanx; **tu,** tuber.

Pelvic Girdle

A single associated pelvis from the left and right sides (FMNH PR 2794) is known for *A. madagaskarensis.* Most other elements of the pelvic girdle were found disarticulated and isolated. The pelvic girdle is formed of equally sized ilia, pubes, and ischia, all three of which contribute to a round acetabulum (fig. 55). The medial wall of the acetabulum is completely ossified, not open as in dinosaurs. The acetabulum must have been deflected ventrally 10° to 25° from vertical given that the lateral articular facets of the sacral ribs are deflected ventrally 10° to 25° from vertical, and the ischial and pubic peduncles must be deflected medially for the pubis and ischium to meet at the midline.

Ilium: A number of complete *A. madagaskarensis* ilia are known, including a complementary pair in FMNH PR 2794, and isolated examples in UA 9-5-98-448, FMNH PR 2769, and FMNH PR 2787 (fig. 56). The iliac component of the acetabulum is shallow and bordered dorsally by a moderately developed supraacetabular crest. The supraacetabular crest stretches from the anterior portion of the pubic peduncle to just anterior to the posteriormost extent of the acetabulum, as in *Proterosuchus alexanderi* (NMQR 1484), *Prolacerta broomi* (BP/1/2676), *Tanystropheus longobardicus* (MCSN BES SC 1018), and *Tanytrachelos ahynis* (AMNH FARB 7206). The supraacetabular crest in *A. madagaskarensis* is thickest dorsally, thinning anteriorly where it meets the pubic peduncle. The depth of the acetabulum exceeds the thickness of the bone forming its medial wall. Bone within the acetabulum is somewhat spongy and not covered in compact bone. The pubic and ischiadic peduncles form the ventral portion of the ilial contribution to the acetabulum. The pubic peduncle joins the ischiadic peduncle at a point just ventral to the thickest part of the supraacetabular crest, at an angle near 135° in lateral view. This angle seems to be consistent in the better-preserved ilia of *A. madagaskarensis,* not variable as reported for *Trilophosaurus buettneri* (Gregory, 1945).

←

Fig. 52. Right manual digits of *Azendohsaurus madagaskarensis* (FMNH PR 3820). Digit one in (**A**) ventral and (**B**) dorsal views with associated drawings (right). Digit two in (**C**) medial and (**D**) ventral views with associated drawings (right). Digit three in (**E**) medial and (**F**) ventral views with associated drawings (right). Digit four in (**G**) medial and (**H**) ventral views with associated drawings (right). Digit five in (**I**) ventral and (**J**) dorsal views with associated drawings (right). Note, some of the phalanges are slightly disarticulated. Scale = 1 cm. Gray in drawings represents matrix. Abbreviations: **a.,** articulates with; **dc1,** distal carpal 1; **mc,** metacarpal; **r,** radius; **ra,** radiale; **tu,** tuber; **un,** ungual; **I,** digit one; **II,** digit two; **III,** digit three; **IV,** digit four; **V,** digit five.

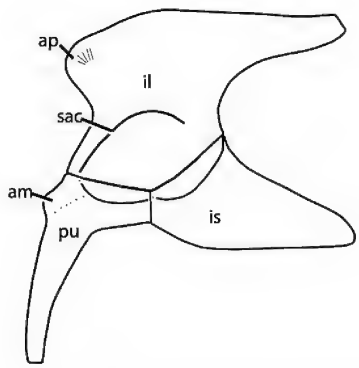

Fig. 55. Reconstruction of the pelvis of *Azendohsaurus madagaskarensis*. Abbreviations: **am,** ambiens process; **ap,** anterior process; **il,** ilium; **is,** ischium; **pu,** pubis; **sac,** supraacetabular crest.

The pubic and ischiadic peduncles of the ilium have straight articular facets where they meet the pubis and ischium, respectively. *Azendohsaurus madagaskarensis* thus lacks the angled ischiadic peduncle seen in *Proterosuchus alexanderi* (NMQR 1484), "*Chasmatosaurus*" *yuani* (Young, 1936), and *Erythrosuchus africanus* (NHMUK R 3592). In ventral view, the pubic peduncle of *A. madagaskarensis* thins posteriorly where it meets the ischiadic peduncle, whereas the ischiadic peduncle thickens posteriorly. The ventral surfaces of both peduncles are rugose and capped by spongy bone.

The iliac blade is nearly as tall dorsoventrally as the greatest dorsoventral height of the acetabular portion of the ilium. The iliac blade bears anterior and posterior processes. A distinct anterior process is present in various archosauromorphs, including *Jesairosaurus lehmani* (MNHN ZAR 12), late-diverging tanystropheids (e.g., *Tanystropheus longobardicus*, MCSN BES SC 1018; *Tanytrachelos ahynis*, AMNH FARB 7206), late-diverging rhynchosaurs (e.g., *Stenaulorhynchus stockleyi*, Huene, 1937; *Hyperodapedon gordoni*, Benton, 1983), *Erythrosuchus africanus* (NHMUK 3592), *Euparkeria capensis* (Ewer, 1965), and members of Archosauria. It is absent, however, in *Prolacerta broomi* (BP/1/2676) and *Trilophosaurus buettneri* (Gregory, 1945). The anterior process of *A. madagaskarensis* joins the dorsal margin of the supraacetabular crest via a mediolaterally thickened, rounded ridge that is directed anterodorsally. This ridge essentially becomes the anterior process, rather than dividing the anterior process from the posterior portion of the ilium as in some poposauroid loricatan archosaurs (see Nesbitt, 2011). In lateral view, the anterodorsal portion of the anterior process is gently rounded and bears long, deep grooves. Just posterior to the anterior process, the lateral surface of the iliac blade is concave; this concavity reaches the posterior end of the iliac blade, similar to the condition in "*Scaphonyx*" *fischeri* (MCZ 1529). In contrast, the lateral surface of the blade is roughly planar in *Erythrosuchus africanus* (NHMUK R 3592) and *Trilophosaurus buettneri* (TMM 31025-73). The dorsal margin of the iliac blade is mediolaterally thin in dorsal view and distinctly convex in lateral view. Convex iliac blades occur in certain rhynchosaurs (*Mesosuchus browni*, SAM 7416; "*Scaphonyx*" *fischeri*, MCZ 1529; *Rhynchosaurus articeps*, Benton, 1990), whereas more flattened dorsal margins occur in *Prolacerta broomi* (BP/1/2676), "*Chasmatosaurus*" *yuani* (Young, 1936), and *Tanystropheus longobardicus* (Wild, 1973). In *A. madagaskarensis* shallow, posterodorsally directed ridges adorn the dorsal edge of the bone in lateral view. The posterior process of the ilium tapers posteriorly, terminating in a rounded process that expands slightly posterodorsally (fig. 56). The ventral surface of the posterior process is rounded.

Medially, the ilium bears two large scars for articulation with the sacral vertebrae

→

Fig. 56. Ilia of *Azendohsaurus madagaskarensis*. Left ilium (FMNH PR 2794) in (**A**) lateral, (**B**) medial, and (**C**) dorsal views. Left ilium (UA 9-5-98-448) in (**D**) lateral and (**E**) medial views. Left ilium (FMNH PR 2769) in (**F**) lateral and (**G**) medial views. Right ilium (FMNH PR 2787) and articulated ischium in (**H**) lateral and (**I**) medial views. Scales = 1 cm. Abbreviations: **a.,** articulates with; **ace,** acetabulum; **ap,** anterior process; **ipi,** ischial peduncle of the ilium; **isc,** ischium; **pp,** posterior process of the ilium; **ppi,** pubic peduncle of the ilium; **sr1,** sacral rib 1; **sr2,** sacral rib 2; **sac,** supraacetabular crest.

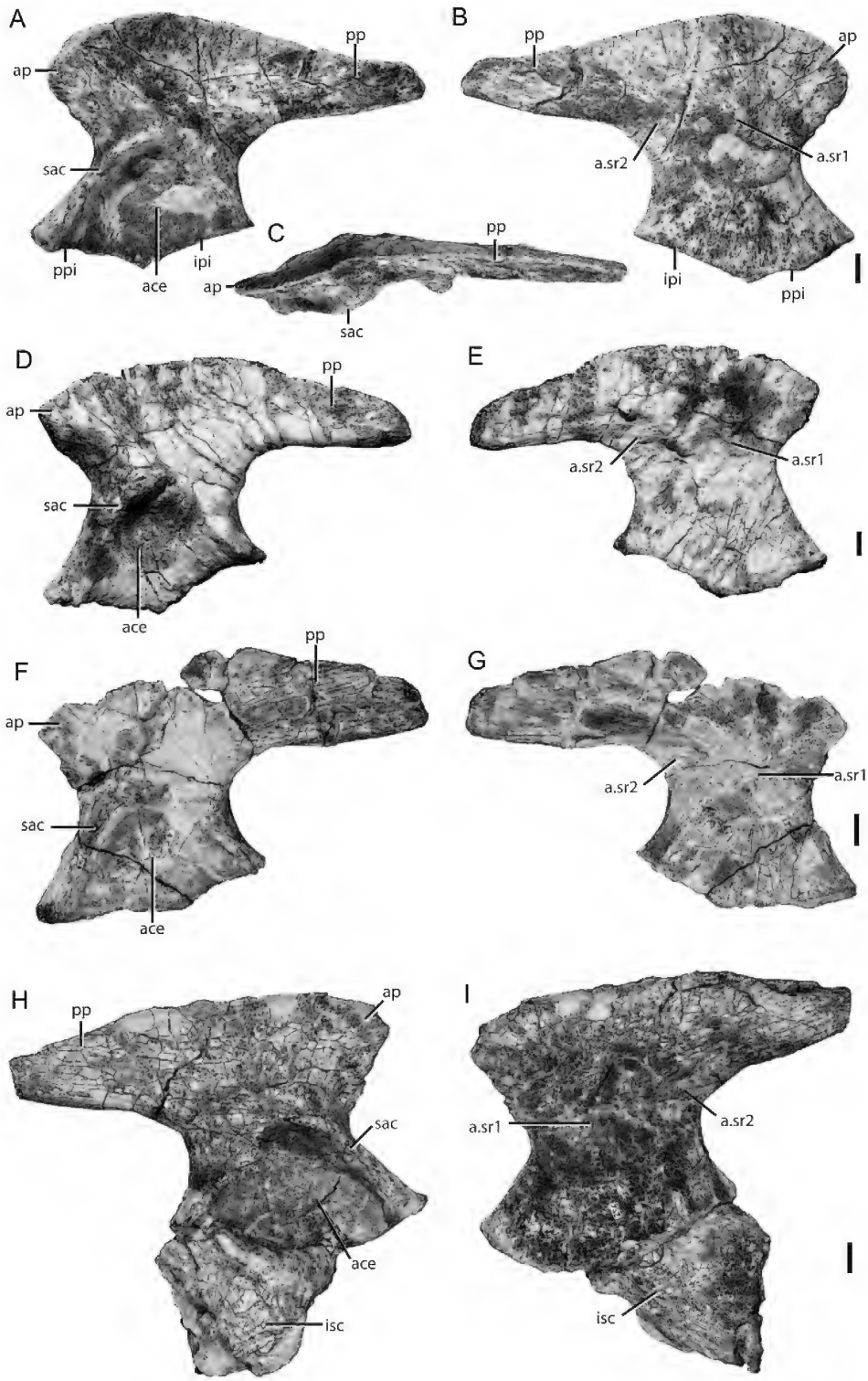
A
pp
ap
sac
ppi
ipi
ace
B
pp
ap
a.sr2
a.sr1
ipi
ppi
C
pp
ap
sac
D
pp
ap
sac
ace
E
a.sr2
a.sr1
F
pp
ap
sac
ace
G
a.sr2
a.sr1
H
pp
ap
sac
ace
isc
I
a.sr1
a.sr2
isc

(fig. 57). The scar for ancestral sacral one (= primordial sacral one of Nesbitt, 2011) corresponds with the comparatively larger, more anterior sacral rib scar. The rounded scar occupies the area medial to the acetabulum and the ventral portion of the iliac blade. The scar for ancestral sacral two (= primordial sacral two of Nesbitt, 2011) is posteriorly elongated at the juncture between the ischial peduncle and the postacetabular process. There is no clear medial ridge with which the ancestral sacral two articulated, in contrast to most archosauriforms (e.g., *Erythrosuchus africanus*; Gower, 2003). The sacral scars from ancestral sacral ribs one and two are similar in relative size to those of other early diverging archosauromorphs, such as *Trilophosaurus buettneri* (Gregory, 1945), *Prolacerta broomi* (BP/1/2676), and rhynchosaurs (e.g., MCZ 1529; Chatterjee, 1974).

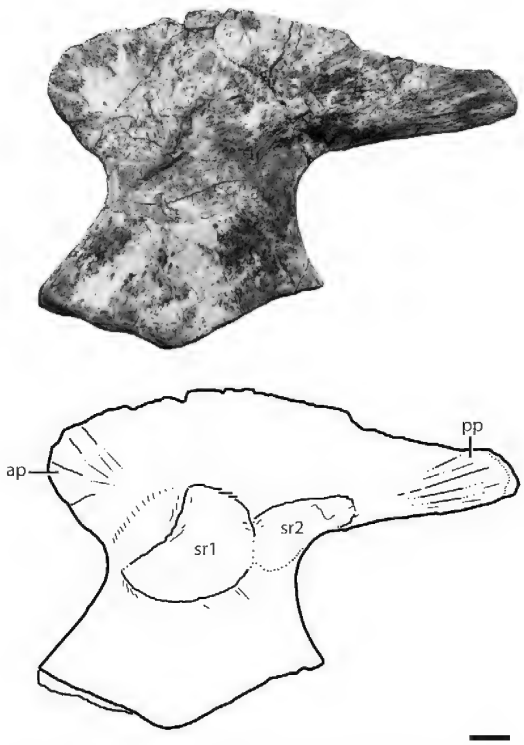

Fig. 57. Right ilium of *Azendohsaurus madagaskarensis* (FMNH PR 2794) in medial view illustrating the sacral rib attachments. Scale = 1 cm. Abbreviations: **ap,** anterior process; **pp,** posterior process of the ilium; **sr1,** attachment with sacral rib 1; **sr2,** attachment with sacral rib 2.

PUBIS: The pubis of *A. madagaskarensis* is represented by a number of relatively uncrushed specimens (FMNH PR 2794), allowing observation of its original three-dimensional structure (fig. 58). The proximal portion of the pubis forms the anteroventral margin of the acetabulum; the articular surface with the ilium is a perfect antimere of the articulation surface of the pubic peduncle of the ilium. The pubis meets the ischium at a short, straight, and dorsoventrally oriented contact. In contrast, a gap in the puboischiadic contact forms a thyroid fenestra in lepidosaurs (Russell and Bauer, 2008) and tanystropheids (e.g., *Macrocnemus bassanii*, MCSN V 457; *Tanystropheus longobardicus*, MCSN BES SC 1018). Small interruptions in the contact also occur in *Youngina capensis* (Gow, 1975) and *Mesosuchus browni* (SAM-PK 7416). In *A. madagaskarensis*, contact between the two elements trends medioventrally at nearly a 45° angle and thins ventrally. A small, dorsally expanded notch is likely present between the pubis and the ischium at the ventral margin. Similar notches occur broadly among archosauromorphs (e.g., rhynchosaurs, Benton, 1990; *Proterosuchus alexanderi*, NMQR 1484). The ventrolaterally directed, oval obturator foramen lies just a few millimeters anterior of the proximal contact between the pubis and the ischium.

Laterally, the pubis of *A. madagaskarensis* bears a thickened, dorsolaterally projecting, and flangelike ambiens process near the acetabular margin. Such a process is common in early archosauromorphs (e.g., *Prolacerta broomi*, BP/1/2676), although others exhibit a broader attachment site (e.g., *Erythrosuchus africanus*, NHMUK 3592; Hutchinson, 2001). In *A. madagaskarensis*, the dorsal portion of the ambiens process connects directly to the acetabulum margin through unfinished bone (FMNH PR 2794), whereas the ambiens process is clearly separated from the acetabular margin in *Trilophosaurus buettneri* (TMM 31025-79B). In lateral view, the shaft of the pubis arcs anteroventrally; it terminates ventrally with a very slight expansion (i.e., the terminal end of the pubic shaft is slightly thicker than the more proximal portion), as in *Trilophosaurus buettneri*

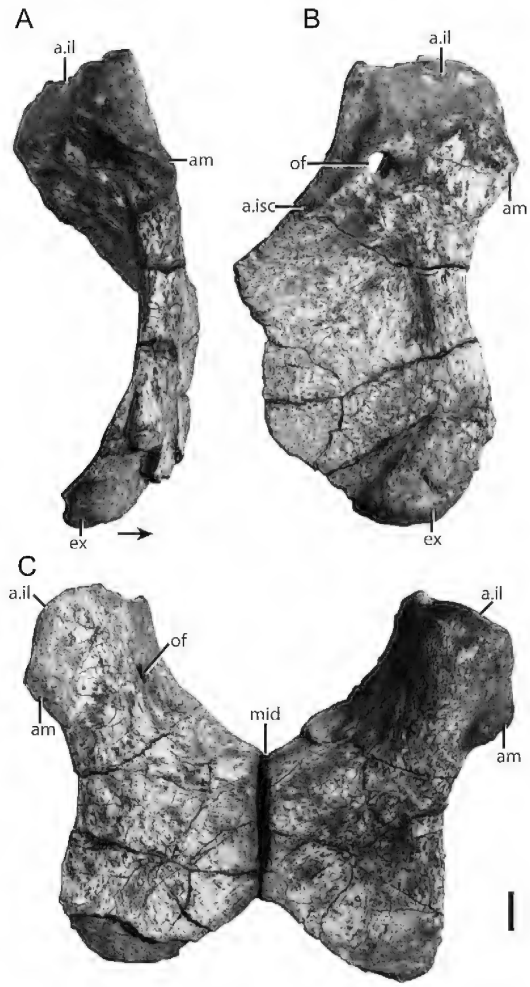

Fig. 58. Right pubis of *Azendohsaurus madagaskarensis* (FMNH PR 2794) in (**A**) lateral and (**B**) posterior views. The left and right pubes (FMNH PR 2794) in articulation **C**, in anterior view. Scale = 1 cm. Arrow indicates anterior direction. Abbreviations: **a.,** articulates with; **am,** ambiens process; **ex,** expansion; **il,** ilium; **isc,** ischium; **mid,** midline; **of,** obturator foramen.

(31025-79B) but in contrast to the greater distal expansion in *Prolacerta broomi* (BP/1/2676), *Proterosuchus alexanderi* (Cruickshank, 1972), *Protorosaurus speneri* (Gottmann-Quesada and Sander, 2009), and most rhynchosaurs (e.g., *Howesia browni*, Dilkes, 1995; *Hyperodapedon gordoni*, Benton, 1983). The distal end is capped in spongy bone.

In anterior view, the articulated pubes of *A. madagaskarensis* form a distinct pubic apron (fig. 58C), as in *Prolacerta broomi* (BP/1/2676), *Pamelaria dolichotrachela* (Sen, 2003), *Trilophosaurus buettneri* (TMM 31025-79B), and archosauriforms (e.g., *Erythrosuchus africanus*, Gower, 2003; *Euparkeria capensis*, Ewer, 1965). The two pubes of *A. madagaskarensis* meet anteriorly at a dorsoventrally oriented contact. More proximally, the contact slopes posterodorsally, becoming nearly horizontal at its posterior termination. The anterior face of the pubic apron is completely flat. The ventral edges of the pubes converge dorsomedially, creating a triangular notch between the pubes ventrally in anterior view (fig. 58C). A similar notch occurs in *Erythrosuchus africanus* (NHMUK R 3592), and one has been illustrated for *Pamelaria dolichotrachela* (Sen, 2003).

ISCHIUM: The ischium of *A. madagaskarensis* is represented by isolated elements (FMNH PR 2777) and specimens directly associated with other parts of the pelvis (FMNH PR 2794; fig. 59). The ischium is triangular in ventrolateral view. A low acetabular rim separates the acetabular portion of the ischium from the main body. The articulation surface with the ilium precisely mirrors its counterpart (the ischiadic peduncle of the ilium). The dorsoventrally oriented articular edge with the pubis ends two-thirds of the way along the length of the ischium from the acetabular edge. The posterior process of the ischium is short; it is shorter anteroposteriorly than the iliac blade, as in a number of early archosauromorphs (e.g., *Macrocnemus bassanii*, MCSN V 457; *Prolacerta broomi*, BP/1/2676). In ventrolateral view, the posterior portion terminates in a gently rounded posteroventral corner; the posterior margin of the ischium is more strongly angled in *Trilophosaurus buettneri* (TMM 31025-78), rhynchosaurs (MCZ 1666; Dilkes, 1998), and archosauriforms (e.g., *Proterosuchus alexanderi*, NMQR 1484; *Euparkeria capensis*, Ewer, 1965). In tanystropheids, the ischium bears a posteriorly directed process posterodorsally (e.g., *Macrocnemus bassanii*, MCSN V 457; *Langobardisaurus pandolfii*, MCSNB 2883). In *A. madagaskarensis*, the entire ventral edge and posterodorsal edges of the posterior portion of the ischium are straight.

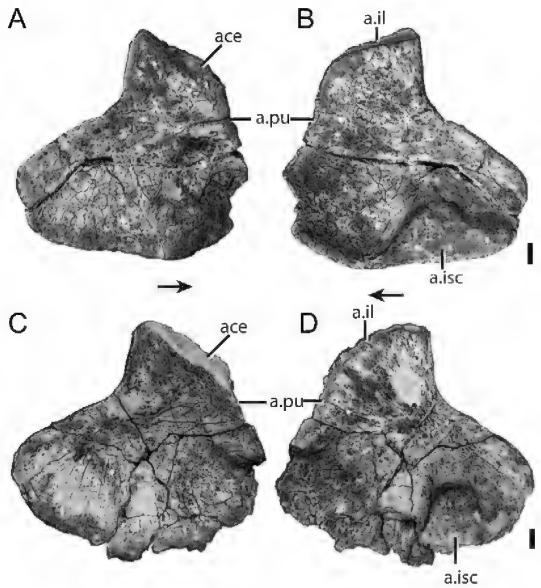

Fig. 59. Ischia of *Azendohsaurus madagaskarensis*. Right ischium (FMNH PR 2794) in (**A**) ventrolateral and (**B**) dorsomedial view. Right ischium (FMNH PR 2777) in (**C**) ventrolateral and (**D**) dorsomedial view. Scales = 1 cm. Arrows indicate anterior direction. Abbreviations: **a.,** articulates with; **ace,** acetabulum; **il,** ilium; **isc,** ischium; **pu,** pubis.

Medially, the main body of the ischium is concave ventral to the iliac articulation. A large articulation surface at the ventral margin marks the contact with its antimere; a similar surface is present in well-preserved specimens of *Trilophosaurus buettneri* (TMM 31025-79), but the area of articulation is proportionally much smaller in *T. buettneri*. The expanded articular surface of *A. madagaskarensis* has not been reported in other archosauromorphs (e.g., rhynchosaurs exhibit a straight, unexpanded ischial symphysis, as in MCZ 1666). In *Azendohsaurus* and *Trilophosaurus*, this large, rugose articulation surface is thickened dorsomedially and occupies ~70% of the ventromedial edge.

Hind Limb

The orientation terminology employed below follows those of Rewcastle (1980) and Gower (1996) for the hindlimb of *Erythrosuchus* and closely related taxa.

Femur: Complete femora are rare within the quarry (table 7). The best-preserved example, FMNH PR 2799, is a complete and nearly uncrushed right element (fig. 60). The shaft is weakly sigmoidal in anterior and dorsal views; the middle of the shaft is straight. The femora of most early archosauromorphs are similar in this respect, with the major exceptions the extremely straight femoral shafts of *Langobardisaurus pandolfii* (MCSNB 2883, MFSN 1921), and tanystropheids (*Tanytrachelos ahynis* [VMNH 120049], Pritchard et al., 2015). In *A. madagaskarensis*, the proximal end is modestly expanded relative to the midshaft, as in some rhynchosaurs (e.g., "*Scaphonyx*" *fischeri*, MCZ 4637) and early archosauriforms (e.g., *Proterosuchus alexanderi*, NMQR 1484; *Erythrosuchus africanus*, NHMUK 3592). The femoral head is more weakly expanded in tanystropheids (e.g., *Tanytrachelos ahynis*, AMNH FARB 7206; unnamed taxon, GR 301). The roughened proximal surface is rounded anteriorly, tapers posterodorsally, and lacks the groove that occurs in other early archosauromorphs and extant lepidosaurs when the proximal femoral epiphyses are removed. The posterodorsally tapered portion of the proximal surface continues distally as a rounded ridge that forms the posterodorsal margin of the femur for approximately one-third of its length. The ridge for attachment of the caudifemoralis musculature (= internal trochanter of some authors) is located ventrally on the proximal end. The ridge is fingerlike proximally and rounded ventrally, as in early diapsids (e.g., Reisz, 1981) and early archosauromorphs (e.g., *Tanystropheus conspicuus*, Wild, 1973; *Trilophosaurus buettneri*, TMM 31025-140). The ridge originates just distal to the proximal surface of the femur, but nearly reaches the midshaft distally. An intertrochanteric fossa is bordered by the posterodorsal ridge (which originates at the proximal surface), the proximoventral edge, and the ridge for attachment of the caudifemoralis musculature. The surface of the fossa is rugose. An intertrochanteric fossa also occurs in *Erythrosuchus africanus* (NHMUK R3592), *Proterosuchus alexanderi* (NMQR 1484), and *Prolacerta broomi* (BP/1/2676). A weakly developed fossa occurs in *Tanystropheus*

TABLE 7
Measurements of femora (in mm) of *Azendohsaurus madagaskarensis*

Specimen	Side	Length	Proximal width	Distal width	Circumference at midshaft
FMNH PR 2794	right	210	55	55	28
FMNH PR 2799 (fig. 60)	left	215	55	55	30
UA 7-13-99-576	left	210	55	70 est	28
UA 7-13-99-576	right	215	55	60	28

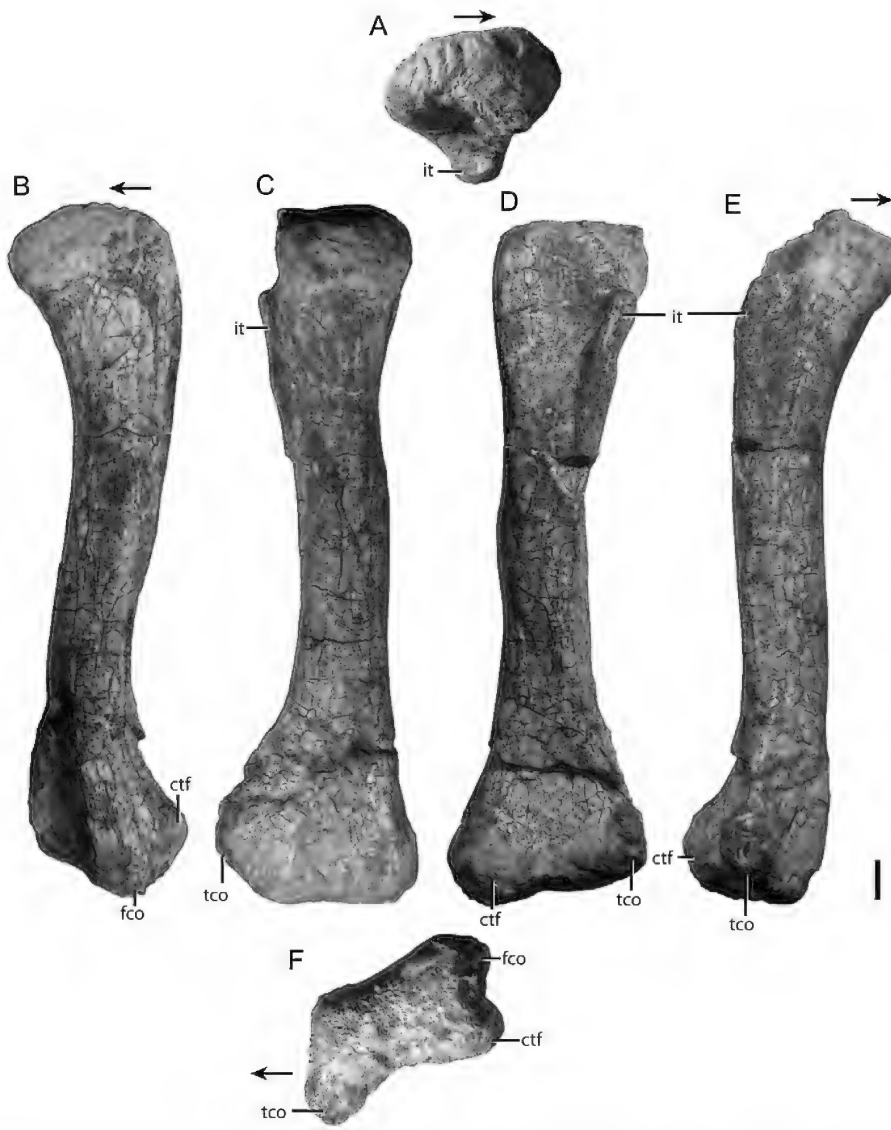

Fig. 60. Left femur of *Azendohsaurus madagaskarensis* (FMNH PR 2799) in (**A**) proximal, (**B**) dorsal, (**C**) anterodorsal, (**D**) posteroventral, (**E**) ventral and (**F**) distal views. Scale = 1 cm. Arrows indicate anterior direction. Abbreviations: **ctf,** crista tibiofibularis; **fco,** fibular condyle; **it,** internal trochanter; **tco,** tibial condyle.

conspicuus (Wild, 1973) and in other tanystropheid femora (Pritchard et al., 2015). The fossa is absent in *Trilophosaurus buettneri* (TMM 31025-67) and *Sphenodon punctatus* (FMNH 197942). The shaft of the femur is twisted, such that the long axes of the proximal and distal ends are offset by ~75° in proximal view. The midshaft is circular in cross section.

The distal end of the femur is greatly expanded anteroposteriorly relative to the midshaft, as in non-archosaurian archosauriforms, *Trilophosaurus buettneri* (TMM 31025-67), rhynchosaurs (e.g., *Noteosuchus colletti*, Carroll, 1976; *Mesosuchus browni*, Dilkes, 1998; *Hyperodapedon gordoni*, Benton, 1983), and *Erythrosuchus africanus* (NHMUK R3592). A less expanded distal end occurs in *Prolacerta broomi* (BP/1/2676) and tanystropheids (e.g., *Tanystropheus conspicuus*, Wild, 1973; unnamed taxon, GR 301, Pritchard et al., 2015). The distal end consists of two ventrally projecting condyles, separated by a gently excavated intercondylar fossa (fig. 60). The tibial condyle (= medial condyle in archosaurs) tapers ventrally whereas the posterior portion of the fibular condyle (= lateral condyle in archosaurs) tapers posteriorly. The fibular condyle is separated from the ventrally shifted crista tibiofibularis by a deep cleft. The crista tibiofibularis lies slightly proximal to the fibular and tibial condyles and tapers posteriorly to a small point. Dorsally, the distal end bears a shallow fossa between the two condyles. The distal surface is gently rounded.

Tibia: Several tibiae are represented from the *A. madagaskarensis* quarry including one particularly well-preserved, nearly undistorted specimen from the right side (FMNH PR 3814; fig. 61), and some elements directly associated with partially or completely articulated pedes (FMNH PR 2776; FMNH PR 2786). The tibia is approximately 75% the length of the femur from the same individual (table 8). The tibia has an enlarged and robust proximal portion and a slightly expanded distal end. In proximal view, the tibia is triangular, as in most early archosauromorphs (e.g., *Trilophosaurus buettneri*, TMM 31025-140; "*Chasmatosaurus*" *yuani*, Young, 1936; *Noteosuchus colletti*, Carroll, 1976). Anteriorly, a weakly developed cnemial crest runs nearly the length of the tibia. Medially, a rounded condyle on the proximal surface marks the contact between the tibia and fibula. The posterior and medial condyles are separated by a shallow cleft visible in proximal view. The proximal surface is gently convex in the well-preserved example (FMNH PR 3814; fig. 61), but slightly concave in FMNH PR 2776 and FMNH PR 2786. A proximodistally elongated depression occurs proximomedially (fig. 61). The same structure occurs in the three tibiae examined here (FMNH PR 3814; FMNH PR 2776; FMNH PR 2786). A similar depression occurs in the same position as the compound attachment site of the *m. puboischiotibialis* and slips of *m. flexor tibialis* in extant lepidosaurs (Romer, 1942; Russell and Bauer, 2008) and archosaurs (Gatesy, 1997; Dilkes, 2000). A deep pit on the equivalent proximomedial aspect of the tibia has been identified as a scar of the *m. puboischiotibialis* in *Erythrosuchus africanus* (Gower, 2003). An additional depression, proximodistally elongated, occurs on the anteromedial surface near the midshaft (fig. 61) in all three specimens of *A. madagaskarensis*. The bone surface within this depression is rugose, suggesting a point of muscle attachment, likely the *m. gastrocnemius* based on comparison to extant lepidosaurs and archosaurs.

The shaft of the tibia is gently curved anteriorly and laterally. In cross section, the shaft is circular at midshaft. A slight ridge arises from the anteromedial side on the distal half of the element. A rounded muscle scar occurs at the base of this ridge, just proximal to the distal surface (fig. 61). The distal end is narrow anterolaterally compared to the midshaft width. The distal surface, oval in outline, consists of a slight posteromedial expansion adjacent to a nearly flat anterolateral portion. Subcircular distal tibiae occur in "*Chasmatosaurus*" *yuani* (Young, 1936), *Prolacerta broomi* (BP/1/2676), and *Trilophosaurus buettneri* (TMM 31025-140).

The tibia of *A. madagaskarensis* is generally similar to that of most archosauromorphs, but is more robust in overall proportions in comparison to those of *Trilophosaurus buettneri* (Gregory, 1945), smaller archosauromorphs (e.g., *Prolacerta*

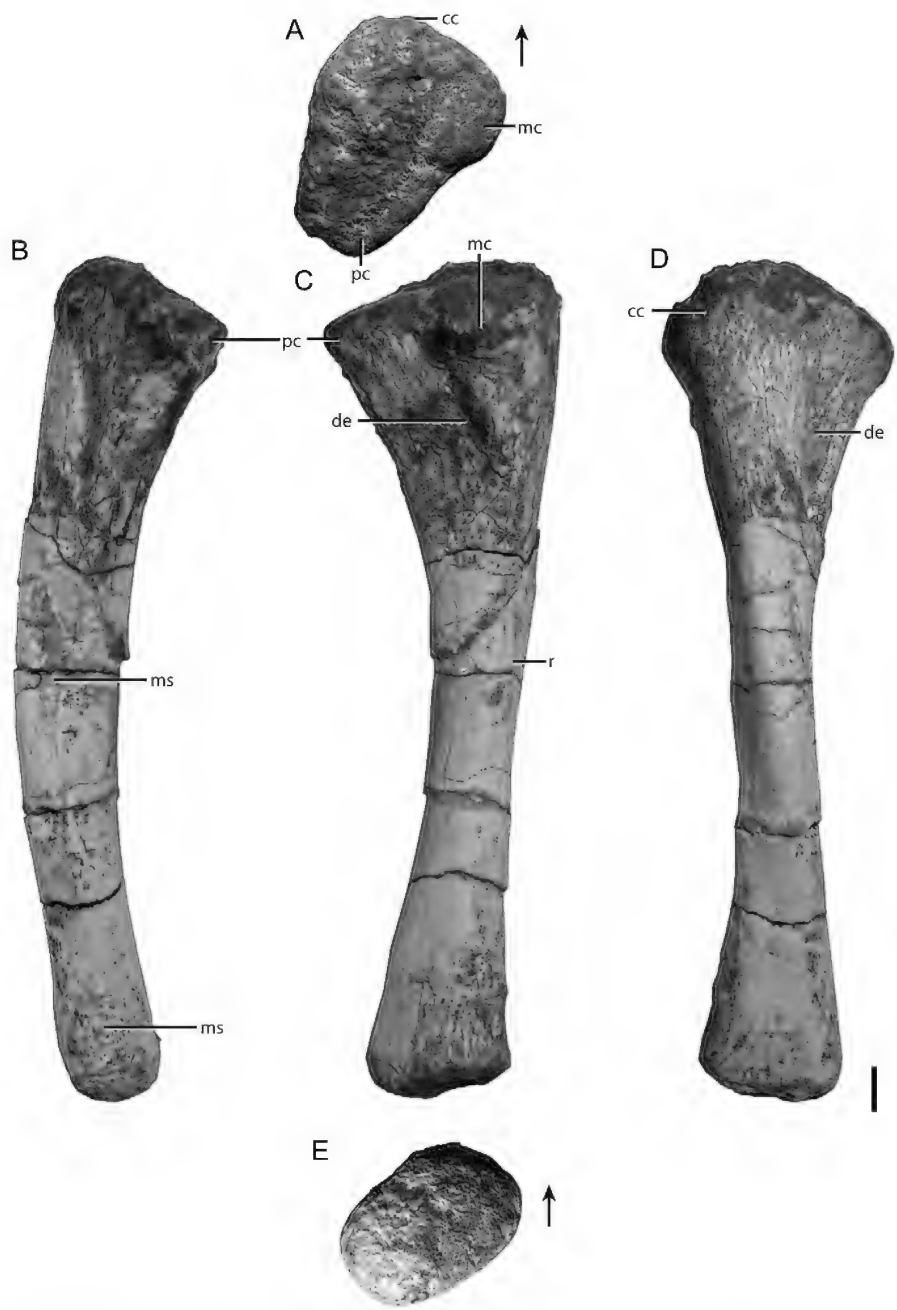

Fig. 61. The right tibia of *Azendohsaurus madagaskarensis* (FMNH PR 3814) in (**A**) proximal, (**B**) medial, (**C**) lateral, (**D**) anterior, and (**E**) distal views. Scale = 1 cm. Arrows indicate anterior direction. Abbreviations: **cc,** cnemial crest; **de,** depression; **mc,** medial condyle; **ms,** muscle scar; **pc,** posterior condyle; **r,** ridge.

broomi, Gow, 1975), and tanystropheids (e.g., *Tanystropheus longobardicus*, Nosotti, 2007). It is less robust, however, than in larger rhynchosaurs (e.g., "*Scaphonyx*" *fischeri*, MCZ 1529; *Stenaulorhynchus stockleyi*, pers. obs.; *Teyumbaita sulcognathus*, Montefeltro et al., 2013).

FIBULA: Four fibulae of *A. madagaskarensis* are known (FMNH PR 2782, UA 7-13-99-576, FMNH PR 3821, and FMNH PR

TABLE 8
Measurements of tibiae (in mm) of *Azendohsaurus madagaskarensis*

Specimen	Side	Length	Proximal width	Distal width	Circumference at midshaft
FMNH PR 2770	right	190	60	37	24
FMNH PR 2782	left	193	58	38	25
FMNH PR 3814 (fig. 61)	right	180	50	32	23
UA 7-13-99-576	right	185	53	35	23

3813), the latter of which is exquisitely preserved (fig. 62). The fibula, slightly sigmoidal in lateral view, is far more slender than the tibia (table 9). The fibula is similarly sigmoidal in *Protorosaurus speneri* (Gottmann-Quesada and Sander, 2009), *Mesosuchus browni* (SAM 7416), *Tanystropheus longobardicus* (MSCN BES SC 1018), *Trilophosaurus buettneri* (TMM 31025-140), and "*Chasmatosaurus*" *yuani* (Young, 1936). Straighter fibulae occur in early diapsids (e.g., *Araeoscelis gracilis*, Vaughn, 1955). Proximally the fibula is highly compressed mediolaterally, convex, and symmetrical in lateral view. The shaft is twisted such that the long axis of the proximal portion is oriented anteroposteriorly and that of the distal portion anteromedially. A low ridge, likely for the attachment of the *m. iliofibularis* as in extant reptiles (Dilkes, 2000), originates dorsolaterally, one-third of the way from the proximal surface, and terminates at midshaft. A sharp ridge occurs ventromedially (opposite the low ridge), possibly for attachment of the *m. iliofibularis*. The distal and proximal halves of the element both gradually expand toward their termini, but to a greater degree in the distal segment. In anterior view, the distal end is asymmetrical, with the posterolateral side much more distally expanded than the anteromedial. In distal view, the posterolateral portion is convex whereas the anteromedial portion is flat; a small posteromedially projecting rim defines the medial portion of the distal end.

Pes: The pes of *A. madagaskarensis* is poorly represented compared to the manus; only two pedes are known from the type locality, yet all portions are preserved (fig. 63). Specimen FMNH PR 2776 (fig. 64) comprises a completely articulated left pes, the tarsals and digit I of which have been removed and completely prepared for study, and FMNH PR 2786 (fig. 65), a disarticulated left pes consisting of all of the proximal and distal tarsals, metatarsals I–IV and associated phalanges (table 10). Isolated pedal elements occur within the bone bed, but also are rare compared to isolated manual elements.

Digits I–IV of the pes diverge from the tarsals in a smooth arc, digit V being posteroventrally deflected relative to the others. The pedal digits, like those of the manus, are short for an early archosauromorph. The longest, digit IV, is about the same length as the tibia in FMNH PR 2776. A similar digit IV:tibia ratio is seen in *Tanystropheus longobardicus* (MSNM BES SC 265; measurements from Nosotti, 2007) and *Protorosaurus speneri* (Simon/Bartholomaus specimen, Gottmann-Quesada and Sander, 2009: fig. 15), whereas digit IV is 117% the length of the tibia in *Trilophosaurus buettneri* (TMM 31025-140; measurements from Gregory, 1945). Digits I and V are similar in length, but the proportions of their constituent elements differ; the three phalanges and short ungual of digit V are about the same combined length as the single phalanx and enlarged ungual of digit I.

Six tarsals are preserved in FMNH PR 2776, including the astragalus (with a fused centrale, see below), calcaneum, and first, second, third, and fourth distal tarsals (fig. 63). A fifth distal tarsal is not present in the articulated or associated pedes, and there is no room for an ossification of an element between metatarsal V and the fourth distal tarsal suggesting that it was absent, or that the fifth distal tarsal fused onto the larger fourth distal tarsal as hypothesized for early diapsids by Caldwell (1994). The tarsals are each fully ossified and bear distinct articular surfaces. Four distal tarsals occur in most early archosauromorphs (e.g., *Meso-*

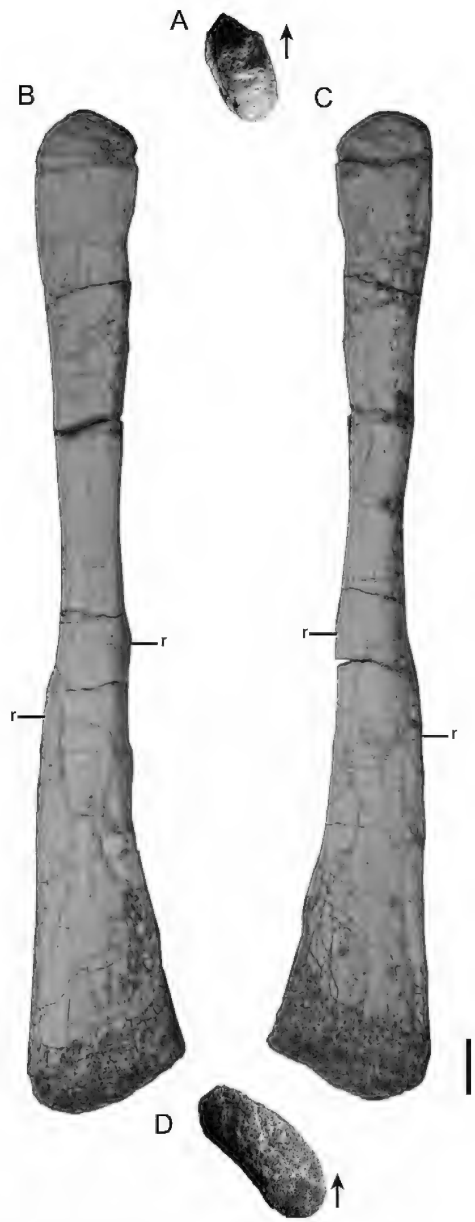

Fig. 62. Right fibula of *Azendohsaurus madagaskarensis* (FMNH PR 3813) in (**A**) proximal, (**B**) lateral, (**C**) medial, and (**D**) ventral views. Scale = 1 cm. Arrows indicate anterior direction. Abbreviation: **r,** ridge.

TABLE 9
Measurements of fibulae (in mm) of *Azendohsaurus madagaskarensis*

Specimen	Side	Length	Proximal width	Distal width	Circumference at midshaft
FMNH PR 2782	left	198	27	35	15
FMNH PR 3813 (fig. 62)	right	180	23	30	14
UA 7-13-99-576	right	190	25	32	15

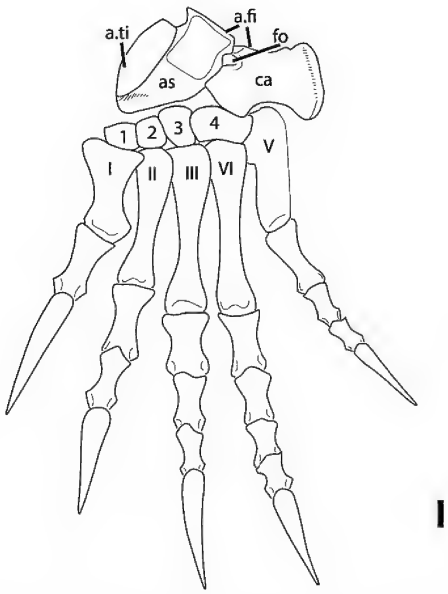

Fig. 63. Reconstruction of the left pes of *Azendohsaurus madagaskarensis*. Scale = 1 cm. Abbreviations: **a.,** articulates with; **as,** astragalus; **ca,** calcaneum; **fi,** fibula; **fo,** foramen; **ti,** tibia; **1,** distal tarsal I; **2,** distal tarsal II; **3,** distal tarsal III; **4,** distal tarsal IV; **I,** digit I; **II,** digit II; **III,** digit III; **IV,** digit IV; **V,** digit V.

suchus browni, SAM 7416; *Protorosaurus speneri,* Gottmann-Quesada and Sander, 2009; *Trilophosaurus buettneri*, TMM 31025-140). Three distal tarsals occur in *Macrocnemus fuyuanensis* (Jiang et al., 2011), and only two in *Tanystropheus longobardicus* (MCSN BES SC 1018, MCSN V 3730). In *A. madagaskarensis,* as in nearly all other early archosauromorphs, the phalangeal formula of the pes is 2-3-4-5-4 (fig. 63).

The **astragalus** is represented in FMNH PR 2776 (figs. 66, 67) and FMNH PR 2786, the former particularly well preserved. None of the articular surfaces are finished in compact bone. In all examples, the centrale and astragalus are fused into a single element, hereafter termed the astragalus (following Rieppel, 1993). In both specimens, a clear cleft between the main body of the astragalus and the primordial centrale persists on the anterior surface (figs. 66, 67); in FMNH PR 2786 the cleft spans the proximal and distal surfaces of the two elements. However, fusion is complete, without a trace of a suture. Likewise, the posterior side of the astragalus shows no indication of two separate elements. Fusion of the centrale and astragular body is polymorphic in *Trilophosaurus buettneri* in similarly sizedindividuals, as it is fused in TMM 31025-unnumbered, whereas the two elements remain distinct in the right pes of TMM 31025-140. Additionally, fusion of the astragular body (classically referred to as the intermedium in archosauromorphs, e.g., Hughes, 1968) and the centrale (classically referred to as the tibiale in archosauromorphs, e.g., Hughes, 1968) is variable within Rhynchosauria. For example, the astragular body and the centrale are separate in the Middle Triassic *Mesosuchus browni* (Dilkes, 1998) and *Stenaulorhynchus stockleyi* (Hughes, 1968: figs. 2, 3), but fused in a Late Triassic rhynchosaur (PVSJ 679) from the Ischigualasto Formation of Argentina. In the latter specimen, a cleft clearly divides the astragular body and centrale in all views. An unfused centrale is present in Archosauriformes, including *Proterosuchus alexanderi* (NMQR 1484) and possibly *Erythrosuchus africanus* (Gower, 1996). In *A. madagaskarensis*, the inferred centrale portion of the astragalus is reduced and forms only about 30% of the mediolateral length of the astragalus. This is similar to the proportions in *Trilophosaurus buettneri* (TMM 31025-140), *Macrocnemus bassanii* (Rieppel, 1989), *Noteosuchus colletti* (Carroll, 1976), and *Proterosuchus* (AMNH FR 2237), whereas it makes up ~50% of the length of the compound element in later rhynchosaurs (e.g., *Mesosuchus browni*, Dilkes, 1998; Ischigualasto rhynchosaur, PVSJ 679) and in a possible *Langobardisaurus* hindlimb (MFSN 26829). No centrale bones appear to be present in *Tanystropheus longobardicus* (MCSN V 3730), although the tibial articular surface is quite elongate; the classical intermedium and centrale thus are possibly indistinguishably fused.

Proximally, the astragalus bears two articular surfaces separated by a gap (figs. 66B, 67B). The larger, medial surface articulates with the tibia. In proximal view, the tibial articulation surface is circular, with a posteriorly expanded lip. The articular surface is complicated: ventrally it is concave, dorsally it is convex, and laterally it is nearly flat. This irregular surface mirrors that of the distal

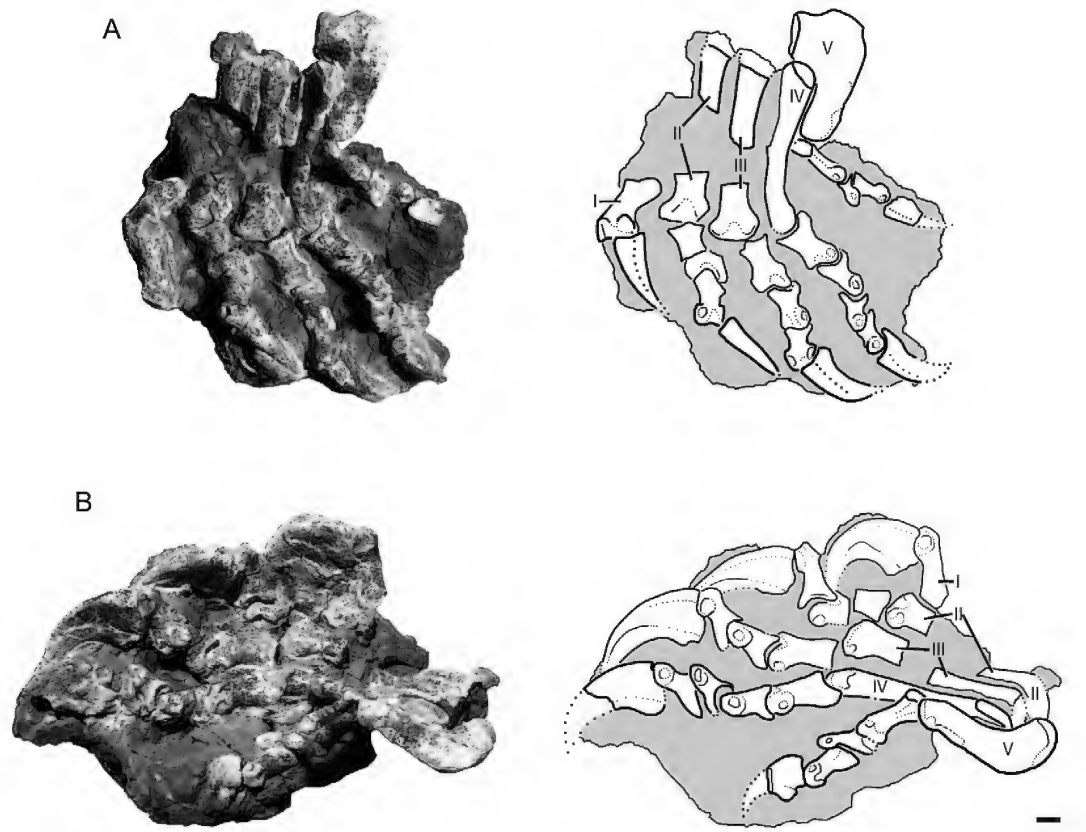

Fig. 64. Nearly completely articulated left pes of *Azendohsaurus madagaskarensis* (FMNH PR 2776) in (**A**) anterodorsal view and drawing (right) and (**B**) dorsolateral view and drawing (right). Scale = 1 cm. Gray in drawings represents matrix. Abbreviations: **I,** digit one; **II,** digit two; **III,** digit three; **IV,** digit four; **V,** digit five.

surface of the tibia; the convex portion of the tibia articulates with the ventral concave surface of the astragalus, and the concave surface on the dorsal part of the distal surface of the tibia matches the convex dorsal portion of the astragalus. This complex tibial-astragular articulation contrasts with the simple concave articular surface seen in the astragalus of *Trilophosaurus buettneri* (TMM 31025-140). A similarly flattened tibial articulation occurs in some rhynchosaurs (e.g., MCZ 4555; Hughes, 1968). *Proterosuchus alexanderi* (MCZ 4301, cast of NMQR 1484) exhibits an intermediate condition between those of *A. madagaskarensis* and *T. buettneri*, with a slight ventral concavity but an otherwise flattened tibial articular surface. The fit between the astragalus and the tibia in *A. madagaskarensis* is not tight, and thus cartilage must have played a structural role in the articulation between the two elements.

The degree to which the centrale portion of the astragalus contributes to the tibial articular surface is unclear (figs. 67A). In FMNH PR 2776 the centrale portion does not contribute to the tibial articular surface, whereas in FMNH PR 2786 the centrale portion seems to form a small contribution. This contrasts with the large contribution of centrale to the tibial articular surface in late diverging rhynchosaurs (e.g., *Teyumbaita sulcognathus*, Montefeltro et al., 2013).

A marked concave gap separates the tibial from the fibular articular surface in *A. madagaskarensis* (figs. 67B), as in other non-archosauriform archosauromorphs (Gower, 1996; Nesbitt et al., 2009). This gap (groove) is deeper posteriorly than dorsally. A low ridge

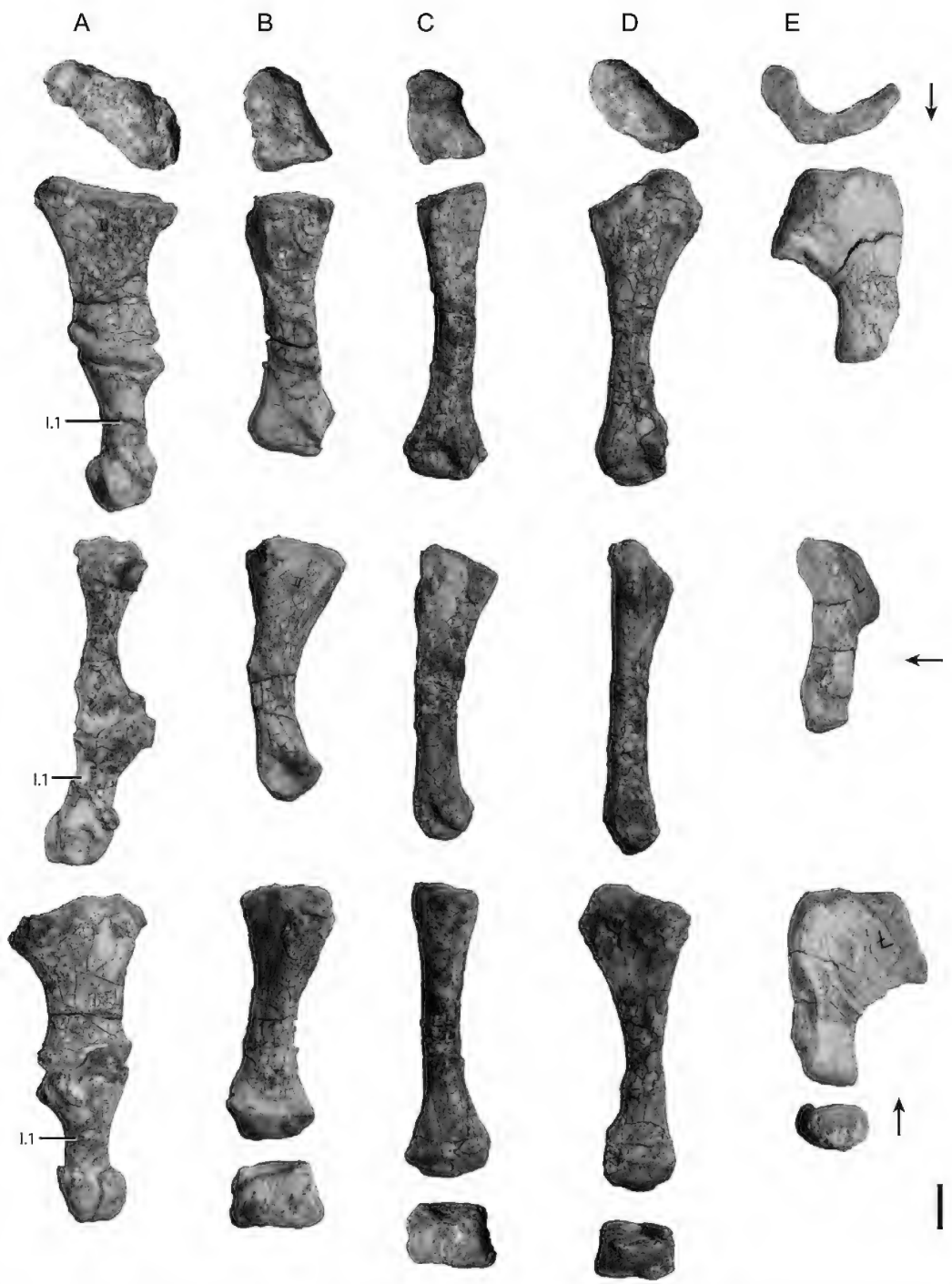

Fig. 65. Left metatarsals (**A–E**) of *Azendohsaurus madagaskarensis* in (from top down) proximal, dorsal, lateral, ventral, and distal views. (**A**) Metatarsal one (FMNH PR 2786); (**B**) metatarsal two (FMNH PR 2786); (**C**) metatarsal three (FMNH PR 2786); (**D**) metatarsal four (FMNH PR 2786); and (**E**) metatarsal V (FMNH PR 3820) in (**E**). Scale = 1 cm. Arrows indicate anterior direction. Abbreviations: **I.1**, first phalanx of digit one.

TABLE 10
Measurements of the complete left pes (in mm; fig. 64) of *Azendohsaurus madagaskarensis* (FMNH PR 2776)
Abbreviation: inc, incomplete.

Digit	Element	Length
I		
	metatarsal I	40
	phalanx I-1	36
	phalanx I-2	46
II		
	metatarsal II	44 inc
	phalanx II-1	30
	phalanx II-2	21
	phalanx II-3	46
III		
	metatarsal III	60 inc
	phalanx III-1	23
	phalanx III-2	21
	phalanx III-3	25
	phalanx III-4	45
IV		
	metatarsal IV	72
	phalanx IV-1	23
	phalanx IV-2	19
	phalanx IV-3	17
	phalanx IV-4	24
	phalanx IV-5	24 inc
V		
	metatarsal V	48
	phalanx V-1	24
	phalanx V-2	19
	phalanx V-3	20
	phalanx V-4	13 inc

extends from the anterior margin of the tibial facet to the anterior margin of the fibular facet. Similar ridges occur in some specimens of *Trilophosaurus jacobsi* (e.g., NMMNHS P-36709) and *Proterosuchus alexanderi* (NMQR 1484).

The fibular facet of the astragalus of *A. madagaskarensis* slopes laterally, and the articular surface is concave. The medial portion of the distal surface of the fibula is a poor match for the fibular articulation of the astragalus, suggesting that this articulation space was filled with cartilage in life. The mismatch of the fibular articulation surface of the calcaneum and the more lateral portion of the distal end of the fibula invites a similar interpretation. The fibular articulation surface of the astragalus is circular, except for the distal portion where it meets the calcaneum, at which point the distal edge of the fibular articulation surface is concave.

In dorsal view (fig. 67A), the astragalus of *A. madagaskarensis* bears a deep concave surface ("dorsal hollow" of Gower, 1996) that appears to be homologous with the "anterior hollow" (sensu Brochu, 1992) in crocodylians. The hollow is partially framed dorsally by the ridge joining the tibial and fibular facets. In early diapsids and archosauromorphs that lack this ridge (e.g., *Araeoscelis gracilis*, MCZ 8288; "*Scaphonyx*" *fischeri*, MCZ 4555; *Tanystropheus longobardicus*, Dalla Vecchia, 2008: fig. 61O), the anterior hollow smoothly grades into the gap between the facets. In *A. madagaskarensis,* small foramina dot the inside surface of the "dorsal hollow." The dorsal edge of the articular surface of the tibia and the distal articular surface between the calcaneum and the astragalus both are visible in dorsal view. The dorsomedial corner of the astragalus is convex and lacks clear articulation surfaces for other elements.

In ventral view (fig. 67D), the astragalus is concave along a proximodistal axis; this concavity is a continuation of the gap that proximally separates the fibular and tibial articular surfaces. This concavity is common in early diapsids (e.g., *Trilophosaurus buettneri*, TMM 31025-582; *Proterosuchus alexanderi*, MCZ 4301). In *A. madagaskarensis*, the proximomedial edge of the astragalus is distinctly convex in posterior view, and the proximolateral edge is nearly straight. The distal portion of the posterior surface of the astragalus bears the distal articulation with the calcaneum. A distinct groove on the lateral side of the astragalus separates the distal articulation with the calcaneum from the proximal half of the element. This groove forms the medial side of the perforating foramen in early tetrapods (e.g., Broom, 1921), early diapsids (e.g., *Araeoscelis gracilis*, MCZ 8288; *Hovasaurus boulei*, MNHN MAP 349), and early archosauromorphs (e.g., Nesbitt, 2011).

The distal view of the astragalus of *A. madagaskarensis* illustrates the complex articulation between the astragalus and calcaneum (fig. 67C). The articular facet with the calcaneum is nearly completely divided by a ventral groove (see above) into two distinct

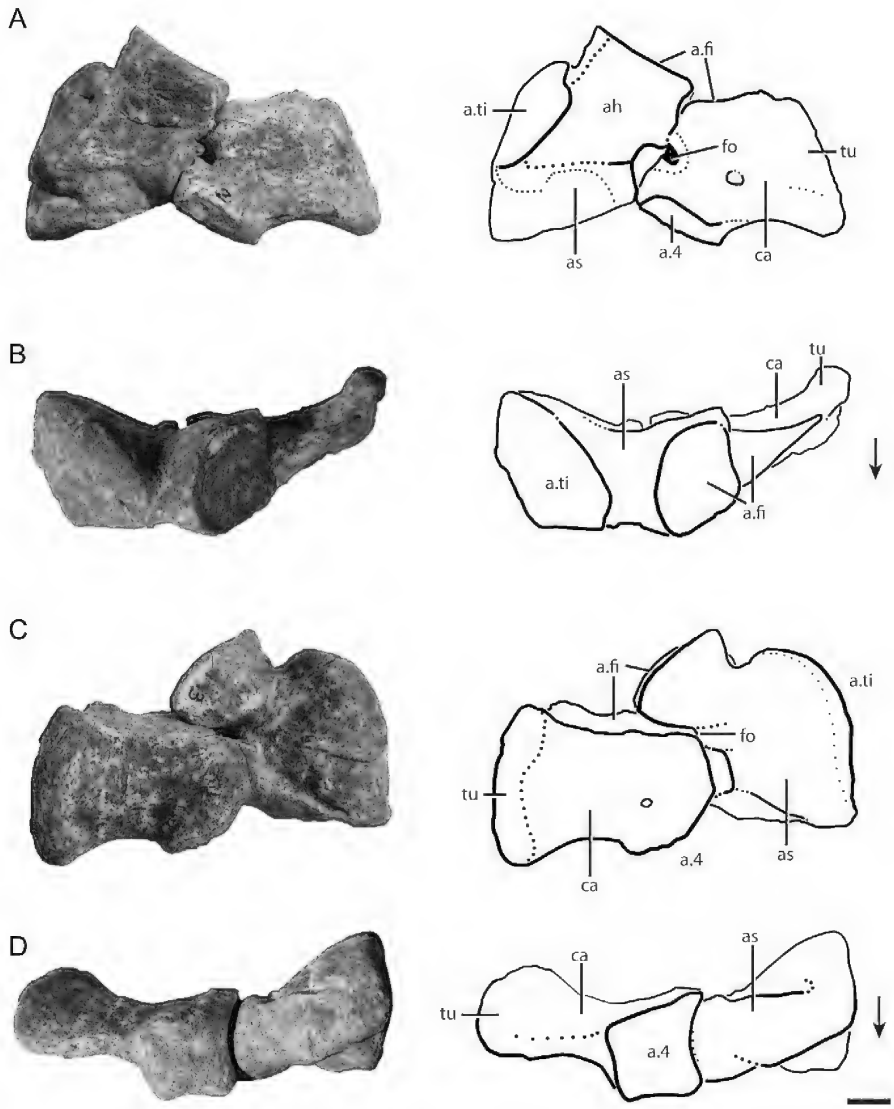

Fig. 66. Articulated left proximal tarsals of *Azendohsaurus madagaskarensis* (FMNH PR 2776) in (**A**) dorsal, (**B**) proximal, (**C**) ventral, and (**D**) distal views. Scale = 1 cm. Arrows indicate dorsal direction. Abbreviations: **a.,** articulates with; **ah,** anterior hallow; **as,** astragalus; **ca,** calcaneum; **fi,** fibula; **fo,** foramen; **ti,** tibia; **tu,** tuber; **4,** distal tarsal 4.

surfaces; the groove disappears at the dorsal portion of the two articulation surfaces. The more distal and medial astragular articulation for the calcaneum is convex and stretches from the anterior surface, around the distal surface, to the ventral surface of the astragalus. A low rim frames the medial edge of the articulation. The more lateral and proximal calcaneal articulation of the astragalus is concave and rectangular, with a mediolateral long axis. This articular surface lies directly distal to that for the fibula. Both articulation surfaces correspond with the astragular articular surfaces of the calcaneum, the concave surface of the astragalus mirroring the convex surface of the calcaneum. This coupled convex-concave and concave-convex articulation between the astragalus and calcaneum, respectively, of *A. madagaskarensis* occurs in a number of

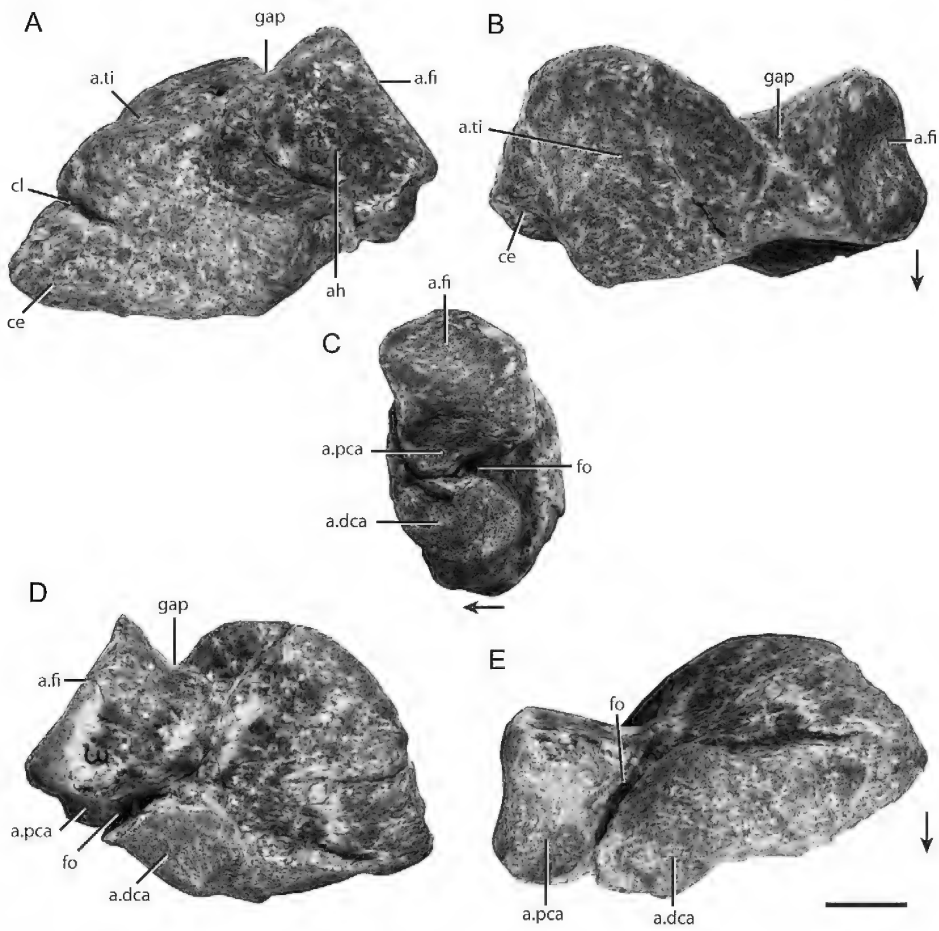

Fig. 67. Left astragalus of *Azendohsaurus madagaskarensis* (FMNH PR 2776) in (**A**) dorsal, (**B**) proximal, (**C**) lateral, (**D**) ventral, and (**E**) distal views. Scale = 1 cm. Arrows indicate dorsal direction. Abbreviations: **a.,** articulates with; **ah,** anterior hallow; **ce,** centrale; **cl,** cleft; **dca,** distal articular facet for the calcaneum; **fi,** fibula; **fo,** foramen; **gap,** gap; **pca,** proximal articular facet for the calcaneum; **ti,** tibia.

other early archosauromorphs, but typically can be observed easily only in larger-bodied taxa having disarticulated proximal tarsals (e.g., rhynchosaurs, MCZ 4555; *Trilophosaurus buettneri*, Gregory, 1945; *Proterosuchus alexanderi,*Sereno, 1991).

The **calcaneum** is also rare in the *A. madagaskarensis* quarry sample, represented only by FMNH PR 2776 (figs. 66, 68) and FMNH PR 2786. The former is complete and exceptionally preserved, whereas the latter is crushed and its fibular articular surface sheared off. As with the astragalus, the calcaneum bears compact bone on the nonarticular surfaces and spongy bone on the articular surfaces. The calcaneum is thickened medially where it articulates with the astragalus. The calcaneal tuber is directed laterally.

Proximally, the calcaneum bears a convex surface that articulates with the fibula (figs. 66, 68). This convex surface is continuous with the proximal astragular facet and stretches laterally to the shaft (but not lateral edge) of the calcaneal tuber. A similar condition occurs in *Tanytrachelos ahynis* (GR 306; Pritchard et al., 2015). Unfinished bone of the fibular facet is continuous with the lateral tuber in some *Trilophosaurus* calcanei (AMNH FARB 30836), *Proterosuchus alexanderi* (MCZ 4301), and *Erythrosuchus africanus* (NHMUK R3592; Gower, 1996). The fibular articular surface of the

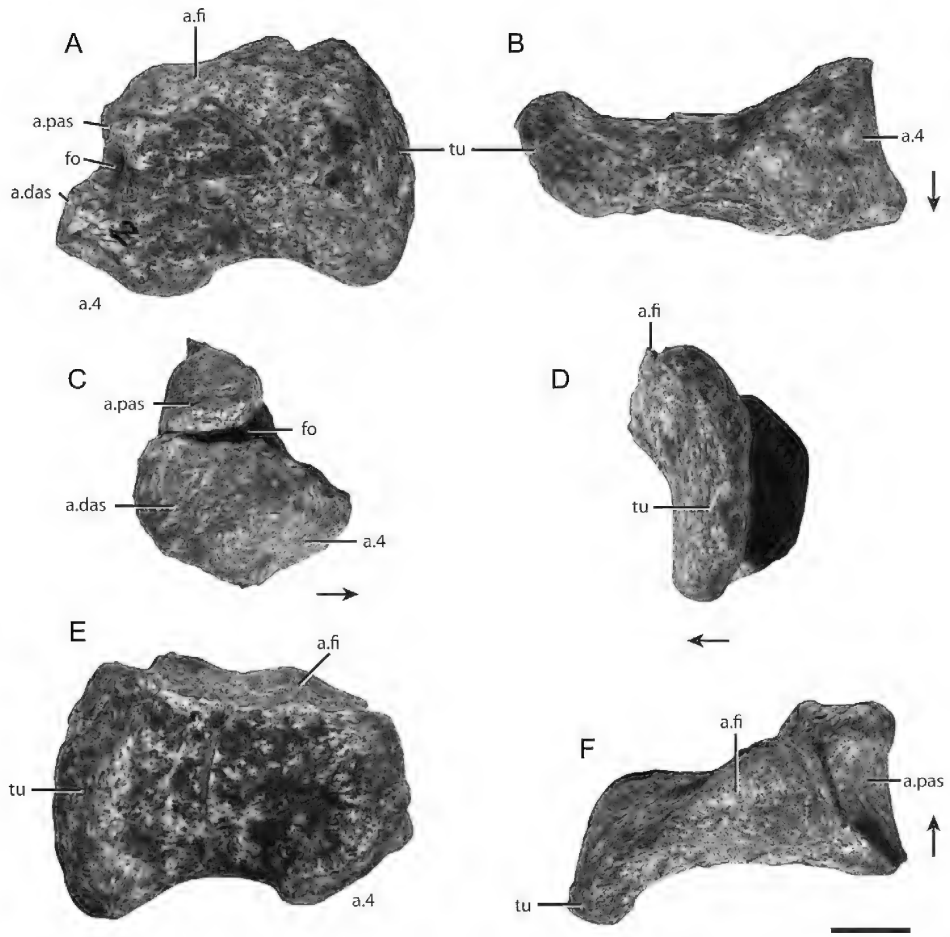

Fig. 68. Left calcaneum of *Azendohsaurus madagaskarensis* (FMNH PR 2776) in (**A**) dorsal, (**B**) distal, (**C**) medial, (**D**) lateral, (**E**) ventral, and (**F**) proximal views. Scale = 1 cm. Arrows indicate dorsal direction. Abbreviations: **a.,** articulates with; **das,** distal facet for the astragalus; **fi,** fibula; **fo,** foramen; **pas,** proximal facet for the astragalus; **tu,** tuber; **4,** distal tarsal 4.

calcaneum tapers laterally; it lies adjacent to a shelf on the ventral side.

The calcaneal tuber expands laterally from the articular surfaces for the astragalus and the fourth tarsal. The tuber is dorsoventrally compressed, and three times longer (proximodistally) than tall (dorsoventrally); similar proportions are seen in most early archosauromorphs (e.g., *Tanytrachelos ahynis*, GR 306; *Trilophosaurus buettneri*, TMM 31025-140). The distal surface of the tuber originates medially from the articular facet for the fourth distal tarsal, and arcs proximally. A similar condition occurs in *Trilophosaurus buettneri* (e.g., AMNH 30836). The concave distal surface of the tuber (figs. 68B) in *A. madagaskarensis* resembles that of some rhynchosaurs (e.g., *Stenaulorhynchus stockleyi*, Hughes, 1968), but the tuber is larger than that of *Trilophosaurus buettneri* (TMM 31025-140) and proterosuchids (AMNH FARB 2237). The lateral side of the calcaneal tuber of *A. madagaskarensis* is expanded distally and ventrally; the ventral expansion is clearly visible (fig. 68D) in proximal view. This contrasts with the tubera of most early archosauromorphs (e.g., *Protorosaurus speneri*, Gottmann-Quesada and Sander, 2009; *Trilophosaurus buettneri*, TMM 31025-140), in which ventral expansion is lacking. In ventral view (fig. 68E), the calcaneal tuber is convex on its lateral edge; its terminus is capped by the spongy bone typical of articular surfaces. The dorsal surface is

convex and bears a central foramen. The ventral surface is slightly concave along its proximodistal axis.

The medial surface of the calcaneum bears most of its articulations. Proximally, the fibular articular facet grades into the proximal astragular articular surface. This convex surface articulates distally to the fibular facets of both the astragalus and the calcaneum. The proximal and distal articular facets for the astragalus are separated by a groove that is deep dorsally but that shallows ventrally. This groove is the lateral component of the perforating foramen that forms when the astragalus and the calcaneum are in articulation. The more distal articular surface is rectangular and concave along a proximodistal axis. The articulation with the fourth distal tarsal is poorly separated from the distal articular surface with the astragalus. In ventral view, the rectangular articular surface with the fourth distal tarsal expands dorsally and forms the portion of the calcaneum with the greatest dorsoventral expansion. The articular surface is mainly convex, with a shallow depression in the center.

The **distal tarsals** are preserved in the left pedes of FMNH PR 2776 and FMNH PR 2786 in various states of articulation (fig. 69). None of the articular surfaces among the distal tarsals, proximal tarsals, and the metatarsals are precise, suggesting that cartilage was an important component of this portion of the pes. The **first distal tarsal** is adjacent to its original articulation on the proximal surface of metatarsal I in FMNH PR 2776; the element is disarticulated in FMNH PR 2786 (fig. 69). A deep fissure that surrounds the first distal tarsal in FMNH PR 2786 is the result of breakage during fossilization, not due to the presence of a separate element in life; this interpretation is confirmed by the well-preserved element in FMNH PR 2776. The proximal and distal surfaces of the triangularly shaped first distal tarsal are nearly flat; the entire element tapers medially. The dorsal surface bears a concave surface with small foramina perforating the compact bone. The ventromedial surface, composed of spongy bone, is nearly flat. The lateral surface is composed mostly of spongy bone, but a small region with compact bone occurs near the distal edge, along with a pair of small foramina. This lateral surface articulates with the second distal tarsal, but not in a precise bone-on-bone articulation.

The **second distal tarsal** is slightly disarticulated from the third distal tarsal in FMNH PR 2776 (fig. 69E–H) and completely separated in FMNH PR 2786. The second distal tarsal lies on the proximal surface of metatarsal II, articulates with the first distal tarsal medially, and the third distal tarsal laterally. Like the proximal surface of the metatarsal, the body of the second distal tarsal is much deeper dorsoventrally than proximodistally. In dorsal and ventral views, the second distal tarsal is square and bears compact bone with small foramina. The proximal, lateral, medial, and distal surfaces are nearly flat and rectangular. A distinct groove on the lateral side near the proximal margin forms the medial side of a foramen created when the second and third distal tarsals articulate.

The **third distal tarsal** is in slight articulation with second distal tarsal FMNH PR 2776 and in full articulation with the fourth distal tarsal in FMNH PR 2786 (fig. 69I–K). The third distal tarsal lies on the proximal surface of metatarsal III, and articulates with the second distal tarsal medially and the fourth distal tarsal laterally. Like the second distal tarsal, the third distal tarsal is more elongate dorsoventrally than proximodistally. Nevertheless, the third distal tarsal is more proximodistally elongate than the second distal tarsal, resulting in a rectangular outline of the dorsal surface of the third distal tarsal. Similar proportions are seen in *Trilophosaurus buettneri* (TMM 31025-140). The ventral surface, less expanded than the dorsal one, is triangular. Both the dorsal and ventral surfaces are covered with compact bone and bear small foramina. The lateral surface for articulation with the fourth distal tarsal is convex, corresponding to a concave surface on the fourth distal tarsal, similar to the articular surfaces in *Protorosaurus speneri* (Gottmann-Quesada and Sander, 2009: fig. 25d), *Trilophosaurus buettneri* (TMM 31025-140), and likely *Tanystropheus longobardicus* (MCSN V 3730). More proximally on this articular surface, a distinct groove forms the medial side of a foramen

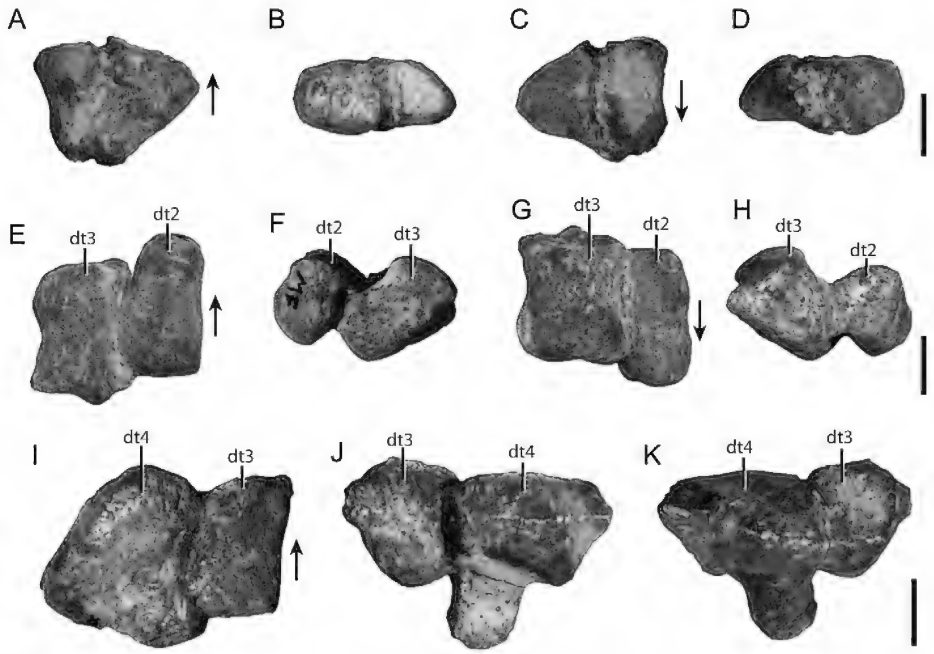

Fig. 69. The right distal tarsals of *Azendohsaurus madagaskarensis*. First distal tarsals 1 (FMNH PR 2786) in (**A**) proximal, (**B**) dorsal, (**C**) distal, and (**D**) ventral view. Second and third distal tarsals (FMNH PR 2776) in (**E**) proximal, (**F**) dorsal, (**G**) distal, and (**H**) ventral view. Third and fourth tarsals (FMNH PR 2786) in (**I**) proximal, (**J**) dorsal, and (**K**) ventral view. Scales = 1 cm. Arrows indicate dorsal direction. Abbreviations: **dt#,** distal tarsal.

that is present when the third and fourth distal tarsals are in articulation.

The **fourth distal tarsal** articulates with the third distal tarsal in FMNH PR 2786 and is isolated in FMNH PR 2776 (fig. 69). About half the size of the calcaneum, it is the largest element of the distal tarsal series. The fourth distal tarsal lies on the proximal surface of metatarsal IV, articulates medially with the third distal tarsal, the calcaneum and possibly the astragalus proximally, and metatarsal V ventrolaterally. The dorsal and ventral surfaces are capped in compact bone dotted with many small foramina. The dorsal surface is distoventrally expanded into a tablike process that tapers distally. Similar expansions occur in *Protorosaurus speneri* (Gottmann-Quesada and Sander, 2009: fig. 25 c) and *Trilophosaurus buettneri* (TMM 31025-140), but not in *Tanystropheus longobardicus* (MCSN V 3730). In *A. madagaskarensis*, a small fossa on the lateral side of the dorsal surface appears to be nonarticular. The markedly convex lateral surface tapers ventrolaterally. The lateral side of the fourth distal tarsal is banked distally for articulation with the proximal portion of metatarsal V.

All **metatarsals** of *A. madagaskarensis* are represented; a full set is known from the two nearly complete specimens, FMNH PR 2776 (fig. 64) and FMNH PR 2786 (figs. 65, 70). Metatarsals were in near articulation in the left pes of FMNH PR 2776 prior to full preparation. Currently, metatarsals II–V remain in articulation proximally in FMNH PR 2776, but are slightly displaced distally (fig. 64). Metatarsals I–IV of FMNH PR 2786, recovered in partial articulation, have been fully prepared in all views (figs. 65, 70). The shafts of all metatarsals parallel each other; metatarsals I–IV fall in roughly the same mediolaterally oriented plane, with metatarsal V lying somewhat more ventrolaterally. Proximally, metatarsals I–IV bear clear articular surfaces medially for articulation with the medially adjacent metatarsal (figs. 65, 70). As in the metacarpals, this overlapping pattern results in lateral imbrication, wherein the more medial metatarsal overlaps its lateral neighbor. Metatarsal V contacts only the fourth distal

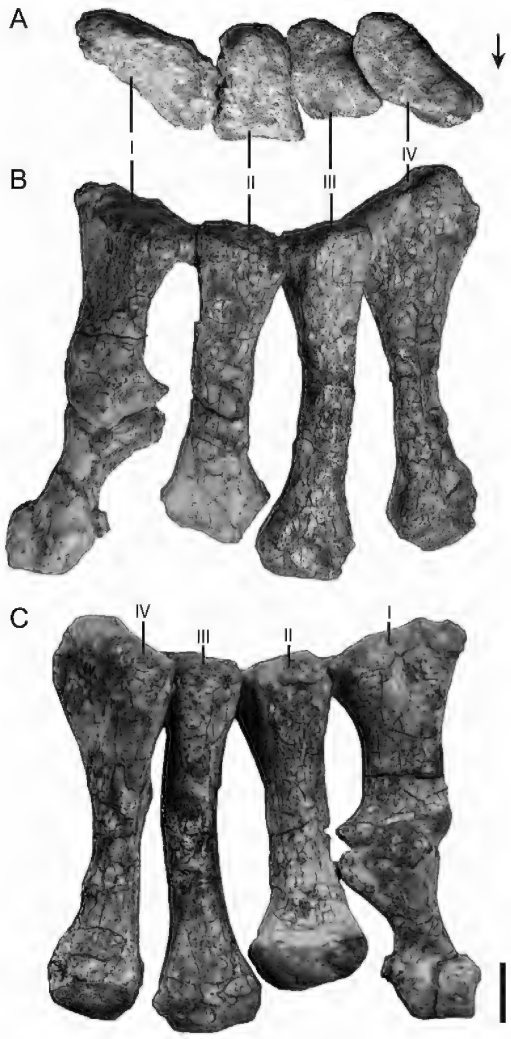

Fig. 70. Articulated left metatarsals of *Azendohsaurus madagaskarensis* (FMNH PR 2786) in (**A**) proximal, (**B**) dorsal, and (**C**) ventral views. Scale = 1 cm. Arrow indicates dorsal direction. Abbreviations: **I,** digit one; **II,** digit two; **III,** digit three; **IV,** digit four.

tarsal, as in all reptiles with hooked fifth metatarsals (e.g., *Proganochelys quenstedti*, Gaffney, 1990; *Trilophosaurus buettneri*, TMM 31025-140; extant lepidosaurs, Robinson, 1975). Metatarsal length increases incrementally from metatarsal I to IV.

Metatarsal I is preserved in articulation with the proximal phalanx in both pedes. Metatarsals I and V are subequal in length, as in *Protorosaurus speneri* (Gottmann-Quesada and Sander, 2009: fig. 24) and *Trilophosaurus buettneri* (TMM 31025-140). In tanystropheids (e.g., *Macrocnemus bassanii*, Peyer et al., 1937; *Tanystropheus longobardicus*, MCSN V 3730), metatarsal I is substantially longer than metatarsal V. In dorsal view, metatarsal I is the mediolaterally broadest of the metatarsal series in *A. madagaskarensis*. The shaft tapers to midshaft and then expands mediolaterally distally. In proximal view, the surface of metatarsal I is concave; the medial surface is expanded more proximally than the lateral surface. A small scar is present on the medioventral surface of the proximal end in FMNH PR 2776 and in FMNH PR 2786. At midshaft, metatarsal I is oval in cross section, the long axis oriented mediolaterally. The distal end is asymmetrical in dorsal view, with the lateral side more distally expanded than the medial. The distal end bears a ligament pit laterally; the typically medial ligament pit (as in *Trilophosaurus buettneri* TMM 31025-140) occurs dorsomedially. A distinct rim defines the proximal portion of the medial pit, whereas the distal portion of the pit is poorly defined. This feature is nearly identical to its counterpart on metacarpal I (see above).

Metatarsals II and III are similar in overall morphology, except that metatarsal III is longer, as in most early archosauromorphs. Both share the following characteristics: deeper than broad in proximal view; distinct medial facets for contact with other metatarsals; circular cross sections at midshaft; distal articular facets that are nearly rectangular, with the long axis oriented mediolaterally; shallow retractor fossae just proximal to the distal articular surface; and lack of a medial ligament pit coupled with well-defined lateral ligament pits. The facet for metatarsal IV on the proximal portion of metatarsal III is much more concave than the articular surface for metatarsal III on metatarsal II.

Metatarsal IV, the longest of the metatarsals in overall length, is slightly shorter than metatarsal III when the proximal articular surfaces of the two metatarsals are aligned (figs. 65, 70). The additional length of metatarsal IV is the result of a proximolateral expansion that is seemingly unique to *A. madagaskarensis*; this portion of metatarsal IV is seldom visible in early archosauromorphs, although no such expansion appears

to occur in referred specimens of *Prolacerta broomi* (AMNH FARB 9502; Colbert, 1987) or tanystropheids (e.g., MCSN BES SC 265). The long axis of the proximal surface of metatarsal IV is nearly mediolaterally oriented, in contrast to dorsoventral orientations of the long axes of metatarsals II and III. Like metatarsals II and III, metatarsal IV bears a shallow retractor fossa just proximal to the distal articular surface, and well-defined lateral (but no medial) ligament pits. Similarly, it is circular in cross section at midshaft. A small tuber occurs dorsomedially near the midshaft; whether a similar tuber occurs on metatarsals II and III is uncertain. No facet for articulation with metatarsal V is present on the proximal portion of metatarsal IV.

Metatarsal V is preserved in approximately natural position with respect to the rest of the pes in FMNH PR 2776 (fig. 64), but disarticulated in FMNH PR 3820. Metatarsals V and I are similar in length. Metatarsal V is distinctively "hooked" in overall shape relative to the other metatarsals, as is typical of saurians (Gregory, 1945; Romer, 1956; Robinson, 1975). The medially directed, dorsoventrally compressed proximal articulation surface contacts the fourth distal tarsal. The posterior portion of the bone bears a small, posteriorly directed expansion, separated from the articular surface for the fourth distal tarsal by a concave gap, as in most archosauromorphs (e.g., *Tanystropheus longobardicus*, MCSN V 3730; *Trilophosaurus buettneri*, TMM 31025-140). In *A. madagaskarensis* this expansion is curved proximolaterally, whereas in *Trilophosaurus buettneri* (31025-435) and *Proterosuchus alexanderi* (NMQR 1484) it forms a longer, proximally pointed process. The shaft of metatarsal V is concave ventrally and convex dorsally along its anteroposterior axis. Much of the lateral side of the element bears a rugose surface that wraps onto the ventral side, likely equivalent to the lateral plantar tubercle of Robinson (1975). A similar rugose surface is present broadly in archosauromorphs (e.g., *Trilophosaurus buettneri*, TMM 31025-140; *Stenaulorhynchus stockleyi*, Hughes, 1968). The distal end bears an anterolaterally directed facet for articulation with the first phalanx. A slight rim proximal to its distal end defines the distal articular surface. In distal view, the articular facet is oval in outline with a mediolaterally oriented long axis.

All **pedal digits** are generally preserved in articulation in FMNH PR 2776, although slight disarticulation occurs at some joints (fig. 64). The nonterminal phalanges are similar in form, but differ in mediolateral symmetry and length. The phalanges of *A. madagaskarensis* are, in general, relatively shorter than those of *Trilophosaurus buettneri* (Gregory, 1945). Pedal phalanges all share the following suite of features: proximal articular surfaces that are dorsoventrally concave; shafts that are waisted relative to the articular ends (nonterminal phalanges only); and oval midshaft cross sections with longer mediolateral than dorsoventral axes. As in the manual phalanges, the distal ends of the pedal phalanges, except for the penultimate, lack a ligament pit medially but possess a marked one laterally. Medial and lateral ligament pits occur in all nonterminal phalanges of *Trilophosaurus buettneri* (TMM 21025-140) and rhynchosaurs (e.g., MCZ 4652).

The first phalanx is the longest and the widest in digits II–V, as in most archosauromorphs (e.g., *Protorosaurus speneri*, Gottmann-Quesada and Sander, 2009; *Tanystropheus longobardicus*, MCSN BES SC 1018). All first phalanges in digits II–V are asymmetrical, as the lateral portion of the distal end expands further distally than the medial portion. Phalanges III.2, IV.2, IV.3, and V.2 are also asymmetric, like the first phalanges of digits II–V. The penultimate phalanx of each digit is distinctive relative to the other nonterminal phalanges; proximally they are asymmetrical, with an elongated medial process underlying the more proximal phalanx or metatarsal. The penultimate phalanges in digits II–V are of the same length, measured on the dorsal surface, as their proximal neighbors in the same digit. Like the distal ends of the penultimate phalanges of the manus, the medial and lateral sides of the distal ends of the penultimate phalanges converge distally in the pedal elements (fig. 71), and are symmetric in dorsal view. The distal ends of the penultimate phalanges are similar to those of *Trilophosaurus*

buettneri (TMM 31025-140). The medial and lateral ligament pits are equally deep, and the articular surfaces with the unguals stretch from the dorsal to the ventral sides.

Terminal phalanges (unguals) occur on all digits of the pes in *A. madagaskarensis* (fig. 64). Pedal unguals share the following character states. The element is highly compressed mediolaterally. A large tubercle occurs ventral to the articulation with the penultimate phalanx. The distal phalanx is longer than its most proximal counterpart. A single groove occurs on the medial and lateral sides, originating near the ventral tubercle and terminating at the tip. Each ungual is highly recurved (typically ~100° of curvature). The ungual of digit I is the largest; unguals progressively decrease in length laterally. The lateral and medial faces of the unguals on digits I–III are flat and striated, whereas the smaller unguals have slightly rounded and smooth surfaces.

The large pedal unguals of *A. madagaskarensis* are unmatched in absolute size among early archosauromorphs. The unguals are longer than most of the phalanges in *Trilophosaurus buettneri* (Gregory, 1945), but in relative size they are not even close to those of *A. madagaskarensis*. The unguals of *A. madagaskarensis* and *Trilophosaurus buettneri* (TMM 31025-140) are similar in possessing large ventral tubercles, highly mediolaterally compressed, and strongly recurved tips. Mediolateral compression also occurs in the pedal unguals of *Protorosaurus speneri* (USNM 442453, cast of NMK S 180) and *"Chasmatosaurus" yuani* (Young, 1936).

PHYLOGENETIC ANALYSIS

TAXON AND CHARACTER SAMPLING: Taxon sampling (table 11) in this analysis was dictated by two primary goals: (1) to understand the relationships of *Azendohsaurus madagaskarensis* relative to other early diverging archosauromorphs, and (2) to employ as many of the anatomical details of *A. madagaskarensis* as possible to strengthen our understanding of higher-level relationships within Archosauromorpha. To attain these goals, we sampled the more anatomically complete representatives of Archosauromorpha using as our starting point the dataset in Pritchard et al. (2015). Additionally, we used a minimum of three terminal taxa to score diverse archosauromorph clades (e.g., Rhynchosauria), following the approach of Brusatte (2010). We excluded the more fragmentary prolacertiform/protorosaur taxa analyzed by Benton and Allen (1997), Jalil (1997), and Rieppel et al. (2003), focusing instead on the more anatomically complete taxa sampled in Dilkes (1998) and other recently described, plausible close relatives of *A. madagaskarensis* (e.g., *Teraterpeton*, Sues, 2003). We acknowledge the potential importance of incorporating poorly known archosauromorph taxa with unique morphologies into the sample, but their inclusion in such an analysis is beyond the scope of the current study, given the many archosauromorph or potential archosauromorph taxa currently in revision and thus still incompletely described (Ezcurra et al., 2013, 2014; Pritchard et al., 2012).

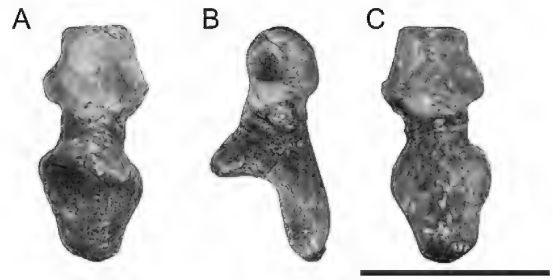

Fig. 71. Penultimate phalanx of the left foot of *Azendohsaurus madagaskarensis* (FMNH PR 2786) in (**A**) dorsal, (**B**) lateral, and (**C**) ventral views. Scale = 1 cm.

We modified the taxon sampling of Pritchard et al. (2015) by excluding the less complete species of *Macrocnemus* (*M. fuyuanensis*). We added the nonarchosaur archosauromorphs *Pamelaria dolichotrachela*, *Azendohsaurus laaroussii*, *Spinosuchus caseanus* (based on the work of Spielmann et al., 2009), and "*Chasmatosaurus*" *yuani*. Additionally, we added the dinosaurs *Coelophysis bauri* and *Plateosaurus engelhardti*, the latter to assess the likely convergence between *A. madagaskarensis* and early sauropodomorphs noted previously in Flynn et al. (2010). We also scored *Proterosuchus* based on new taxonomic work on the taxon published by Ezcurra and Butler (2015). We scored

TABLE 11
Terminal taxa and sources used in the phylogenetic analysis

Taxon	Sources
Amotosaurus rotfeldensis	Fraser and Rieppel, 2006
Azendohsaurus madagaskarensis	See text
Azendohsaurus laaroussii	See appendix 3
Batrachotomus kupferzellensis	Gower, 1999, 2002; Gower and Schoch, 2009
Coelophysis bauri	Colbert, 1989; Rinehart et al., 2009; NMMNH and AMNH specimens
"Chasmotosaurus" yuani	See appendix 3
Erythrosuchus africanus	NHMUK R 3592, BP/1/5207 Gower, 2003
Euparkeria capensis	SAM specimens; Ewer, 1965.
Gephyrosaurus bridensis	Evans, 1980, 1981
Langobardisaurus pandolfii	MCSNB 2883, 4860; MFSN, 1921; Saller et al., 2013
Macrocnemus bassanii	MCSN BES SC 111, V 457; Peyer, 1937
Mesosuchus browni	SAM specimens; Dilkes, 1998
Pamelaria dolichotrachela	See appendix 3
Petrolacosaurus kansensis	Reisz, 1981
Plateosaurus engelhardi	See Nesbitt, 2011
Prolacerta broomi	BP/1/2675, 2676, 5375; Modesto and Sues, 2004
Proterosuchus (composite)	NMQR 1484; SAM-PK-K140; Hughes, 1963; Cruickshank, 1972; Welman, 1998
Proterosuchus alexanderi	NMQR 1484; Ezcurra and Butler, 2015
Protorosaurus speneri	USNM 442453, YPM 2437; Gottmann-Quesada and Sander, 2009
Rhynchosaurus articeps	NHMUK R 1235, 1236; Benton, 1990
Shinisaurus crocodilurus	Bever et al., 2005; Conrad, 2004, 2006
Spinosuchus caseanus	See appendix 3
Tanystropheus longobardicus	MCSN BES SC 61, SC 265, BES SC 1018, V 3663, V 3730; Wild, 1973; Nosotti, 2007
Tanytrachelos ahynis	AMNH FARB 7206; YPM 7482, 8600; VMNH #2826, 3423, 120015, 120016
Teyumbaita sulcognathus	Montefeltro et al., 2010, 2013
Teraterpeton hrynewichorum	Sues, 2003
Trilophosaurus buettneri	Hundreds of specimens from TMM, largely TMM 31025-140
Trilophosaurus jacobsi	Hundreds of specimens from NMMNH; Spielmann et al., 2008
Uromastyx sp.	complete skeleton in Stony Brook University comparative anatomy collection; El-Toubi, 1949
Youngina capensis	BP/1/375, BP/1/2871; Gow; 1975; Currie, 1981; Gardner et al., 2010

a terminal taxon *Proterosuchus* based on all of the *Proterosuchus* spp. from the *Lystrosaurus* AZ of South Africa, following the previous work of Nesbitt et al. (2009), Nesbitt (2011), and Pritchard et al. (2015). We also scored only the holotype of *Proterosuchus alexanderi* as a terminal taxon (see appendix 3). Our discussion of apomorphies is based on the composite terminal taxon *Proterosuchus* only, although we ran *Proterosuchus alexanderi* in place of the broader composite *Proterosuchus* in our analysis (see below). Our ingroup thus consisted of 28 taxa, with *Petrolacosaurus kansensis* designated as the outgroup. The use of *P. kansensis* as an outgroup was chosen because (1) it is almost completely represented anatomically, by many individuals (Reisz, 1981), (2) it is clearly an early diapsid outside of the saurian split (Reisz, 1981; Müller, 2004; Ezcurra et al., 2014), and (3) it is used as an outgroup in other studies focusing on the relationships of Archosauromorpha (e.g., Dilkes, 1998).

Taxon scoring is based on firsthand observations, published morphological descriptions, and photos taken by the authors (see table 11). Nearly every specimen discussed has been observed (and photographed) by one of the authors over the past

five years. Descriptions of those taxa not previously included in phylogenetic analyses are provided in appendix 3.

Character sampling includes the 200 archosauromorph characters from Pritchard et al. (2015) combined with additional archosauromorph characters from previous diapsid datasets (Juul, 1994; Gower and Sennikov, 1996; 1997; Dilkes, 1998; Nesbitt et al., 2009; Nesbitt, 2011, Ezcurra et al., 2010), as well as characters employed here for the first time. Novel characters are described in appendix 4. In total, 247 skeletal characters were scored over the taxa considered (appendix 5). The dataset is available online (http://morphobank.org/927) on MorphoBank (O'Leary and Kaufman, 2012).

TREE SEARCH STRATEGY: Phylogenetic analysis was performed using the Tree Analysis using New Technology software package (TNT) v. 1.1 (Goloboff et al., 2003; 2008). We used a heuristic search (1000 replicates of Wagner trees, using random addition sequences), followed by tree bisection and reconnection (TBR), holding 10 trees per TBR replicate. Zero-length branches were collapsed if they lacked support under any of the most parsimonious reconstructions. As a confirmatory test, the phylogenetic analysis also was run in PAUP* version v4.0b1 (Swofford, 2002) using heuristic searches with 10,000 random addition replicates. Nodal support was assessed using nonparametric bootstrapping (1000 pseudoreplicates, TBR branch swapping, and 1000 random addition sequences), and decay indices (= Bremer support values) were calculated manually in PAUP* by accepting trees progressively longer than the maximally parsimonious one identified in the original analysis (e.g., >618 steps); consensus trees were produced from the results of each of these runs. Consistency (CI) and retention (RI) indices were calculated in PAUP*. Characters 2, 5, 10, 11, 20, 32, 52, 72, 204, and 212 were ordered, given that these multistate characters represent potential nested sets of character states. Our tree structure is not dependent on ordering these characters (i.e., the resultant most parsimonious trees are the same when these characters are ordered or not). The results from TNT and PAUP were identical.

RESULTS AND DISCUSSION

Our phylogenetic analyses of early Archosauromorpha yielded a single, maximally parsimonious tree (tree length = 616 steps; CI = 0.422; RI = 0.624) *Azendohsaurus madagaskarensis* is robustly supported as an archosauromorph falling outside Archosauriformes (fig. 72), and hence also far outside Dinosauria, differing from earlier hypotheses on the relationships of *Azendohsaurus* (Gauffre, 1993; Flynn et al., 1999) but consistent with a previous study of craniodental evidence alone for *A. madagaskarensis* (Flynn et al., 2010). Our analysis identified the following cranial features (or complexes) as plesiomorphic retentions that clearly exclude *Azendohsaurus madagaskarensis* from Archosauria (and, by extension, Dinosauria): presence of an extensive dentition on all elements of the palate (chars. 47–51); the presence of a pineal foramen (22-0); the absence of an external mandibular fenestra (84-0); the absence of an antorbital fenestra (13-0); an incomplete lower temporal bar (32-1); teeth ankylosed to their bone of attachment (= ankylothecodont) (97-1). As predicted earlier (Flynn et al., 2010), the lack of an antorbital fenestra and an incomplete lower temporal bar exclude *A. madagaskarensis* from Archosauriformes. The following plesiomorphic character states (or complexes) of the postcranium clearly exclude *A. madagaskarensis* from Archosauria: presence of a nearly full set of carpals (nine elements total); a femur with a large attachment for the caudifemoralis muscles near the proximal surface (= internal trochanter); a foramen formed between the astragalus and calcaneum when in articulation; and four distal tarsals. Collectively, these cranial and postcranial data, convincingly place *A. madagaskarensis* as an early diverging member of Archosauromorpha outside Archosauriformes.

The wealth of anatomical data now available for *A. madagaskarensis* has helped identify new phylogenetically meaningful characters, strengthened previous hypotheses of relationships among early archosauromorphs, and provided several unanticipated insights. In particular, *Azendohsaurus*-like taxa were found to be closely related to *Trilophosaurus*-like taxa, a pairing not predicted by

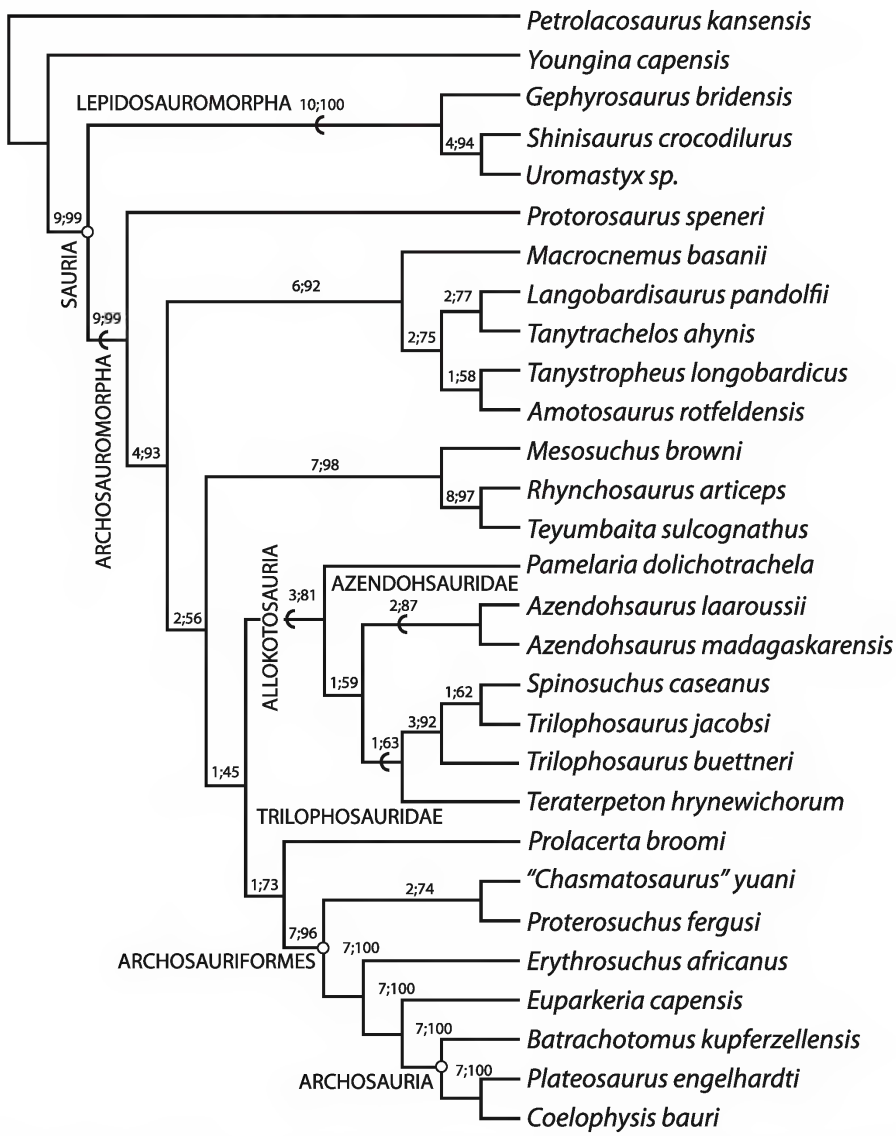

Fig. 72. The results of the phylogenetic analyses of early Archosauromorpha incorporating *Azendohsaurus madagaskarensis*. The analysis obtains a unique tree (tree length = 616 steps; CI = 0.422; RI = 0.624) with support values indicated (left number = Bremer support: left number = bootstrap values).

prior analyses of cranial evidence, even though some resemblances were noted previously (Flynn et al., 2010). This clade, here named Allokotosauria (see above), is in turn closely related to Archosauriformes (fig. 72). This phylogenetic arrangement has a subtle effect (e.g., clade relationships, character support) on the remainder of the archosauromorph tree. As in the initial application of the bulk of this archosauromorph dataset in Pritchard et al. (2015), and those of other datasets (e.g., Dilkes, 1998), the monophyly of Lepidosauromorpha, Tanystropheidae, Rhynchosauria, Trilophosauridae (in Pritchard et al., 2015), and Archosauriformes are relatively well supported to strongly supported (Bremer = 2–10), but relationships among these clades are somewhat more tenuous (Bremer = 1–4). Our results are generally congruent with the results obtained

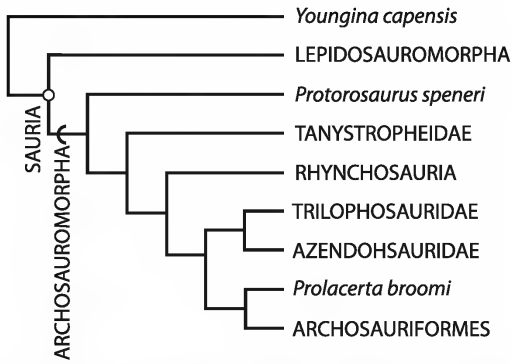

Fig. 73. The relationships of the major clades of early archosauromorphs found in the analyses of this study.

by Pritchard et al. (2015) except for the positions of Tanystropheidae and Rhynchosauria. In the present analysis, Rhynchosauria is more closely related to Archosauriformes than is Tanystropheidae, although with weak support (Bremer = 1) whereas Pritchard et al. (2015) found the reverse (fig. 73).

Our higher-level phylogeny generally agrees with the findings of Dilkes (1998), with one prominent exception. Dilkes (1998) found *Trilophosaurus* to be the proximal outgroup of Rhynchosauria + *Prolacerta* + Archosauriformes, whereas here *Trilophosaurus* is much more closely related to Archosauriformes (figs. 72, 73). It may be noted that our association of *Trilophosaurus* as a near outgroup to Archosauriformes is maintained even if the other taxa that form the Allokotosauria clade with *Trilophosaurus* (*Azendohsaurus madagaskarensis*, *A. laaroussii*, and *Pamelaria dolichotrachela*) are excluded from the analysis. Without inclusion of these three taxa, however, Rhynchosauria falls outside Tanystropheidae + Archosauria. Furthermore, even if all of the taxa (except lepidosauromorphs and archosauriforms) that were not considered in or were unknown to Dilkes (1998) are excluded, our analysis still yields a pairing of *Trilophosaurus* with Archosauriformes to the exclusion of Rhynchosauria. In this variation of the analysis excluding other allokotosaurians, Rhynchosauria, Tanystropheidae, and *Trilophosaurus* + *Prolacerta* + Archosauriformes form a polytomy, with *Protorosaurus speneri* as its nearest outgroup. Comparisons of our full higher-level phylogenetic results for archosauromorphs with that of Dilkes (1998) highlight the instability of current understanding of the interrelationships of Allokotosauria, Archosauriformes, Rhynchosauria, and Tanystropheidae.

Although our analysis identified *Prolacerta broomi* as the proximal outgroup of Archosauriformes, as did those of Dilkes (1998), followed by Modesto and Sues (2004), Gottmann-Quesada and Sanders (2009), and Pritchard et al. (2015), we note that this phylogenetic arrangement is poorly supported, requiring the acceptance of only one additional step to force *P. broomi* as the outgroup of Allokotosauria + Archosauriformes. In our analysis, the only nonhomoplastic character state supporting *P. broomi* + Archosauriformes is the posteriormost extent of the dentary positioned ventral to the surangular rather than on the dorsal margin of the mandible (246-1). Other character support for the clade of *P. broomi* + Archosauriformes is the presence of recurved (91-1), mediolaterally compressed teeth (98-1). The distribution of recurved, mediolaterally compressed teeth among reptiles is complex, however; teeth of this form occur in the outgroups Sauria and *Protorosaurus speneri*, within Tanystropheidae, and in Azendohsauridae, but are absent in Trilophosauridae and Rhynchosauria. Given the inarguable homoplasy of this tooth form across Reptilia, tooth morphology constitutes relatively weak support for the pairing of *P. broomi* and Archosauriformes, although parsimony results indicate that this is an unambiguous synapomorphy for that clade. The position of Archosauriformes closer to *Prolacerta broomi* than to *Azendohsaurus* has interesting implications. For example, *Azendohsaurus* and Archosauriformes both have serrated marginal teeth, but *P. broomi* does not. This implies a "reversal" of the condition in *P. broomi* (from an ancestor with serrated teeth), or the convergent acquisition of serrated teeth in *Azendohsaurus* and Archosauriformes. Similarly, *A. madagaskarensis* and Archosauriformes share an ossified laterosphenoid, a feature lacking in *P. broomi* and *T. buettneri*.

Additionally, determining the phylogenetic position of *Prolacerta broomi* is further

complicated by taxon sampling. For example, we used the newly erected taxon *Proterosuchus alexanderi* (sensu Ezcurra and Butler, 2015) based on NMQR 1484 in place of *Proterosuchus*, which was also based on NMQR 1484 and other specimens attributed to the genus. All the scores are the same except that *Proterosuchus alexanderi* has fewer characters scored because of the lack of appendicular elements, the premaxilla, and a few other anatomical elements. When we used *Proterosuchus alexanderi* in our phylogenetic analysis, we obtained two most parsimonious trees (instead of a unique tree) with the same tree length (616) and other scores (RI and CI) as the tree including only *Proterosuchus*. The difference in the phylogenetic analysis that includes *Proterosuchus alexanderi* is the position of *Prolacerta broomi*; it is either the sister taxon to Archosauriformes (as found above when all taxa are included) or as the sister taxon of Allokotosauria + Archosauriformes (when *P. alexanderi* is excluded).

Clearly, *P. broomi* is crucial for understanding archosauriform relationships, yet our understanding of character distribution in this part of the tree is far from certain. The phylogenetic uncertainty in this portion of the tree is not caused by missing character data in *P. broomi*, but instead demonstrates the rampant character homoplasy that occurred among these early forms. Additionally, the variation of phylogenetically crucial morphological features (e.g., presence or absence of a pineal foramen) within *P. broomi* is poorly understood (Bhullar et al., 2011) and has led to inconsistencies in scoring the taxon into phylogenetic matrices.

Below, we present unambiguous synapomorphies and possible synapomorphies (contingent on whether character evolution is optimized using ACCTRAN or DELTRAN) diagnosing the major clades just outside and within Allokotosauria, with an emphasis on those features for which study of *A. madagaskarensis* has contributed new phylogenetic information. Ambiguous synapomorphies are included in the discussion largely because their uncertain optimizations often reflect missing data rather than character conflict, and may therefore be of use in future analyses with more complete character sampling. Unambiguously optimized characters denoted by an asterisk are those with low occurrences of homoplasy (a high consistency index) among Triassic archosauromorphs.

Allokotosauria and Early Archosauromorpha: Tree Topology and Clade Support

Figure 74

Allokotosauria + (*Prolacerta* + Archosauriformes) (Bremer = 1)

Support: Unambiguous synapomorphies include: pubic apron present, with distinct anteroventral downturn of the symphyseal region (173-0*); medial surface of the tibial condyle of the femur is triangular and sharply pointed (182-1); ventral surface of the fibular (= medial) condyle of the femur rounded and moundlike (183-1).

Other potential synapomorphies: **ACCTRAN:** Exoccipitals contact on floor of foramen magnum (61-1); serrations of the marginal dentition present (90-1); manual ungual distinctly longer than the last phalanx of the same digit (222-1); prominent ridge separates tibial and fibular facets from anterior hollow in the astragalus (239-1); distal half of the posterior margin of the quadrate convex (242-1). **DELTRAN:** Ventral ramus of the opisthotic expanded ventrally into a club shape (57-1); foramen positioned directly anterolateral to glenoid fossa on the lateral surface of the surangular (81-1); posterior articular surfaces of the presacral vertebrae concave (102-1); costal facets of the posterior trunk vertebrae inverted L-shape (123-1).

Discussion: As with other subgroups of early archosauromorphs, the phylogenetic position of the newly recognized and named Allokotosauria within Archosauromorpha is contentious. The present analysis yielded a close relationship between Allokotosauria and *Prolacerta broomi* + Archosauriformes. As mentioned above, support for the major internodes (= the backbone) of Archosauromorpha is sparse; the acceptance of just one or two steps beyond the minimum (618) renders a polytomy of all major archosauromorph subgroups sampled here. The character state that clearly supports this clade in our analysis is the presence of an anteroventral

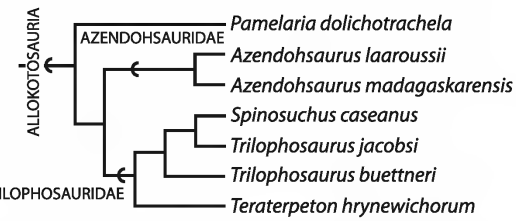

Fig. 74. The relationships of Allokotosauria found in the analyses of this study.

directed pubic apron (173-0). The significance of most other character states for resolving the phylogeny, both unambiguous and ambiguous, is highly sensitive to taxon sampling.

Allokotosauria (Bremer = 3)

SUPPORT: Unambiguous synapomorphies include: prominent tubercle developed distal to glenoid fossa of the scapula (146-0); distal condyle morphology of the humerus has distinct trochlear and capitular articulations (156-0); ossified olecranon process of the ulna present (157-0); posterior side of the quadrate head expanded and hooked (207-1)*; lateral surface of the orbital margin of the frontal rugose (237-1)*.

Other possible synapomorphies: **ACCTRAN:** Pineal foramen position within the frontoparietal suture (23-1); medial process of the postorbital situated deep to the postfrontal (27-0); supratemporals absent (36-0); tympanic crest of the quadrate absent (43-0); one field of dentition on the anterior process of the pterygoid (49-0); paroccipital contribution of the prootic contributes laterally tapering lamina to the anterior surface of the prootic (75-1); distinct depression on the ventral surface of the parabasisphenoid (68-2); chevron shaft maintains breadth along its length (136-1); marked expansion of the posterior stem of the interclavicle (144-1); medial centrale of manus present (158-1); prominent, bulbous rugosity superior to acetabulum of the ilium (167-1); primordial sacral rib one is longer anteroposteriorly than primordial sacral rib two (216-0); lateral and medial sides of the distal pedal phalanges converging anteriorly (234-1); gastralia small in number (= well separated) (238-1). **DELTRAN:** Anterior margin of neural spine of the anterior postaxial cervical vertebrae inclined anterodorsally (116-1); posteriorly pointed projections (epipophyses) present on the dorsal surface of postzygapophyses cervical vertebrae (119-1); two (dichocephaly) pectoral costal facets in the anterior trunk vertebrae (122-1); neural spines of the anterior caudal vertebrae inclined posteriorly (217-0); manual ungual distinctly longer than the last phalanx of the same digit (222-1).

DISCUSSION: Our most parsimonious tree provides the following topology for interrelationships of taxa within Allokotosauria: ((Trilophosauridae, Azendohsauridae), *Pamelaria dolichotrachela*) (figs. 71, 73).

Although Allokotosauria is diagnosed by a large number of characters (five unambiguous, and many ambiguous [some only in ACCTRAN and others only in DELTRAN] optimizations), we consider the group's monophyly well supported but still open to question, as more than half of the apomorphies diagnostic of Allokotosauria represent "reversals" to more plesiomorphic character states typical of Sauria (e.g., ossified olecranon process of the ulna present). On the other hand, two character states that are unambiguously diagnostic of the clade (posterior side of the quadrate head expanded and hooked 207-1; lateral surface of the orbital margin of the frontal rugose 237-1) occur uniquely within this clade among archosauromorphs, providing unequivocal support for this hypothesis of relationships.

Character states ambiguously diagnosing Allokotosauria include a distinct depression on the ventral surface of the parabasisphenoid (68-2) and a manual ungual distinctly longer than the last phalanx of the same digit (222-1).

Within Allokotosauria, the optimization of the following character states is ambiguous because the characters cannot be scored in *Pamelaria dolichotrachela*: supratemporals absent (36-0); marked expansion of the posterior stem of the interclavicle (144-1); lateral and medial sides of the distal pedal phalanges converging anteriorly (234-1); and gastralia low in number (= well separated) (238-1). Nevertheless, these four derived character states are uniformly present in all members of Allokotosauria that can be scored, and serve as potential diagnostic synapomorphies for the clade or for a subclade within it that excludes *P. dolichotrachela*.

Azendohsauridae + Trilophosauridae
(Bremer = 1)

SUPPORT: Unambiguous synapomorphies include: prominent postglenoid process on coracoid, terminating in thickened margin (148-1*); entire anterior margin of scapula markedly concave (219-1*); constricted scapula blade, the anteroposterior length of the constriction less than one-quarter the proximodistal length of the scapula (220-1*); ventral tubercle of the pedal (or manual) ungual well developed and extended ventral to the articular portion (233-1*); anteroventrally deflected anterior end of the dentary (241-1*); atlas centrum fused to axial intercentrum (243-1*).

Other possible synapomorphies: **ACCTRAN**: Parabasisphenoid, orientation more vertical (208-1). **DELTRAN**: Medial process of the postorbital situated deep to the postfrontal (27-0); supratemporals absent (36-0); tympanic crest of the quadrate absent (43-0); one field of dentition on the anterior process of the pterygoid (49-0); exoccipitals and opisthotic fused (62-1); paroccipital contribution of the prootic contributes laterally tapering lamina to the anterior surface of the paroccipital process (75-1); medial centrale of manus present (158-1); lateral and medial sides of the distal pedal phalanges converging anteriorly (234-1); gastralia small in number (= well separated) (238-1).

DISCUSSION: Within Allokotosauria, Trilophosauridae and Azendohsauridae form a pairing. This relationship, despite being poorly supported by decay indices, is supported by a number of unambiguous character states that can be scored in the nearest outgroup, *Pamelaria dolichotrachela.* For example, *A. madagaskarensis* and *Trilophosaurus* share a very long postglenoid process of the coracoid (148-1), a feature clearly absent in *Pamelaria dolichotrachela* (fig. 72). The scapulae of *A. madagaskarensis* and *Trilophosaurus* are tall relative to their widths and have highly constricted shafts, whereas the scapula of *P. dolichotrachela* (Sen, 2003) is proportionally shorter and more similar to that of the outgroup taxon *Prolacerta broomi* (BP/1/2675). The atlas centrum is fused to the axial intercentrum in *A. madagaskarensis* and *Trilophosaurus*, but is clearly separate in *P. dolichotrachela* (Sen, 2003). *Azendohsaurus madagaskarensis* and *Trilophosaurus* share large unguals with prominent ventral tubercles, whereas the ungual tubercle of *P. dolichotrachela* (Sen, 2003) is small. *Azendohsaurus, Trilophosaurus,* and *Teraterpeton hrynewichorum* share an anteroventrally deflected anterior end of the dentary, whereas the anterior portion of the dentary of *P. dolichotrachela* (Sen, 2003) is horizontal. Lastly, the presence of epipophyses on the cervical postzygapophyses of *A. madagaskarensis* and *Trilophosaurus*, and the plesiomorphic absence of epipophyses in *P. dolichotrachela*, also unites Azendohsauridae + Trilophosauridae to the exclusion of *P. dolichotrachela*, even though this is not a character state optimized outside Azendohsauridae + Trilophosauridae because of a complex distribution as a result of homoplasy and missing data.

Although *Pamelaria dolichotrachela* is identified as the nearest outgroup of Trilophosauridae + Azendohsauridae, curiously a number of derived character states occur in Azendohsauridae and *Pamelaria dolichotrachela* to the exclusion of trilophosaurids, apparently homoplastically (see below).

Azendohsauridae = *Azendohsaurus*
(currently *A. madagaskarensis* + *A. laaroussii*)
(Bremer = 2)

SUPPORT: Unambiguous synapomorphies include: prominent anteroposteriorly oriented ridge present on the medial surface of the maxilla (201-1*); dorsal apex of the maxilla is a separate, distinct process having a posteriorly concave margin (202-1*); crown height of the upper dentition is lower than that of the lower dentition (211-1*).

Other possible synapomorphies: **ACCTRAN:** Nasal oriented parasagitally at contact with prefrontal (9-0); pineal foramen present (22-0); posterior process of the postorbital contributes to more than one-half the length of the supratemporal bar (28-1); anteroposteriorly slender descending process of the squamosal (34-1); posterior margin of quadrate straight and vertical (41-0); internal carotids appear not to enter braincase (67-2); basipterygoid processes of

the parabasisphenoid oriented anterolaterally (70-0); laterosphenoid ossification present but fails to reach the ventral surface of frontals (72-1); retroarticular process absent (86-1); ribs fused on the posteriormost trunk vertebra (124-1); neural spines of the trunk vertebrae long and low, lesser in dorsoventral height than anteroposterior length (129-1); chevrons broaden distally, forming subcircular expansion (136-3); proximal end of head of the femur well ossified and convex (178-0); internal trochanteric crest of the femur does not reach proximal surface of femoral head (179-0); pedal centrale absent as distinct ossification, fused to astragalus (184-0); ventrolateral margin of the lateral process of the calcaneum "curls" externally (190-1); transverse width of the distal end of the humerus equal to or greater than 2.5 times the minimum width of the shaft (221-1). **DELTRAN**: Anterodorsal process (= nasal process) of the premaxilla absent, creating a confluent external naris (3-1); marginal dentition serrated (90-1); Interdental plates present in the marginal dentition (96-1).

DISCUSSION: The two members of Azendohsauridae, *Azendohsaurus madagaskarensis* and *A. laaroussii,* are obviously closely related. Both taxa share a prominent anteroposteriorly oriented ridge on the medial surface of the maxilla, a "pseudoantorbital fenestra" where the dorsal apex of the maxilla forms a separate, distinct process with a posteriorly concave margin, and a distinct difference in crown height between the upper and lower dentitions as well as other characters noted as unambiguous or ambiguous synapomorphies (fig. 7). These taxa likely share many additional character states exclusive of those that are present in other archosauromorphs, but *A. laaroussii* is currently described on the basis of only a few elements (e.g., teeth, maxilla, dentary) even though postcrania are preserved and under study by other investigators (Jalil and Knoll, 2002).

Our phylogenetic analysis identified *Pamelaria dolichotrachela* as the nearest outgroup of Azendohsauridae + Trilophosauridae, based on numerous character states (see above). Even so, a number of character states shared by *P. dolichotrachela* and *A. madagaskarensis* to the exclusion of Trilophosauridae emerged during construction of our data matrix. For example, *P. dolichotrachela* (Sen, 2003) and *A. madagaskarensis* lack an anterodorsal process (= nasal process) of the premaxilla (3-1). This character state is also present in rhynchosaurs, but the premaxillae of *P. dolichotrachela* (Sen, 2003) and *A. madagaskarensis* are nevertheless very similar in this respect. Furthermore, the marginal teeth of *P. dolichotrachela* (Sen, 2003) and *A. madagaskarensis* are serrated (90-1). Additionally, *P. dolichotrachela* (Sen, 2003) and *A. madagaskarensis* share a deep depression on the ventral surface of the basicranium that is restricted to the parabasisphenoid (68-2). Whereas serrated teeth and a deep depression on the ventral surface of the parabasisphenoid occur among some Archosauriformes, they occur infrequently outside that clade among archosauromorphs. The cervical vertebrae of *P. dolichotrachela* and *A. madagaskarensis* are similar in their dorsoventrally short neural spines and strong transverse waisting of the centra. Comparison of *P. dolichotrachela* and *A. madagaskarensis* is hampered, however, by our inability to score many skull characters for *P. dolichotrachela*, owing to poor preservation and high fracturing of the bone surfaces. To investigate this pairing further, we built a constraint tree in PAUP with *P. dolichotrachela* and *Azendohsaurus* as sister taxa and ran the analysis using the same methodology as stated above. As a result, the relationships of Allokotosauria remained the same, although some support values changed at the base of the clade and at Trilophosauridae. The constrained analysis added only two more steps over the original analysis, thus indicating that the phylogenetic position of *P. dolichotrachela* is poorly supported within Allokotosauria. Nonetheless, irrespective of which placement of *P. dolichotrachela* ultimately is most strongly supported, homoplasy of many craniodental features within Allokotosauria is unavoidable.

Trilophosauridae (Bremer = 1)

SUPPORT: Unambiguous synapomorphies include: postorbital, jugal, and squamosal fit against one another as a "lateral temporal plate" present, with squamosal extending anteriorly to slot into a notch on the jugal

(29-1*); ascending process of the jugal intersects between postorbital and squamosal within the supratemporal bar (31-1*); marginal dentition on anteriormost portions of premaxilla and dentary absent (88-1*); crowns of marginal teeth are flattened platforms bearing pointed cusps (93-1*); large anteriorly opening foramen on the anterolateral surface of the maxilla absent (203-1).

Other possible synapomorphies: **ACCTRAN:** Anterodorsal process (= nasal process) of the premaxilla present (3-0); paroccipital process of the opisthotic unflattened and tapered (63-0); parasphenoid crests absent such that a ventral floor of the vidian canal is lacking (66-0); distinct depression on the ventral surface of the braincase at the suture between the basioccipital and the parabasisphenoid (68-1); splenials contribute to mandibular symphysis (85-0); nonserrated marginal teeth (90-0); costal facets very closely appressed to one another with little or no finished bone separation in the anterior postaxial cervical vertebrae (112-1); transverse processes of the anterior caudal vertebrae perpendicular to the long axis of the vertebra (134-0); anterior surface anteromedial to clavicular articulations of the interclavicle smooth (143-0); entepicondylar crest of the humerus exhibits a prominently angled proximal margin (155-1); proximal postaxial margin of metatarsal V forms prominent, pointed process (196-1); postzygapophyses of the anterior cervical vertebrae (presacral vertebrae 3–5) connected through a horizontal lamina (= transpostzygapophyseal lamina) with a notch at the midline (213-1); posterior caudal vertebrae much longer than the anterior caudal vertebrae (218-1); penultimate phalanges of the pes significantly longer than the more proximal phalanges (235-1); tibial and fibular facets of the astragalus grade smoothly into the anterior hollow (239-0); midcaudal chevrons bears an anterior process resulting in an inverted-T shape (240-1); palatal process of the premaxilla present (247-1). **DELTRAN:** None.

Discussion: *Teraterpeton hrynewichorum*, *Trilophosaurus buettneri*, *Trilophosaurus jacobsi*,and *Spinosuchus caseanus* form a monophyletic group in our analysis (herein termed Trilophosauridae). The clade is poorly supported from the perspective of decay index (Bremer support), although *Te. hrynewichorum* and *Tr. buettneri* share a number unambiguous synapomorphies (as first hypothesized by Sues, 2003). Trilophosauridae is diagnosed by cranial character states of the maxilla and premaxilla (crowns of marginal teeth consist of flattened platform with pointed cusps [93-1]; marginal dentition on anteriormost portions of premaxilla and dentary absent [88-1]), and in the region posterior of the orbit (jugal and squamosal abut to form a "lateral temporal plate," with squamosal extending anteriorly to slot into a notch on the jugal [29-1]; ascending process of the jugal intersects postorbital and squamosal within the supratemporal bar [31-1]). Although no characters of the postcranium unambiguously diagnose Trilophosauridae, it is important to note that Sues's (2003) hypothesis is supported by the highly constricted scapula blade (220-1) shared by *Te. hrynewichorum* and *Tr. buettneri*.

Trilophosaurus (including *Spinosuchus caseanus*) (Bremer = 3)

Support: Unambiguous synapomorphies include: lacrimal limited to orbital margin (11-2*); coronoid process present (79-1*); tooth shape (marginal dentition) labiolingually wider than mesiodistally long at crown base (98-2*); posterior articular surface of the centrum of the presacral vertebrae convex (102-2*); diapophysis located in the anteroposterior middle of the neural arch/centrum in the trunk vertebrae (215-1*).

Other possible synapomorphies: **ACCTRAN:** Palatal teeth absent (44-1); posterior surface of the supraoccipital smooth (55-0); Shape of the supraoccipital pillarlike (56-1); angular exposure on lateral mandibular surface extends to the glenoid (83-1); Intercentra in the trunk vertebrae present (128-0). **DELTRAN:** Splenials contribute to mandibular symphysis (85-0); moderate development of posterior articular surface convexity of the presacral vertebrae (103-0); costal facets very closely appressed to one another with little or no finished bone separation in the anterior postaxial cervical vertebrae (112-1); entepicondylar crest of the humerus exhibits a prominently angled proximal margin (155-1); postzygapophyses of the

anterior cervical vertebrae (presacral vertebrae 3–5) connected through a horizontal lamina (= transpostzygapophyseal lamina) with a notch at the midline (213-1); posterior caudal vertebrae much longer than the anterior caudal vertebrae (218-1); penultimate phalanges of the pes significantly longer than the more proximal phalanges (235-1).

DISCUSSION: Because of its unusual dental anatomy, the relationships of *Trilophosaurus buettneri* have been hotly contested since its initial description from a partial maxilla (Case, 1928a, 1928b; Gregory, 1945; Romer, 1956; DeMar and Bolt, 1981; Carroll, 1988). Since the advent of cladistic analyses, *Trilophosaurus buettneri* has been consistently placed as a non-archosauriform archosauromorph (Gauthier et al., 1988b; Dilkes, 1998; Spielmann et al., 2008; Gottmann-Quesada and Sanders, 2009; Ezcurra et al., 2014; Pritchard et al., 2015), among various early diverging archosauromorph clades (Dilkes, 1998). Our analysis indicates a clear relationship between *Trilophosaurus* (and kin) and *Azendohsaurus*, and a fairly well-resolved placement for this clade outside Archosauriformes. The best-known trilophosaurid, *Trilophosaurus buettneri*, obviously embodies a bizarre mix of cranial features. This mix includes many unique character states (e.g., tricuspid teeth with a beaklike rostrum), plesiomorphic archosauromorph character states (e.g., lack of an antorbital fenestra), and characters present in archosaurs (e.g., complete loss of palatal dentition). Our examination of character state changes in the postcrania of allokotosaurs with regard to *T. buettneri* yielded unexpected results, particularly that the taxon's "lizardlike" features (e.g., long tail, elongated manus and pes, procoelous vertebrae, general "lizardlike" proportions: Gregory, 1945) all are autapomorphic, rather than retentions of plesiomorphic saurian conditions. Thus, *T. buettneri* and its closest relatives are even more specialized than previously suspected. In fact, most of the unique character states described originally by Gregory (1945) are now useful in grouping the closest relatives of *T. buettneri* into a monophyletic clade of basal archosauromorphs. We found that various character states, particularly in the teeth and skull, unite *T. buettneri* and *T. jacobsi*, and that additional postcranial character states unite *T. buettneri, T. jacobsi,* and *Spinosuchus caseanus*. Some postcranial character states shared by *T. buettneri, T. jacobsi,* and *S. caseanus* were originally detailed by Spielmann et al. (2009) but were not incorporated into a phylogenetic analysis. We tested these character states in a numeric phylogenetic analysis and found that a diapophysis located in the anteroposterior middle of the neural arch/centrum in the trunk vertebrae (215-1) was an unambiguous synapomorphy, but others detailed by Spielmann et al. (2009) (e.g., postzygapophyses of the anterior cervical vertebrae [presacral vertebrae 3–5] connected through a horizontal lamina [= transpostzygapophyseal lamina] with a notch at the midline [213-1]) were ambiguous synapomorphies, because they could not be scored in the closest outgroup, *Teraterpeton hrynewichorum*. Moreover, we identified two other potential "lizardlike" synapomorphies for *T. buettneri, T. jacobsi,* and *S. caseanus* that could not be scored in *Te. hrynewichorum*: posterior caudal vertebrae much longer than the anterior caudal vertebrae, and penultimate phalanges of the pes significantly longer than the more proximal phalanges.

The results of our phylogenetic analysis with *Trilophosaurus buettneri, Trilophosaurus jacobsi,* and *Spinosuchus caseanus* raised the question of whether *Trilophosaurus jacobsi* and *Spinosuchus caseanus* are in fact the same animal. Collectively a comparison of the holotypes of *Spinosuchus caseanus* and *Trilophosaurus jacobsi,* their cooccurrence at the Kahle *Trilophosaurus* Quarry, and our phylogenetic results suggest that *Trilophosaurus jacobsi* is a subjective synonym of *Spinosuchus caseanus*, which is discussed next.

The absence of overlapping elements between the holotypes of *Spinosuchus caseanus* (UMMP 7507) and *Trilophosaurus jacobsi* (MNA V3192) complicates our proposed synonymy. The holotype of *Spinosuchus* consists of an axial column, and the holotype of *Trilophosaurus jacobsi* is an anterior portion of the maxilla with four teeth, three partial and one nearly complete (Murry, 1987). Our case for synonymy thus hinges on correct referral of skeletal elements

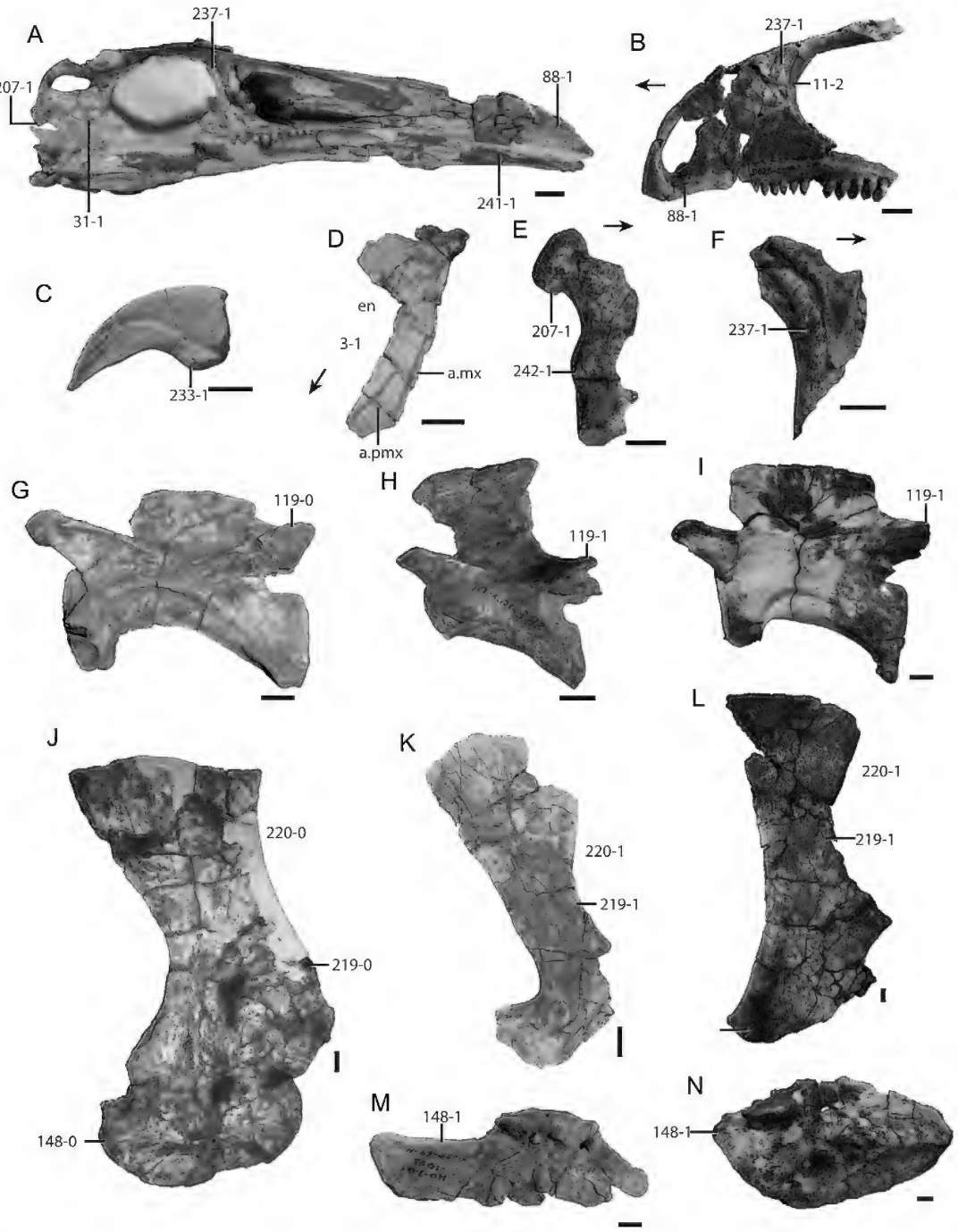

Fig. 75. Selected characters states supporting Allokotosauria and clades within Allokotosauria. (**A**) The skull of *Teraterpeton hrynewichorum* (NSM 999GF041) in right lateral view. (**B**) Anterior portion of the skull of *Trilophosaurus buettneri* (TMM 31025-207) in left lateral view. (**C**) Pedal ungual of *Azendohsaurus madagaskarensis* (FMNH PR 3815) in lateral view. (**D**) Left nasal of *Azendohsaurus madagaskarensis* (FMNH PR 2785) in dorsolateral view demonstrating the confluent external naris. (**E**) Right quadrate of *Azendohsaurus madagaskarensis* (FMNH PR 2751) in lateral view. (**F**) Right prefrontal of *Azendohsaurus madagaskarensis* (FMNH PR 2751) in lateral view. (**G**) Anterior cervical vertebra of

not represented in the holotypes; these referrals are based on direct association or particular apomorphies identified over the course of this comparative anatomical and phylogenetic analysis.

Perhaps the strongest evidence that *Spinosuchus caseanus* and *Trilophosaurus jacobsi* represent the same taxon comes from their cooccurrence at Kahle *Trilophosaurus* Quarry in the Tecovas Formation of the Dockum Group (Borden County, Texas) (they also cooccur at other localities, e.g., at Rotten Hill in the Tecovas Formation of the Dockum Group, northern Texas [Spielmann et al., 2013].) Tooth-bearing elements and teeth from the Kahle *Trilophosaurus* Quarry were assigned to *Trilophosaurus* Heckert et al., 2001), and subsequently to *Trilophosaurus jacobsi* (Heckert et al., 2006). Nearly all the postcranial material from the Kahle *Trilophosaurus* Quarry found alongside the tooth-bearing elements referred to *Trilophosaurus jacobsi* were referred to the same taxon (Heckert et al., 2006; Spielmann et al., 2008), largely because of the similarity of these postcrania to those of *Trilophosaurus buettneri* from the Otis Chalk quarries in Howard County, Texas (Gregory, 1945). *Trilophosaurus jacobsi* is currently known from hundreds of elements, including cranial material, forelimbs, hindlimbs, pectoral and pelvic girdles, and vertebrae. Other than reptile teeth clearly not belonging to *T. jacobsi* (Heckert et al., 2001), the only tetrapod elements from the Kahle *Trilophosaurus* Quarry not identified as *T. jacobsi* are vertebrae bearing tall neural spines. These vertebrae were assigned to *Spinosuchus caseanus* (Heckert et al., 2001; Spielmann et al., 2009). Justification for the assignment of these elements to *S. caseanus* is clearly spelled out by Spielmann et al. (2009). In sum, all tooth-bearing elements from these deposits that can be compared directly to *T. jacobsi*, and all *Trilophosaurus*-like postcrania, historically have been assigned to *T. jacobsi,* whereas vertebrae with tall neural spines have been assigned to *S. caseanus.*

Few vertebrae from the Kahle *Trilophosaurus* Quarry have been assigned to *Trilophosaurus jacobsi* (see Spielmann et al., 2008) whereas all the complete or nearly complete vertebrae (with tall neural spines) are assigned to *Spinosuchus caseanus*. On the other hand, none of the *Trilophosaurus buettneri*–like postcrania have been assigned to *S. caseanus* even though Spielmann et al. (2009) convincingly argue that *S. caseanus* is closely related to *Trilophosaurus*. Here, we posit that all of the *Trilophosaurus*-like crania and postcrania assigned to *T. jacobsi*, and the vertebrae assigned to *S. caseanus*, pertain to a single species-level taxon. In other words, *T. jacobsi* and *S. caseanus* represent the same species, and given the rules of priority, all this material from the Kahle *Trilophosaurus* Quarry should be assigned to *S. caseanus.*

To further test our proposition that the *Trilophosaurus*-like elements from the Kahle *Trilophosaurus* Quarry represent a single taxon (*Spinosuchus caseanus*), we scored the holotype of *S. caseanus,* and all the Kahle *Trilophosaurus* Quarry elements referred to *T. jacobsi* by Spielmann et al. (2008) or to *S. caseanus* by Spielmann et al. (2009) as three separate terminal taxa. A similar method has been used to test the synonymy of the "*Chatterjeea elegans*" and *Shuvosaurus inexpectatus* (Nesbitt and Norell, 2006; Nesbitt, 2007).

Our phylogenetic analysis identified *S. caseanus* and *T. jacobsi* as nearest relatives (fig. 72); both are scored identically in our data matrix, sharing one unique character state (spinopostzygapophyseal laminae present on the posterior edge of the neural arch of

←

Pamelaria dolichotrachela (ISRI 316/9) in lateral view. (**H**) Anterior cervical vertebra of *Trilophosaurus buettneri* (TMM 31025-46) in lateral view. (**I**) Anterior cervical vertebra (reversed) of *Azendohsaurus madagaskarensis* (FMNH PR 2791) in lateral view. (**J**) Right scapulocoracoid of *Pamelaria dolichotrachela* (ISRI 316/47) in in lateral view. (**K**) Right scapula of *Trilophosaurus buettneri* (TMM 31025-68R) in lateral view. (**L**) Left scapula (reversed) of *Azendohsaurus madagaskarensis* (FMNH PR 2798) in lateral view. (**M**) Right coracoid of *Trilophosaurus buettneri* (TMM 31025-69h) in lateral view. (**N**) Left coracoid (reversed) of *Azendohsaurus madagaskarensis* (FMNH PR 3822) in lateral view. Scales = 1 cm. Arrows indicate anterior direction. Abbreviations: **a.,** articulates with; **en,** external naris; **mx,** maxilla; **pmx,** premaxilla.

most presacral vertebrae [245-1]), a feature absent in *T. buettneri*.

If our hypothesized synonymy is correct, *Spinosuchus caseanus* is more abundant in the Upper Triassic of the southwestern United States than previously recognized. The taxon would now be known from the Chinle Formation in Arizona (*Placerias* Quarry UCMP A269, holotype of *T. jacobsi* MNA V3192), possibly the Chinle Formation of New Mexico (NMMNH Locality 2739, NMMNH P-34448), and potentially over a substantial stratigraphic range in the Dockum Group (MOTT VPL 3869, TTU-P10413). Even accepting this proposed range extension, secure occurrences of *S. caseanus* in the Revueltian land-vertebrate faunachron are lacking (Lucas, 1998).

Implications for the Divergence of Archosauromorpha

All recent phylogenetic analyses concur that the origin and lineage diversification of early archosauromorphs occurred prior to the end of the Permian (e.g., Dilkes, 1998; Muller, 2004; Nesbitt, 2011; Butler et al., 2011; Ezcurra et al., 2014). This is well supported, given that Archosauriformes, represented by *Archosaurus rossicus*, diverged from the rest of Archosauromorpha by the end of the Permian (Tatarinov, 1960; Nesbitt, 2011; Ezcurra et al., 2014). This divergence indicates that all successive outgroups to Archosauriformes (e.g., Rhynchosauria, Tanystropheidae) were also present by that time. Regrettably, the fossil record of archosauromorphs prior to the Triassic is exceptionally poor (Ezcurra et al., 2014). Not only is the record highly fragmentary, anatomical evidence of phylogenetic character transformations (or plesiomorphies) at the base of Archosauromorpha and along the spine leading to Archosauriformes is extremely limited. Consequently, it is difficult to understand whether the subgroups of archosauromorphs form successive outgroups (see Dilkes, 1998) or some of the subgroups pair with each other (e.g., the proposed affiliation of Rhynchosauria and Trilophosauridae by Merck, 1997).

This uncertainty, in turn, raises a number of other questions including: How many archosauromorph subgroups crossed the Permian-Triassic boundary and when did the highly disparate subgroups of archosauromorphs diversify and transform into the strange animals that appear in the Middle or Late Triassic? Answering these questions requires a much broader evaluation and more complete taxon sampling than is possible here, but the new anatomical and phylogenetic information gleaned from *Azendohsaurus madagaskarensis* provides important clues toward unraveling this puzzle. The phylogenetic conclusions presented here suggest that Tanystropheidae, Rhynchosauria, Archosauriformes, *Prolacerta broomi*, and Allokotosauria (containing Azendohsauridae and Trilophosauridae) all crossed the Permian-Triassic (P-T) boundary. Although the number of crossing lineages proposed here is comparable to that suggested elsewhere (e.g., Dilkes, 1998), our study departs from its predecessors in comprehensiveness of the taxon and character analyses, as well as by placing *Trilophosaurus*/Trilophosauridae within a clade (Allokotosauria) that likely diversified by the end of the Middle Triassic based on current sampling of confirmed members of this clade. A recent report on the possibility of Early Triassic trilophosaurids from Russia (Arkhangelskii and Sennikov, 2008) suggests that Trilophosauridae is much older than all other records for this clade. Although their report is intriguing, at this time we limit our analysis to the confirmed trilophosaurid forms with crania and postcrania. Nevertheless, the ghost lineage leading to *Trilophosaurus* originated in the Permian according to Dilkes (1998), but here we suggest that this ghost lineage is much shorter, and likely confined to the Triassic. Incorporating late Middle Triassic–aged *A. madagaskarensis* into the archosauromorph tree truncates the long *Trilophosaurus* ghost lineage hypothesized in previous analyses (e.g., Dilkes, 1998).

Moreover, the beautifully represented and almost completely sampled skeleton of *A. madagaskarensis* helps lessen the morphological gap between *Trilophosaurus* and other archosauromorphs in two respects. First, *A. madagaskarensis* helps demonstrate that *Trilophosaurus* is more closely related to the "protorosaur" *Pamelaria dolichotrachela*

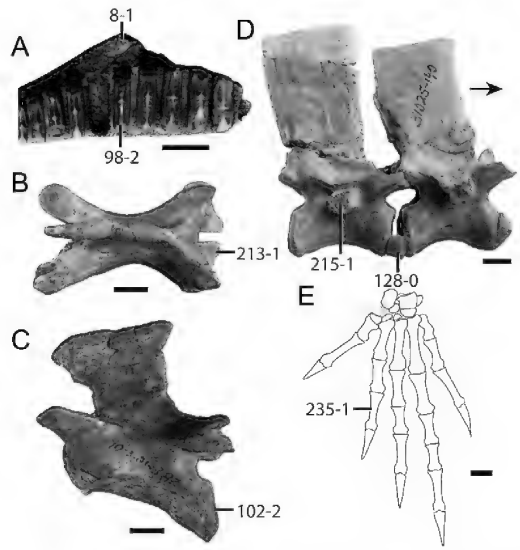

Fig. 76. *Trilophosaurus* character states (including *Spinosuchus caseanus*). (**A**) Maxilla of *Trilophosaurus buettneri* (TMM 31025-207) in ventral/occlusial view. Anterior cervical vertebra of *Trilophosaurus buettneri* (TMM 31025-46) in (**B**) dorsal and (**C**) left lateral views. (**D**) Two articulated trunk vertebrae of *Trilophosaurus buettneri* (TMM 31025-140) in right lateral view. (**E**) Reconstruction of the left manus of *Trilophosaurus buettneri* in dorsal view (note, char. state 235-1 is for the pes, but the manus has the same char. state). Scales = 1 cm. Arrow indicates anterior direction.

than previously thought, and, thus, that the autapomorphic body plan of *Trilophosaurus* does not stretch into the Permian, but instead is derived within the Triassic from a "protorosaur"-like common ancestor with other allokotosaurs. This further supports the polyphyly of "protorosaurs" (= prolacertiforms) and illustrates that "protorosaurs" possess a plesiomorphic archosauromorph body plan rather than a derived one. Second, the close relationship of *A. madagaskarensis* and *Trilophosaurus* (with *Pamelaria dolichotrachela* outside this clade) indicates that the "lizardlike" morphology of the skeleton of *Trilophosaurus* is independently derived from the plesiomorphic condition found in Sauria (see above). This highlights the tremendous disparity in body plans among even closely related Triassic archosauromorphs; the body plan of *Pamelaria dolichotrachela* resembles that of *Protorosaurus*, the body plan of *Trilophosaurus* resembles generalized squamates, and the body plan of *Azendohsaurus* is more similar to that of a sauropodomorph dinosaur (cranial features, elongated neck, large mani) than to any other early archosauromorph.

The age, geographic distribution, anatomical features, and phylogenetic information furnished by *A. madagaskarensis* has the following additional implications: (1) Allokotosauria diverged from other archosauromorphs by the end of the Permian; (2) the plesiomorphic (= *Protorosaurus*-like) body plan of Allokotosauria survived well into the Triassic; and (3) the sauropodomorph-like body plan of *Azendohsaurus* and "lizardlike" body plan of *Trilophosaurus* evolved by the end of the Middle Triassic. This great diversification in morphological disparity by the Middle Triassic is perhaps not unexpected given the rapid, almost simultaneous diversification of archosauriforms (Brusatte et al., 2011; Butler et al., 2011; Nesbitt, 2011) within five million years of the end-Permian extinction.

Convergence and the Prevalence of Herbivory in Triassic Archosauromorpha

We have previously noted the convergent similarities of skull morphology and form of the marginal teeth between *A. madagaskarensis* and early sauropodomorph dinosaurs (Flynn et al., 2010), many of which have been interpreted as herbivorous adaptations in early sauropodomorphs (Weishampel and Norman, 1989; Barrett, 2000; Sues, 2000; Goswami et al., 2005). For example, both *A. madagaskarensis* and early sauropodomorphs share convergences in marginal tooth crown structure and hemimandible architecture (see Flynn et al., 2010). As highlighted in the descriptions above, however, homoplasious similarities between *A. madagaskarensis* and early sauropodomorphs extend beyond craniodental features, occurring throughout much of the skeleton. In particular, the forelimbs of *Azendohsaurus* and sauropodomorphs are notably robust compared with those of their closest relatives; the humerus is relatively short with greatly expanded proximal and distal ends, the ulna and radius are

stocky, and the phalanges are short but bear large unguals. The presacral axial column is also similar in both taxa: the cervical series is elongate compared to the trunk series, and accessory intervertebral articulations (i.e., hypantrum-hyposphene) are present in much of the vertebral column. These strong convergences of the forelimb and axial column of *Azendohsaurus* and sauropodomorphs contrast with the remarkable dissimilarity of their hindlimbs. The hindlimb of *A. madagaskarensis* closely resembles that of lepidosauromorphs; the femur was held nearly horizontally and the complicated tarsus includes nine ossified elements. The hindlimbs of early sauropodomorphs were strikingly different in being vertically oriented directly beneath the pelvis and in having a simplified tarsus (four elements or fewer). Additionally, the tail of *Azendohsaurus* is much shorter (scaled for body size) than that of early sauropodomorphs (e.g., *Plateosaurus,* AMNH FR 6810). Thus, the convergences between *A. madagaskarensis* and early sauropodomorphs rest entirely within the skull and anterior half of the postcranial skeleton. The relatively large body size of *Azendohsaurus* is also unusual among early archosauromorphs and is even larger than most early diverging sauropodomorphs. Based on femoral length as a proxy body size (Carrano, 2006; Sookias et al., 2012; Turner and Nesbitt, 2013), *Azendohsaurus* (femoral length [FL] = 215 mm, table 7) was larger than all known early diverging sauropodomorphs from the Carnian (e.g., *Saturnalia tupiniqim*, FL = 157 mm) but is clearly smaller than Norian and younger sauropodomorphs (e.g., *Plateosaurus engelhardti*, FL = 750 mm). Nevertheless, the length and morphology of the elongated cervical vertebrae of *Azendohsaurus* are more similar to those of Norian sauropodomorphs than to the earliest diverging sauropodomorphs (e.g., *Eoraptor lunensis*, Sereno et al., 2013). Although early sauropodomorph dinosaurs were hypothesized to be the earliest high browsers, based on neck length and body size (Weishampel and Norman, 1989), the convergences with *Azendohsaurus* suggest that the high browser resource zone may have been already occupied by early archosauromorphs that diverged prior to the origin of dinosaurs. Alternatively, the sprawling posture of *Azendohsaurus* may have inhibited high browsing.

Extraordinarily, nearly all the craniodental and postcranial features identified in this study as having arisen convergently in *A. madagaskarensis* and early sauropodomorphs, are restricted to Azendohsauridae, and were not acquired sequentially in a stepwise pattern across more inclusive clades in Archosauromorpha. The divergent craniodental and anterior skeleton morphology in *Azendohsaurus* relative to other early archosauromorphs has a number of implications for the evolution of herbivory in early archosauromorphs, particularly within Allokotosauria. Three distinct craniodental character suites that occur within Allokotosauria possibly reflect divergent styles of herbivory: (1) the *Azendohsaurus* character suite (long, mediolaterally compressed crowns with denticles present throughout the dentary, premaxilla, and the maxilla), (2) the *Trilophosaurus* character suite (mediolaterally expanded teeth with distinct cusps, short edentulous portion in the anterior portion of the skull), and (3) the *Teraterpeton* character suite (bulbous teeth with an anterior cusp, long edentulous gap in the upper jaw and the mandible). Even within its relatively low taxonomic diversity, the craniodental disparity of Allokotosauria is extremely high, and the differences between these morphological suites are as profound as the variations in herbivorous features seen across Triassic archosaurs as a whole (e.g., aetosaurs versus silesaurids). Results from our phylogenetic analysis indicate that the three distinct craniodental suites in Allokotosauria are derived from a common herbivorous ancestor (see fig. 74). Nevertheless, the radically different dental specializations among the three terminal taxa make it unclear what pattern typified their common ancestor. This common ancestor may have borne none of the herbivorous traits present in any the three terminal taxa or it may have had a few of the character states from the distinct suites observed in the terminal taxa. However, their marked, unusual specializations have obscured the plesiomorphic anatomical condition or ancestral herbivorous character states in the common ancestor. Nevertheless, few discrete craniodental features correlated with

TABLE 12
Reinterpretation of the manus of *Trilophosaurus buettneri*

Gregory (1945) identifications	Revised identifications
radiale (?)	ulnare
intermedium	pisiform
ulnare	intermedium
centrale	lateral centrale
first distal carpal	first distal carpal
second distal carpal	second distal carpal
third distal carpal	secord distal carpal
fourth distal carpal	fourth distal carpal
fifth distal carpal	fifth distal carpal
missing	not ossified

an herbivorous diet are shared across the three lineages of allokotosaurs; the three distinct character suites are each unique among early archosauromorphs.

Timing of the acquisition of these suites is poorly constrained. *Azendohsaurus*, *Trilophosaurus*, and *Teraterpeton* appear in the fossil record during either the late Middle, or early Late Triassic (late Carnian or early Norian). The lack of terminal taxa having bridging suites of craniodental characters suggests two alternatives regarding the timing of the origin of these herbivorous specializations: (1) these lineages diverged during the Middle Triassic, and each of the three distinct craniodental suites arose quite rapidly; or (2) they diverged considerably earlier and intermediate forms simply have yet to be uncovered. Both scenarios seem equally plausible given the uncertainty surrounding the timing in the Triassic when these lineages diverged, and the currently poor sampling of early diverging, nonrhynchosaur archosauromorphs from the Early and Middle Triassic.

The considerations above regarding the origin of herbivory within Allokotosauria also shed light on shifts to herbivory in other Triassic archosauromoph subgroups. Our recovery of a clade of bizarre herbivores, Allokotosauria, demonstrates that herbivory among archosauromorphs was far more prevalent early in the Triassic than previously realized. Beyond the herbivorous groups that have been known for over a century (e.g., rhynchosaurs Huxley, 1869; Benton, 1983; aetosaurs, Agassiz, 1844, Walker, 1961; and sauropodomorphs von Meyer, 1861, Weishampel and Norman, 1989), a wealth of presumably herbivorous archosauromorphs have come to light from the Triassic in recent years (e.g., *Revueltosaurus callenderi*, Parker et al., 2005; silesaurids, Langer et al., 2010, Brusatte et al., 2010; and possibly shuvosaurids, Nesbitt and Norell, 2006), as have other postTriassic lineages (crocodylomorphs, Buckley et al., 2000). Additionally, taxa that have a typically "carnivorous" dentition such as *Protorosaurus speneri* have been found with plant fragments in their digestive track (Munk and Sues, 1993). We can now say with some confidence that within Archosauromorpha herbivorous specializations (see Barrett, 2000, and Zanno and Makovicky, 2011) arose at least seven times independently during the Triassic (in Rhynchosauria, Allokotosauria, *Revueltosaurus* + Aetosauria, silesaurids, silesaurids, sauropodomorphs, ornithischians).

The new data gleaned from *A. madagaskarensis* suggests that two episodes of multiple lineage shifts to herbivory may have occurred among amniotes. The first shift, during the early portion of the Middle Triassic, involved early-diverging archosauromorphs (rhynchosaurs, Allokotosauria), non-dinosaurian ornithodirans (silesaurids), and gomphodont cynodonts (Reisz and Sues, 2000). The second shift occurred by the end of the Carnian (Late Triassic), involving both dinosaurs and further diversification of herbivorous pseudosuchians (e.g., aetosaurs, *Revueltosaurus*). It is noteworthy that the convergent morphologies that evolved in the taxa from the first wave overlap little in space and time those from the second wave. For example, the timing of acquisition of convergences observed between *Azendohsaurus* and early sauropodomorphs are completely offset in time. Even though *Azendohsaurus* may have temporally overlapped the earliest sauropodomorphs (e.g., *Eoraptor lunensis*), although this is uncertain because of uncertainties in the age of the Makay Formation, the convergent herbivorous features shared by *Azendohsaurus* and sauropodomorphs occur *only* in younger sauropodomorphs (e.g., *Plateosaurus*) from later in the Late Triassic. The proposed pattern of twin shifts to

herbivory by amniotes during the Triassic is only beginning to emerge through discovery and analysis of well-preserved and complete fossils like *Azendohsaurus madagaskarensis*. Constraining the full extent and timing of these shifts or testing for additional episodes in early archosauromorphs history through additional analyses of existing taxa and discovery of Middle Triassic precursors represents a promising avenue of continuing research.

CONCLUSIONS AND PERSPECTIVE

Azendohsaurus madagaskarensis incorporates a seemingly incongruous mix of archosauromorph character states, some of which are found only within Archosauriformes and others within Dinosauria (discussed in Gauffre, 1993; Flynn et al., 1999, 2010). Two character states, the presence of serrated teeth and an ossified laterosphenoid in the skull, were regarded as placing *A. madagaskarensis* closer to Archosauriformes than *Prolacerta broomi* was to Archosauriformes (Flynn et al., 2010). Our current analysis, including of postcranial evidence for *A. madagaskarensis* for the first time and all available data in a comprehensive phylogenetic study, suggests a more complex distribution of these features than previously envisioned. The serrated teeth in *A. madagaskarensis* and other closely related taxa (i.e., *Pamelaria dolichotrachela*, see below) also occur in Archosauriformes, but homoplastically, as serrated teeth now appear to have evolved independently in more than Archosauriformes. In addition, an ossified laterosphenoid in *A. madagaskarensis* optimizes as an autapomorphy of the taxon among basal archosauromorphs, not as a character state uniting *A. madagaskarensis* with Archosauriformes. This is not surprising, however, given that the laterosphenoid of *A. madagaskarensis* has a unique morphology not shared by any other archosauriform (see Clark et al., 1993). This finding may weaken the notion that turtles are closely related to archosauriforms (Bhullar and Bever, 2009), given that an ossified laterosphenoid is more broadly distributed within Archosauromorpha. Vertebral character states of *A. madagaskarensis* also hint at a more complicated distribution of character states among archosauromorphs than previously realized. The sauropodomorph-like cervical vertebrae, complex laminae of the neural arches of the presacral vertebrae, and hypantrum-hyposphene intervertebral articulation of *A. madagaskarensis* otherwise are more typical of members of Archosauria (see Butler et al., 2012) than of early archosauromorphs (see description above). Moreover, *A. madagaskarensis* lacks any postaxial intercentra, a character state that is synapomorphic well within Archosauriformes (for *Vancleavea campi* + Archosauria; see Nesbitt et al., 2009). This suite of character states in a highly autapomorphic taxon illustrates a continued theme in recent discovery and descriptions of Triassic archosauromorphs (e.g., *Effigia okeeffeae*, Nesbitt and Norell, 2006; Nesbitt, 2007): rampant convergence. This pattern of frequent convergence urges caution in the identification of isolated, disarticulated remains in multitaxic bone beds or even of partial skeletons.

Deciphering early archosauromorph diversification currently lies at an interesting crossroads. Recent studies are rapidly advancing our understanding, particularly those focused on long-standing taxonomic enigmas (Proterosuchia; Ezcurra et al., 2013; Tanystropheidae; Pritchard et al., 2015) and those detailing the anatomy of previously discovered taxa (e.g., Dilkes, 1998) as well as new taxa (Sues, 2003; our contribution here for *A. madagaskarensis*) with an eye focused on distinguishing plesiomorphy from synapomorphy at various hierarchical levels of phylogenetic analysis. Despite the progress such studies have brought, a number of challenges persist, especially the dearth of "transitional" morphologies between the "stem" of the archosauromorph tree and later diverging, more autapomorphic lineages. Additionally, the apparent high rates of homoplasy in character evolution for early archosauromorphs have hindered our ability to tease apart plesiomorphy from derived character states. Targeting Lower and Middle Triassic sediments for discovery of more (and more complete specimens) of these early forms provides perhaps the only potential solution to this dilemma.

ACKNOWLEDGMENTS

This work has been supplemented and expanded through discussions with J.B. Desojo, M.D. Ezcurra, M.R. Stocker, H.-D. Sues, and R.J. Butler. We especially thank the many members of the field crews, including R. Andriantompohavana, G. Buckley, D. Croft, J. Finarelli, A. Gandhi, A. Goswami, R. Hill, G. Kampouris, J.A. Rabarison, T. Rajoelisolo, H. Rakotomalala, B. Randriamanpionona, H. Raveloson, M. Ravokatra, J.C. Razafimahazo, L. Razafimanantsoa, W. Simpson, A. Toto Volahy, P. Vavisaro, G. Wesley, R. Whatley, A. Yoder, J.R. Zaonarivelo, our World Wildlife driver Kose, and our friends and local assistants Mena, Dada (F. D'A. Randriamanendrika), and Hari (B. Zafimahefa), for their assistance in collecting material of *Azendohsaurus madagaskarensis* and other Isalo II specimens. William Simpson showed exceptional skills in overseeing many aspects of the excavation and preservation of this important archosauromorphs material, as well as invaluable collections assistance. Preparation of *Azendohsaurus madagaskarensis* was completed by M. Brown, D. Wagner, L. Herzog, C. Van Beek, M. Eklund, P. Brinkman, A. Smith, R. Vodden, J. Holstein, W. Simpson and many volunteers from the Field Museum of Natural History.

Financial support was provided by the Meeker Postdoctoral Fellowship at the Field Museum and the American Museum of Natural History to S.J.N., and additional support was provided by Ministere de l'Energie et des Mines of Madagascar, National Geographic Society, the Field Museum, the University of California–Santa Barbara, and the American Museum of Natural History. Photographs of the *Pamelaria* were provided by C. Kammerer and J.B. Desojo, and photographs of the skull of *Teraterpeton* were provided by Tim Fedak. Access to the free version of TNT 1.1 was provided by the Willi Henning Society.

We thank the following people for access to specimens: B. Zipfel and B. Rubidge (Bernard Price Institute of Paleontological Research, Johannesburg, South Africa); R. Smith and S. Kaal (Iziko South African Museum, Cape Town, South Africa); J. Both and E. Butler (National Museum, Bloemfontein, South Africa); A. Bhart-Bhullar, F. Jenkins, and J. Cundiff of the Museum of Comparative Zoology (Harvard, MA); M. Brett-Surman of the National Museum of Natural History (Washington, DC); C. Dal-Sasso of the Museo Civico di Storia Naturale (Milano, Italy); A. Downs of the Ruth Hall Museum of Paleontology (Ghost Ranch, NM); C. Mehling of the American Museum of Natural History (New York, NY); L. Murray and J.C. Sagebiel of the Texas Memorial Museum (Austin, TX); G. Muscio and L. Simonetto of the Museo Friulano di Storia Naturale (Udine, Italy); C. Norris and D. Brinkman of the Peabody Museum of Natural History (New Haven, CT); A. Dooley and N. Fraser of the Virginia Museum of Natural History (Martinsville, VA); A. Paganoni of the Museo Civico di Storia Naturale Enrico Caffe (Bergamo, Italy); and L. Steel of the Natural History Museum of the United Kingdom (London, England). We thank Martin Ezcurra and Nicholas Fraser for detailed and helpful reviews.

REFERENCES

Abdala, V., and R. Diogo. 2010. Comparative anatomy, homologies and evolution of the pectoral and forelimb musculature of tetrapods with special attention to extant limbed amphibians and reptiles. Journal of Anatomy 217: 536–573.

Agassiz, L. 1844. Monographie des poisons fossils du Vieux Grès Rouge ou Système dévonien (Old Red Sandstone) des Îles Britanniques et de Russie. Neuchatel: Jent et Gassman, 171 pp.

Arkhangelskii, M.S., and A.G. Sennikov. 2008. Subclass Synaptosauria. *In* M.F. Ivakhnenko, and E.N. Kurochkin (editors), Fossil vertebrates of Russia and adjacent countries: 224–241. Moscow: Geos. [in Russian]

Bandyopadhyay, S. 1988. A kannemeyeriid dicynodont from the Middle Triassic Yerrapalli Formation. Philosophical Transactions of the Royal Society of London Series B Biological Sciences 320: 185–233.

Barrett, P.M. 2000. Prosauropod dinosaurs and iguanas: speculations on the diets of extinct reptiles. *In* H.-D. Sues (editor), Evolution of herbivory in terrestrial vertebrates: perspectives from the fossil record: 42–78. Cambridge: Cambridge University Press.

Bassani, F. 1886. Sui fossili e sull'eta degli schisti bituminosi Triasici di Besano in Lombardia. Atti Societa Italiana di Scienze Naturali 29: 15–72.

Behrensmeyer, A.K. 1978. Taphonomic and ecologic information from bone weathering. Paleobiology 4: 150–162.

Benton, M.J. 1983. The Triassic reptile *Hyperodapedon* from Elgin: functional morphology and relationships. Philosophical Transactions of the Royal Society B 302: 605–718.

Benton, M.J. 1985. Classification and phylogeny of the diapsid reptiles. Zoological Journal of the Linnaean Society 84: 97–164.

Benton, M.J., and J.L. Allen. 1997. *Boreopricea* from the Lower Triassic of Russia, and the relationships of the prolacertiform reptiles. Palaeontology 40: 931–953.

Benton, M.J., and J.M. Clark. 1988. Archosaur phylogeny and the relationships of the Crocodylia. *In* M.J. Benton (editor), The phylogeny and classification of the tetrapods. Vol. 1, Amphibians, reptiles, birds: 295–338. Oxford: Clarendon Press.

Besairie, H. 1936. Recherches géologiques à Madagascar, première suite; la géologie du nordouest. Mémoires de l'Académie Malgache 21: 1–259.

Besairie, H. 1972. Géologie de Madagascar I. Les terraines sédimentaires. Annales Géologiques de Madagascar, Service des Mines 35: 1–463.

Bever, G.S., C.J. Bell, and J.A. Maisano. 2005. The ossified braincase and cephalic osteoderms of *Shinisaurus crocodilurus* (Squamata, Shinisauridae). Paleaeontologica Electronica 8: 1–36.

Bhullar, B.-A.S., and G.S. Bever. 2009. An archosaur-like laterosphenoid in early turtles (Reptilia: Pantestudines). Breviora 518: 1–11.

Bhullar, B.-A.S., G.S. Bever, J. Merck, T. Lyson, and J. Gauthier. 2011. Uniting microevolutionand macroevolution in deep time: the zone of variability in Archosauromorpha. Journal of Vertebrate Paleontology, 2011 Annual meeting of the Society of Vertebrate Paleontology: 71.

Biron, P.-E., and J.M. Dutuit. 1981. Figurations sédimentaires et traces d'activité au sol dans le Trias de la formation d'Argana et de l'Ourika (Maroc). Bulletin du Muséum National d'Histoire Naturelle, 4ème série 3: 339–427.

Bonaparte, J.F. 1976. *Pisanosaurus mertii* Casamiquela and the origin of the Ornithischia. Journal of Paleontology 50: 808–820.

Brochu, C.A. 1992. Ontogeny of the postcranium in crocodylomorph archosaurs. *In* Geological sciences. Master's thesis, University of Texas, Austin.

Broili, F., and J. Schroeder. 1934. Beobachtungen an Wirbeltieren der Karroformation. V. Über *Chasmatosaurus van hoepeni* Haughton. Sitzungsberichte der Bayerischen Akademie der Wissenschaften, Mathematisch-naturwissenschaftliche Abteiliung 3: 225–264.

Broom, R. 1903. On a new reptile (*Proterosuchus fergusi*) from the Karoo beds of Tarkastad, South Africa. Annals of the South African Museum 4: 159–164.

Broom, R. 1921. On the structure of the reptilian tarsus. Proceedings of the Zoological Society of London 91: 143–156.

Brusatte, S.L. 2010. Representing supraspecific taxa in higher-level phylogenetic analyses: guidelines for palaeontologists. Palaeontology 53: 1–9.

Brusatte, S.L., M.J. Benton, M. Ruta, and G.T. Lloyd. 2008. Superiority, competition, and opportunism in the evolutionary radiation of dinosaurs. Science 321: 1485–1488.

Brusatte, S., et al. 2010. The origin and early radiation of dinosaurs. Earth-Science Reviews 101: 68–100.

Brusatte, S.L., M.J. Benton, G.T. Lloyd, M. Ruta, and S.C. Wang. 2011. Macroevolutionary patterns in the evolutionary radiation of archosaurs (Tetrapoda: Diapsida). Earth and Environmental Science Transactions of the Royal Society of Edinburgh 101: 367–382.

Buckley, G.A., C.A. Brochu, D.W. Krause, and D. Pol. 2000. A pug-nosed crocodyliform from the Late Cretaceous of Madagascar. Nature 405: 941–944.

Buffetaut, E. 1983. *Isalorhynchus genovefae*, n. g. n. sp. (Reptilia, Rhynchocephalia), un nouveau rhynchosaure du Trias de Madagascar. Neues Jahrbuch für Geologie und Paläontologie, Monatshefte 1983: 465–480.

Butler, R.J., et al. 2011. The sail-backed reptile *Ctenosauriscus* from the latest Early Triassic of Germany and the timing and biogeography of the early archosaur radiation. PLoS ONE 6 (10): e25693.

Butler, R.J., P.M. Barrett, and D.J. Gower. 2012. Reassessment of the evidence for postcranial skeletal pneumaticity in Triassic archosaurs, and the early evolution of the avian respiratory system. PLoS ONE 7 (3): e34094.

Caldwell, M.W. 1994. Developmental constraints and limb evolution in Permian and extant lepidosauromorph diapsids. Journal of Vertebrate Paleontology 14: 459–471.

Caldwell, M.W. 1996. Ichthyosauria: a preliminary phylogenetic analysis of diapsid affinities. Neues Jahrbuch für Geologie und Paläontologie. Abhandlungen 200: 361–386.

Cao, Y., M.D. Sorenson, Y. Kumazawa, D.P. Mindell, and M. Hasegawa. 2000. Phylogenetic position of turtles among amniotes: evidence from mitochondrial and nuclear genes. Gene 259: 139–148.

Carrano, M.T. 2006. Body-size evolution in the Dinosauria. *In* M.T. Carrano, T.J. Gaudin, R.W. Blob, and J.R. Wible (editors), Amniote paleobiology: perspectives on the evolution of mammals, birds, and reptiles: 225–268. Chicago: University of Chicago Press.

Carrano, M.T., S.D. Sampson, and C.A. Forster. 2002. The osteology of *Masiakasaurus knopfleri*, a small abelisauroid (Dinosauria: Theropoda) from the Late Cretaceous of Madagascar. Journal of Vertebrate Paleontology 22: 510–534.

Carroll, R.L. 1976. *Noteosuchus*—the oldest known rhynchosaur. Annales of the South African Museum 72: 37–57.

Carroll, R.L. 1988. Vertebrate paleontology. London: Unwin-Hyman, 377 pp.

Case, E.C. 1922. New reptiles and stegocephalians from the Upper Triassic of western Texas. Carnegie Institution of Washington, Publication 321: 1–84.

Case, E.C. 1927. The vertebral column of *Coelophysis* Cope. Contributions of the Museum of Paleontology, University of Michigan 2: 209–222.

Case, E.C. 1928a. A cotylosaur from the Upper Triassic of western Texas. Journal of the Washington Academy of Sciences 18: 177–178.

Case, E.C. 1928b. Indications of a cotylosaur and of a new form of fish from the Triassic beds of Texas, with remarks on the Shinarump Conglomerate. Contributions of the Museum of Paleontology, University of Michigan 3: 1–14.

Charig, A.J. 1980. Differentiation of lineages among Mesozoic tetrapods. Mémoires de la Société Géologique de France 139: 207–210.

Charig, A.J., and H.-D. Sues. 1976. Proterosuchia. *In* O. Kuhn (editor), Handbuch der Paläoherpetologie: 11–39. Stuttgart: Gustav Fischer.

Chatterjee, S. 1974. A rhynchosaur from the Upper Triassic Maleri Formation of India. Philosophical Transactions of the Royal Society B 267: 209–261.

Chatterjee, S. 1978. A primitive parasuchid (phytosaur) reptile from the Upper Triassic Maleri Formation of India. Palaeontology 21: 83–127.

Clark, J.M., J. Welman, J.A. Gauthier, and J.M. Parrish. 1993. The laterosphenoid bone of early archosauriforms. Journal of Vertebrate Paleontology 13: 48–57.

Colbert, E.H. 1952. A pseudosuchian reptile from Arizona. Bulletin of the American Museum of Natural History 99 (10): 561–592.

Colbert, E.H. 1987. The Triassic reptile *Prolacerta* in Antarctica. American Museum Novitates 2882: 1–19.

Colbert, E.H. 1989. The Triassic dinosaur *Coelophysis*. Museum of Northern Arizona Bulletin 57: 1–160.

Conrad, J.L. 2004. Skull, mandible, and hyoid of *Shinisaurus crocodilurus* (Squamata: Anguimorpha). Zoological Journal of the Linnaean Society 141: 399–434.

Conrad, J.L. 2006. Postcranial skeleton of *Shinisaurus crocodilurus* (Squamata: Anguimorpha). Journal of Morphology 267: 759–775.

Cruickshank, A.R.I. 1972. The proterosuchian thecodonts. *In* K.A. Joysey and T.S. Kemp (editors), Studies in vertebrate evolution: 89–119. Edinburgh: Oliver and Boyd.

Currie, P.J. 1981. The vertebrae of *Youngina* (Reptilia: Eosuchia). Canadian Journal of Earth Sciences 18: 815–818.

Dalla Vecchia, F.M. 2008. Vertebrati fossili del Friuli. Pubblicazioni del Museo Friulano di Storia Naturale 50: 1–303.

Demar, R., and J.R. Bolt. 1981. Dentitional organization and function in a Triassic reptile. Journal of Paleontology 55: 967–984.

Desojo, J.B., M.D. Ezcurra, and C.L. Schultz. 2011. An unusual new archosauriform from the Middle-Late Triassic of southern Brazil and the monophyly of Doswelliidae. Zoological Journal of the Linnean Society 161: 839–871.

Dilkes, D.W. 1995. The rhynchosaur *Howesia browni* from the Lower Triassic of Africa. Palaeontology 38: 665–685.

Dilkes, D.W. 1998. The Early Triassic rhynchosaur *Mesosuchus browni* and the interrelationships of basal archosauromorph reptiles. Philosophical Transactions of the Royal Society of London Series B 353: 501–541.

Dilkes, D.W. 2000. Appendicular myology of the hadrosaurian dinosaur *Maiasaura peeblesorum* from the Late Cretaceous (Campanian) of Montana. Transactions of the Royal Society of Edinburgh 90: 87–125.

Dilkes, D.W., and H.-D. Sues. 2009. Redescription and phylogenetic relationships of *Doswellia kaltenbachi* (Diapsida: Archosauriformes) from the Upper Triassic of Virginia. Journal of Vertebrate Paleontology 29: 58–79.

Dutuit, J.M. 1972. Découverte d'un dinosaure ornithischien dans le Trias supérieur de l'Atlas occidental marocain. Comptes Rendus d l'Académie des Sciences 275: 2841–2844.

El-Toubi, M.R. 1949. The post-cranial osteology of the lizard *Uromastyx aegyptia* (Forskal). Journal of Morphology 84: 281–292.

Evans, S.E. 1980. The skull of a new eosuchian reptile from the Lower Jurassic of South Wales.

Zoological Journal of the Linnaean Society 70: 203–264.

Evans, S.E. 1981. The postcranial skeleton of the Lower Jurassic eosuchian *Gephyrosaurus bridensis*. Zoological Journal of the Linnaean Society 73: 81–116.

Ewer, R.F. 1965. The anatomy of the thecodont reptile *Euparkeria capensis* Broom. Philosophical Transactions of the Royal Society of London B 248: 379–435.

Ezcurra, M.D., and R.J. Butler. 2015. Taxonomy of the proterosuchid archosauriforms (Diapsida: Archosauromorpha) from the earliest Triassic of South Africa, and implications for the early archosauriform radiation. Palaeontology 58: 141–170.

Ezcurra, M.D., A. Lecuona, and A. Martinelli. 2010. A new basal archosauriform diapsid from the Lower Triassic of Argentina. Journal of Vertebrate Paleontology 30: 1433–1450.

Ezcurra, M.D., R.J. Butler, and D.J. Gower. 2013. 'Proterosuchia': the origin and early history of Archosauriformes. *In* S.J. Nesbitt, J.B. Desojo, and R.B. Irmis (editors), Anatomy, phylogeny and palaeobiology of early archosaurs and their kin: 9–33. London: Geological Society Special Publications.

Ezcurra, M.D., T.M. Scheyer, and R.J. Butler. 2014. The origin and early evolution of Sauria: reassessing the Permian saurian fossil record and the timing of the crocodile-lizard divergence. PLoS ONE 9 (2): e89165.

Feduccia, A. 1993. Evidence from claw geometry indicating arboreal habits of *Archaeopteryx*. Science 259: 790–793.

Flynn, J.J., et al. 1999. A Triassic fauna from Madagascar, including early dinosaurs. Science 286: 763–765.

Flynn, J.J., et al. 2000. New traversodontids (Synapsida: Eucynodontia) from the Triassic of Madagascar. Journal of Vertebrate Paleontology 20: 422–427.

Flynn, J.J., S.J. Nesbitt, J.M. Parrish, L. Ranivoharimanana, and A.R. Wyss. 2010. A new taxon of *Azendohsaurus* (Archosauromorpha, Diapsida, Reptilia) from the Triassic Isalo Group of southwest Madagascar: part 1, cranium. Palaeontology 53: 669–688.

Fraser, N.C., and O. Rieppel. 2006. A new protorosaur (Diapsida) from the Upper Buntsandstein of the Black Forest, Germany. Journal of Vertebrate Paleontology 26: 866–871.

Gaffney, E.S. 1990. The comparative osteology of the Triassic turtle *Proganochelys*. Bulletin of the American Museum of Natural History 194: 1–263.

Galton, P.M. 1985. Cranial anatomy of the prosauropod dinosaur *Sellosaurus gracilis* from the Middle Stubensandstein (Upper Triassic) of Nordwürttemberg, West Germany. Stuttgarter Beiträge zur Naturkunde B 118: 1–39.

Galton, P.M. 1990. Basal Sauropodomorpha-Prosauropoda. *In* D.B. Weishamppel, P. Dodson, and H. Osmolska (editors), The Dinosauria: 320–344. Berkeley: University of California Press.

Gardner, N.M., C.M. Holliday, and F.R. O'Keefe. 2010. The braincase of *Youngina capensis* (Reptilia, Diapsida): new insights from high-resolution CT scanning of the holotype. Palaeontologia Electronica 13: 1–16.

Gatesy, S.M. 1997. An electromyographic analysis of hindlimb function in *Alligator* during terrestrial locomotion. Journal of Morphology 234: 197–212.

Gauffre, F. 1993. The prosauropod dinosaur *Azendohsaurus laaroussii* from the Upper Triassic of Morocco. Palaeontology 36: 897–908.

Gauthier, J.A. 1986. Saurischian monophyly and the origin of birds. Memoirs of the California Academy of Science 8: 1–55.

Gauthier, J.A., A.G. Kluge, and T. Rowe. 1988a. The early evolution of the Amniota. *In* M.J. Benton (editor), The phylogeny and classification of the tetrapods. Vol. 1, Amphibians, reptiles, birds: 103–155. Oxford: Clarendon Press.

Gauthier, J.A., A.G. Kluge, and T. Rowe. 1988b. Amniote phylogeny and the importance of fossils. Cladistics: 105–209.

Goloboff, P.A., J.S. Farris, and K. Nixon. 2003. TNT: Tree analysis using new technologies. Program and documentation available from the authors and online (http://www.zmuc.dk/public/phylogeny).

Goloboff, P., J. Farris, and K. Nixon. 2008. TNT: a free program for phylogenetic analysis. Cladistics 24: 774–786.

Goswami, A., J.J. Flynn, L. Ranivoharimanana, and A.R. Wyss. 2005. Dental microwear in Triassic amniotes: implications for paleoecology and masticatory mechanics. Journal of Vertebrate Paleontology 25: 320–329.

Gottmann-Quesada, A., and P.M. Sander. 2009. Redescription of the early archosauromorph *Protorosaurus speneri* Meyer, 1832, and its phylogenetic relationships. Palaeontographica Abteilung A 287: 123–220.

Gow, C.E. 1975. The morphology and relationships of *Youngina capensis* Broom and *Prolacerta broomi* Parrington. Palaeontologia Africana 18: 89–131.

Gower, D.J. 1996. The tarsus of erythrosuchid archosaurs (Reptilia), and implications for early diapsid phylogeny. Zoological Journal of the Linnean Society 116: 347–375.

Gower, D.J. 1999. The cranial and mandibular osteology of a new rauisuchian archosaur from the Middle Triassic of southern Germany. Stuttgarter Beiträge zur Naturkunde Serie B (Geologie und Paläontologie) 280: 1–49.

Gower, D.J. 2001. Possible postcranial pneumaticity in the last common ancestor of birds and crocodilians: evidence from *Erythrosuchus* and other Mesozoic archosaurs. Naturwissenschaften 88: 119–122.

Gower, D.J. 2002. Braincase evolution in suchian archosaurs (Reptilia: Diapsida): evidence from the rauisuchian *Batrachotomus kupferzellensis*. Zoological Journal of the Linnean Society 136: 49–76.

Gower, D.J. 2003. Osteology of the early archosaurian reptile *Erythrosuchus africanus* Broom. Annals of the South African Museum 110: 1–84.

Gower, D.J., and R. Schoch. 2009. Postcranial anatomy of the rauisuchian archosaur *Batrachotomus kupferzellensis*. Journal of Vertebrate Paleontology 29: 103–122.

Gower, D.J., and A.G. Sennikov. 1996. Braincase morphology in early archosaurian reptiles. Palaeontology 39: 883–906.

Gower, D.J., and A.G. Sennikov. 1997. *Sarmatosuchus* and the early history of the Archosauria. Journal of Vertebrate Paleontology 17: 60–73.

Gregory, J.T. 1945. Osteology and relationships of *Trilophosaurus*. University of Texas Publication 4401: 273–359.

Haas, G. 1970. Eine bemerkenswerte Interclavicula von (?) *Tanystropheus* aus dem Muschelkalk des Wadi Ramon, Israel. Paläontologische Zeitschrift 44: 207–214.

Haines, R.W. 1939. A revision of the extensor muscles of the forearm in tetrapods. Journal of Anatomy 73: 211–233.

Harris, J.D., and A. Downs. 2002. A drepanosaurid pectoral girdle from the Ghost Ranch (Whitaker) *Coelophysis* Quarry (Chinle Group, Rock Point Formation, Rhaetian), New Mexico. Journal of Vertebrate Paleontology 22: 70–75.

Heckert, A.B., S.G. Lucas, and R. Kahle. 2001. New occurrence of *Trilophosaurus* (Reptilia: Archosauromorpha) from the Upper Triassic of West Texas and its biochronological significance. New Mexico Geological Society Guidebook 52: 115–122.

Heckert, A.B., et al. 2006. Revision of the archosauromorph reptile *Trilophosaurus*, with a description of the first skull of *Trilophosaurus jacobsi*, from the Upper Triassic Chinle Group, West Texas, USA. Palaeontology 49: 621–640.

Hoffman, A.C. 1965. On the discovery of a new thecodont from the Middle Beaufort Beds. Navorsinge van die Nasionale Museum Bloemfontein 2: 33–40.

Hoffstetter, R., and J.-P. Gasc. 1969. Vertebrae and ribs of modern reptiles. *In* C. Gans, A.d.A. Bellairs, and T.S. Parsons (editors), Biology of the Reptilia. Vol. 1, Morphology: 201–309. New York: Academic Press.

Holz, M., and C.L. Schultz. 1998. Taphonomy of the south Brazilian Triassic herpetofauna: fossilization mode and implications for morphological studies. Lethaia 31: 335–345.

Huene, F.v. 1932. Die fossile Reptil-Ordung Saurischia, ihre Entwicklung und Geschichte. Monographien zur Geologie und Palaeontologie 1 (4): 1–361.

Huene, F.v. 1937. *Stenaulorhynchus*, ein Rhynchosauride der ostafrikanische Obertrias. Nova Acta Leopoldina 6: 7–121.

Huene, F.v. 1946. Die grossen Stämme der Tetrapoden inden geologischen Zeiten. Biologisches Zentralblatt 65: 268–275.

Hughes, B. 1963. The earliest archosaurian reptiles. South African Journal of Science 59: 221–241.

Hughes, B. 1968. The tarsus of rhynchocephalian reptiles. Journal of the Zoological Society of London 156: 457–481.

Hunt, A.P., S.G. Lucas, A.B. Heckert, R.M. Sullivan, and M.G. Lockley. 1998. Late Triassic dinosaurs from the Western United States. Geobios 31: 511–531.

Hutchinson, J.R. 2001. The evolution of pelvic osteology and soft tissues on the line to extant birds. Zoological Journal of the Linnean Society 131: 123–168.

Huxley, T.H. 1869. On *Hyperodapedon*. Quarterly Journal of the Geological Society of London. 25: 138–152.

Irmis, R.B., R. Mundil, C. Marsicano, and A. Mancuso. 2013. U-Pb dating of redeposited volcanics in non-marine sedimentary strata: case studies from the early Mesozoic. Journal of Vertebrate Paleontology (suppl.) 33: 147.

Jalil, N.-E. 1997. A new prolacertiform diapsid from the Triassic of North Africa and the interrelationships of the Prolacertiformes. Journal of Vertebrate Paleontology 17: 506–525.

Jalil, N.-E., and F. Knoll. 2002. Is *Azendohsaurus laaroussii* (Carnian, Morocco) a dinosaur. Journal of Vertebrate Paleontology 22 (suppl. to no. 3): 70A.

Jiang, D.-Y., et al. 2011. New information on the protorosaurian reptile *Macrocnemus fuyuanensis* Li et al., 2007, from the Middle/Upper Triassic of Yunnan, China. Journal of Vertebrate Paleontology 31: 1230–1237.

Juul, L. 1994. The phylogeny of basal archosaurs. Palaeontologia Africana 31: 1–38.

Kammerer, C.F., J.J. Flynn, L. Ranivoharimanana, and A.R. Wyss. 2010. The first record of a probainognathian (Cynodontia: Chiniquodontidae) from the Triassic of Madagascar. Journal of Vertebrate Paleontology 30: 1889–1894.

Kuhn-Schnyder, E. 1959. Han und Fuss von *Tanystropheus longobardicus* (Bassani). Eclogae Geologicae Helveticae 52: 921–941.

Langer, M.C., M.D. Ezcurra, J.S. Bittencourt, and F.E. Novas. 2010. The origin and early evolution of dinosaurs. Biological Reviews 85: 55–110.

Li, C., L. Zhao, and L. Wang. 2007. A new species of *Macrocnemus* (Reptilia: Protorosauria) from the Middle Triassic of southwestern China and its palaeogeographical implication. Science in China Series D 50: 1601–1605.

Linnaeus, C. 1758. Systema naturae per regna tria naturae, secundum classes, ordines, genera, species, cum characteribus, differentiis, synonymis, locis. 10th ed., tom. 1–2. Holmiae [Stockholm]: Laurentii Salvii.

Long, R.A., and P.A. Murry. 1995. Late Triassic (Carnian and Norian) tetrapods from the southwestern United States New Mexico Museum of Natural History and Science Bulletin 4: 1–254.

Lucas, S.G. 1998. Global Triassic tetrapod biostratigraphy and biochronology. Palaeogeography, Palaeoclimatology, Palaeoecology 143: 347–384.

Meers, M.B. 2003. Crocodylian forelimb musculature and its relevance to Archosauria. Anatomical Record 274A: 891–916.

Meyer, H.v. 1861. Reptilien aus dem Stubensandstein des obern Keupers. Palaeontographica A 6: 253–346.

Modesto, S.P., and H.-D. Sues. 2004. The skull of the Early Triassic archosauromorph *Prolacerta broomi* and its phylogenetic significance Zoological Journal of the Linnean Society 140: 335–351.

Montefeltro, F.C., J.S. Bittencourt, M.C. Langer, and C.L. Schultz. 2013. Postcranial anatomy of the hyperodapedontine rhynchosaur *Teyumbaita sulcognathus* (Azevedo and Schultz, 1987) from the Late Triassic of southern Brazil. Journal of Vertebrate Paleontology 33: 67–84.

Montefeltro, F.C., M.C. Langer, and C.L. Schultz. 2010. Cranial anatomy of a new genus of hyperodapedontine rhynchosaur (Diapsida, Archosauromorpha) from the Upper Triassic of southern Brazil. Earth and Environmental Science Transactions of the Royal Society of Edinburgh 101: 27–52.

Munk, W., and H.-D. Sues. 1993. Gut contents of *Parasaurus* (Pareisauria) and *Protorosaurus* (Archosauromorpha) from the Kupferschiefer (Upper Permian) of Hessen, Germany. Paläontologische Zeitschrift 67: 169–176.

Müller, J. 2004. The relationships among diapsid reptiles and the influence of taxon selection. *In* M.V.H. Wilson, G. Arratia, and R. Cloutier (editors), Recent advances in the origin and early radiation of vertebrates: 379–408. Munich: Verlag Dr. Friedrich Pfeil.

Murry, P.A. 1987. New reptiles from the Upper Triassic Chinle Formation of Arizona. Journal of Paleontology 61: 773–786.

Nesbitt, S.J. 2003. *Arizonasaurus* and its implications for archosaur divergences. Proceedings of the Royal Society of London B 270 (suppl. 2): S234–S237.

Nesbitt, S.J. 2007. The anatomy of *Effigia okeeffeae* (Archosauria, Suchia), theropod-like convergence, and the distribution of related taxa. Bulletin of the American Museum of Natural History 302: 1–84.

Nesbitt, S.J. 2011. The early evolution of archosaurs: relationships and the origin of major clades. Bulletin of the American Museum of Natural History 352: 1–292.

Nesbitt, S.J., and M.A. Norell. 2006. Extreme convergence in the body plans of an early suchian (Archosauria) and ornithomimid dinosaurs (Theropoda). Proceedings of the Royal Society of London B 273: 1045–1048.

Nesbitt, S.J., R.B. Irmis, and W.G. Parker. 2007. A critical re-evaluation of the Late Triassic dinosaur taxa of North America. Journal of Systematic Palaeontology 5: 209–243.

Nesbitt, S.J., M.R. Stocker, B. Small, and A. Downs. 2009. The osteology and relationships of *Vancleavea campi* (Reptilia: Archosauriformes). Zoological Journal of the Linnean Society 157: 814–864.

Nesbitt, S.J., J. Liu, and C. Li. 2011. A sail-backed suchian from the Heshanggou Formation (Early Triassic: Olenekian) of China. Earth and Environmental Science Transactions of the Royal Society of Edinburgh 101: 271–284.

Nosotti, S. 2007. *Tanystropheus longobardicus* (Reptilia, Protorosauria): re-interpretations of the anatomy based on new specimens from the Middle Triassic of Besano (Lombardy, northern Italy). Memoire della Civico di Storia Naturale di Milano 35: 1–88.

O'Leary, M.A., and S.G. Kaufman. 2012. MorphoBank 3.0: web application for morphological phylogenetics and taxonomy. Online resource (http://www.morphobank.org).

Olsen, P.E. 1979. A new aquatic eosuchian from the Newark Supergroup (Late Triassic–Early Jurassic) of North Carolina and Virginia. Postilla 176: 1–14.

Owen, R. 1842. Report on British fossil reptiles. Report of the British Association for the Advancement of Science 11: 60–204.

Parker, W.P. 2008. Description of new material of the aetosaur *Desmatosuchus spurensis* (Archosauria: Suchia) from the Chinle Formation of Arizona and a revision of the genus *Desmatosuchus*. Paleo Bios 28: 1–40.

Parker, W.G., R.B. Irmis, S.J. Nesbitt, J.M. Martz, and L.S. Brown. 2005. The Late Triassic pseudosuchian *Revueltosaurus callenderi* and its implications for the diversity of early ornithischian dinosaurs. Proceedings of the Royal Society of London B 272: 963–969.

Parrish, J.M. 1993. Phylogeny of the Crocodylotarsi, with reference to archosaurian and crurotarsan monophyly. Journal of Vertebrate Paleontology 13: 287–308.

Peyer, B. 1937. Die Triasfauna der Tessiner Kalkalpen XII. *Macrocnemus bassanii* Nopcsa. Abhandlungen der Schweizerischen Palaeontologischen Gesellschaft 59: 1–140.

Pritchard, A.C., A.H. Turner, S.J. Nesbitt, R.B. Irmis, and N.D. Smith. 2012. A new drepanosaurid from the Late Triassic of New Mexico: insights into the forelimb evolution and biogeography of drepanosaurs. Journal of Vertebrate Paleontology 32 (suppl.2): 158.

Pritchard, A.C., A.H. Turner, S.J. Nesbitt, R.B. Irmis, and N.D. Smith. 2015. Late Triassic tanystropheids (Reptilia, Archosauromorpha) from northern New Mexico (Petrified Forest Member, Chinle Formation) and the biogeography, functional morphology, and evolution of Tanystropheidae. Journal of Vertebrate Paleontology e911186. [doi: 10.1080/02724634.2014.911186]

Razafimbelo, E. 1987. Le basin de Morondava (Madagascar). Synthèse géologique et structurale. Ph.D. dissertation, Université Louis Pasteur, Strasbourg, France, 189 pp.

Reisz, R. 1981. A diapsid reptile from the Pennsylvanian of Kansas. Special Publication of the Museum of Natural History, University of Kansas 7: 1–74.

Reisz, R.R., and H.-D. Sues. 2000. Herbivory in late Paleozoic and Triassic terrestrial vertebrates. *In* H.-D. Sues (editor), Evolution of herbivory in terrestrial vertebrates: perspectives from the fossil record: 9–41. Cambridge University Press, Cambridge.

Reisz, R., D.S. Berman, and D. Scott. 1984. The anatomy and relationships of the Lower Permian reptile *Araeoscelis*. Journal of Vertebrate Paleontology 4: 57–67.

Renous-Lécuru, S. 1973. Morphologie comparée du carpe chez les lepidosauriens actuels (rhynchocéphales, lacertiliens, amphisbéniens). Gegenbaurs Morphologisches Jahrbuch Leipzig 119: 727–766.

Rewcastle, S.C. 1980. Forma and function in lacertilian knee and mesotarsal joints: a contribution to the analysis of sprawling locomotion. Journal of Zoology, London 191: 147–170.

Richards, H.R.I. 1999. Osteology and relationships of *Spinosuchus caseanus* Huene, 1932 from Texas (Dockum Group, Upper Triassic): a new interpretation. M.S. thesis, Fort Hays State University, Fort Hays, Kansas.

Rieppel, O. 1989. The hind limb of *Macrocnemus bassanii* (Nopcsa) (Reptilia, Diapsida): development and functional anatomy. Journal of Vertebrate Paleontology 9: 373–387.

Rieppel, O. 1993. Studies on skeletal formation in reptiles. IV. The homology of the reptilian (amniote) astragalus revisited. Journal of Vertebrate Paleontology 13: 31–47.

Rieppel, O., N.C. Fraser, and S. Nosotti. 2003. The monophyly of Protorosauria (Reptilia, Archosauromorpha): a preliminary analysis. Atti della Società Italiana di Scienze Naturali e del Museo Civico di Storia Naturale di Milano 144: 359–382.

Rieppel, O., et al. 2010. *Tanystropheus* cf. *T. longobardicus* from the early Late Triassic of Guizhou Province, southwestern China. Journal of Vertebrate Paleontology 30: 1082–1089.

Rinehart, L.F., S.G. Lucas, A.B. Heckert, J.A. Spielmann, and M.D. Celeskey. 2009. The paleobiology of *Coelophysis bauri* (Cope) from the Upper Triassic (Apachean) Witaker quarry, New Mexio, with detailed analysis of a single quarry block. New Mexico Museum of Natural History and Science Bulletin 45: 1–260.

Robinson, P.L. 1975. The functions of the hooked fifth metatarsal in lepidosaurian reptiles. Colloque international C.N.R.S. 218: 461–483.

Romer, A.S. 1922. The locomotor apparatus of certain primitive and mammal-like reptiles. Bulletin of the American Museum of Natural History 46 (10): 517–603.

Romer, A.S. 1942. The development of tetrapod limb musculature—the thigh of *Lacerta*. Journal of Morphology 71: 251–298.

Romer, A.S. 1944. The development of tetrapod limb musculature—the shoulder region of *Lacerta*. Journal of Morphology 74: 1–47.

Romer, A.S. 1956. The osteology of the Reptilia Chicago: University of Chicago Press, 772 pp.

Russell, A.P., and A.M. Bauer. 2008. The appendicular locomotor apparatus of *Sphenodon* and normal-limbed squamates. *In* C. Gans, A.S. Gaunt, and K. Adler (editors), Biology of the Reptilia. Vol. 21, Morphology I: the skull and appendicular locmotor apparatus of Lepidosauria: 1–465. Ithaca, NY: Society for the Study of Amphibians and Reptiles.

Saller, F., S. Renesto, and F.M. Dalla Vecchia. 2013. First record of *Langobardisaurus* (Diapsida, Protorosauria) from the Norian (Late

Triassic) of Austria, and a revision of the genus. Neues Jahrbuch für Geologie und Paläontologie Abhandlungen 268: 83–95.

Sen, K. 2003. *Pamelaria dolichotrachela*, a new prolacertid reptile from the Middle Triassic of India. Journal of Asian Earth Sciences 21: 663–681.

Sereno, P.C. 1991. Basal archosaurs: phylogenetic relationships and functional implications. Journal of Vertebrate Paleontology 10 (suppl. to 3): 1–53.

Sereno, P.C. 1994. The pectoral girdle and forelimb of the basal theropod *Herrerasaurus ischigualastensis*. Journal of Vertebrate Paleontology 13: 425–450.

Sereno, P.C. 1999. The evolution of dinosaurs. Science 284: 2137–2147.

Sereno, P.C., R.N. Martinez, and O.A. Alcober. 2013. Osteology of *Eoraptor lunensis* (Dinosauria, Sauropodomorpha). Journal of Vertebrate Paleontology (Memoir 12) 32 (suppl. to no. 6): 83–179.

Sookias, R.B., R.J. Butler, and R.B.J. Benson. 2012. Rise of dinosaurs reveals major body size transitions are driven by passive processes of trait evolution. Proceedings of the Royal Society B 279: 2180–2187.

Spielmann, J.A., S.G. Lucas, and A.B. Heckert. 2005. The Late Triassic archosauromorph *Trilophosaurus* as an arboreal climber. Rivista Italiana di Paleontologia e Stratigrafia 111: 395–412.

Spielmann, J.A., S.G. Lucas, L.F. Rinehart, and A.B. Heckert. 2008. The Late Triassic archosauromorph *Trilophosaurus*. New Mexico Museum of Natural History and Science Bulletin 43: 1–177.

Spielmann, J.A., S.G. Lucas, A.B. Heckert, L.F. Rinehart, and H.R. Richards. 2009. Redescription of *Spinosuchus caseanus* (Archosauromorpha: Trilophosauridae) from the Upper Triassic of North America. Paleodiversity 2: 283–313.

Spielmann, J.A., S.G. Lucas, and P. Huber. 2013. New record of *Spinosuchus caseanus* (Archosauromorpha: Trilophosauridae) from the Late Triassic (Adamanian) of West Texas. New Mexico Museum of Natural History and Science Bulletin 61: 573–576.

Sues, H.-D. 2000. Herbivory in terrestrial vertebrates: an introduction. *In* H.-D. Sues (editor), Evolution of herbivory in terrestrial vertebrates: perspectives from the fossil record: 1–8. Cambridge: Cambridge University Press.

Sues, H.-D. 2003. An unusual new archosauromorph reptile from the Upper Triassic Wolfville Formation of Nova Scotia. Canadian Journal of Earth Sciences 40: 635–649.

Swofford, D.L. 2002. PAUP* (phylogenetic analysis using parsimony and other methods), version 4.0b10. Sunderland MA: Sinauer Association.

Tatarinov, L.P. 1960. [Discovery of pseudosuchians in the Upper Permian of the USSR]. Paleontologicheskii Zhurnal 1960: 74–80. [in Russian]

Thulborn, R.A. 1973. Teeth of ornithischian dinosaurs from the Upper Jurassic of Portugal, with description of a hypsilophodontid (*Phyllodon henkeli* gen. et sp. nov.) from the Guimarota Lignite. Memorias dos Servicos Geologicos de Portugal 22: 89–134.

Tixeront, M. 1973. Lithostratigraphie et minéralisations cuprifères et uraniferer stratiformes syngénétiques et familières des formations détritiques Permo-Triassiques du couloir d'Argana, Haut-Atlas occidental (Maroc). Notes du Service Géologique de Maroc 33: 147–177.

Trotteyn, M.J., R.N. Martinez, and O.A. Alcober. 2012. A new proterochampsid *Chanaresuchus ischigualastensis* (Diapsida, Archosauriformes) in the early Late Triassic Ischigualasto Formation, Argentina. Journal of Vertebrate Paleontology 32: 485–489.

Turner, A.H., and S.J. Nesbitt. 2013. Body size evolution during the Triassic archosauriform radiation. *In* S.J. Nesbitt, J.B. Desojo, and R.B. Irmis (editors), Anatomy, phylogeny, and palaeobiology of early archosaurs and their kin. Geological Society of London special volume 379: 573–597.

Tschanz, K. 1988. Allometry and heterochrony in the growth of the neck of Triassic prolacertiform reptiles. Palaeontology 31: 997–1011.

Vaughn, P.P. 1955. The Permian reptile *Araeoscelis* restudied. Bulletin of the Museum of Comparative Zoology 113: 305–467.

Walker, A.D. 1961. Triassic reptiles from the Elgin area: *Stagonoleplis*, *Dasygnathus*, and their allies. Philosophical Transactions of the Royal Society of London 244: 103–204.

Weishampel, D.B., and D.B. Norman. 1989. Vertebrate herbivory in the Mesozoic: jaws, plants, and evolutionary metrics. *In* J.O. Farlow (editor), Paleobiology of the dinosaurs. Geological Society of America Special Paper 238: 87–100.

Welman, J. 1998. The taxonomy of the South African proterosuchids (Reptilia, Archosauromorpha). Journal of Vertebrate Paleontology 18: 340–347.

Whatley, R.L. 2005. Phylogenetic relationships of *Isalorhynchus genovefae*, the rhynchosaur (Reptilia, Archosauromorpha) from Madagascar. Ph.D. dissertation, University of California, Santa Barbara, Santa Barbara, California, 276 pp.

Wild, R. 1973. Die Triasfauna der Tessiner Kalkalpen XXII. *Tanystropheus longobardicus* (Bassani). Schweizerische Paläontologische Abhandlungen 95: 1–162.

Wilson, J.A. 1999. A nomenclature for vertebral laminae in sauropods and other saurischian dinosaurs. Journal of Vertebrate Paleontology 19: 639–653.

Yates, A.M. 2003. A new species of the primitive dinosaur *Thecodontosaurus* (Saurischia: Sauropodomorpha) and its implications for the systematics of early dinosaurs. Journal of Systematic Palaeontology 1: 1–42.

Young, C.C. 1936. On a new *Chasmatosaurus* from Sinkiang. Bulletin of the Geological Society of China 15: 291–311.

Young, C.C. 1963. Additional remains of *Chasmatosaurus yuani* Young from Sinkiang, China. Vertebrata PalAsiatica 7: 215–222.

Young, C.C. 1978. On a new *Chamatosaurus* from Sinkiang. Bulletin of the Geological Society of China 15: 291–320.

Zanno, L.E., and P.J. Makovicky. 2011. Herbivorous ecomorphology and specialization patterns in theropod dinosaur evolution. Proceedings of the National Academy of Sciences 108: 232–237.

APPENDIX 1

REFERRED MATERIAL OF *AZENDOHSAURUS MADAGASKARENSIS*

No.	Field Number	Elements
FMNH PR 2752	8-22-97-91	left maxilla, left angular, left prearticular, tooth
FMNH PR 2753	8-22-97-92	left maxilla, palatine, teeth
UA 8-28-97-138	8-28-97-138	small braincase
UA 8-28-97-139	8-28-97-139	left maxilla
UA 8-28-97-140	8-28-97-140	pterygoid
UA 8-28-97-141	8-28-97-141	posterior cervical vertebra, middorsal vertebra, anterior caudal vertebra, metacarpal V, rib fragments, two articulated phalanges, right palatine, partial frontal, fragments
UA 8-28-97-143	8-28-97-143	proximal right ulna, poorly preserved humerus fragments, anterior caudal vertebra, partial squamosal, partial surangular
UA 10604	8-28-97-144	left dentary
FMNH PR 2754	8-28-97-147	right dentary
FMNH PR 2755	8-29-97-151	right humerus, anterior caudal vertebra, atlas neural arches, ribs, braincase, right dentary, left angular
UA 8-29-97-152	8-29-97-152	pterygoid
UA 8-29-97-153	8-29-97-153	left ulna, left radius
FMNH PR 2769	8-29-97-155	left ilium
UA 8-29-97-156	8-29-97-156	right dentary
UA 8-29-97-159	8-29-97-159	left maxilla
FMNH PR 2756	8-29-97-160	right maxilla
FMNH PR 2770	8-29-97-165	right tibia
FMNH PR 2771	8-29-97-168	right scapula, right coracoid
UA 8-29-97-169	8-29-97-169	three articulated anterior caudal vertebrae
FMNH PR 2757	8-29-97-171	left dentary
FMNH PR 2772	8-29-97-172	articulated distal caudal vertebrae with chevrons
FMNH PR 2773	8-29-97-173	two articulated midcaudal vertebrae, six chevrons
FMNH PR 2774	8-29-97-174	ten articulated mid- to distal caudal vertebrae
UA 10603	8-29-97-178	right maxilla
UA 8-25-98-213	8-25-98-213	left humerus, right ilium
FMNH PR 2775	8-25-98-220	left ilium, partial right ischium, anterior caudal vertebra
FMNH PR 2776	8-25-98-231	left tibia, completely articulated pes
FMNH PR 2777	8-25-98-239	right ischium, first sacral vertebra
UA 8-26-98-250	8-26-98-250	middorsal vertebra
FMNH PR 2778	8-26-98-264	anterior caudal, distal radius, four articulated midcaudal vertebrae, rib fragments, ribs
FMNH PR 2779	8-26-98-265	middorsal vertebra, complete dorsal rib
FMNH PR 2780	8-27-98-270	first sacral vertebra, posterior dorsal vertebra
FMNH PR 2781	8-27-98-271	interclavicle
UA 8-27-98-273	8-27-98-273	right palatine
UA 8-27-98-281	8-27-98-281	tooth
FMNH PR 2758	8-27-98-284	right premaxilla
FMNH PR 2782	8-27-98-285	left tibia and fibula
FMNH PR 2783	8-27-98-290	three articulated posterior cervical vertebrae
FMNH PR 2784	8-27-98-291	two articulated midcervical vertebrae
UA 8-27-98-292	8-27-98-292	left scapula, partial left coracoid
FMNH PR 2785	8-28-98-293	left nasal, left splenial, fragments
FMNH PR 2786	8-28-98-295	right dentary, left tibia, left fibula, astragalus, calcaneum, distal tarsals, metatarsals I-IV, phalanges, unguals other fragments
FMNH PR 2787	8-28-98-296	right ilium and articulated ischium
UA 8-28-98-297	8-28-98-297	rib
FMNH PR 2788	8-28-98-298	three articulated anterior cervical vertebrae and ribs
FMNH PR 2789	8-28-98-299	articulated dorsal vertebrae with associated ribs
FMNH PR 2759	8-28-98-300	left dentary and other bones

APPENDIX 1
(Continued)

No.	Field Number	Elements
FMNH PR 2790	8-28-98-303	left ulna
FMNH PR 2791	8-28-98-306	anterior cervical vertebra
UA 8-28-98-307	8-28-98-307	left radius
UA 8-29-98-325	8-29-98-325	posterior dorsal vertebra
FMNH PR 2792	8-29-98-328	ribs
FMNH PR 2793	8-29-98-334	right ulna, right radius, articulated proximal carpals
UA 8-29-98-340	8-29-98-340	left humerus
UA 8-30-98-348	8-30-98-348	left ulna
UA 8-30-98-349	8-30-98-349	posterior cervical vertebra
FMNH PR 2760	8-30-98-352	left dentary, right dentary, right palatine, left postfrontal, right surangular, right humerus, interclavicle, right scapula, left coracoid, right coracoid, left ulna, right ulna, left radius, right radius, five dorsal vertebrae, partial hand (phalanges), ribs, gastralia
UA 8-30-98-355	8-30-98-355	ribs, right clavicle
FMNH PR 2794	8-30-98-375	right femur, left ilium, right ilium, left pubis, right pubis, left ischium, right ischium, second sacral vertebra, posteriormost dorsal vertebra
UA 9-5-98-447	9-5-98-447	right vomer
UA 9-5-98-448	9-5-98-448	left ilium, fragments
UA 9-5-98-449	9-5-98-449	left coracoid, left ulna, left radius, left intermedium
FMNH PR 2795	9-5-98-451	left clavicle
FMNH PR 2761	9-5-98-454	tooth
UA 9-5-98-457	9-5-98-457	left humerus, fragments, right vomer
FMNH PR 2796	9-5-98-458	anterior caudal vertebra, partial ungual
FMNH PR 2797	9-5-98-459	radius, ribs, ulnare, carpals
FMNH PR 2810	9-8-98-495	atlas/axis
UA 9-8-98-497	9-8-98-497	metacarpal, phalanx, ungual
UA 9-8-98-498	9-8-98-498	left manus (carpals, metacarpals, phalanges, unguals)
FMNH PR 2798	9-8-98-501	left scapula
FMNH PR 2799	9-8-98-502	left femur
FMNH PR 2800	9-8-98-508	right fibula
FMNH PR 2801	9-8-98-509	right tibia
FMNH PR 2762	9-8-98-519	right vomer
FMNH PR 2802	9-8-98-522	three unguals
FMNH PR 2763	9-8-98-524	tooth
FMNH PR 2764	9-8-98-549	right pterygoid, fragments
UA 7-12-99-560	7-12-99-560	right premaxilla
UA 7-12-99-564	7-12-99-564	two midcervical vertebrae
UA 7-13-99-570	7-13-99-570	left maxilla
UA-7-13-99-571	7-13-99-571	right maxilla
UA 7-13-99-576	7-13-99-576	left femur, right femur, right tibia, right fibula, pes elements
FMNH PR 2803	7-13-99-577	left and right humerus, left coracoid, left ulna, left radius
FMNH PR 2804	7-13-99-578	left ulna, left radius, manus, left humerus
FMNH PR 2805	7-13-99-583	atlas/axis, posterior cervical vertebra, ribs
UA 7-15-99-592	7-15-99-592	left radius
FMNH PR 2765	7-15-99-597	braincase, right pterygoid, right dentary, postcranial bones
FMNH PR 2806	7-15-99-598	cervical rib
UA 7-15-99-599	7-15-99-599	distal caudal vertebrae, unguals, rib heads
UA 7-15-99-600	7-15-99-600	eleven articulated caudal vertebrae with chevrons, one isolated caudal vertebra
FMNH PR 2807	7-16-99-607	right ulna, right radius, articulated right manus (proximal and distal carpals, metacarpals, phalanges, unguals), left metatarsal V, two distal caudal vertebrae
FMNH PR 2766	7-16-99-608	teeth
FMNH PR 2808	7-16-99-611	left fibula

APPENDIX 1
(Continued)

No.	Field Number	Elements
FMNH PR 2767	7-16-99-612	left premaxilla, midcaudal vertebra, dorsal ribs
UA 7-16-99-614	7-16-99-614	right premaxilla
UA 7-16-99-619	7-16-99-619	right pterygoid
UA 7-16-99-620	7-16-99-620	left humerus, pathologic interclavicle, left? radius, ribs, ungual, interclavicle
UA 7-16-99-621	7-16-99-621	dorsal rib
UA 7-16-99-622	7-16-99-622	left dentary
FMNH PR 2768	7-20-99-647	maxilla, teeth, anterior cervical vertebra, middorsal vertebra, anterior caudal vertebra, rib fragments, articular, podial, phalanges
FMNH PR 2809	7-20-99-654	anterior cervical vertebra, left coracoid, first sacral vertebra, posterior dorsal vertebra, midcaudal vertebra, cervical rib

APPENDIX 2

The Manus of *Trilophosaurus buettneri*

In seeking material to compare with the available specimens of *Azendohsaurus madagaskarensis*, we turned to the well-represented and described material of *Trilophosaurus buettneri*. The manus of *T. buettneri* was fully described by Gregory (1945) from a seemingly nearly complete and articulated manus (Gregory, 1945: fig. 10) found with the most complete skeleton of a single individual of the taxon (TMM 31025-140). This manus subsequently has formed the basis of comparative descriptions among reptiles (Romer, 1956), a redescription of *T. buettneri* and *Trilophosaurus jacobsi* (Spielmann et al., 2008), phylogenetic character scores for *T. buettneri* (e.g., Dilkes, 1998), and as the basis for the mounted skeletons of *T. buettneri* on display at the Texas Memorial Museum on the campus of the University of Texas at Austin and at the American Museum of Natural History in New York. However, our close comparison between the mani of *Azendohsaurus madagaskarensis* and *Trilophosaurus buettneri* demonstrates that the identifications and, consequently, the position of the carpals is incorrect. Particularly, the proximal carpals are incorrectly identified when compared with the articulated mani of *A. madagaskarensis*. This is not too surprising given that the carpals were found "displaced" and rearticulated based on "relatively closely fitting articular surfaces" (Gregory, 1945: 309). Additionally, one of us (S.J.N.) found an unprepared, partially articulated *T. buettneri* manus (TMM 31025-141; fig. 77) among the originally material collected from the *Trilophosaurus* Quarry in 1939–1941. The following redescription of the proximal carpals of *T. buettneri* is based on the recently reprepared and disassembled manus of TMM 31025-140 (figs. 78–80) combined with the fully prepared, nearly articulated right carpus of TMM 31025-141 (fig. 77). TMM 31025-141 includes most of the proximal and distal carpals in near articulation with the metacarpals. The slight disarticulation (e.g., the articulation between the intermedium and lateral centrale) of the carpal elements allows examination of some of the articulation surfaces that are directly comparable to that of the disarticulated manus. For a detailed description of the distal carpals (refigured here), metacarpals (refigured here) and phalanges, see Gregory (1945).

Ulnare: It is now clear from the articulated manus of *Trilophosaurus buettneri* (TMM 31025-141; fig. 77) that the element originally identified by Gregory (1945) as the radiale is actually the ulnare (fig. 78). The ulnare of *T. buettneri* is the largest carpal of the series. The ulnare articulates with the ulna proximally, the intermedium proximomedially, the pisiform posterolaterally, the lateral centrale distomedially, and the fourth distal carpal distally. The proximal and distal surfaces are distinctly concave and dorsal, ventral, and medial surfaces are composed of finished bone surfaces. A slight depression adjacent to the articular surface with the ulna forms the posterolateral articular facet with the pisiform. The medial surface of the ulnare bears a proximomedial articular surface for articulation with the intermedium and a ventromedial articular facet for the lateral centrale. The articular surface with the lateral centrale is canted ventromedially as in *Azendohsaurus madagaskarensis* (see above). The articular facets for the intermedium and the lateral centrale are separated by a channel with small foramina within it. This channel represents the lateral portion of the perforating foramen, whereas the intermedium and lateral centrale form the rest of the perforating foramen. This perforating foramen is also clearly present in *Sphenodon punctatus* (FMNH 197942) and early archosauromorphs (fig. 49).

Intermedium: The element originally hypothesized as the ulnare (upside down in Gregory, 1945: fig. 10; fig. 79) is reidentified as the intermedium. The dorsoventrally compressed intermedium bears dorsal and ventral surfaces with finished bone surfaces. The medial surface is rounded but does not appear to be articulated with another bone. The intermedium articulates with the ulna proximolaterally and the

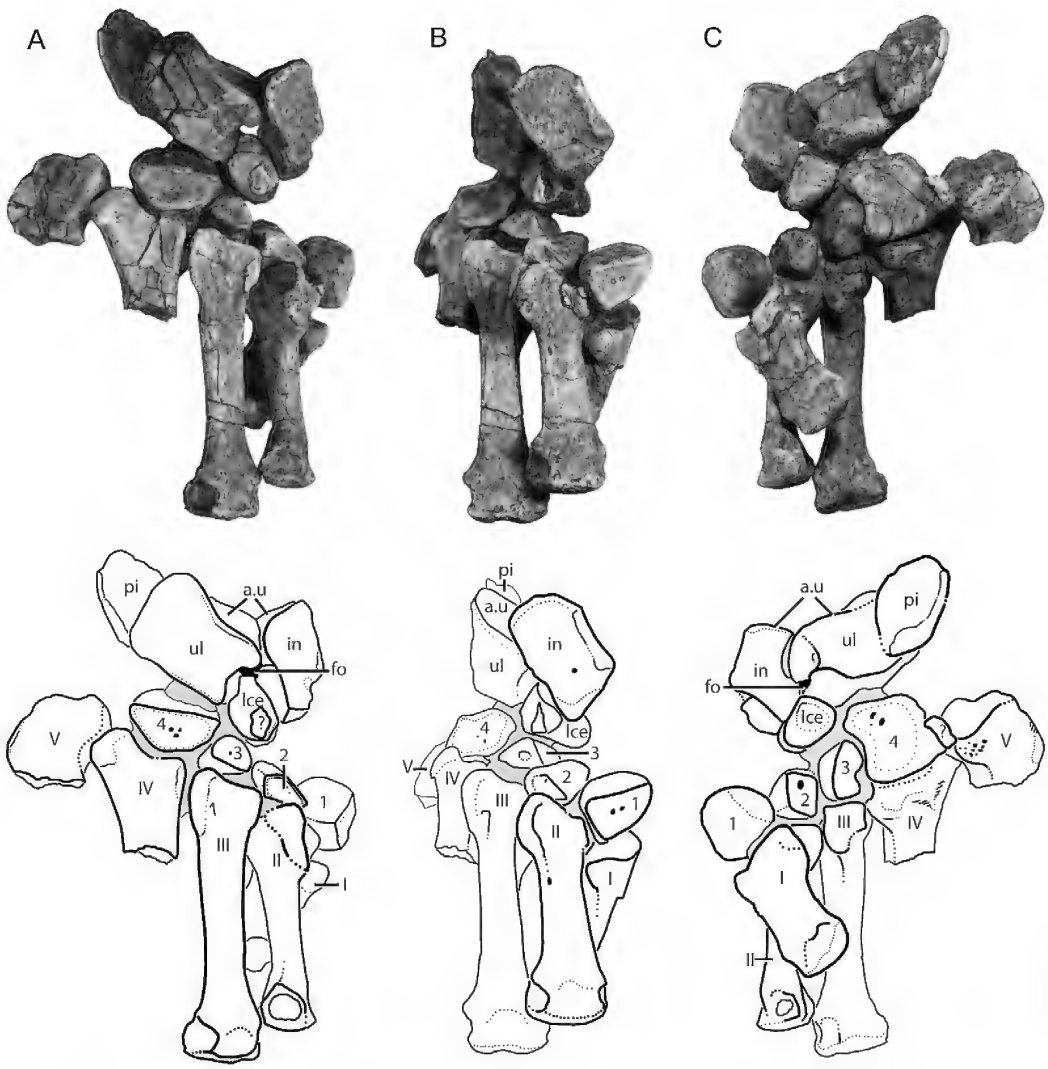

Fig. 77. Partially articulated right manus of *Trilophosaurus buettneri* (TMM 31025-141) in (**A**) dorsal view and drawing (below), (**B**) dorsolateral view and drawing (below), and (**C**) ventral view and drawing (below). Note, some of the phalanges are slightly disarticulated. Scale = 1 cm. Gray in drawings represents matrix. Abbreviations: **a.,** articulates with; **fo,** foramen; **pi,** pisiform; **in,** intermedium; **lce,** lateral centrale; **r,** radius; **u,** ulna; **ul,** ulnare; **1,** distal carpal 1; **2,** distal carpal 2; **3,** distal carpal 3; **4,** distal carpal 4; **I,** digit I; **II,** digit II; **III,** digit III; **IV,** digit IV; **V,** digit V.

ulnare proximolaterally just distal to the articular facet with the ulna, the lateral centrale distolaterally, and presumably the radiale mediodistally. The articular surface with the ulna is convex, and this surface forms the medial third of the complete carpus contribution of the articular surface with the ulna. The articular surface with the lateral centrale is large and flat. The medial edge of the perforating foramen lies between the articular surface with the ulna and the lateral centrale. The expression of the foramen is more apparent on the ventral surface (fig. 77) in comparison with the dorsal surface.

PISIFORM: The pisiform was originally described as the intermedium by Gregory (1945). The pisiform remains in near articulation with the ulnare in TMM 31025-141. The element is composed of compact bone surfaces on the dorsolateral and ventromedial surfaces in TMM 31025-140 (fig. 80) but spongy bone surfaces in TMM 31025-141. Pisiforms from both sides share the presence of lateral rims composed of finished bone. The proximal and dorsal edges of the pisiform are spongy and there is a distinct groove along these surfaces. The pisiform articulates only with the ventrolateral surface of the ulnare.

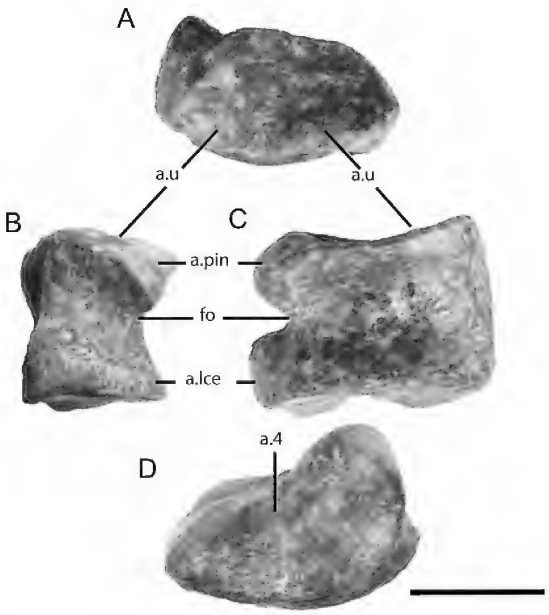

Fig. 78 Left ulnare of *Trilophosaurus buettneri* (TMM 31025-140) in (**A**) proximal, (**B**) preaxial (lateral), (**C**) dorsal, and (**D**) distal views. Scale bar = 1 cm. Abbreviations: **a.,** articulates with; **fo,** foramen; **lce,** lateral centrale; **pin,** proximal articulation with the intermedium; **u,** ulna; **4,** distal carpal 4.

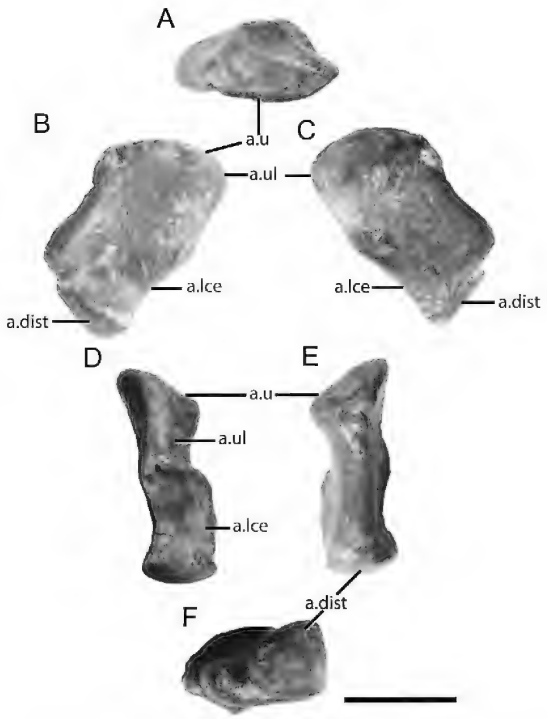

Fig. 79. Left intermedium of *Trilophosaurus buettneri* (TMM 31025-140) in (**A**) proximal, (**B**) palmar, (**C**) dorsal, (**D**) preaxial (lateral), (**E**) postaxial (medial), and (**F**) distal views. Scale bar = 1 cm. Abbreviations: **4,** distal carpal 4; **a.,** articulates with; **dist,** distal carpal; **lce,** lateral centrale; **u,** ulna; **ul,** ulnare.

LATERAL CENTRALE: The lateral centrale (centrale of Gregory, 1945) was correctly identified, but oriented upside down by Gregory (1945). Unfortunately, the lateral centrale of TMM 31025-140 is now missing, but TMM 31025-141 preserves the lateral centrale in articulation (fig. 77). The lateral centrale has concave and finished bone surfaces both dorsally and ventrally. Small foramina lie in these depressions. The lateral centrale forms the ventral border of the perforating foramen, articulates with the intermedium proximomedially, possibly the medial centrale distomedially, the third distal carpal distally, the fourth distal carpal distolaterally, and the ulnare proximolaterally. All of these articulations lack clear facets for each of these elements because the edges of the lateral centrale are rounded without distinct articulation surfaces.

OTHER CARPAL ELEMENTS: A radiale is not present in the associated (TMM 31025-140) or articulated (TMM 31025-141) manus of *Trilophosaurus buettneri.* Furthermore, we have not been able to identify a radiale with confidence from the abundant *T. buettneri* remains from the *Trilophosaurus* Quarry (TMM 31025). However, the articular facet on the intermedium indicates that the radiale was ossified. The space between the proximal and distal carpals suggests that the radiale was rather small and may have been similar in relative proportions to that of *Azendohsaurus madagaskarensis.*

Like the radiale, we have not been able to identify a medial centrale. This is not surprising given that the medial centrale in *A. madagaskarensis* is a rounded and small carpal with few distinguishing characteristics. However, the articular facets of the surrounding elements (lateral centrale, second and third distal carpals), the gap between these elements in the articulated manus (fig. 77), and the similarity in the hands of *Trilophosaurus buettneri* and *A. madagaskarensis* all indicate that a medial centrale was likely ossified.

Gregory (1945) hypothesized that the fifth distal carpal was lost during preservation or was cartilaginous. Here, we support that that fifth distal carpal was not lost after the death of the animal, but may have been lost completely in evolutionary history, given that there is no sign of an ossified element in TMM 31025-141 and there are no clear articular facets on the surrounding elements. This may have

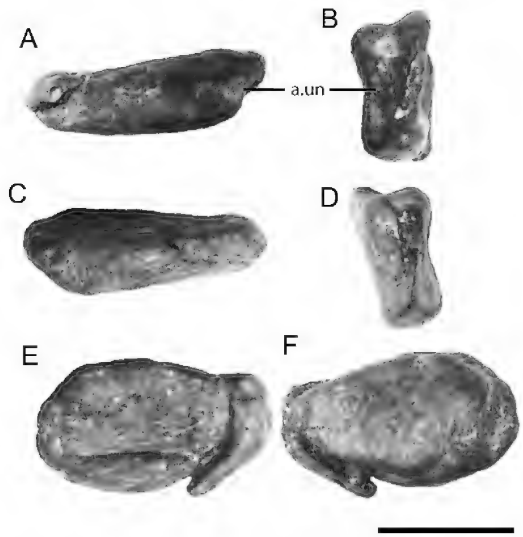

Fig. 80. Left pisiform of *Trilophosaurus buettneri* (TMM 31025-140) in (**A**) proximal, (**B**) preaxial (lateral), (**C**) distal, (**D**) postaxial (medial), (**E**) dorsal, and (**F**) palmar views. Scale bar = 1 cm. Abbreviations: **a.,** articulates with; **ul,** ulnare.

a wider phylogenetic implication (see Phylogenetic Analysis).

Implications

We present a newly reconstructed hand of *Trilophosaurus buettneri* in figure 81 based on the new specimen (fig. 77), comparisons with other saurians (e.g., *Azendohsaurus madagaskarensis*, *Sphenodon punctatus*), and the repreparation of the originally described hand (TMM 31025-140). The new anatomical arrangement has a number of implications. First, the arrangement of the proximal carpals in *T. buettneri* is now more similar to the plesiomorphic condition for Sauria (exemplified by *S. punctatus*). The ulna and radius are well separated from each other by means of a mediolaterally wide intermedium, and a large pisiform is present. Second, there is more cartilage in the manus of *T. buettneri* than originally described. The carpal elements of *T. buettneri* are well ossified and most have distinct articular facets with other elements, but some of the surfaces are simply rounded without clear articular surfaces. This indicates that cartilage was still a major structural component of the manus. Third, the identification of carpal elements by Gregory (1945) led directly to the identification of carpal elements in *Trilophosaurus jacobsi* (Spielmann et al., 2008). For example, the element identified by Spielmann et al. (2008) as a radiale for *T. jacobsi* (NMMNH P-36707; fig. 104) is actually the ulnare, whereas the element identified as the ulnare (NMMNH P-36765) by Spielmann et al. (2008) is the intermedium.

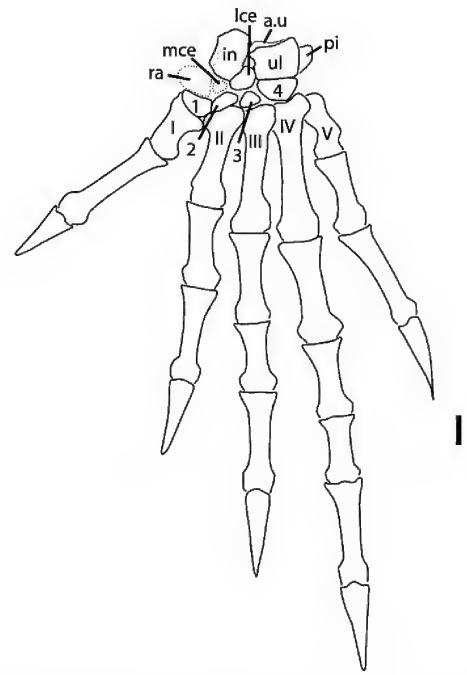

Fig. 81. Reconstruction of the left hand of *Trilophosaurus buettneri* from specimens TMM 31025-140 and TMM 31025-141.**a.,** articulates with; **pi,** pisiform; **in,** intermedium; **lce,** lateral centrale; **mce,** medial centrale; **ra,** radiale; **u,** ulna; **ul,** ulnare; **1,** distal carpal 1; **2,** distal carpal 2; **3,** distal carpal 3; **4,** distal carpal 4; **I,** digit I; **II,** digit II; **III,** digit III; **IV,** digit IV; **V,** digit V.

APPENDIX 3

Extended Description of Newly Added or Revised Terminal Taxa in the Phylogenetic Analysis

Spinosuchus caseanus von Huene, 1932

Age: Early Norian, Late Triassic (Spielmann et al., 2009), based on biostratigraphy.

Occurrence: The holotype is from the Spur-Crosbyton locality, possibly the Tecovas Formation, West Texas; Kahle *Trilophosaurus* Quarry in the base of the Trujillo Formation, West Texas; Rotten Hill in the Tecovas Formation, West Texas; Walker's Tank in the Tecovas Formation, West Texas (Spielmann et al., 2009; 2013).

Holotype: UMMP 7507, a presacral vertebral column, consisting of four cervical, three transitional and 15 trunk vertebrae, with 17 complete, nearly complete or fragmentary neural spines.

REFERRED TO AND SCORED MATERIAL: Material from the Kahle *Trilophosaurus* Quarry (NMMNH L-3775): NMMNH P-57852 to P-57865, including presacral, sacral, and caudal vertebrae.

REMARKS: For over 70 years, *Spinosuchus caseanus* was known only from a single articulated vertebral from the Tecovas Formation of West Texas and as a result of the paucity of material, the taxon has been identified as a dinosaur (Case, 1922; von Huene, 1932; Hunt et al., 1998), an indeterminate neodiapsid (Long and Murry, 1995), an archosauromorph or archosauriform (Nesbitt et al., 2007), or a taxon closely related to *Trilophosaurus* (Richards, 1999). After the discovery of additional vertebral material from the Kahle *Trilophosaurus* Quarry in the base of the Trujillo Formation, Spielmann et al. (2009) weaved a well-supported argument that *Spinosuchus caseanus* was closely related to *Trilophosaurus* and belonged in the same "family level" clade. Here, we test this proposed relationship in a comprehensive phylogeny. Additionally, we propose that *Spinosuchus caseanus* and referred material of *Trilophosaurus jacobsi* belong to the same species-level taxon (detailed in the main text).

KEY REFERENCES: Case, 1922; von Huene, 1932; Spielmann et al., 2009.

Pamelaria dolichotrachela Sen, 2003

AGE: Middle Triassic (Bandyopadhyay, 1988), based on biostratigraphy.

OCCURRENCE: Yerrapalli Formation, Gondwana Supergroup, Pranhita-Godavari Basin, south India (Sen, 2003).

HOLOTYPE: ISIR 316, an almost complete, partially articulated skeleton.

REFERRED TO AND SCORED MATERIAL: ISIR 317, a partially preserved associated skeleton consisting mainly of a cervical series and a partial skull and ISIR 318–333, isolated bones found among the remains of the ?archosaur *Yarasuchus deccanensis* Sen, 2005.

REMARKS: Sen (2003) coined the name *Pamelaria dolichotrachela* for relatively complete remains from multiple specimens from the same horizon in the Middle Triassic Yerrapalli Formation from India. Somewhat poorly preserved, much of the material of *P. dolichotrachela* is three-dimensionally preserved and prepared. Although some of the disarticulated referred material was found mixed with disarticulated remains of the ?archosaur *Yarasuchus deccanensis*, the nearly complete holotype skeleton allows relatively easy referral of isolated remains.

Sen (2003) first identified *Pamelaria dolichotrachela* as a "prolacertid"—a likely paraphyletic or polyphyletic group of long-necked archosauromorphs from the Triassic (Dilkes, 1998; Rieppel et al., 2003). Here, we are the first to incorporate *P. dolichotrachela* into a phylogenetic dataset given its importance to biogeography and age.

KEY REFERENCES: Sen, 2003.

"Chasmotosaurus" yuani Young, 1936

AGE: Early Triassic, *Lystrosaurus* AZ (Young, 1936; Rubidge, 2005).

OCCURRENCE: Lowermost Jiucaiyuan Formation, Cangfanggou Group, western Xinjiang, China.

HOLOTYPE: IVPP V36315 (field collection 90002); partial skull, jaw, partial postcranial skeleton.

REFERRED TO AND SCORED MATERIAL: Cast of holotype (rostrum and mandible), IVPP V2719, V2720 (jaw fragments, postcranial fragments), IVPP V4067 (nearly complete skeleton).

REMARKS: "*Chasmatosaurus*" *yuani* was first described based on a skull and partial postcranial skeleton by Young (1936), who recognized the close resemblance with the sharply downturned rostrum and recurved, serrated teeth of *Chasmatosaurus vanhoepeni* (now referred to *Proterosuchus,* see Welman, 1998, and Ezcurra and Butler, 2015) materials described by Broili and Schröder (1934). Young (1963) later described more material that he referred to the taxon (IVPP V2719 and V2720). Young (1978) preliminarily described a nearly complete skeleton, which he attributed to *Chasmatosaurus yuani.* Welman (1998) revised the taxonomy of South African *Proterosuchus* and *Chasmatosaurus*, assigning all South African material to the first-described species, *Proterosuchus fergusi.* This choice renders the type species of *Chasmatosaurus*, *C. vanhoepeni*, a junior objective synonym of *Proterosuchus fergusi.* Further complicating the picture, Ezcurra and Butler (2015) split *Proterosuchus fergusi* (sensu Welman, 1998) into four species of *Proterosuchus.* Yet, this recent work also concludes that *Chasmatosaurus* a junior synonym of *Proterosuchus.* Thus, the Chinese taxon is in need of taxonomic revision with these reassignments. We refer to it throughout as "*Chasmatosaurus*" *yuani*, pending further revision to the taxonomy of specimens referred to "*Chasmatosaurus*" *yuani* (Ezcurra et al., 2013; Ezcurra and Butler, 2015).

KEY REFERENCES: Young, 1936, 1963, 1978; Cruickshank, 1972; Charig and Sues, 1976; Ezcurra and Butler, 2015.

Azendohsaurus laaroussii Dutuit, 1972

AGE: Carnian to early Norian, Late Triassic (Biron and Dutuit, 1981), based on biostratigraphy.

OCCURRENCE: Argana Formation, base of t5 level (of Tixeront, 1973), near Azendoh, Morocco.

HOLOTYPE: MNHN-ALM XVI 1, fragment of mandible.

REFERRED TO AND SCORED MATERIAL: MNHN-ALM 424-5 isolated tooth; MNHN-ALM 424-4, isolated tooth; MNHN-ALM 351, left dentary; MNHN-ALM 365-20, right dentary; MNHN-ALM 353, MNHN-ALM 365-17, MNHN-ALM 365-18 dentary fragments; MNHN-ALM 355-3, left maxilla; MNHN-ALM 365-21, right maxilla; MNHN-ALM 365-16, right premaxilla.

REMARKS: Dutuit (1972) named *Azendohsaurus laaroussii* based on teeth and tooth-bearing elements from one locality in the t5 horizon in the Argana Formation in Morocco. First identified as an ornithischian dinosaur (Dutuit, 1972), *A. laaroussii* has been reidentified as a sauropodomorph dinosaur (Thulborn, 1973; Bonaparte, 1976; Gauffre, 1993; Flynn et al., 1999), and most recently as a non-archosaurian archosauromorph (Flynn et al., 2010). The published material of *A. laaroussii* is limited to cranial material, but postcranial material collected with the type series has been preliminarily reported (Jalil and Knoll, 2002). Here, we test the proposed close relationship of *Azendohsaurus laaroussii* and *Azendohsaurus madagaskarensis.*

KEY REFERENCES: Dutuit, 1972; Gauffre, 1993; Flynn et al., 2010.

Proterosuchus alexanderi Hoffman, 1965, sensu Ezcurra and Butler, 2015

AGE: Lystrosaurus AZ (Induan–?early Olenekian; Rubidge, 2005).

OCCURRENCE: Upper Balfour Formation or lower Katberg Formation, Beaufort Group, Karoo, Supergroup Farm Zeekoegat, four miles from Venterstad, Joe Gqabi District, Eastern Cape Province, South Africa (Hoffman, 1965; Ezcurra and Butler, 2015).

HOLOTYPE: NMQR 1484, nearly complete and postcranial skeleton.

REMARKS: During a recent taxonomic assessment of the *Proterosuchus* taxa from the Early Triassic of South Africa, Ezcurra and Butler (2015) divided *Proterosuchus fergusi* (sensu Welman, 1998) into four taxa, *Proterosuchus fergusi*, *Proterosuchus goweri*, *Proterosuchus alexanderi*, and *Proterosuchus vanhoepeni.* This division complicates previous treatments of *Proterosuchus fergusi* in recent phylogenetic analyses (e.g., Nesbitt et al., 2009; Nesbitt, 2011) of archosauriform relationships given that each *Proterosuchus* species is now known by less material. However, much of the scoring of *Proterosuchus fergusi* in Nesbitt et al., (2009) and Nesbitt (2011) was based on the new taxon *Proterosuchus alexanderi.* Therefore, in this study we ran the analysis twice regarding *Proterosuchus*, once scoring only the holotype of *Proterosuchus alexanderi* and once scoring *Proterosuchus* as a composite based on specimens assigned to both *Proterosuchus alexanderi* and *Proterosuchus fergusi* (see above).

APPENDIX 4

PHYLOGENETIC CHARACTERS

1. Premaxilla, external sculpturing: surface is smoothly sculptured (0); premaxilla is marked by anteroventral striations (1).
2. Premaxilla, orientation of ventral margin: horizontal, roughly inline with maxillary ventral margin (0); slight downturn, such that the margin trends anteroventrally (1); extensive downturn, premaxilla extends to ventral margin of dentary (2). ORDERED
3. Premaxilla, anterodorsal process (= nasal process): present, separating the nares (0); absent or reduced, creating a confluent external naris (1).
4. Premaxilla, posterodorsal process (= maxillary process = subnarial process): absent, such that premaxilla contributes a small ventral margin for the naris (0); posterodorsal process present, framing the posteroventral margin of the naris (1).
5. Premaxilla, length of posterodorsal process (= maxillary process = subnarial process): short, failing to exclude maxilla from narial margin (0); long, excluding maxilla from narial margin (1); extremely long, reaching the anteriormost part of the prefrontal (2). ORDERED
6. Premaxilla, posterodorsal process/maxilla contact: contact is a simple, straight margin (0); knob on the posterior margin of the posterodorsal process of the premaxilla fits into notch in the anterior surface of the maxilla (1).
7. Maxilla, orientation of ventral margin: ventral margin of maxilla is horizontal (0); ventral margin of maxilla is convex (1).
8. Maxilla, posterolateral surface: directly adjacent to alveolar margin (0); lateral process of maxilla present, creating distinct space between maxillary alveoli and posterolateral surface of the maxilla (1).
9. Nasal, orientation of contact with prefrontal: oriented parasagitally (0); oriented anterolaterally (1).
10. Prefrontal, contact with contralateral prefrontal: no contact, due to frontonasal contact (0); prefrontals approach medially, constricting frontonasal contact (1); contact present (2). ORDERED
11. Lacrimal, facial contribution: forms a portion of lateral surface of the face, reaching anteriorly to the external naris (0); forms a portion of the lateral surface of the face, but does not reach naris (1); limited to orbital margin (2). ORDERED

12. Lacrimal, anterior extension: lacrimal extends dorsally to reach the ventral margin of the nasal externally (0); lacrimal fails to reach nasal (1).
13. Antorbital fenestra: absent (0); present (1).
14. Frontals, degree of fusion: frontals unfused to one another (suture patent) (0); frontals fused in the midline (1).
15. Frontals, shape: frontal maintains transverse width throughout its anteroposterior length (0); frontals expand transversely posteriorly (1).
16. Frontal, shape of contact with parietal in dorsal view: roughly transverse in orientation (0); frontal exhibits posterolateral processes, forming anteriorly curved U-shaped contact (1).
17. Frontal and postfrontal, surface texture: dorsal surface relatively smooth (0); dorsal surface exhibits distinct pitting (1).
18. Postfrontal, medial contact with frontal and parietal: postfrontal forms broad contact with midline skull elements, without bifurcation (0); postfrontal bifid, fitting broadly across both parietal and frontal (1).
19. Parietals, degree of fusion: parietals unfused to one another (patent suture) (0); parietals fused at the midline (1).
20. Parietal, dorsal surface: parietal skull table flattened (0); dorsal exposure of parietal forms a raised margin, elevated above lateral excavation for jaw adductor musculature (1); thin, bladelike sagittal crest (2). ORDERED
21. Parietal, orientation of posttemporal process: roughly transverse (0); strong posterolateral angling (1).
22. Pineal foramen: present (0); absent (1).
23. Pineal foramen, position: entirely surrounded by parietals (0); situated within the frontoparietal suture (1).
24. Postparietals: absent (0); present (1).
25. Postparietals, degree of fusion: unfused to one another (0); fused as a midline interparietal (1).
26. Postorbital, presence of medial process: medial process absent, with contributions of the frontal, parietal or postfrontal forming the posterodorsal orbital margin (0); present, postorbital contributing to posterodorsal orbital margin (1).
27. Postorbital, location of medial process: situated deep to postfrontal (0); dorsally excludes postfrontal from supratemporal fenestra margin (1).
28. Postorbital, length of posterior process: contributes to less than one-half the length of the supratemporal bar (0); contributes to more than one-half the length of the supratemporal bar (1).
29. Infratemporal fenestrae, conformation: present, distinct opening framed by squamosal, postorbital, and jugal (0); postorbital, jugal, and squamosal fit against one another as a "lateral temporal plate" present, with squamosal extending anteriorly to slot into a notch on the jugal (1).
30. Jugal, ornamentation of lateral surface: unornamented (0); distinct anteroposteriorly trending shelf present (1).
31. Jugal, ascending process relative to supratemporal bar: process terminates ventral to bar (0); process intersects between postorbital and squamosal within bar (1).
32. Jugal, posterior process: absent (0); present, but failing to contact the quadratojugal posteriorly (1); present, contacting the quadratojugal posteriorly (2). ORDERED
33. Squamosal, descending process: present (0); absent (1).
34. Squamosal, size of descending process: forms massive flange that covers the quadrate almost entirely or entirely in lateral view (0); anteroposteriorly slender (1).
35. Squamosal, posterior process: no posterior process (0); posterior process, extending beyond quadrate contact (1).
36. Supratemporals: absent (0); present (1).
37. Tabulars: absent (0); present (1).
38. Quadratojugal: present (0); absent (1).
39. Quadratojugal, shape of anterior process: paralleling dorsal and ventral borders (0); anteriorly tapering anterior process (1).
40. Quadratojugal, extent of dorsal process: process tall (0); weakly developed or absent dorsal process (1).
41. Quadrate, shape of posterior margin: straight, vertical posterior margin (0); concave, excavated posterior margin (1).
42. Quadrate foramen/quadratojugal foramen, position: foramen positioned between quadrate and quadratojugal (0); foramen positioned within the quadrate (1).
43. Quadrate, tympanic crest: absent, quadrate has no lateral expansion (0); present, flattened tympanic crest projects from lateral surface of quadrate (1).
44. Palatal teeth: present (0); absent (1).
45. Vomerine teeth: present (0); absent (1).
46. Vomer, contact with maxilla: absent, vomer only contacts premaxilla (0); present, vomer-premaxilla contact expands onto maxilla (1).
47. Palatine teeth: present (0); absent (1).
48. Pterygoid, anterior process dentition: present (0); absent (1).
49. Pterygoid, anterior process, number of dentition fields: one field (0); two fields (1); three fields (2).
50. Pterygoid, transverse process dentition: absent (0); present (1).
51. Pterygoid, number of tooth rows on transverse process: multiple rows (0); one row (1).
52. Pterygoid, midline contact with contralateral pterygoid: absent (0); present, small contact anteriorly (1); present, broad contact throughout length (2). ORDERED
53. Pterygoid, orientation of transverse process in ventral view: lateral (0); anterolateral (1).
54. Pterygoid, shape of interpterygoid vacuity: pterygoids meet to form anteriorly tapering space (0); pterygoids meet to form anteriorly curved space (1).

55. Supraoccipital, texture of posterior surface: smooth (0); distinct dorsoventrally running crest in the midline (1).
56. Supraoccipital, shape: consists of a flattened posterior lamina (0); pillarlike (1).
57. Opisthotic, shape of ventral ramus: slender process (0); distinct club-shaped expansion ventrally (1).
58. Opisthotic, paroccipital process contact with squamosal: absent, ends freely (0); present (1).
59. Exoccipital, dorsal contact with occipital elements: exoccipital columnar throughout dorsoventral height, forming transversely narrow dorsal contact with more dorsal occipital elements (0); dorsal portion of exoccipital exhibits dorsomedially inclined process that forms transversely broad contact with more dorsal occipital elements (1).
60. Exoccipital, contralateral contact dorsal to foramen magnum: absent, supraoccipital contributes to foramen magnum (0); present, excluding supraoccipital from foramen magnum (1).
61. Exoccipital, contralateral contact on floor of foramen magnum: absent, basioccipital contributes to floor of foramen magnum (0); present, excluding basioccipital from floor of the foramen magnum (1).
62. Exoccipitals, fusion with opisthotic: absent (0); present (1).
63. Opisthotic, paroccipital process morphology: unflattened and tapered (0); anteroposteriorly flattened distally (1).
64. Basioccipital, basal tubera: absent (0); present (1).
65. Parabasiphenoid, dentition on cultriform process: absent (0); present (1).
66. Parabasisphenoid, parasphenoid crests: absent such that there is no ventral floor for the vidian canal (0); present as prominent ventrolateral extensions of the caudoventral processes, framing the ventromedial floor of the vidian canal (1).
67. Parabasisphenoid, passage for internal carotid arteries: within lateral wall of braincase (0); within ventral surface of the parabasisphenoid (1); passage of the internal carotids do not enter the braincase (2).
68. Braincase, conformation of ventral surface: roughly planar (0); distinct depression at the suture between the basioccipital and the parabasisphenoid (1); distinct depression within the parabasisphenoid (2).
69. Parabasisphenoid, cultriform process: extremely elongate, reaching to the level of the nares (0); shorter, failing to reach nares (1).
70. Parabasisphenoid, basipterygoid process orientation in transverse plane: anterolateral (0); lateral (1).
71. Parabasisphenoid, location of abducens foramina: within the dorsum sella (0); track across dorsal surface of dorsum sella, between it and the prootic (1).
72. Laterosphenoid ossification: absent (0); present but fails to reach the ventral surface of frontals (1); present and reaches the frontals (2). ORDERED
73. Prootic, crista prootica: present (0); absent (1).
74. Prootic, anterior inferior process: process present, sitting anterior to trigeminal foramen (0); absent, trigeminal foramen unframed anteriorly (1).
75. Prootic, paroccipital contribution: does not contribute to anterior surface of paroccipital process (0); contributes laterally tapering lamina to the anterior surface of the prootic (1).
76. Stapes, dorsal process: absent (0); present (1).
77. Stapes, foramen for stapedial artery: present (0); absent (1).
78. Dentary, anterior portion, symphyseal region of mandible: dentaries do not diverge, thus contributing to symphysis (0); dentaries diverge, and only splenials contribute to symphysis (1).
79. Coronoid process: absent (0); present (1).
80. Surangular, lateral surface, foramen positioned near surangular-dentary contact: absent (0); present (1).
81. Surangular, lateral surface, foramen positioned directly anterolateral to glenoid fossa: absent (0); present (1).
82. Angular, exposure on lateral mandibular surface: broadly exposed (0); limited to posteroventral sliver by dentary and surangular (1).
83. Angular, exposure on lateral mandibular surface: terminates anterior to the glenoid (0); extends to the glenoid (1).
84. External mandibular fenestra (EMF): absent (0); present (1).
85. Splenial, contribution to mandibular symphysis: splenials contribute to symphysis (0); splenials fail to contribute (1).
86. Retroarticular process: present (0); absent (1).
87. Retroarticular process, composition: articular only (0); fused articular-prearticular (1).
88. Marginal dentition on anteriormost portions of premaxilla and dentary: present (0); absent (1).
89. Marginal dentition, enlarged caniniform teeth in maxilla: present (0); absent, maxillary teeth subequal in size (1).
90. Marginal dentition, serrations: nonserrated (0); serrated (1).
91. Marginal dentition, shape of the posterior margin of tooth: convex or straight (0); concave (1).
92. Marginal dentition, arrangement: single row of marginal teeth (0); multiple *zahnreihe* in maxilla (1).
93. Marginal dentition, morphology of crown base: single, pointed crown (0); flattened platform with pointed cusps (1); mesiodistally arranged cusps (2).
94. Marginal dentition, implantation: teeth situated in shallow groove (pleurodonty + thecodonty) (0); teeth on dorsal surface of tooth-bearing bones (acrodonty) (1).
95. Marginal dentition, lingual surface: teeth walled by minimal lingual wall (0); no lingual wall (= pleurodonty) (1).
96. Marginal dentition, lingual surface: teeth walled by minimal lingual wall only (0); interdental plates are present (1).

97. Marginal dentition, rooting: tooth crowns are not attached to dentigerous bones (0); teeth ankylosed to bones of attachment (1).
98. Marginal dentition, tooth shape at crown base: circular (0); labiolingually compressed (1); labiolingually wider than mesiodistally long (2).
99. Palatal dentition, morphology: small, buttonlike teeth (0); small, conical teeth (1).
100. Marginal dentition, procumbency: anteriormost marginal teeth have similar apicobasal orientation to posterior teeth (0); anteriormost teeth are procumbent (1).
101. Presacral vertebrae, shape of anterior articular surface: planar (0); concave (1).
102. Presacral vertebrae, shape of posterior articular surface: planar (0); concave (1); convex (2).
103. Presacral vertebrae, development of posterior articular surface convexity: moderate (0); balllike (1).
104. Anterior cervical ribs, shaft shape: tapering rapidly, roughly triangular in lateral view (0); ribs taper gradually, elongate and splintlike in lateral view (1).
105. Cervical ribs, anterior process: absent (0); present (1).
106. Intercentra in the cervical column: present (0); absent (1).
107. Anterior postaxial cervical vertebrae, shape of anterior articular surface: subcircular, roughly equivalent in dorsoventral height and transverse width (0); compressed, with a greater transverse width than dorsoventral height (1).
108. Cervical vertebrae, ventral keel: present (0); absent (1).
109. Anterior postaxial cervical vertebrae, shape of ventral surface excluding keel: ventrally rounded (0); ventral face flattened (1).
110. Cervical vertebrae, number of costal facets: one (0); two (1).
111. Anterior postaxial cervical vertebrae, position of diapophysis (or dorsal margin of synapophyses): at or near dorsoventral level of pedicles (0); further ventrally, near the dorsoventral midpoint of the centrum (1).
112. Anterior postaxial cervical vertebrae, relative location of costal facets: facets distinctly offset from one another (0); facets very closely appressed to one another with little or no finished bone separation (1).
113. Anterior postaxial cervical vertebrae, shape of neural spine base: elongate, subequal in length to the neural arch (0); short, spine restricted to posterior half of neural arch (1).
114. Anterior postaxial cervical vertebrae, neural spine shape in cross section: transversely narrow (0); elliptical or circular (1).
115. Anterior postaxial cervical vertebrae, shape of anterior margin of neural spine in lateral view: straight and linear (0); anterodorsal process present forming an anterior notch (1).
116. Anterior postaxial cervical vertebrae, anterior margin of neural spine, direction of inclination: inclined posterodorsally (0); inclined anterodorsally (1).
117. Cervical vertebra, transverse width of dorsal tip of neural spine: transversely slender (0); expanded transversely with a midline cleft (1).
118. Cervical vertebrae, relative location of dorsal margin of midcervical neural spines: spines are equivalent in height and length to other cervical neural spines (0); spines are dorsoventrally depressed at their anteroposterior midpoints, leaving them little more than midline dorsal ridges (1).
119. Cervical vertebra, dorsal surface of postzygapophyses: smooth and rounded (0); posteriorly pointed projections (epipophyses) present (1).
120. Anterior trunk vertebrae, position of parapophysis (or ventral margin of dorsal synapophysis): positioned partially on lateral margin of centrum (0); positioned entirely on neural spine (1).
121. Posterior trunk vertebra, position of parapophysis (or ventral margin of dorsal synapophysis) in trunk vertebrae: positioned partially on lateral margin of centrum (0); positioned entirely on neural spine (1).
122. Anterior trunk vertebra, number of pectoral costal facets: one (holocephaly) (0); two (dichocephaly) (1); three (tricephaly) (2).
123. Posterior trunk vertebrae, costal facets: single rib facet (0); "inverse-L" (inverted-L) rib facet (suggesting partial confluence of diapophysis and parapophysis) (1); double rib facet (2).
124. Posterior trunk vertebra, ribs, and vertebrae: unfused (0); fused (1).
125. Trunk vertebrae, neural spine, dorsal portion: similar width as the more distal portion of the neural spine (0); expanded transversely into a flattened tip (= spine table) (1).
126. Trunk vertebra, breadth of neural spine expansion: little lateral expansion relative to the neural spine base (0); transversely broad, much wider than neural spine base (1).
127. Trunk vertebra, texturing on dorsum of neural spine expansion: marked by irregular rugosities (0); marked by transverse striations (1).
128. Trunk vertebrae, intercentra: present (0); absent (1).
129. Trunk vertebrae, height of neural spines: tall, greater in dorsoventral height than anteroposterior length (0); long and low, lesser in dorsoventral height than anteroposterior length (1).
130. Trunk vertebra, accessory zygosphene-zygantrum articulations: absent (0); present (1).
131. Second sacral rib, shape: rib is a single unit (0); rib bifurcates posteriorly into anterior and posterior processes (1).
132. Second sacral rib, morphology of posterior process: terminally blunted (0); sharp distally (1).
133. Anterior caudal vertebrae, shape of transverse processes: processes curve posterolaterally (0); processes straight (1).
134. Anterior caudal vertebrae, orientation of transverse processes: base of process perpendicular to the long axis of the vertebra (0); processes angled posterolaterally from base (1).

135. Caudal vertebrae, autotomic septa within the centrum: absent (0); present (1).
136. Chevron, shape of hemal spine: tapers along its anteroposterior length (0); maintains breadth along its length (1); broadens distally, forming inverted-T shape (2); broadens distally, forming subcircular expansion (3).
137. Gastralia, ossification: present (0); absent (1).
138. Gastralia, pairs of lateral gastralia: two (0); one (1).
139. Epiphyses of limb elements, secondary ossification centers: absent (0); present (1).
140. Cleithrum: present (0); absent (1).
141. Clavicle, portion articulated with the interclavicle, shape: broader than distal portion of clavicle (0); similar in narrowness to the distal portion of the clavicle (1).
142. Interclavicle, shape: transversely robust, forming broad diamond anteriorly (0); transversely gracile anteriorly, forming anchorlike shape anteriorly (1).
143. Interclavicle, shape of anterior surface anteromedial to clavicular articulations: smooth margin (0); prominent notch in margin (1).
144. Interclavicle, shape of posterior stem: slender, tapering (0); marked expansion (1).
145. Scapula, scapular blade, orientation of the long axis: blade oriented directly dorsally (0); curves posterodorsally (1).
146. Scapula, supraglenoid morphology: prominent tubercle developed distal to glenoid fossa (0); smooth bone dorsal to glenoid, lacking tubercle (1).
147. Coracoid, number of ossifications: two (0); one (1).
148. Coracoid, infraglenoid morphology: no development of coracoid posteroventral to glenoid (0); prominent postglenoid process on coracoid, terminating in thickened margin (1).
149. Sternum, ossification of sternal plates: absent (0); present (1).
150. Humerus, ectepicondyle, presence of radial nerve groove: absent (0); present (1).
151. Humerus, ectepicondyle, radial nerve groove: groove has no roof (0); groove roofed, forming ectepicondylar foramen (1).
152. Humerus, ectepicondyle preaxial crest: prominent (0); absent (1).
153. Humerus, entepicondylar foramen: absent (0); present (1).
154. Humerus, entepicondyle morphology: smooth margin between shaft and postaxial condyle (0); prominent entepicondylar crest present (1).
155. Humerus, entepicondylar crest: exhibits a curved proximal margin (0); exhibits a prominently angled proximal margin (1).
156. Humerus, distal condyle morphology: distinct trochlear and capitular articulations (0); low, double condyle (1).
157. Ulna, ossified olecranon process: present (0); absent (1).
158. Medial centrale of manus: absent (0); present (1).
159. Distal carpal five: absent (0); present (1).
160. Manual intermedium: present (0); absent (1).
161. Ulnare and intermedium, perforating foramen between elements: present (0); absent (1).
162. Manual digit four, phalangeal formula: five phalanges (0); four phalanges (1).
163. Puboischiadic plate, fenestration: no fenestra (0); thyroid fenestra within plate (1).
164. Ilium, orientation of long axis of orientation for iliac blade: horizontal orientation (0); posterodorsal orientation (1).
165. Ilium, anteroventral process extending from anterior margin of pubic peduncle: absent (0); present, process draping across anterior surface of pubis (1).
166. Ilium, supraacetabular crest: crest absent, posterodorsal margin of acetabulum similar in development of anterodorsal margin (0); prominent anterodorsal bony lamina frames the anterodorsal margin of the acetabulum (1).
167. Ilium, shape of supraacetabular margin: dorsalmost margin of acetabulum unsculptured (0); prominent, bulbous rugosity superior to acetabulum (1).
168. Ilium, acetabulum shape: irregular, marked by posterodorsal invasion by finished bone (0); roughly circular, no posterodorsal invasion (1).
169. Ilium, anterior margin of iliac blade, anterior process or tuber: absent, smooth anterior margin (0); process or tuber present (1).
170. Ilium, anterior process/tuber of ilium: anterior process/tuber small, with anterodorsal margin of ilium curving smoothly into dorsal margin of iliac blade (0); large and anteriorly projecting tuber, with dorsal margin of tuber nearly continuous with dorsal margin of iliac blade (1).
171. Ilium, development of posterior process: weakly developed, failing to extend well posterior of acetabulum (0); strongly developed, extending well posterior to the acetabulum (1).
172. Ilium, dorsal blade margin: smoothly textured dorsal border (0); distinct dorsoventral striations running from acetabulum to dorsal margin of iliac blade (1).
173. Pubis, morphology of symphysis, public apron: pubic apron present, with distinct anteroventral downturn of the symphyseal region (0); pubic apron absent, symphyseal region only in coronal plane (1).
174. Pubis, pubic tubercle: absent (0); present (1).
175. Pubis, lateral surface, development of a lateral tubercle (sensu Vaughn, 1955): present (0); absent (1).
176. Ischium, shape of posterior margin: linear posterior margin (0); posterior process extends from posterodorsal ischiadic margin (spina ischii sensu El-Toubi, 1949) (1).
177. Femur, profile in preaxial view: femoral shaft exhibits sigmoidal curvature (0); femoral shaft linear with slight ventrodistal curvature (1).
178. Femur, morphology of proximal end of head: well-ossified convex head, hemispherical (0); concave surface with groove (1).
179. Femur, development of internal trochanter crest: trochanteric crest does not reach femoral head (0); trochanteric crest reaches far proximally, continuous with the femoral head (1).
180. Femur, size of distal condyles (medial and lateral), comparison: about equal in size (0);

unequal, lateral condyle larger than the medial condyle (1).

181. Femur, expansion of distal condyles relative to femoral shaft: distinct expansion beyond the circumference of the femoral shaft (0); limited expansion beyond the circumference of the femoral shaft (1).
182. Femur, shape of tibial condyle in distal view: medial surface is rounded and moundlike (0); medial surface is triangular and sharply pointed (1).
183. Femur, fibular (= medial) condyle, shape of ventral surface: flattened and planar (0); rounded and moundlike (1).
184. Pedal centrale: absent as distinct ossification, fused to astragalus (0); present as distinct ossification (1).
185. Astragalus-calcaneum, extent of coossification: present as distinct ossifications (0); coossified (1).
186. Astragalus-calcaneum, perforating foramen at contact: distinct foramen situated between astragalus and calcaneum (0); no foramen evident between astragalus and calcaneum (1).
187. Calcaneum, distal facet: distal facet is little broader than is the proximal facet (0); distal facet is markedly expanded, more than twice the breadth of the distal facet (1).
188. Calcaneum, lateral margin: calcaneum terminating in unthickened margin (0); roughened tuberosity present laterally (1).
189. Calcaneum, expansion of lateral margin: calcaneum has little postaxial expansion (0); lateral wing of calcaneum is twice as broad as or broader than the distal calcaneal facet (1).
190. Calcaneum, lateral projection: ventrolateral margin of calcaneum projection coplanar with dorsolateral margin of projection (0); ventrolateral margin of calcaneum "curls" externally (1).
191. Distal tarsal four, morphology of proximal contact: smooth contact surface for proximal tarsals (0); prominent process for contact with proximal tarsals (1).
192. Pedal centrale, contact with tibia: absent (0); present (1).
193. First distal tarsal: present (0); absent (1).
194. Second distal tarsal: present (0); absent (1).
195. Fifth distal tarsal: present (0); absent (1).
196. Metatarsal five, shape of proximal postaxial margin: smooth, curved margin (0); prominent, pointed process (outer process sensu Robinson, 1975) (1).
197. Metatarsal five, angling of primary shaft with proximal tarsal articulation: metatarsal is straight, with proximal tarsal articulation forming straight line with primary shaft (0); metatarsal is hooked, with proximal tarsal articulation forming right angle with primary shaft (1).
198. Metatarsal five, concavity along preaxial margin: prominent concavity present (0); concavity absent, creating blocky metatarsal five (1).
199. Pedal digits, morphology of digit five: proximal phalanx shorter than proximal phalanx of digit four (0); proximal phalanx elongate, longer than all other proximal phalanges (1).
200. Heterotopic ossifications: absent in a minimum of 5 individuals (0); present (1).
201. Maxilla, medial surface dorsal to tooth row: smooth (0); prominent anteroposteriorly oriented ridge present (1). (New)

    In most archosauromorphs, the medial surface of the maxilla is smooth (e.g., *Trilophosaurus buettneri*, TMM 31025-207; *Proterosuchus goweri*, NMQR 880; *Tanystropheus longobardicus*, MCSN BES SC265). In contrast, a prominent longitudinal keel is located on the medial side of the maxillae of *Azendohsaurus madagaskarensis* and *Azendohsaurus laaroussii*. In *A. madagaskarensis,* the ridge is restricted to the posterior half of the maxilla (fig. 7) whereas, in *A. laaroussii*, the anteroposteriorly oriented ridge is present along the entire length of the maxilla (fig. 7).

202. Maxilla, dorsal portion, shape: simply tapers to point dorsally (0); the dorsal apex of the maxilla is a separate, distinct process that has a posteriorly concave margin (1). (New)

    This character describes a distinct dorsal (= ascending) process of the maxilla. All archosauriforms with an antorbital fenestra have a posteriorly directed dorsal process of the maxilla that has a vertical or concave posterior margin. With the exception of juvenile specimens of *Tanystropheus longobardicus* (e.g., MCSN BES SC265) and *Tanytrachelos ahynis* (YPM VP 7482), most archosauromorph taxa without antorbital fenestra usually have a dorsal portion of the maxilla that tapers to point dorsally and is not segregated into a distinct process. In lateral view, the overall shape of the maxillae of most non-archosauriform archosauromorph taxa is triangular with a dorsal apex.

    Azendohsaurus madagaskarensis (fig. 7) and *Azendohsaurus laaroussii* (Gauffre, 1993: fig. 2) have a distinct maxillary process that projects posterodorsally and has a concave posterior margin. The archosauriform-like dorsal process in *Azendohsaurus* led to the suggestion that the taxon had an antorbital fenestra (Gauffre, 1993; Flynn et al., 1999). At least in *A. madagaskarensis*, it is now clear that the lacrimal and prefrontal occupy the space that was thought to be the antorbital fenestra (Flynn et al., 2010). The presence of state (1) occurs in *A. madagaskarensis* and *A. laaroussii* and all taxa with an antorbital fenestra plesiomorphically.

203. Maxilla, anterolateral surface, large anteriorly opening foramen: present, positioned just anterodorsal to primary row of neurovascular foramina (0); absent (1). (Modified from Nesbitt, 2011: char. 31)

204. Maxilla, anteromedial surface, palatal process: absent (0); present but fails to reach the midline (1); present and touches its antimere at the midline (2). (Modified from Nesbitt et al., 2009: char. 2) ORDERED
205. Jugal, anterior process: slender and tapering (0); broad and expanded anteriorly (1). (Gower and Sennikov, 1997; Nesbitt et al., 2009: char. 12)
206. Ectopterygoid, articulation with the pterygoid: contacts part of the lateral edge of the pterygoid (0); contacts the entire lateral edge of the pterygoid (1). (Modified from Nesbitt et al., 2009: char. 17)
207. Quadrate, proximal portion, posterior side: continuous with the shaft (0); expanded and hooked (1). (New)

    The posterior portion of the head of the quadrate has a smooth transition from posterior surface to the portion that articulates with squamosal in most archosauromorphs. For example, *Prolacerta broomi* (BP/1/5375), *Proterosuchus fergusi* (BP/1/3993), *Mesosuchus browni* (SAM-PK 6536), *Protorosaurus speneri* (USNM 442453 [cast]), and *Tanystropheus longobardicus* (Wild, 1973) lack any posteroventral expansion of the posterior portion of the quadrate head. In contrast, *Pamelaria dolichotrachela* (ISIS 316/1), *Teraterpeton hrynewichorum* (NSM 99GF041), *Azendohsaurus madagaskarensis* (FMNH PR 2751), and *Trilophosaurus buettneri* (TMM 31025-140) all have a quadrate head that extends posterior of the articulation with the squamosal and arches posteroventrally, so that the ventral surface of the quadrate, in lateral view, is highly concave (fig. 75).

    Additionally, the head of the quadrate is mediolaterally compressed in *Azendohsaurus madagaskarensis* (FMNH PR 2751) and *Trilophosaurus buettneri* (TMM 31025-140), whereas *Prolacerta broomi* (BP/1/5375) and *Tanystropheus longobardicus* (Wild, 1973) have hemispherical quadrate heads. We are not scoring this as a separate character in this analysis because of difficulties of scoring some of the crushed "slab specimens" and it is not clear whether the posterior elongation of the taxa with a hooked posterior end of the quadrate adds to the mediolateral compression.

208. Parabasisphenoid, orientation: horizontal (0); more vertical (1). (Nesbitt, 2011: char. 97)
209. Parabasisphenoid, semilunar depression on the lateral surface of the basal tubera: present (0); absent (1). (Gower and Sennikov, 1996; Nesbitt, 2011: char. 98)
210. Dentary, posteroventral portion: just meets the angular (0); laterally overlaps the anteroventral portion of the angular (1). (Nesbitt, 2011: char. 164)
211. Dentition, crown height of the upper dentition compared with lower dentition: similar tooth crown height (0); the upper dentition is shorter relative to the taller lower dentition (1). (New)

    The crown height of the maxillary dentition and the dentary dentition is similar in most archosauromorphs. In *Azendohsaurus madagaskarensis* and *Azendohsaurus laaroussii*, the crown length of the maxillary dentition is much shorter relative to the crown length of that of the dentary teeth (fig. 7). The disparity in the size of the upper and lower dentition has led to confusion regarding the relationships of *A. laaroussii*. For example, the maxillary fragments were considered to belong to an ornithischian dinosaur and the dentary was considered to belong to a basal sauropodomorph (= prosauropod) (Galton, 1985; 1990). Similarly, the differences in the size of the maxillary and dentary teeth originally led Flynn et al. (1999) to hypothesize that the bone bed that produced *A. madagaskarensis* (M-28) contains the remains of two "prosauropod dinosaurs." It is now clear that all the bones from (M-28) belong to *A. madagaskarensis* because of articulated and associated material. Thus, both *A. madagaskarensis* and *A. laaroussii* have relatively long dentary tooth crowns relative to the maxillary tooth crowns.

    In contrast, the maxillary teeth in many early archosauromorphs are longer than the mandibular teeth. Such taxa include tanystropheids (e.g., *Macrocnemus bassannii*, MCSN V 457; *Tanystropheus longobardicus*, MCSN BES SC 1018), *Prolacerta broomi* (BP/1/5375), and *Proterosuchus alexanderi* (NMQR 1484).

212. Antorbital fossa: restricted to the lacrimal (0); restricted to the lacrimal and dorsal process of the maxilla (1); present on the lacrimal, dorsal process of the maxilla and the dorsal margin of the posterior process of the maxilla (the ventral border of the antorbital fenestra) (2). (Nesbitt, 2011: char. 137) ORDERED
213. Anterior cervical vertebrae (presacral vertebrae 3–5), postzygapophyses: separated posteriorly (0); connected through a horizontal lamina (= transpostzygapophyseal lamina) with a notch at the midline (1). (New)

    The postzygapophyses of most early archosauromorphs are typically connected at their ventral edge (e.g., *Prolacerta*, BP/1/2675; *Tanystropheus*, Wild, 1973). In a revised diagnosis of Trilophosauridae, Spielmann et al. (2009) showed that *Trilophosaurus buettneri*, *Trilophosaurus jacobsi*, and *Spinosuchus caseanus* share the presence of a transpostzygapophyseal lamina between the postzygapophyses in the third through fifth cervical vertebrae. Additionally, a cleft, located at the midline, interrupts the horizontally oriented transpostzygapophyseal lamina (fig. 76) in these taxa. Small, posteriorly projecting spurs of bone are located on the posterior edge of the lamina in some

Trilophosaurus buettneri anterior cervical vertebrae but are absent in others. A transpostzygapophyseal lamina is also present in *Tanystropheus longobardicus* (Wild, 1973) among non-archosauriform archosauromorphs, but the lamina in continuous across the postzygapophyses and not interrupted by a cleft like in *Trilophosaurus* and *S. caseanus.*

214. Cervical centra 3–5, length versus height: length greater than height (0); subequal (1). (Nesbitt et al., 2009: char. 26)

215. Trunk vertebrae, diapophysis, position: anterior portion of the neural arch/centrum (0); anteroposterior middle of the neural arch/centrum (1). (New)

In most archosauromorphs the diapophysis of the anterior to middle trunk vertebrae is located in the anterior third of the vertebra either on the border of the neural arch and the centrum as in early archosauromorphs (e.g., *Macrocnemus*, MCSN V 457; *Proterosuchus*, Hughes, 1963) or completely on the neural arch as in Archosauria. In *Trilophosaurus buettneri* (TMM 31025-140) and *Spinosuchus caseanus* (UMMP 7507), the diapophysis or synapophysis (= diapophysis and parapophysis combined) is located at the anteroposterior middle of the vertebra on the neural arch (fig. 76). Spielmann et al. (2009) used the presence of the position of the middle position of the trunk rib articulation to unite *Spinosuchus caseanus* and *Trilophosaurus buettneri.*

216. Sacral ribs, anteroposterior length of the first primordial sacral rib versus the second primordial sacral rib, dorsal view: primordial sacral rib one is longer anteroposteriorly than primordial sacral rib two (0); primordial sacral rib two is about the same length or longer anteroposteriorly than primordial sacral rib one (1). (New)

In early diapsids (e.g., *Petrolacosaurus kansensis*), the ilium articulation surface of the first sacral rib is bigger relative to that of the second sacral rib. Moreover, the difference in size of the ilium articulation surface of both sacral ribs is reflected in the anteroposterior length of the ilium articulation surfaces in dorsal view. Additionally, the first sacral rib extends laterally whereas the second sacral rib extends anterolaterally from the centrum body. The presence of a larger first sacral rib is clearly present in squamates, non-archosauriform archosauromorphs (e.g., *Azendohsaurus madagaskarensis*, fig. 23; *Mesosuchus browni*, SAM-PK 7416), and *Proterosuchus alexanderi* (NMQR 1484). In *Erythrosuchus africanus* (Gower, 2003) and other non-archosaurian archosauriforms more closely related to Archosauria than *Proterosuchus*, the anteroposterior length of the first and second sacral ribs at the articulation with the ilium are about the same length. In early members of the Archosauria (= basal archosaurs) with two sacral vertebrae, the second sacral rib is longer anteroposteriorly at the articulation with the ilium than the first sacral rib. The comparison between anteroposterior length of the primordial first and second sacral ribs becomes difficult in archosaurs with more than two sacral vertebrae (see Nesbitt, 2011, for a discussion of sacral vertebra identification in archosaurs). Nevertheless, the archosaur pattern of a second sacral rib larger than the first is still clearly present in extant Crocodylia.

217. Anterior caudal vertebrae, neural spines: inclined posteriorly (0); vertical (1). (Dilkes, 1998)

218. Caudal vertebrae, length of the anterior caudal vertebrae (caudal vertebrae 1–10) relative to posterior caudal vertebrae (25+): nearly the same length (0); posterior caudal vertebrae much longer (1). (New)

The caudal vertebrae of early archosauromorphs either remain the same length or decrease in length posteriorly. This is the case in *Protorosaurus speneri* (YPM VP 2437 [cast]), *Langobardisaurus pandolfii* (MFSN 1921), *Rhynchosaurus articeps* (Benton, 1990), *Azendohsaurus madagaskarensis* (fig. 26), and *Tanystropheus longobardicus* (PIMUZ T/2819). The lengths of the caudal vertebrae in the archosauriforms "*Chasmatosaurus*" *yuani* (Young, 1936) and *Erythrosuchus africanus* (Gower, 2003) also decrease posteriorly.

In *Trilophosaurus buettneri* (TMM 31025-140) and *Trilophosaurus jacobsi* (NMMNH various, Spielmann et al., 2008), the middle to posterior caudal vertebrae are clearly longer than the anterior caudal vertebrae. This elongation of the caudal vertebrae reaches a likely maximum in the middle portion of the tail and the posterior caudal vertebrae retain a similar length to that of the middle caudal vertebrae.

219. Scapula, entire anterior margin: straight/convex or partially concave (0); markedly concave (1). (Nesbitt, 2011: char. 217)

220. Scapula, constriction distal to the glenoid: anteroposterior length greater than one-quarter the proximodistal length of the scapula (0); anteroposterior length less than one-quarter the proximodistal length of the scapula (1). (New)

Among most early archosauromorphs, the scapular shaft just distal to the glenoid is usually as wide as the distal portion of the scapula. In lateral view, this configuration of the scapula results in a general rectangular shape and this is what is present in taxa such as *Prolacerta broomi* (BP/1/2675), *Proterosuchus alexanderi* (NMQR 1484), and *Protorosaurus speneri* (Gottmann-Quesada and Sander, 2009). In *Trilophosaurus buettneri* (TMM 31025-140), *Teraterpeton hrynewichorum*

(NSM 99GF041), rhynchosaurs (e.g., *Teyumbaita sulcognathus,*Montefeltro et al., 2013), and *Azendohsaurus madagaskarensis* (fig. 75), the constriction of the scapular shaft distal to the glenoid is strong like that of members of Archosauria (Nesbitt, 2011).

The distribution of this character is currently complex and the plesiomorphic condition is not clear throughout the tree. A wide, short, platelike scapula is present at the base of Archosauromorpha (*Protorosaurus*) and just outside (*Prolacerta broomi*) and at the base of Archosauriformes (*Proterosuchus*). Within Allokotosauria, members of Trilophosauridae and *Azendohsaurus madagaskarensis* have a tall, constricted scapula, but *Pamelaria dolichotrachela* (ISIS 316/1) has a wide, platelike scapula. Additionally, the tall, constricted scapula is present in rhynchosaurs and *Erythrosuchus africanus* + Archosauria.

221. Humerus, distal end, transverse width: less than 2.5 times the minimum width of the shaft (0); equal or greater than 2.5 times the minimum width of the shaft (1). (Ezcurra et al., 2010: char. 93)
222. Manual ungual, length: about the same length or shorter than the last phalanx of the same digit (0); distinctly longer than the last phalanx of the same digit (1). (New)

The manual unguals of most archosauromorphs (e.g., *Protorosaurus speneri*, Gottmann-Quesada and Sander, 2009; *Tanystropheus longobardicus*, MSCN BES SC 1018) are about the same length as the attached nonterminal phalanx. *Trilophosaurus buettneri* (TMM 31025-140), *Teraterpeton hrynewichorum* (NSM 99GF041), and *Azendohsaurus madagaskarensis* (fig. 52) have large, mediolaterally compressed manual unguals that are significantly longer than the attached phalanx.

223. Ilium, ventral margin of the acetabulum: convex (0); concave (1). (Nesbitt, 2011: char. 273)
224. Ilium, iliac blade, maximum length: less than 3 times its maximum height (0); more than 3 times its maximum height (1). (Ezcurra et al., 2010: char. 94)
225. Ischium length: about the same length or shorter than the dorsal margin of iliac blade (0); markedly longer than the dorsal margin of iliac blade (1). (Juul, 1994; Nesbitt, 2011: char. 298)
226. Femur, ridge of attachment of the *M. caudifemoralis*: bladelike with a distinct asymmetric apex located medially (0); low and without a distinct medial asymmetrical apex (= fourth trochanter) (1). (Nesbitt et al., 2009: char. 36)
227. Femur, anterior trochanter (*M. iliofemoralis cranialis* insertion): absent (0); present (1). (Nesbitt, 2011: char. 308)
228. Astragalus, tibial and fibular articulations: separated by a gap (or notch of Gower, 1996) (0); continuous (1). (Nesbitt, 2011: char. 365)
229. Calcaneum, calcaneal tuber, shaft proportions at the midshaft of the tuber: taller than broad (0); about the same or broader than tall (1). (Nesbitt, 2011: char. 376)
230. Calcaneum, articular surfaces for fibula and distal tarsal IV: separated by a nonarticular surface (0); continuous (1). (Sereno, 1991; Nesbitt, 2011: char. 380)
231. Calcaneum, calcaneal tuber, orientation relative to the transverse plane: lateral, less the 20° posteriorly (0); deflected between 21°–49° posterolaterally (1); between 50°–90° posteriorly (2). (Nesbitt, 2011: char. 377)
232. Metatarsal IV: longer than metatarsal III (0); about the same length or shorter than metatarsal III (1). (Nesbitt, 2011: char. 393)
233. Pes, unguals, ventral tubercle: absent or small (0); well developed and extended ventral to the articular portion of the ungual (1). (New)

The ventral margins of the proximal end of the unguals of diapsids (e.g. most Lepidosauria, *Petrolacosaurus kansensis*) either lack a tubercle or have a very small tubercle (e.g., "*Chasmatosaurus*" *yuani*, Young, 1936; *Protorosaurus speneri*, USNM 442453 [cast]). This is the case in most archosauromorphs from the Triassic. *Azendohsaurus madagaskarensis* (figs. 64, 75), *Trilophosaurus buettneri* (TMM 31025-140), and *Trilophosaurus jacobsi* (Spielmann et al., 2008) have very large tubercles on the ventral surface of the proximal surface of the pedal unguals. It appears that a ventral tubercle is either absent or very small in *Pamelaria dolichotrachela* (ISIR 316/1). The absence of a tubercle is somewhat difficult to determine in small diapsids.

234. Distal nonterminal pedal phalanges, distal articular portion: lateral and medial sides parallel or near parallel (0); lateral and medial sides converging anteriorly (1). (New)

In most diapsids, the lateral and medial sides of the distal ends of the distal pedal phalanges have parallel or subparallel sides. This character state is present in the non-archosauriform archosauromorph *Protorosaurus speneri* (Gottmann-Quesada and Sander, 2009) and the archosauriform *Euparkeria capensis* (SAM-PK-K8309). In *Azendohsaurus madagaskarensis* (figs. 64, 71), *Trilophosaurus buettneri* (TMM 31025-140), and *Trilophosaurus jacobsi* (NMMNH L-3775, Spielmann et al., 2008), the lateral and medial edges of the distal end of the distal phalanges converge anteriorly in dorsal view. This is the first formulation of this character, and the distribution of this feature is not yet fully understood. For example, state (1) is present not only in *Azendohsaurus* and *Trilophosaurus* but also in *Sphenodon punctatus* (FMNH 197942). This character is difficult to determine in small diapsids.

235. Pes, penultimate phalanges (last phalanx before the ungual): shorter than the more proximal phalanges (0); significantly longer than the more proximal phalanges (1). (New)

The penultimate phalanx of the pes of most archosauromorphs are either the same length or shorter than the more proximal phalanx to which it is attached (e.g., *Euparkeria capensis,* SAM-PK-K8309; *Azendohsaurus madagaskarensis*, fig. 64; *Protorosaurus speneri*, Gottmann-Quesada and Sander, 2009). In *Trilophosaurus buettneri* (TMM 31025-140) and *Trilophosaurus jacobsi* (NMMNH L-3775, Spielmann et al., 2008), the penultimate phalanx is significantly longer than the attached, more proximal phalanx (Gregory, 1945; fig. 11). Moreover, the penultimate phalanx for all pedal digits of *Trilophosaurus buettneri* (TMM 31025-140) is the longest of each pedal digit.

236. Osteoderms: absent (0); present (1). (Juul, 1994)

237. Prefrontal, orbital margin, lateral surface: smooth or slight grooves present (0); rugose sculpturing present (1). (New)

The anterolateral surface of the prefrontal of most archosauromorphs is either smooth or slightly grooved or sculptured. This is the state present in *Protorosaurus speneri* (Gottmann-Quesada and Sander, 2009), tanystropheids (*Tanystropheus longobardicus*; MCSN BES SC 1018), and in archosauriforms (*Euparkeria capensis*; SAM 5867; *Plateosaurus engelhardti*; AMNH FR 6810). In the early-diverging rhynchosaur *Mesosuchus browni* (SAM-PK 6536), and in the close relatives *Pamelaria dolichotrachela* (Sen, 2003), *Azendohsaurus madagaskarensis* (FMNH PR 2751; fig. 75), and *Trilophosaurus buettneri* (TMM 31025-140; fig. 75), the lateral surface of the prefrontal is covered in a seemingly random pattern of fine ridges and grooves.

238. Gastralia: abundant, with individual gastral elements nearly contacting (0); small in number (= well separated) or unossified (1). (New)

239. Astragalus, margin between tibial and fibular facets: margin grades smoothly into anterior hollow (0); prominent ridge separates margin from anterior hollow (1). (New; taxa that exhibit confluent tibial and fibular facets [state 1 of char. 228] scored as "-" for this character)

In plesiomorphic diapsid reptiles (e.g., *Araeoscelis*, MCZ 8228) and certain taxa of early archosauromorphs (e.g., *Noteosuchus colletti*, Carroll, 1976; *Trilophosaurus buettneri*, TMM 31025-140), there is a smooth margin between the tibial and fibular facets of the astragalus in dorsal view, such that the anterior grades smoothly into the proximal gap between the two facets. In *Prolacerta broomi* (BP/1/2676), *Proterosuchus* (AMNH FARB 2237), and *Azendohsaurus madagaskarensis* (FMNH PR 2776) there is a ridge that runs from the dorsal margin of the fibular facet to the tibial facet, separating the anterior hollow from the dorsum of the astragalus. Although certain taxa (e.g., *Proterosuchus*, rhynchosaurs) appear consistent in the presence or absence of this ridge, trilophosaur materials from the Kahle Quarry (*Spinosuchus caseanus*) appear to be polymorphic for this feature based on multiple specimens from the Kahle *Trilophosaurus* Quarry (NMMNHS P-36709 exhibits a ridge, whereas NMMNHS P-36720 does not). Thus, these are scored as "0&1."

240. Midcaudal chevrons, anterior process: absent, hemal spine only exhibits posteroventral projection (0); present, hemal spine T-shaped (1). (New)

In most early archosauromorphs, the chevrons have simple shafts that are round in cross section and project posteroventrally. In *Trilophosaurus buettneri* (Gregory, 1945: pl. 24, part 3), the chevrons distally expand in the anterior and posterior directions forming an inverted T-shape.

241. Dentary, anterior portion in lateral view: in the same horizontal plane as the middle portion of the dentary (0); anteroventrally deflected (1). (New for an early archosauromorph dataset)

The ventral deflection of the anterior end of the dentary was initially used in sauropodomorph dinosaur phylogenetic datasets (Sereno, 1999; Yates, 2003) and then coopted for early archosaurs (Nesbitt, 2011) and a similar character was used for theropod dinosaurs (Zanno and Makovicky, 2011). In these taxa, the anterior end of the dentary arcs anteroventrally relative to the rest of the mandible and the dentition is either vertical (e.g., *Plateosaurus engelhardti*; AMNH FR 6810) or procumbent (e.g., *Masiakasaurus knopfleri*; Carrano et al., 2002). The anteroventrally directed dentary is also present in the "sauropodomorph mimics" *Azendohsaurus madagaskarensis* and *Azendohsaurus laaroussii* (fig. 7) and members of Trilophosauridae *Trilophosaurus buettneri* (Gregory, 1945) and *Teraterpeton hrynewichorum* (NSM 99GF041). A slight downturn at the anterior end of the dentary is also evident in *Tanystropheus longobardicus* (MCSN BES SC 1018), and possibly in *Protorosaurus speneri* (Gottman-Quesada and Sander, 2009) but appears rarely in Archosauromorpha.

242. Quadrate, posterior margin, distal half, lateral view: concave (0); convex (1). (New)

The posterior margin of the quadrate of most non-archosauriform archosauromorphs is typically concave for body of the quadrate. This

concave morphology is clearly present in *Tanystropheus longobardicus* (Wild, 1973), *Protorosaurus speneri* (USNM 442453 [cast]), *Pamelaria dolichotrachela* (ISIR 316/1), *Prolacerta broomi* (BP/1/5375; Modesto and Sues, 2004), and *Mesosuchus browni* (SAM-PK 6536). *Trilophosaurus buettneri* (TMM 31025-140), *Proterosuchus fergusi* (BP/1/3993), and *Azendohsaurus madagaskarensis* (FMNH PR 2751) have a large convex margin to the ventral half of the quadrate (fig. 75). The posterior margin of the quadrate is simply concave in *Teraterpeton hrynewichorum* (NSM 99GF041).

243. Atlas, centrum: separate from axial intercentrum (0); fused to axial intercentrum (1). (New)

This character describes the coossification of the atlantal centrum and axial intercentrum, forming a wedge-shaped element with a stout odontoid process that sits between the axis and the atlantal intercentrum/neural arch complex. Such a coossification occurs in *Azendohsaurus madagaskarensis* (UA 7-20-99-653; fig. 10) and *Trilophosaurus buettneri* (NMMNH-P 40927). Separate ossifications occur in numerous early diapsids and archosauromorphs, occurring in *Petrolacosaurus kansensis* (Reisz, 1981), *Tanystropheus longobardicus* (Wild, 1973), *Prolacerta broomi* (BP/1/2675), *Proterosuchus fergusi* (Broili and Schroeder, 1934), and rhynchosaurs (e.g., Montefeltro et al., 2013). A distinct pattern of coossification occurs in certain rhynchosaurs (e.g., *Teyumbaita sulcognathus,* Montefeltro et al., 2013), in which the axial intercentrum and atlantal centrum fuse to independent sites on the axial centrum, suggesting that further variation in the coossification of these elements is present.

244. Axis, neural spine, shape: dorsal margin inclined anteroventrally (0); dorsal margin inclined anterodorsally (1). (New for early archosauromorphs)

This character describes the relative inclination of the dorsal margin of the axial neural spine. An anterodorsal incline to the dorsal margin of the spine occurs in very early diapsids, such as *Araeoscelis gracilis* (Vaughn, 1955) and *Petrolacosaurus kasensis* (Reisz, 1981), whereas most archosauromorphs exhibit a strong posterodorsal incline to the dorsal margin of the spine (e.g., *Trilophosaurus buettneri*, TMM 31025-140; *Proterosuchus alexanderi*, NMQR 1484). The degree of posterodorsal inclination can vary; in *Azendohsaurus madagaskarensis* (UA 7-20-99-653) the incline is very shallow, whereas in *Proterosuchus alexanderi* and *Trilophosaurus buettneri* the incline is far steeper. Within Archosauromorpha, tanystropheids exhibit anterodorsally inclined axial spines as occurs in *Macrocnemus bassanii* (MCSN V 457; Peyer, 1937) and *Tanystropheus longobardicus* (MCSN BES SC 265, 1018).

245. Presacral vertebrae, fifth vertebra to the sacrum, neural arch, posterior edge: spinopostzygapophyseal laminae absent (0); spinopostzygapophyseal laminae present (1). (New)

In most archosauromorphs presacral vertebrae, the dorsal margin of the postzygapophyses and the posterior portion of the base of the neural arch are usually rounded without any sharp ridge. In the holotype of *Spinosuchus caseanus* (UMMP 7505) and specimens recently referred to *S. caseanus* (e.g., NMMNH P-57859) by Spielmann et al. (2009), the dorsal margin of the postzygapophyses thins anterodorsally into sharp spinopostzygapophyseal laminae (sensu Wilson, 1999) that define the posterolateral portions of the neural spine. The posterolateral divergence of the spinopostzygapophyseal laminae creates a dorsoventrally oriented trough at the midline of the neural spine. In the more anterior presacral vertebrae (e.g., presacral vertebrae 5–9), a thin posteriorly expanded lamina lies at the midline between the spinopostzygapophyseal laminae; this results in the varied cross section throughout the neural spine of *S. caseanus* described by Case (1927). The more posterior presacral vertebrae lack the midline lamina on the posterior edge of the neural spine. A posterior cervical vertebra (NMMNH P-44274) assigned to *Trilophosaurus jacobsi* from the Kahle *Trilophosaurus* Quarry (NMMNH Locality 3775) has spinopostzygapophyseal laminae (see Results and Discussion). Taxa scored as having epipophyses on the dorsal margin of the postzygapophyses are not scored as "1" unless the anterior portion of the epipophyses thins into a lamina that marks the posterior edges of the neural spine.

246. Dentary, lateral exposure, posterior extent: posteriormost extent of dentary on dorsal margin of mandible (0); posteriormost extent of dentary positioned ventral to surangular (1). (New)

This character describes, in lateral view, the posterior contact of the dentary with the surangular and angular. In most early archosauromorphs, the posteriormost-exposed portion of the dentary in lateral view occurs at the anterodorsal corner of the surangular, at the dorsal margin of the mandible. Examples of this condition include *Mesosuchus browni* (SAM-PK 6536), *Tanystropheus longobardicus* (MCSN BES SC 1018), and *Pamelaria dolichotrachela* (Sen, 2003). In *Prolacerta broomi* (UCMP 37151), *Proterosuchus alexanderi* (NMQR 1484), "*Chasmatosaurus*" *yuani* (IVPP V4067), and derived archosauriforms in this analysis (e.g., *Batrachotomus kupferzellensis*, Gower, 1999; *Erythrosuchus africanus*, Gower, 2003), the posteriormost-exposed portion of the dentary is positioned between the anteriormost portions of the surangular and angular. In these taxa, the surangular appears to occupy a rela-

tively greater length of the lateral mandibular surface. In addition to *Prolacerta broomi* and Archosauriformes, *Gephyrosaurus* also exhibits a dentary with its greatest posterior extent positioned between the surangular and angular (Evans, 1980). Such a condition is common in rhynchocephalians, which exhibit apomorphically elongated dentaries.

247. Premaxilla, medial surface, palatal process: absent (0); present (1). (New)

This character describes the presence of flattened palatal processes extending medially from the premaxillae. These contact one another medially in the taxa in which they occur. The premaxillae do not contribute to the secondary palate in most early diapsids (e.g., *Petrolacosaurus kansensis*, Reisz, 1981) and early archosauromorphs (e.g., *Azendohsaurus madagaskarensis*, FMNH PR 2751; *Tanystropheus longobardicus*, Wild, 1973). Palatal processes of the premaxillae do occur in the early diapsid *Youngina capensis* (BP/1 2871), *Prolacerta broomi* (Gow, 1975), and archosauriforms (e.g., "*Chasmatosaurus*" *yuani*, IVPP 90002; *Erythrosuchus africanus*, NHMUK R 3592). Such palatal processes occur widely in advanced archosauriforms and archosaurs (Nesbitt, 2011). Palatal processes also occur in *Trilophosaurus buettneri* (TMM 31025-207), although their presence may relate to the edentulous beak in the taxon.

APPENDIX 5

Character Scores

A = [0,1]; B = [0,2]; C = [1,2]; I = "-."

Petrolacosaurus kansensis
0000II0000000001000000101100002010110
0100000001010100000000010110000?0???
1000000011I000000000000011I00000010?
1000000000100II0000I00010?000100011?
0100110001100?0100000I0I110000010?I
1000000000000I0I0?00100000?00I00001000
00000000I0I000000?0?0I01000

Youngina capensis
0000II0000100001010000010101000200
0100110000000111110000010000010100100
01101000????0?000101000000000I0I??00?
0 0 0 I 0 1 0 1 0 0 0 0 ? ? 0 0 0 I I 0 0 0 1 0 1 0 0 1 ?
??111000?10110111?0001??0110?010I0?11
1?01?0???10000?000000I0I0??0100000?00I
00001?000000000I0000?010?000I???0?1

Gephyrosaurus bridensis
0000II00002I0100011010000100000100000
I11010000110I100????0000?10100?00
0?????01?0??0?0101000001I000010I
00?0?000I00000?000?000II?111011110?
?11100001O?11011???????1110011I10111
?000000?01100?01????110??00000000?10I
0111??001?000000I0I?1?????0?00100?0

Shinisaurus crocodilurus
0000II00101I01100110100OIII000001I0101
II1110101100I01I1001000111010011000O
10101111001010101000lI000012100001000
I1000000000000II1100I101111111100011
00100111001101011000101011100001000O
11010?1?00101000O?1?0100100I000?00110
10000?0I0I10001010 000100?0

Uromastyx sp.
0000II00102I01100?101010I0??00101I0
001II1111I0IIIII01I11010I0101010010001
100101101?0101010000lIII0I002100000000
I1000000000000II1110I10110111110001101
100111001101011107?11I1011110000100011
00001I11111000001007?00?0?I010010?000?0
00?0I0I0000001000000000

Protorosaurus speneri
0000II0000100000001101I?01100001000
100I11010??????????10??00010?????????
?????001?000?000100000?00?010I1110??
1110000000???000II0000I?0010??1?110001
?0101000101000000?????1?111?011????1
000000000001?1000?0100?0??00I?00010000
0000000?0I00?000000000?0?

Langobardisaurus pandolfii
100???00????0?????????????????00???????
??????????????????????????????????????
???0?????0???11000200?00?01211111?111
1001?101????1???1?011110?00011110????
010100I11??0?010??11111??1111110??010
0?1?001??10111?????????????0?0?0??00
00?0?0???1??00?000????0??

Tanystropheus longobardicus
00011000?01100000001001??11000011I?10
??11?10000100I1001???0001010??011?00?
??100??0?01000100OB001001011I111001111
001?01101?1111110011110100011110111O
10100I1100001100111101111110110000000
01000I1110111101100000?00I10110000000
00000?0I1?00000001001000

Tanytrachelos ahynis
0001?000?01?00000000?01??110?001?I
??????1?1000?100I100???????0?????????
??????????0?0?0?01000000?000012111110
1??10011?01????11?110?0I100?000?????1
?11010100I11????1100?111111111111100?
?0001??1??11?0111100?00?????0I?000100
00?0000?00001??00?0?00??1???

Macrocnemus basanii
0001100010110001000111???1100001000
?0??11?100?0110I?????????????0???11?0
?????00??0?010?0101000000001011I1110?0
1110011000I???01?0100111101000111011
11010100I11?00?0100111110111?1101100?0
10000?00101101001007?00?00?00I?00?1000
000100?0???0?00000000001?00

Amotosaurus rotfeldensis
?0?????0?????0?????????????????0001?????
??????01?01?????????????????????????

????????????0100000????1001I1110??11
100???11??????????011??0??????????1?11
????????????100???101?1??0??????00
0???0?I101???1??11?0??????I?0????00??0
10??0?0?0???0??????????

Mesosuchus browni
00112?00111I000010A11000I111000100010
0I0101001011OI20?10110000110110111000
???00?011000001001000?100010I?1101011
?110000110?000II000101101002?11110
0?110??10101100002100??10011111001100
0010001100100111002000000000I000100
110000000000000000010000000000

Rhynchosaurus articeps
011120101111I0000101101I0I1110102000100
001011I?IIIII20?????????11001011100?
???11??0?000011001002?10II10I??00?01
00110100011?000II?000I100100?1111
10110010101011O?000000?011111111001?I
0??1000??00100101002?0000100?00I01010
011000000000000000000000?? 000

Teyumbaita sulcognathus
011120101111I0000001201I0I101010201O?00
001011I1IIIII201110110001107???1?000
???1001100I00110010002?10II11I??1000100
1?0000101?0?0II100????0?0?01????0110
?10100I1?????????????????????1010??10
??????1?????????0000100?00I011???111?
???000???????00?000000?00

Pamelaria dolichotrachela
??1???00?0??0???0??0?????1??0001?????
0????000?00??????????00???1???2??????
???01??0?0100011000000101011I???00011
000010010011?0II??00I??0???0?????
0010?10101000????00001?1101????001100
1110011??????010??????0?10?00I00000?
0001000000000?0?001???0?00000

Azendohsaurus madagaskarensis
00111000001000000010010I101000101000
0?00000000100I?001?1?1011110122101100
1010011000111001000001100011I
11100011000010010011101I1100I11030I0
11111001101010100010000000111?110110
0000011000?11010010100011000011001I0
0000011110A0000000011001110110000

Azendohsaurus laaroussii
00111I00?????????????????????????????
????????????????????????????????????
????0????????011000001107?0???????????
????????????????????????????????????
????????????????????????????????????
??????????????1100??????1I??????????
??????????????1??1????00

Trilophosaurus buettneri
00011001102I0000000201I0I100101I000000
??1011I0IIIII10?01111011?1001111100
010101?10100001100010012II12011100
011100010011011110I0000I10020?01110100
11010101100100000001111101101100110001
11000110010011100?00100011000I1010111
10100000000001110110111 10001

Trilophosaurus jacobsi
0?0???01002I000?000101??0102101
?000??0?0??1?????????????????????????
?????????01??0?00??11000100?12?I120??
?000111000l?01???????????0I??0???????
??0?11?10101100??00?000101101???1001
10011?0001100?????????0010I0???00I
10?0?1??0?000000000?1110??0?1?1?1??

Spinosuchus caseanus
??????????????????????????????????????
??????????????????????????????????????
??????????????????????????120???00011
100??001001100II?00?????????????????
??????????????????????????????????
??????????????????????????????101?0?
?????????????????0????????1??

Teraterpeton hrynewichorum
000100001O1?000000001??0?0I0101?000000
??1010?0010?????10?100010?0???11?00???
?00?1000?00110001002?10?I11I?1101010
?0001001????0???100??????0??111x?00
??????????????????????????????????????
?????????????????????01?0010?00I??0??
?11?1?????????????01???10?????

Prolacerta broomi
000110001010000100010A00I1100001000100
I11010000111111002A011110011011111100
000100110001000101000011100111I1110001
10000100000?100II00010110????110100
110010100I11????000010100100110011001
110001100100111002000000000I0001100
0000000000000???00?100100011

Chasmatosaurus yuani
02011000001010100001111I1?11?0002001?
00I01010?0??????0?????????1????????
?????00??0?1?0???110000?11?011I???0?0
1?0????00000??0100?0?0I10?1??0100?101
11010111100??00?000101101101100110011
10?011001??11100?0100010??00I00010000
1100000000001?000???01???11

Proterosuchus
02011000001010100001111I101110002000
100I0101000011110OI10111111110111
1112000??0011001?000111000011100101I11
00101100000000??2?0110?0010100100?100
11011001010102?1?????000111?1111110010
00111000110010011100?0100010000I0001
0?000?000000000000?01?0100011

Proterosuchus alexanderi
?2????000010101000?11I101110?0200010
0?01010???1111?0?10111?1111???111?200
0??00??001?000011000??11001??11001011
00000000????0110?0010102?1000100110110
0101010?0?????000111?1110010?10????10
00110010011102???1??0?00000?00010?00??
0000000000???0001?0?00?1?

Erythrosuchus africanus
000111100010101000011II11110000200010
000100??0?????100001?111111001O?11200
1??00110011000111000010lI010I0?000011

0100000001210OII0000I10010001111100?1
00101010111????000111111110110010000100
0??1000???1??00?011111010101010?0101
?0100000000???0???000??011

Euparkeria capensis

0001110000101001000 1?1I11111000201100
0001010?00110?100??1?1?11110?11?11210
?0100110 11?000111000010100 11I01000010
0?00?000??2??1100000I??0?0??11??00??0
???1?0I11?????0001?11111??1?01
I0111000011 00I1111100001011101010101
0110110001111011011000100I000??01?

Batrachotomus kupferzellensis

0001011010101010000000111I0I11100
0020110000010 11I0 III0I1001011101011
?001?1020?1??00?100100 001110000101I
011I0110001 10A00100111210100 1000
I??0100011???00100101000 10?????000101
1111011001I01?1001011?0I???110??0112

1101110201011?110?01110?1121?0?1?0I00
0?1011

Coelophysis bauri

0101I10000101000000111I0I110010201100
0001?011?11I0I100100?1001110?01
11?20?10100??00110001110000101I011I1
1100011100010011111100II1100I10010?01I
III011000I10001000 11I0001011110011000
I01110A10III0I11100II0011201011102
0001?1110111111 1I1I000001I000010??

Plateosaurus engelhardti

v0001I10000101000000111I0I11001020110
00001001 1?11I0I?00100?1001110001110C0
0101 00?1001100011000000100I011I1
1100011000010011111100II1100I1001??01?
III011000I10001000 11I0001011110011?00
I0111001 0III0I11100II0011201011102000
1001111111111 1I1I000011I00000011